

**UNCERTAINTY ANALYSIS OF
LAKE ERIE NET BASIN SUPPLIES**

**UNCERTAINTY ANALYSIS OF LAKE ERIE NET BASIN SUPPLIES
AS COMPUTED USING THE RESIDUAL METHOD**

By

JACOB BRUXER, B.ENG., P.ENG.

A Thesis

Submitted to the School of Graduate Studies

in Partial Fulfilment of the Requirements

for the Degree

Master of Applied Science

McMaster University

© Copyright by Jacob Bruxer, March 2011

Master of Applied Science (2010)
(Civil Engineering)

McMaster University
Hamilton, Ontario

TITLE: Uncertainty Analysis of Lake Erie Net Basin Supplies as
Computed Using the Residual Method

AUTHOR: Jacob Bruxer, B.Eng. (McMaster University)

SUPERVISORS: Dr. S.M.A. Moin, Ph.D., P.Eng.

Dr. Y. Guo, Ph.D., P.Eng.

NO. OF PAGES: xii, 238

Abstract

The Lake Erie net basin supply (NBS) is defined as the net volume of water entering or exiting the lake from its own drainage basin over a specified period of time. NBS can be computed using either the component or residual method. In this research, an uncertainty analysis was performed on the residual method of computing Lake Erie NBS using both the First-Order Second Moment (FOSM) method and a Monte Carlo simulation approach. Uncertainties in each of the various inputs, including the inflows, outflows, and change in storage, among other sources, were first defined through analysis of data, when available, or with alternative methods when necessary. Estimating the uncertainty in each of the NBS model inputs was found to be the most difficult and time consuming component of this study, and also the component prone to the most subjectivity. The results obtained using the FOSM and Monte Carlo approaches were found to be nearly identical when applied to the residual method of computing Lake Erie NBS. Comparison of the results of this study to the results from other research showed that the overall uncertainties in NBS are of similar magnitude. However, the uncertainty in the change in storage was found to be greater than estimates given in previous studies, and greater than perhaps generally believed, being of a similar magnitude to the uncertainty in the Lake Erie inflows and outflows, which have normally been cited as the greatest sources of uncertainty in Lake Erie residual NBS.

Acknowledgements

I would like to thank my thesis supervisors, Dr. Syed Moin and Dr. Yiping Guo, for getting me interested in water resources engineering during my years as an undergraduate student, for encouraging me to continue with my studies at the graduate level, and for agreeing to oversee this research and providing advice and guidance along the way.

I would also like to acknowledge the financial support I received from the International Upper Great Lakes Study. I hope that this research will prove to be as worthwhile an investment to the Study as pursuing my graduate degree has been to me personally.

I would also like to thank a number of my colleagues – notably Chuck Southam, Len Falkiner, Aaron Thompson, Jeanette Fooks and Rob Caldwell at Environment Canada, Tim Hunter and Carlo De Marchi at NOAA, and Nanette Noorbakhsh at the U.S. Army Corps of Engineers – for going to great lengths to provide me with complete and accurate data and information needed for this research, for patiently answering my many questions, and for reviewing this thesis once it was completed. These contributions have been very much appreciated.

Lastly, I would like to thank my family for their encouragement and support, and especially my wife Jen, who has always supported me in everything I do, and without whom I would not have achieved this goal.

Table of Contents

Abstract.....	iii
Acknowledgements.....	iv
Table of Contents.....	v
List of Figures.....	viii
List of Tables.....	ix
List of Acronyms and Abbreviations.....	xi
1 Introduction.....	1
1.1 General Introduction.....	1
1.2 Study Area.....	2
1.3 Thesis Objectives.....	3
1.4 Thesis Overview.....	5
2 Literature Review.....	7
2.1 Uncertainty Analysis.....	7
2.2 Net Basin Supplies.....	9
2.3 Flow Measurement and Uncertainty.....	11
2.4 Change in Storage and Uncertainty.....	16
2.5 Additional NBS Inputs and Sources of Uncertainty.....	19
3 Computation of NBS.....	20
3.1 Derivation of NBS Equations.....	20
3.2 Computation Methods Overview.....	21
3.3 Lake Erie Residual NBS Computation.....	22
3.3.1 Change in Storage.....	22
3.3.2 Inflow.....	25
3.3.3 Outflow.....	25
3.3.4 Additional Diversions.....	33
3.3.5 Consumptive Use.....	34
3.3.6 NBS Summary for Lake Erie.....	34
4 Uncertainty Analysis Concepts and Methods.....	36
4.1 Statistical Terms and Concepts.....	36
4.2 First-Order Second Moment (FOSM) Method.....	37
4.3 Monte Carlo Simulation Method.....	39
5 Discussion of Open-Channel Flow Measurement Uncertainty.....	41
5.1 Overview.....	41
5.2 Uncertainty in Gauged Discharge Measurements.....	41
5.3 Uncertainty in Discharge Determined from a Linear Model.....	43
5.4 Uncertainty in Model Predictor Variables.....	54
5.5 Combined Uncertainty in Modelled Flows.....	55

5.6	Combined Uncertainty in the Average Discharge in a Period	56
5.7	Additional Sources of Uncertainty and Systematic Errors.....	59
6	Sources and Estimates of Uncertainty in Niagara River Flow	61
6.1	Niagara River Flow Overview	61
6.2	Niagara Maid-of-the-Mist (MOM) Pool Flow	61
6.3	Hydropower Diversions	69
6.4	New York State Barge Canal (NYSBC) Diversion	72
6.5	Upper Niagara River Local Runoff.....	75
6.6	Welland River Diversion.....	81
6.7	Combined Uncertainty in Niagara River Flow at Buffalo	83
6.8	Alternative Niagara River Flow Estimation Methods.....	87
7	Sources and Estimates of Uncertainty in Welland Canal Flow	90
7.1	Welland Canal Overview	90
7.2	Welland Canal Supply Weir Flow	90
7.3	Uncertainty in Flows into the Welland Canal	95
7.4	Uncertainty in Flows Distributed Along the Welland Canal	96
7.5	Comparison of Flows Into and Distributed Along Welland Canal	98
7.6	Combined Uncertainty in Welland Canal Flows	100
7.7	Alternative Welland Canal Flow Estimation Methods	100
8	Sources and Estimates of Uncertainty in Detroit River Flow	102
8.1	Detroit River Overview	102
8.2	Stage-Fall-Discharge Equations.....	102
8.3	Flow Transfers.....	114
8.4	Additional Sources of Error	121
8.5	Combined Uncertainty in Detroit River Flows	124
8.6	Alternative Detroit River Flow Estimation Methods	124
9	Sources and Estimates of Uncertainty in Change in Storage.....	127
9.1	Change in Storage Overview.....	127
9.2	Accuracy of Gauged Water Levels	128
9.3	Temporal Variability	129
9.4	Spatial Variability	137
9.5	Glacial Isostatic Adjustment (GIA)	143
9.6	Lake Area	143
9.7	Combined Uncertainty in Change in Storage.....	146
9.8	Thermal Expansion and Contraction.....	150
9.9	Alternative Change in Storage Estimation Methods	160
10	Sources and Estimates of Uncertainty in Consumptive Use.....	162
11	Overall Uncertainty in Residual NBS.....	165
11.1	Hydrologic Data	165

11.2	Combined Residual NBS Uncertainty: FOSM Method	167
11.3	Combined Residual NBS Uncertainty: Monte Carlo Method.....	172
11.4	Comparison of FOSM and Monte Carlo Analysis Results	176
11.5	Sensitivity Analysis.....	178
11.6	Comparison to Previous Estimates of NBS Uncertainty.....	181
11.6.1	Neff and Nicholas (2005).....	181
11.6.2	De Marchi et al. (2009).....	181
11.6.3	NBS Uncertainty Results Comparison.....	182
11.7	Summary of Overall NBS Uncertainty	186
12	Conclusions and Recommendations	188
12.1	Conclusions	188
12.2	Recommendations	189
13	References.....	191
	Appendix A: Comparison of Upper Niagara River Local Runoff to fitted probability distributions	202
	Appendix B: Niagara River flow at Buffalo 2008 Monte Carlo analysis results histograms	209
	Appendix C: Spatial variability in mean Lake Erie water level error comparison to fitted probability distributions.....	212
	Appendix D: Environment Canada 1967-1982 bathythermograph survey vertical temperature data for Lake Erie and fitted temperature profiles	219
	Appendix E: Lake Erie beginning-of-month fitted vertical temperature profile comparisons	225
	Appendix F: Thermal expansion and contraction results comparison to fitted probability distributions	232

List of Figures

Figure 1-1: The Great Lakes-St. Lawrence River system.....	4
Figure 3-1: Active Lake Erie water level gauges.....	25
Figure 3-2: Map of Niagara River flow inputs and other important features	27
Figure 3-3: Niagara River simplified flow schematic.....	28
Figure 3-4: Map of Welland Canal flow inputs	31
Figure 6-1: Ashland Ave. rating compared to ADCP measurements	63
Figure 6-2: Ashland Ave. rating compared to conventional flow measurements (pre-2001) and ADCP measurements (post-2001).....	65
Figure 6-3: Six-minute vs. hourly Ashland Ave. water level data (1 April, 2010).....	67
Figure 6-4: Boxplot comparison of upper Niagara River local runoff estimates.....	79
Figure 7-1: Welland Canal supply weir index-velocity rating vs. mean velocities from ADCP measurements	92
Figure 7-2: Difference in Welland Canal flow estimates (Apr. 2005 – Apr. 2010).....	99
Figure 8-1: Detroit River water level gauges.....	103
Figure 8-2: St. Clair River water level gauges.....	116
Figure 9-1: BOM lake-wide mean water level error schematic.....	127
Figure 9-2: Lake Erie daily mean water level comparison	138
Figure 9-3: EC bathythermograph survey locations (1967-1982)	153
Figure 11-1: Lake Erie monthly mean residual NBS (1900-2008).....	166

List of Tables

Table 6-1: Measured NYSBC flows: 1923-1926 navigation season	73
Table 6-2: Measured NYSBC flows: 1927 non-navigation season	74
Table 6-3: Niagara River local runoff values	75
Table 6-4: Upper Niagara River tributary gauge information	77
Table 6-5: Comparison of upper Niagara River local runoff estimates	78
Table 6-6: Probability distributions used for local runoff uncertainty estimation	80
Table 6-7: Niagara River mean input flows (1962-2008) and uncertainty estimates	84
Table 6-8: Niagara River Monte Carlo analysis input distributions and parameters	86
Table 6-9: Niagara River FOSM and Monte Carlo analysis results comparison.....	87
Table 7-1: Comparison of Welland Canal flow estimates (Apr. 2005 - Apr. 2010).....	100
Table 8-1: Detroit River stage-fall-discharge rating equations.....	104
Table 8-2: Detroit River rating equation standard error estimates (%).....	104
Table 8-3: Standard uncertainty in 24-hour mean Detroit River water levels	106
Table 8-4: Detroit River rating equation sensitivity coefficients.....	107
Table 8-5: Detroit River mean daily water level correlation coefficients.....	109
Table 8-6: Detroit River combined standard uncertainty	109
Table 8-7: Mean difference in Detroit River flow estimates (1994-2009)	112
Table 8-8: Root mean squared deviation in Detroit R. flow estimates (1994-2009)	113
Table 8-9: St. Clair River stage-fall-discharge rating equations.....	117
Table 8-10: St. Clair River rating equation standard error estimates (%).....	118
Table 8-11: Number of days flows were affected each month by ice.....	122
Table 9-1: Change in storage error due to true changes in mass volume of water	134
Table 9-2: Average standard deviation of two-day lake-wide mean water levels	135
Table 9-3: Correlation coeff. of deviations from 4-gauge lake-wide mean water level .	136
Table 9-4: Standard error of the two-day lake-wide mean water level.....	137
Table 9-5: Lake Erie water level gauge Thiessen weights	139
Table 9-6: Lake Erie water level differences (9-gauge Thiessen network)	141
Table 9-7: Spatial variability errors: logistic distribution parameters and SEs.....	142
Table 9-8: Summary of standard uncertainty estimates in BOM water levels.....	147
Table 9-9: Summary of uncertainty estimates in change in storage	148
Table 9-10: FOSM vs. Monte Carlo analysis estimates of ch. in storage uncertainty ...	149
Table 9-11: Mean thermal volume change (GLSEA surface temperature data)	156
Table 9-12: Mean thermal volume change (GLERL model surface temperature data)..	156
Table 9-13: Comparison of mean thermal volume change results.....	157
Table 9-14: Uniform and triangular distribution mean and variance equations	159
Table 9-15: Thermal volume change uncertainty PDFs and parameters	159
Table 10-1: Lake Erie total withdrawals, diversions and consumptive use estimates	163
Table 11-1: L. Erie monthly mean residual NBS and input estimates (1900-2008).....	165
Table 11-2: L. Erie monthly mean residual NBS and input estimates (1962-2008).....	167
Table 11-3: Standard uncertainty estimates for L Erie residual NBS inputs	169
Table 11-4: Combined uncertainty in Lake Erie residual NBS using FOSM method....	170
Table 11-5: Mean systematic error in Lake Erie residual NBS	171
Table 11-6: Distributions & parameters used in residual NBS Monte Carlo analysis...	173
Table 11-7: Residual NBS mean Monte Carlo analysis results (1900-2008)	174

Table 11-8: Residual NBS mean Monte Carlo analysis results (1962-2008)	174
Table 11-9: Monthly range and SD of residual NBS Monte Carlo analysis results	175
Table 11-10: Mean FOSM and Monte Carlo analysis results for residual NBS	176
Table 11-11: Mean systematic error in monthly residual NBS.....	177
Table 11-12: Residual NBS sensitivity analysis results.....	180
Table 11-13: Residual NBS sensitivity analysis results (relative uncertainty)	180
Table 11-14: Comparison of residual NBS input uncertainty estimates	184
Table 11-15: Comparison of overall uncertainty estimates in NBS	186

List of Acronyms and Abbreviations

ADCP – Acoustic Doppler Current Profiler
AVM – Acoustic Velocity Meter
BOD – Beginning-of-Day
BOM – Beginning-of-Month
CaPA – Canadian Precipitation Analysis
CDF – Cumulative Distribution Function
CGIP – Chippawa-Grass Island Pool
CHS – Canadian Hydrographic Service
Coordinating Committee – Coordinating Committee on Great Lakes Basic Hydraulic and Hydrologic Data
DFO – Department of Fisheries and Oceans (Canada)
EC – Environment Canada
EOD – End-of-Day
FOSM – First-Order Second Moment method
GEM – Global Environment Multiscale
GIA – Glacial Isostatic Adjustment
GLC – Great Lakes Commission
GLERL – Great Lakes Environmental Research Laboratory
GLSEA – Great Lakes Surface Environmental Analysis
HPG – Hydraulic Performance Graph
IEC - International Electrotechnical Commission
IGLD – International Great Lakes Datum
IJC – International Joint Commission
INBC – International Niagara Board of Control
INC – International Niagara Committee
INWC – International Niagara Working Committee
ISO – International Organization for Standardization

IUGLS – International Upper Great Lakes Study
IUGLSB – International Upper Great Lakes Study Board
MOM – Maid-of-the-Mist
NBS – Net Basin Supply
NOAA – U.S. National Oceanic and Atmospheric Administration
NOS – U.S. National Ocean Service
NYPA – New York Power Authority
NYSBC – New York State Barge Canal
OPG – Ontario Power Generation
PDF – Probability Distribution Function
RM – Robert Moses
SAB – Sir Adam Beck
SINB – Special International Niagara Board
SLSMC – St. Lawrence Seaway Management Corporation
USACE – United States Army Corps of Engineers
USGS – United States Geological Survey
WSC – Water Survey of Canada
ZETG – Zero of the Electric Tape Gauge

1 Introduction

1.1 General Introduction

The Laurentian Great Lakes (hereinafter referred to as the Great Lakes) are a series of large, connected freshwater lakes located in Canada and the United States. In water balance studies of these lakes, an individual lake's net basin supply (NBS) is defined as the net volume of water entering (or exiting) the lake from its own basin over a specified period of time. More specifically, NBS is defined as the precipitation that falls directly onto the lake, plus the drainage basin runoff that enters the lake, minus the evaporation from the lake itself, plus or minus the direct groundwater flux.

NBS have traditionally been computed in the Great Lakes basin using either of two methods: the component method, which computes NBS directly from measurements and modelled estimates of the hydrologic components themselves, namely over-lake precipitation, lake evaporation and basin runoff (groundwater flow is normally considered negligible); or the residual method, which computes the NBS to a lake as the residual of a lake's change in storage, inflows from upstream lakes, outflows downstream, and diversions into and/or out of a lake. Of the two methods, the residual method was the first used by water resources engineers in the Great Lakes basin, as it could be computed primarily from readily available water level data; however, with the advent of modern computers and numerical models, and the ability to manage and analyze large datasets, the component method became feasible (Lee, 1992). The NBS determined using the residual method (known as the *residual NBS* for short) are computed and coordinated in the Great Lakes basin by Canadian and U.S. agencies, notably Environment Canada (EC) and the U.S. Army Corps of Engineers (USACE), respectively, and have been back-calculated to the year 1900. The National Oceanic and Atmospheric Administration's (NOAA) Great Lakes Environmental Research Laboratory (GLERL) in the U.S. has developed models and methods for computing NBS estimates using the component method (known as the *component NBS* for short), and has back-calculated these estimates to 1948. Prior to this date, the data required for the component method is insufficient. More recently, EC researchers have begun computing a second estimate of component NBS using a suite of alternative methods and models.

Accurate estimates of NBS are required in the Great Lakes basin for operational regulation of Lake Superior and Lake Ontario, for the formulation and evaluation of regulation plans, for water level forecasting, for time series analyses using statistical methods, and to provide an indicator of climate change (Lee, 1992). This thesis will focus primarily on uncertainty in Lake Erie NBS computed using the residual method, with some additional discussion and comparisons made with regard to the component NBS.

1.2 Study Area

The Great Lakes form one of the largest fresh surface-water systems in the world. The Great Lakes basin has a total drainage area of approximately 765,990 km², of which approximately one third (244,160 km²) consists of the surface area of the lakes themselves. The total volume of water in the Great Lakes is approximately 22,684 km³, and this volume represents approximately 18-percent of the world's fresh surface water (Fuller et al., 1995).

This huge resource is shared by Canada and the United States, and is of tremendous importance to both countries. The regional importance of the Great Lakes cannot be understated: the basin is home to millions of people who rely on the Great Lakes for drinking water, irrigation, and recreational opportunities; the lakes support diverse ecosystems, providing for a wealth of plant and animal life; and they provide the foundation for major industries, including commercial navigation, hydropower, tourism, and fishing, among others.

The Great Lakes system (Figure 1-1) consists of the five Great Lakes themselves (Lake Superior, Lake Michigan, Lake Huron, Lake Erie and Lake Ontario), one secondary lake (Lake St. Clair), four connecting channels (the St. Marys, St. Clair, Detroit and Niagara rivers), and an outlet channel that drains to the Atlantic Ocean (the St. Lawrence River). Lake Superior is the most upstream of the Great Lakes. Its outflow is regulated, and passes through the St. Marys River before entering Lake Huron. Lake Huron is connected hydraulically to Lake Michigan through the Straits of Mackinac, and in this respect is considered one lake. Lake Michigan-Huron's outflow passes through the St. Clair River, entering the relatively small Lake St. Clair, which then flows through the Detroit River into Lake Erie. Lake Erie's outflow consists of both the flow that

passes through its natural outlet, the Niagara River, and the flow diverted through the Welland Canal, both of which flow into Lake Ontario. Lake Ontario flows into the St. Lawrence River, which is also regulated, and after passing through the regulation works, the outflow from the Great Lakes travels by way of the St. Lawrence River through Canada to the Gulf of St. Lawrence and the Atlantic Ocean.

Though still one of the largest lakes in the world, of the five Great Lakes, Lake Erie is the second smallest in terms of surface area, the shallowest of the five, and the one having the smallest volume; however, its shores are heavily populated by a number of major metropolitan areas, it is heavily industrialized, and is biologically the most productive of the Great Lakes, supporting one of the greatest freshwater fisheries in the world (Fuller et al., 1995). It is also one of the more complex in terms of computing NBS by the residual method and estimating its uncertainty. This is due to the complicated nature of determining Lake Erie's inflow and outflow and their large magnitude relative to the NBS, as well as the effects of wind and thermal expansion and contraction on measured water levels and the computed change in storage.

1.3 Thesis Objectives

The main objective of this thesis is to quantify the uncertainty in the residual NBS for Lake Erie. The thesis will provide a detailed description of how the residual NBS for Lake Erie is computed; identify sources of error in the computations and methods for evaluating the uncertainty resulting from them; use a subset of these methods and available data and models to accurately quantify the uncertainty in each element of the computations; and combine these individual sources of uncertainty using appropriate methods to determine the total uncertainty in residual NBS. The uncertainty results will be compared to those from other studies, and will be used to resolve differences observed in the different methods of computing NBS. Methods will also be suggested that could be used to reduce uncertainty. The findings of this study can be applied by the engineering community to similar problems, including application of the methods proposed for the other Great Lakes.



Figure 1-1: The Great Lakes-St. Lawrence River system

1.4 Thesis Overview

This thesis consists of a total of twelve chapters, plus references and a set of Appendices. This first chapter provides an introduction to the topic and motivation for completing an uncertainty analysis on Lake Erie residual NBS.

Chapter 2 contains the literature review that was conducted for this study. The chapter provides an overview of NBS, sources of uncertainty, and methods that have been proposed to quantify them. It also discusses uncertainty analysis in general, the different methods available for quantifying uncertainty, and their uses and limitations.

In Chapter 3 the mathematical equations used to compute the NBS are derived in general, and then for Lake Erie specifically. Additionally, a general overview of the methods used to compute each of the quantities that are used in the equations is given.

In Chapter 4, the basic statistical concepts and uncertainty analysis methods used in this research are presented. Definitions are given for a number of important terms used throughout this report, and the First-Order Second Moment (FOSM) and Monte Carlo simulation methods of performing uncertainty analysis are described.

In Chapters 5 through 10, the specific sources of uncertainty in each of the inputs to the Lake Erie residual NBS are evaluated in detail. Chapter 5 provides an introductory section on the statistical methods available to compute open-channel flow uncertainty, an overview of how they were applied in this research, and their assumptions and limitations. In Chapters 6, 7 and 8 the uncertainties in the Niagara River, Welland Canal, and Detroit River flows, respectively, are estimated using statistical methods when possible, and more general approaches when necessary. In Chapter 9, uncertainty in Lake Erie lake-wide mean water levels is assessed, including the uncertainty resulting from gauge accuracy limitations, temporal and spatial variability, and other sources. How this uncertainty propagates to uncertainty in the computed monthly change in storage is also determined. In Chapter 10, one additional source of uncertainty in residual NBS is investigated, namely consumptive use. Consumptive use is normally

assumed negligible in NBS computations, and the error that results from this assumption is discussed in this chapter.

In Chapter 11 the uncertainty estimates derived in Chapters 5 through 10 are summarized and then used to provide an estimate of the overall combined uncertainty in residual Lake Erie NBS. The overall uncertainty estimate is determined on a monthly basis using both the FOSM method and a Monte Carlo simulation approach, and the results from both methods are compared. The uncertainty analysis results are also compared to previous estimates of uncertainty in NBS from the literature.

Finally, Chapter 12 provides a summary and conclusions of this research, and offers recommendations for further study.

2 Literature Review

2.1 *Uncertainty Analysis*

Uncertainty can be defined in many ways. In general terms, the uncertainty of a result or measured value (measurand) can be understood as a quantifiable estimate of the quality of the measurand; more specifically, it is a parameter that describes the dispersion of values that could reasonably be attributed to the quantity being observed (ISO, 1995). Uncertainty is related to but not the same as accuracy or error. The accuracy of a measurement refers to how close the measurements of a quantity are to the true value of that quantity; similarly, the error is the difference between the measured value and the true value. Since the true value is rarely if ever known, the accuracy and the error must be estimated, and this estimate is the uncertainty of the measured value (Coleman and Steele, 1995).

Uncertainty results from imperfect information about the quantity being measured (ISO, 1995). In scientific problems, uncertainty arises from many sources, including the natural variability and randomness of natural physical processes; the uncertainty due to incomplete knowledge of the true physical processes being observed; uncertainty that results from representing complex physical systems with simplified models or designs having uncertain parameters; data uncertainties resulting from inaccuracy and errors in measurement of the variables being studied, as well as inconsistencies, non-homogeneous data, and spatial and temporal limitations of the data; and uncertainties resulting from additional human factors (Yen et al., 1986; ISO, 1995). An uncertainty analysis involves determining how uncertainty in each of these individual sources propagates to uncertainty in the output of interest. Uncertainty analysis is also sometimes referred to as risk or reliability analysis (Ang and Tang, 1984), in reference to the risk associated with a decision or course of action, or the expected reliability of the outcome, given the uncertainty of the information available on which the final outcome depends.

Uncertainty analysis is increasingly being performed in a number of areas of water resources engineering, including, for example, water quality modelling (Beck, 1987), statistical climate model downscaling (Khan et al, 2006), urban

stormwater analysis (Guo and Adams, 1998a; 1998b), groundwater flow modelling (Dettinger and Wilson, 1981), hydrologic models (Blasone et al., 2008) and hydraulic models (Thompson et al., 2008). There are numerous techniques available for performing uncertainty analysis, and a number of reference texts are available that describe these (e.g. Ang and Tang, 1984; Coleman and Steele, 1989; ISO, 1995; Mishra, 2009). One of the more recent is provided by Tung and Yen (2005), who thoroughly reviewed a number of uncertainty analysis methods and their application to problems specific to the field of hydrosystems engineering.

Four types of uncertainty analysis methods were considered in this project to assess how uncertainty in the various inputs propagates to uncertainty in the total residual NBS. The four methods were direct integration method, Monte Carlo analysis, FOSM method and Point Estimation method.

The direct integration or derived distribution method, as it is also known, is an analytical or exact uncertainty analysis method. With this method, derived probability distribution theory is used to determine the exact probability distribution function (PDF) of the dependant random variable directly from the PDFs of the independent random variables used as inputs to the model. In this research the dependant random variable, or model output, is the total residual NBS. The direct integration method requires the determination and integration of the PDFs of the input variables, which can be difficult. Furthermore, applying this method becomes quite complicated in a high-dimensional problem, and therefore the direct integration method was not used in this research.

The Monte Carlo method can be used to provide a numerical approximation of the full PDF of the model output. To do this, the probability distributions of the random variables used as model inputs must first be determined. Random samples are then drawn from the distributions of the model inputs and substituted into the model to evaluate the model output. This is done repeatedly to create a subset of probabilistic model outputs, the PDF of which defines the uncertainty in the model output. The Monte Carlo method can be computationally demanding, especially when applied to highly complex numerical models: however, as will be shown, the residual NBS model used in this research is dimensionally large, yet mathematically simple, making application of the Monte Carlo method relatively uncomplicated.

Two additional approximate uncertainty analysis methods were considered. Rather than estimating the full PDF of the model output, these two approximate methods only estimate certain statistical properties of the probability distributions. The FOSM method is one such method, and it can be used to estimate the mean and variance of the model output. This method is supported by a number of international standards organizations, including the International Organization for Standardization (ISO, 1995). It is also known as the first-order variance method or the variance propagation method (Tung and Yen, 2005). The FOSM method involves representing the model as a function of any number of stochastic input variables using a Taylor series expansion to estimate the mean and variance of the model output. The FOSM method is relatively simple to apply, and can be used for nearly any problem, though the accuracy of the method can be compromised when the distributions of the input variables are highly asymmetric, since in such cases the distributions are not sufficiently described by their means and standard deviations alone.

Lastly, the point estimation method is another approximate uncertainty analysis method. Similar to the FOSM method, the point estimation method can be used to estimate the statistical moments of a model output, but unlike the FOSM method, the point estimation method is also able to account for asymmetry in the PDF of the input variables. However, while this method is feasible when one or two input variables are used, it becomes highly complicated for higher dimensional problems (Tung and Yen, 2005). Therefore, given the high dimensionality of the residual NBS model, the point estimation method was not chosen for this study.

2.2 Net Basin Supplies

NBS have been computed in the Great Lakes for many years. Lee (1992), Croley and Hunter (1994) and Neff and Nicholas (2005) have each provided overviews and a comparison of the different methods (i.e. component and residual) used to compute NBS in the Great Lakes, and they have also described sources of error affecting these computations.

The computation of NBS using the residual method was the first of the two methods used in the Great Lakes (Lee, 1992) as it was the simpler method to apply, since the change in storage, inflows and outflows can be computed from

readily available water level measurements. However, currently this is only partly true, especially for Lake Erie. For example, determination of the Niagara River outflow involves measurement of hydropower flows using rating tables that relate discharge to measured power output in addition to water levels. As another example, part of the Welland Canal flow is currently modelled using measured velocities and an index-velocity relationship in addition to water levels; likewise, velocity measurements and index-velocity relationships have also recently been established in the St. Clair and Detroit rivers. Furthermore, the development of any type of flow model, including those that use only water levels as the model parameters, requires gauged discharge measurements for model calibration. Neff and Nicholas (2005) provided some detail regarding the complexity of the residual NBS computations for Lake Erie and the other Great Lakes, but a full description is not available. The Coordinating Committee on Great Lakes Basic Hydraulic and Hydrologic Data (commonly referred to simply as the *Coordinating Committee*) has in the past provided documentation on Lake Erie inflows (Coordinating Committee, 1982) and outflows (Coordinating Committee, 1976), as well as documentation on Great Lakes physical data (Coordinating Committee, 1977). Otherwise, documentation (and in many cases computation) of NBS and the various subcomponents of these computations has come about mainly as a result of the work of the various International Joint Commission (IJC) boards (e.g. INBC, 2009), or the occasional international studies that have occurred (e.g. IUGLSB, 2009).

The component method of estimating NBS, specifically the method used by GLERL, has been well documented. Croley and Hunter (1994) provided a general overview of the GLERL method, while more detailed reports have been produced for each of the individual components, including runoff and precipitation (De Marchi et al., 2009) and evaporation (Croley, 1989; Croley and Assel, 1994). Documentation is also becoming available for the more recent component NBS estimates being developed by EC (e.g. Pietroniro et al., 2006; Spence et al., 2009).

Until recently there have been few attempts to quantify the uncertainty in the computed NBS estimates. Lee (1992) and Croley and Hunter (1994) outlined potential sources of error in NBS. Quinn and Guerra (1986) analyzed the Lake Erie water balance and the continuity of the system in particular. Neff and Nicholas (2005) provided the most comprehensive study of uncertainty in the Great Lakes water balance to date. This analysis, which was done for the purpose

of illustrating how well the hydrology of the Great Lakes-St. Lawrence River system is understood, included estimates of uncertainty in both the residual and component NBS computations for each lake; however, the authors noted that the uncertainty estimates provided were based primarily on best professional judgment since published uncertainty calculations associated with most of the flows and levels of the Great Lakes were unavailable. De Marchi et al. (2009) completed an assessment of uncertainty in GLERL's component NBS estimates as part of the IJC's International Upper Great Lakes Study (IUGLSB, 2009). Another recent study by Quinn (2009) provided a statistical comparison of residual and component NBS estimates for the upper Great Lakes, specifically Lake Superior, Lake Michigan-Huron and Lake Erie. In addition, uncertainty in the change in storage was estimated from an analysis of the measured water levels at different gauge stations as compared to the mean water level computed for each lake. This uncertainty estimate was combined with the uncertainty estimates for the inflows and outflows provided by Neff and Nicholas (2005) to obtain the total uncertainty in the computed residual NBS.

2.3 Flow Measurement and Uncertainty

There are numerous techniques that can be employed to measure flow in open channels, with the choice of which to use depending on the individual application (Herschy, 2009). The literature on flow measurement methods as well as methods of estimating flow measurement uncertainty can be divided into two groups: gauged flows and modelled flows.

Gauged flows refer to single determinations of discharge from actual field measurements. These are often assumed to be instantaneous or near-instantaneous measurements, taken at a specific point in time. Gauged flows are often measured using conventional current meters and the velocity-area method. With this method, velocity is measured using a current meter at specific locations in the channel cross-section, such that an estimate of the average velocity in the channel or a specific portion of it can be determined and then multiplied by the corresponding measured area to give the discharge. More recently, acoustic technologies, such as Acoustic Doppler Current Profilers (ADCP), have been used to measure velocity and discharge in open channels. An ADCP measures water velocity by measuring the Doppler shift of a sound wave transmitted through and reflected off small particles present in the water column (Simpson, 2001).

Additional methods of measuring flow, such as moving-boat, dilution techniques, and float methods, also exist (Hersch, 2009). Gauged flows are often referred to as measured flows, and are collected periodically throughout the Great Lakes region. Gauged flows are also used in conjunction with other measured variables (such as water level and/or channel velocity, for example) in the calibration and validation of flow models.

Modelled flows refer to indirect measurements of flow based on additional measured and modelled predictor variables. Models are often used to determine continuous or near-continuous measurements of flow, since continuous direct gauged measurements are impractical. There are a number of different models that can be used to estimate flow, many of which have been described by Hersch (2009) among others. Examples include stage-discharge rating equations, which relate measured water level at a channel cross-section to channel discharge; stage-fall-discharge equations, which relate water level measured at two cross-sections and the fall between these sections to channel discharge; index-velocity relationships, which relate a measured index velocity acquired using acoustic or other technology to the average velocity in the channel cross-section, which when multiplied by the measured cross-sectional area gives the channel discharge; Hydraulic Performance Graphs (HPG), which are similar to stage-fall-discharge equations in that they relate water level measured upstream and downstream to discharge in the channel (González-Castro and Ansar, 2003); and numerical hydrodynamic models, which are used to solve mathematical equations governing flow in an open channel. Many of these methods and others are currently in use in the Great Lakes region. For example, stage-discharge rating equations are utilized in the Niagara River (Quinn and Noorbakhsh, 2001; INBC, 2009); stage-fall-discharge equations are employed in the St. Clair and Detroit rivers (Quinn, 1979b; Fay and Noorbakhsh, 2010); index-velocity relationships are used to measure the Lake Michigan Diversion at Chicago (Espey et al., 2001; Duncker et al., 2006), the flow through the Welland Canal supply weir (Jeanette Fooks, WSC, personal communication, 8 April, 2010), and more recently, the St. Marys, St. Clair and Detroit River flows (IUGLSB, 2009); HPGs have been applied to the St. Clair and Detroit rivers (Schmidt et al., 2009; Fay and Noorbakhsh, 2010); and numerical hydrodynamic models have been developed for the St. Marys River, the St. Clair and Detroit River system (Holtschlag and Koschik, 2002), and the St. Lawrence River (Thompson et al., 2008).

The uncertainty in gauged flows measured using conventional current meters and the velocity area method has been examined by a number of researchers (Pelletier, 1988). There are many sources of uncertainty in a conventional gauged discharge measurement, including uncertainty resulting from the accuracy of the current meter; uncertainty in estimating the mean section velocity in both time and space resulting from natural fluctuations and the fact that discrete point measurements of velocity are used to estimate the mean velocity of the cross-section; and uncertainties in measuring the cross-sectional area. Mathematical models for each of the error components in discharge determination have been developed in order to better understand the various sources of uncertainty (e.g. Dickinson, 1967), and methods for quantifying the uncertainty in each component and suggested estimates have been given based on a review of a number of studies and field observations (Carter and Anderson, 1963; ISO, 1979; Sauer and Meyer, 1992; Herschy, 2009).

Being a relatively new and evolving technology, the uncertainty in gauged discharge measurements collected using an ADCP has received less attention. Similar to conventional gauged discharge measurements, a number of sources of error cause uncertainty in ADCP flow measurements. Uncertainty results from both errors in the actual measurement of velocity and discharge, and also in the estimation of velocity and discharge in the areas immediately below the ADCP instrument and at the channel boundaries where velocity and flow cannot be measured directly. Simpson (2001) provided detailed explanations of the principles behind ADCP discharge measurements, and outlined sources of error and guidelines for reducing the error in ADCP measurements. Muste et al. (2004a) laid out a framework for computing ADCP uncertainty based on relevant standards for uncertainty analysis, including ISO (1993). González-Castro and Muste (2007) also discussed errors in ADCP discharge measurements, and derived the data reduction equations used to compute flow from the ADCP-measured variables, which formed the basis of an analytical framework for estimating uncertainty in ADCP measurements. Similarly, Kim and Yu (2010) developed an analytical framework for uncertainty in velocity measurements collected by ADCP. Examples of the practical application of these methods were not found.

The uncertainty in modelled flows has been given less attention in the past, although recent research has started to improve on this. Uncertainty in modelled flows results from natural, random variability; from using a simplified

model to represent the true hydraulic conditions and physics in the channel; from errors in the model parameters; from uncertainty in calibration data; and from uncertainty in measurement of the predictor variables used in the model.

Given that it is one of the more commonly used flow models, it is not surprising that much of the literature on uncertainty in modelled flows has been devoted to discharge determined from stage-discharge equations. The stage-discharge equation relates water level to discharge in a channel, and normally takes the form of a power equation. Much of the research on uncertainty in discharge determined from stage-discharge relationships has focused primarily on statistical analyses of deviations of gauged discharge measurements from the fitted stage-discharge equation, as developed from linear regression theory (e.g. Draper and Smith, 1998). For example, in addition to investigating the sources of error in gauged discharge measurements, Dickinson (1967) also considered uncertainty in determination of a single discharge estimate from a rating curve, estimating uncertainty from the standard error of the mean relation at the mean stage value. Venetis (1970) explained that discharge measurements show a spread around the straight-line log-log fit mainly because of errors in the measurements or gauged discharges themselves, but also because the stage-discharge model is an approximation, noting specifically that the flow may not be strictly uniform and the channel roughness may vary with depth. Venetis (1970) also discussed the least squares regression estimates for the parameters, and derived the equations for the maximum likelihood estimators and the variance-covariance matrix of these estimators, which could be used to estimate the variance of the discharge obtained from the stage-discharge relationship. Herschy (1970) gave the same estimate for the error in the stage-discharge curve as Dickinson (1967), but later revised his approach to include increasing confidence bounds as one moves further from the mean stage value (Herschy, 1978). Ibbitt (1975) gave the uncertainty estimate as the standard error of the residuals, and did not account for the number of measurements made. Dymond and Christian (1982) reviewed and summarized these previous studies, and identified three types of errors that cause the random error of a single discharge measurement determined from a rating curve, specifically rating curve error, water level measurement error, and the error resulting from ignoring all physical parameters other than water level that affect discharge. Freeman et al. (1995; 1996) used statistical approaches to determine the uncertainty in polynomial relationships of stage and discharge throughout the United States for the purposes of flood damage reduction studies. Clarke (1999) and Clarke et al. (2000) suggested that

errors arising from incorrect form of the rating curve can be ignored, since the hydraulic justification for using a power-law equation is sufficiently strong, but suggested that the standard error of the mean relation underestimates the uncertainty in discharge obtained from a rating curve since it does not account for the random variations as captured in the gauged discharge measurements. This argument is supported by others, such as Tung and Yen (2005), who discussed application of uncertainty analysis techniques to hydrosystems in general.

In more recent years alternative methods to the statistical approaches described have been proposed. For example, Di Baldassarre and Montanari (2009) investigated uncertainty in stage-discharge curves developed for an Italian river using a one-dimensional hydraulic model. Pappenberger et al. (2006), Krueger et al. (2009) and others have used variations on a fuzzy rating curve method. McMillan et al. (2010) applied a variation of this method to a gravel-bed river in New Zealand. This involved developing multiple rating curves from subsets of available discharge and corresponding stage measurements, which themselves were described by PDFs, in order to incorporate errors in the measured variables into the flow model. All rating curves formulated in this manner were retained if they passed through the error PDFs of all remaining discharge measurements in the group, and these were combined to provide the uncertain or envelope rating curve. Alternative methods such as these are computationally intense, especially when a large number of gauged discharge measurements are available, as is the case in the Great Lakes connecting channels. Nonetheless, an adaptation of either of these methods may be a useful tool to employ at a later date, but was considered beyond the scope of this thesis. Instead, statistical methods as discussed above were used primarily in this research to assess the uncertainty in modelled discharge.

Uncertainty in discharge determined from other models in addition to stage-discharge equations has not been given equal attention. For example, the uncertainty in discharge determined from stage-fall-discharge equations, in particular the form of equation used in the Great Lakes, has not been evaluated specifically. However, the statistical methods applied to stage-discharge equations can be adapted for other linear discharge models, including stage-fall-discharge equations and index-velocity relationships.

The methods described above deal primarily with uncertainty in the model and model parameters. However, error and resulting uncertainty is normally

assumed to be greater than might be suggested by these methods alone when flows are subjected to additional systematic effects. Systematic effects have been observed in the Great Lakes connecting channels, and include weed growth (Sellinger and Quinn, 2001), ice impacts (Derecki and Quinn, 1986), channel erosion or deposition (IUGLSB, 2009), and channel obstructions (Quinn and Noorbakhsh, 2001). These sources of error may be far greater than any other error sources, and must be considered when appropriate.

In addition to the linear models relating measured water level(s) and velocity to discharge described above, Lake Erie outflows are also determined in part by other means. For example, the hydropower companies use rating tables to relate discharge to measured power output and head difference, while a combination of other models and methods are used to estimate flow through the Welland Canal. The hydropower companies use the Gibson method, which is well-documented (e.g. IEC, 1982), to measure flows for use in the development and calibration of their rating tables; however, documentation of the actual rating table development was unavailable. Similarly, there is little documentation available regarding the flows in the Welland Canal.

2.4 Change in Storage and Uncertainty

Change in storage is the increase or decrease in the volume of water stored in the lake over a given time period, and is determined by multiplying the change in measured water level by the area of the lake. Uncertainty results from the precision and resolution of measured water levels at individual gauges; from temporal variability and the choice of averaging period used to estimate the mean water level at the beginning of each month; from spatial variability of water levels resulting from winds, barometric pressure and seiche effects; from the effects of glacial isostatic adjustment (GIA), i.e. the slow rebounding of the Earth's crust due to the removal of the weight of the glaciers some 10,000 years ago; from error in the computed area of the lake and the assumption that it remains constant through the full range of water levels on the lake; and from the effects of thermal expansion and contraction due to heating and cooling of the water volume.

The accuracy of individual water level measurements at a gauge station is determined from the instrument manufacturer's specifications and depends on the type of instrument used. The water level gauges on the Great Lakes are installed,

operated and maintained primarily by the Department of Fisheries and Oceans (DFO) in Canada, and by NOAA in the U.S. The individual agencies are responsible for processing the water level data and for quality control (NOAA, 2009), and the data collection methodologies and processing algorithms used must be taken into consideration in the uncertainty analysis.

There has been much research on the effects of winds, barometric pressure and seiches on measured Great Lakes water levels. Hayford (1922) described these effects and provided one of the first and most comprehensive studies on their impacts on water levels. Sustained winds affect the slope of the lake surface, causing water levels at the downwind end of a lake to rise, and the water levels at the upwind end to fall. This is known as wind-setup or storm-surge. The slope of the lake surface also adjusts to differences in barometric pressure over the Great Lakes, such that water levels are lower under high pressure areas, and higher under low pressure areas (Hayford, 1922). Seiches normally occur when wind intensity subsides, such that inertia of the water body as it returns to an equilibrium state causes free oscillations of the water body, such that water levels rise and fall, back and forth, at opposite ends of the lake (Hayford, 1922; Hunt, 1959).

Hayford (1922) developed methods and equations for determining and correcting for the effects of barometric pressure and winds on water levels at gauges on lakes Erie and Huron, and compared the accuracy of the observed water levels to the corrected water levels by comparing plots of the values to each other and to plots of combined inflow, outflow and precipitation estimates. Hayford (1922) also computed the probable errors for each gauge, and computed weights to use in averaging lake-wide water levels. Hunt (1959) developed a method for calculating and forecasting water level setup due to wind events on Lake Erie by relating such events to measured land and lake-based wind data, as well as temperature difference between the air and water. The largest effects of wind setup and seiche were noted along the longitudinal axis of the lake, running west to east from Toledo to Buffalo, but three other local seiches were also noted, including seiches between the east end of Lake Erie and Long Point, as observed between water levels at Buffalo and Port Colborne; between the south and north shores of the lake, as observed between water levels at Cleveland and Port Stanley; and between the west end of Lake Erie and Point Pelee, as observed between water levels at Toledo and Monroe. The effects of local harbour disturbances and the variability of the effects of wind-setup at different locations

was also discussed. For example, the water level rises caused by wind setup at Buffalo were observed to be much sharper than the corresponding water level falls observed at Toledo, a result of the orientation and shape of the lake, and local geographic features.

Quinn and Derecki (1976) and Quinn et al. (1979) investigated beginning-of-month (BOM) water levels (i.e. the lake-wide mean water level at midnight on the first day of the month) for Lake Erie and the other Great Lakes, respectively, using Thiessen polygons as an alternative to straight averaging. Croley (1987) used a numeric hydrodynamic model to investigate the long-term wind setup error in water levels measured at gauges on Lake Erie. Historic gauge networks were analyzed and spatial-optimum networks and gauge weightings were suggested to minimize the errors observed.

In addition to comparing residual and component NBS, Quinn (2009) analyzed BOM water levels and their uncertainty for each of Lake Superior, Lake Michigan-Huron and Lake Erie. For Lake Superior, this was accomplished by adjusting the recorded water level data for GIA, and comparing the lake-wide mean to the standard deviations of measured water levels at the gauges used to compute the mean. For Lake Erie, the coordinated mean water levels and change in storage values were compared to the values obtained from the weighted gauge network values from Quinn and Derecki (1976). Additionally, the average of the beginning and end of month water levels was also compared to the monthly mean water levels, and correction factors were suggested. This analysis did not consider the uncertainty resulting from gauge accuracy and resolution or the averaging period used.

GIA has long been recognized as having an impact on measured water levels and water balance studies in the Great Lakes (Clark and Persoage, 1970). More recent studies have also looked at the effect of GIA on Great Lakes water levels (Coordinating Committee, 2001; Bruxer and Southam, 2008). However, Quinn et al. (1979) dismissed the effects of GIA on monthly change in storage as negligible due to the extremely small impact it has over a monthly time period.

There have been many investigations regarding the seasonal thermal structure of Lake Erie (e.g. Derecki, 1976; Schertzer et al., 1987), but few have considered its effects on the Lake Erie water balance. Meredith (1975) provided the first and most comprehensive study to date on the effects of thermal expansion

and contraction on the Great Lakes water balance. The mean monthly error caused by thermal expansion and contraction was investigated by developing dimensionless temperature profiles for the beginning of each month, relating these to measured surface water temperatures to estimate the vertical temperature distributions, and then using the differences from the beginning to the end of each month to estimate the change in volume. Results suggested that the monthly NBS could be in error by as much as 100% if thermal expansion and contraction is not considered. Other researchers have investigated and discussed the effects of thermal expansion and contraction on the Lake Erie water balance using similar methods (e.g. Quinn and Guerra, 1986), but a lack of sufficient water temperature data has precluded any more detailed investigation.

2.5 Additional NBS Inputs and Sources of Uncertainty

Two additional sources of error in the residual NBS will be investigated in this study, namely consumptive use and minor diversions. Both of these should be included as inputs in residual NBS computations, but because they are so small compared to other components of the Great Lakes water balance, each of these is typically assumed negligible (Lee, 1992). Similarly, direct groundwater flow to or from the Great Lakes should be accounted for in the component NBS but is normally omitted due to its small magnitude. However, neglecting any of these quantities causes uncertainty in the computed NBS, and comparisons of the two different NBS estimates must take the omitted quantities into consideration.

There are few studies and little data available on these three components of the water balance. The Great Lakes Commission (GLC) acts as a repository for Great Lakes water use data, including consumptive use, which is estimated by the Great Lakes provinces and states and is thought to be highly uncertain (GLC, 2003a). Minor diversions are those normally assumed to have a negligible effect on the Great Lakes water balance. Quinn and Edstrom (2000) described and quantified most of both the major and minor diversions in the Great Lakes, but additional diversions may exist. Lastly, a handful of studies have investigated groundwater discharge to the Great Lakes at various locations (Grannemann and Weaver, 1998), but the rate of flow varies throughout the basin, and few have tried to quantify the total groundwater flow to any of the Great Lakes in particular (e.g. Haefeli, 1972).

3 Computation of NBS

3.1 Derivation of NBS Equations

Mathematical expressions for the two methods of computing NBS (i.e. residual and component) can be derived from analyzing the water balance on a large lake. The water balance can be expressed in full as (Lee, 1992):

$$\Delta S \pm \Delta S_{Th} = I - O + P + R - E \pm D \pm G - C \quad (1)$$

where ΔS is the total measured change in storage; ΔS_{Th} is the change in storage due to thermal expansion or contraction; I is the inter-basin inflow; O is the inter-basin outflow; P is over-lake precipitation; R is basin runoff; E is lake evaporation; D is inter-basin diversions into or out of the lake; G is direct groundwater flow into or out of the lake; and C is consumptive use of lake water. The NBS can then be defined directly as:

$$NBS = P + R - E \pm G \quad (2)$$

Determination of NBS directly from estimates of precipitation, runoff and evaporation has been termed the component method. In practice, groundwater has been considered negligible, such that the component NBS are normally computed as:

$$NBS = P + R - E \quad (3)$$

Substituting equation (2) into (1) and rearranging gives the residual method of determining NBS:

$$NBS = \Delta S \pm \Delta S_{Th} - I + O \pm D + C \quad (4)$$

In practice, both the change in storage due to thermal expansion and contraction as well as the consumptive use are assumed negligible and omitted, and as a result the residual NBS is normally computed as:

$$NBS = \Delta S - I + O \pm D \quad (5)$$

3.2 Computation Methods Overview

The Great Lakes component NBS are computed by estimating each component (i.e. precipitation, runoff and evaporation) directly. Traditionally, GLERL has been the primary agency involved in computing component NBS in the Great Lakes. The methods and models used by GLERL to estimate precipitation and runoff were described recently by De Marchi et al. (2009). Over-lake precipitation is estimated by GLERL using precipitation gauge measurements at points throughout the basin, which are extrapolated to the lake surface area using a Thiessen polygon weighting scheme. GLERL estimates direct runoff using a combination of measured runoff from gauged basins, and the extrapolation of measured runoff to ungauged areas and basins using area ratios. Evaporation is estimated by GLERL using a one-dimensional energy balance model, which has been calibrated to measurements of surface temperature and ice cover (Croley, 1989; Croley and Assel, 1994). More recently, EC has begun producing its own estimates of component NBS using its Modélisation Environnementale Communautaire – Surface Hydrology (MESH) modelling system (Pietroniro et al., 2006). To estimate over-lake precipitation, measured precipitation observations are assimilated with historical short-term Global Environment Multiscale (GEM) meteorological model forecasts to produce the Canadian Precipitation Analysis (CaPA) product. For runoff, a coupled land-surface scheme and hydrologic routing model is used to model flows from gauged and ungauged areas, and then route the total flow downstream to the Great Lakes. Lastly, evaporation is computed by EC using short-term GEM forecasts calibrated to data collected from eddy covariance systems recently installed on Lake Superior (Spence et al., 2009) and Lake Huron. Both GLERL and EC continue to improve the component NBS estimates by improving the models and their calibration, and collecting and incorporating additional data as it becomes available.

The residual NBS are computed from inflows, outflows, change in storage, and diversions. Inflows and outflows, as well as some diversions, are measured primarily using a combination of various streamflow estimation techniques, including stage-discharge equations, stage-fall-discharge equations, HPGs and index-velocity ratings, each of which is calibrated using gauged discharge measurements and measured water level and velocity data. Change in storage is determined from averaging measured water levels from gauges at a number of locations on a lake, and determining the difference in average water level from the start to the end of a time period.

In practice, groundwater flux, change in storage due to thermal expansion and contraction, minor diversions, and consumptive use have traditionally been considered negligible; however, for a comprehensive assessment of uncertainty in NBS calculations these terms must also be considered.

3.3 Lake Erie Residual NBS Computation

As shown in equation (4), the residual NBS for any lake is given as a residual of the change in storage, inflows, outflows, diversions and consumptive use. Equation (4) can be defined for Lake Erie specifically by describing each term in the equation individually and combining the results.

3.3.1 Change in Storage

The first two terms in equation (4), the change in storage terms, can be expressed together as:

$$\Delta S \pm \Delta S_{Th} = \Delta H \cdot CF \quad (6)$$

where ΔH is the change in water level (head) on Lake Erie; and CF is the conversion factor used to convert the change in head to discharge units. The conversion factor is a function of the area of the lake and the number of seconds in a month, and is computed from:

$$CF = \frac{A}{d_t \cdot 86400} \quad (7)$$

where A is the mean surface area of Lake Erie; d_t is the number of days in month t ; and 86400 is the number of seconds in a day. As stated, the change in storage due to thermal expansion and contraction is assumed negligible and is not computed. The remaining terms are evaluated as follows.

For a given month t the change in head on Lake Erie for that month (ΔH_t) is calculated as the change in water level from the beginning to the end of the month in metres. That is

$$\Delta H_t = BOM_{t+1} - BOM_t \quad (8)$$

where BOM_t is the mean Lake Erie water level at the beginning of month t ; BOM_{t+1} is the mean Lake Erie water level at the end of month t , or the mean water level at the beginning of the subsequent month $t + 1$. The BOM water level is meant to represent the mean water level of Lake Erie at midnight at the beginning of the first day of the month. In reality, since instantaneous water levels are assumed to be highly error-prone due to short term impacts resulting primarily from meteorological effects, the level at midnight is instead estimated using a two-day mean of the daily average Lake Erie water levels from the last day of the previous month and first day of the current month. That is

$$BOM_t = \frac{\bar{h}_{(m=t, d=1st)} + \bar{h}_{(m=t-1, d=last)}}{2} \quad (9)$$

where $\bar{h}_{(m=t, d=1st)}$ is the average daily Lake Erie water level for the first day of month t ; $\bar{h}_{(m=t-1, d=last)}$ is the average daily Lake Erie water level for the last day of month $t - 1$.

The daily mean water levels at gauges in Canada and the United States are used to calculate the average daily lake-wide mean water level for Lake Erie. There are currently a total of fourteen active water level gauges on Lake Erie, of which six are located in Canada, and eight are located in the United States

(Figure 3-1). Current practice of the Coordinating Committee is to use a network of only four of these gauges to calculate the lake-wide mean BOM water level. These include the gauges at Port Colborne and Port Stanley in Ontario, and Cleveland and Toledo in Ohio. More specifically, for Lake Erie the daily lake-wide mean water level (\bar{h}) is calculated from:

$$\bar{h} = \frac{(\bar{h}_{CL} + \bar{h}_{PS}) + (\bar{h}_{TO} + \bar{h}_{PC})}{4} \quad (10)$$

where \bar{h}_{CL} is the mean daily water level at Cleveland, OH; \bar{h}_{PS} is the mean daily water level at Port Stanley, ON; \bar{h}_{TO} is the mean daily water level at Toledo, OH; \bar{h}_{PC} is the mean daily water level at Port Colborne, ON. These four gauges have been chosen based on their reliability and their long periods of record, and in order to balance the gauges between the two countries and to spatially balance the gauges approximately around the area of the lake. The spatial balancing is necessary to deal with meteorological effects, such as wind, barometric pressure and seiches. The individual water level gauges are paired in parentheses because if data from one gauge in any gauge pair is unavailable for a given period of time, neither gauge in that pair is used to calculate the mean water level for that time period, and instead the other two gauges are averaged to determine the mean Lake Erie water level. It should also be noted that the Fairport, OH gauge was at one time used to compute the mean Lake Erie water level; however, water level difference plots suggest that this gauge is subject to local subsidence (e.g. Bruxer and Southam, 2008), and therefore this gauge is no longer used in Lake Erie change in storage computations, and historic BOM levels have been revised accordingly (Nanette Noorbakhsh, USACE, personal communication, 24 August, 2010).

Lastly, as discussed, the change in storage due to thermal expansion and contraction (ΔS_{Th}) is currently omitted from residual NBS computations, but it should be included in addition to the measured change in storage identified above.

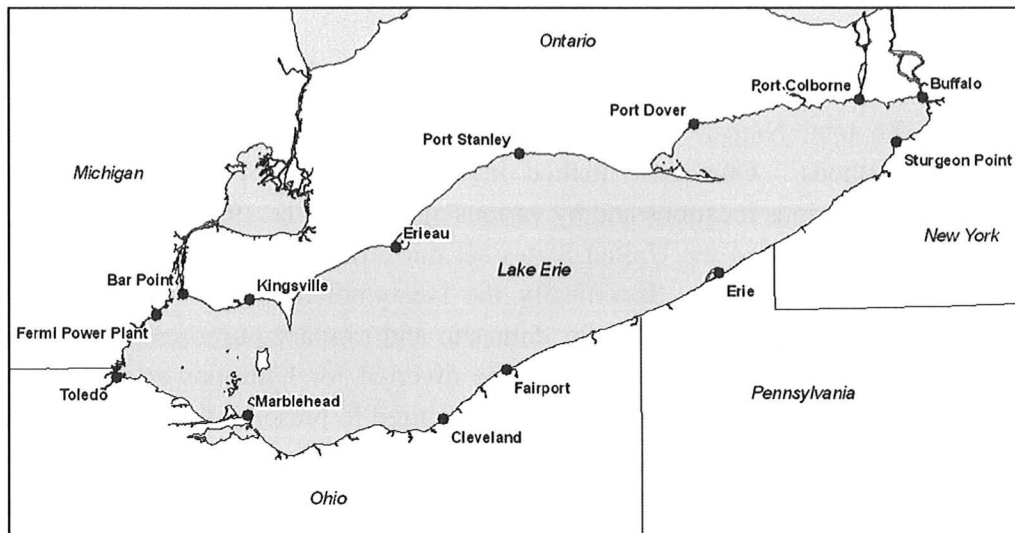


Figure 3-1: Active Lake Erie water level gauges

3.3.2 Inflow

The inflow term (I) from equation (4) can be defined simply as the Detroit River flow, I_{Det} , entering Lake Erie.

$$I = I_{Det} \quad (11)$$

While this is relatively straight forward, the accounting is quite complicated, since monthly Detroit River flow is measured using a combination of a number of stage-fall-discharge equations, hydraulic models, and by transferring the St. Clair River flow using estimates of the Lake St. Clair NBS and change in storage. Additional detail is provided in Section 8.

3.3.3 Outflow

The computation of the outflow term for Lake Erie is more complicated. Lake Erie outflow is computed by summing the flow out of Lake Erie through both the Niagara River at Buffalo ($O_{N@Buf}$) and through the Welland Canal (O_{WC}). Thus, the Lake Erie outflow (O) is given as:

$$O = O_{N@Buf} + O_{WC} \quad (12)$$

The total Niagara River outflow at Buffalo, can be determined using various methods. One such method involves summing a number of flows measured at various locations and by various agencies. The 1950 Niagara Treaty signed by Canada and the United States set out orders of precedence for water uses on the Niagara River. Specifically, the Treaty noted that the total Lake Erie outflow, minus the flow needed for domestic and sanitary purposes and for the service of canals for navigation, could be diverted for hydropower production only after ensuring that the minimum flow required to preserve the scenic beauty of Niagara Falls, as set out in the Treaty, was met. The International Niagara Committee (INC) was established by the two governments following the signing of the Treaty, and is responsible for reporting back to the governments on the amount of water available under the Treaty for scenic flow over Niagara Falls, as well as the amount diverted for hydropower production. As a result of this Treaty, the flow over Niagara Falls and the total diverted for hydropower must be carefully measured.

As such, the current practice when computing residual NBS is to determine the total Niagara River flow at Buffalo by summing six separate flow estimates, including the Niagara Falls and hydropower flows, which make up the majority of the total. This is referred to as the *summation equation* method for the purposes of this study. The Niagara River flow at Buffalo can be measured using available stage-discharge equations, or alternatively, it could be estimated using other flow models; however, currently these methods are limited in their usefulness due to the effects of weeds and ice.

Figure 3-2 provides a map of the Niagara River with the six separate flow estimates used in the summation equation indicated, while Figure 3-3 provides a simplified schematic of the Niagara River flow at Buffalo. Referring to these two figures, the summation equation for the Niagara River flow at Buffalo can be stated as:

$$O_{N@BUF} = N_{MOM} + P_{SAB1\&2} + P_{RM} + D_{NYSBC} - R_N - D_{WR} \quad (13)$$

where N_{MOM} is the computed Maid-of-the-Mist (MOM) pool outflow; $P_{SAB1\&2}$ is the flow diverted to the Ontario Power Generation (OPG) Sir Adam Beck (SAB)

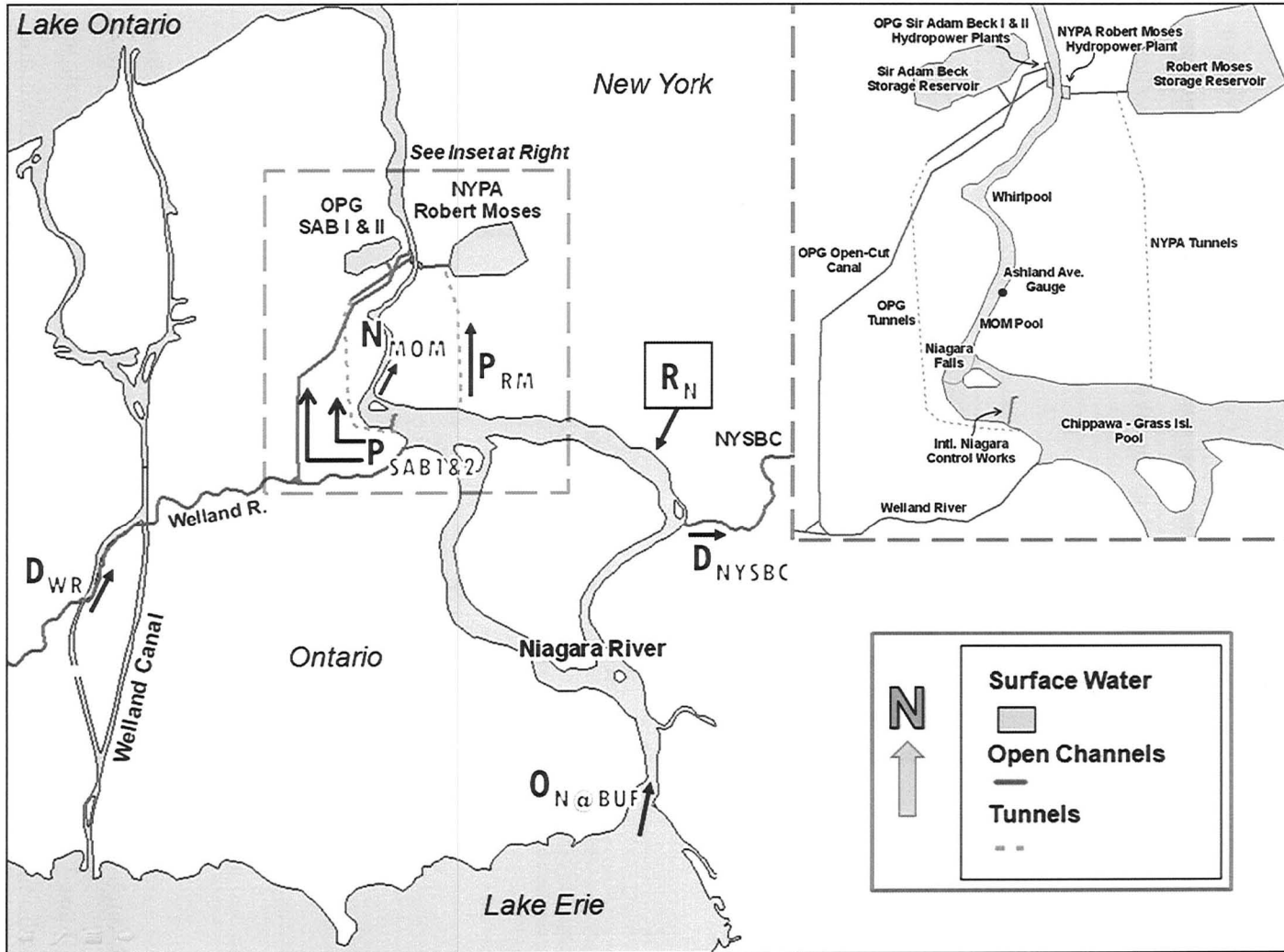


Figure 3-2: Map of Niagara River flow inputs and other important features

hydropower plants One and Two; P_{RM} is the flow diverted to the New York Power Authority (NYPA) Robert Moses (RM) hydropower plant; D_{NYSBC} is the flow diverted to the New York State Barge Canal (NYSBC) from the Niagara River at Tonawanda, NY; R_N is the local runoff entering the upper Niagara River; and D_{WR} is the flow diverted to the Welland River from the Welland Canal.

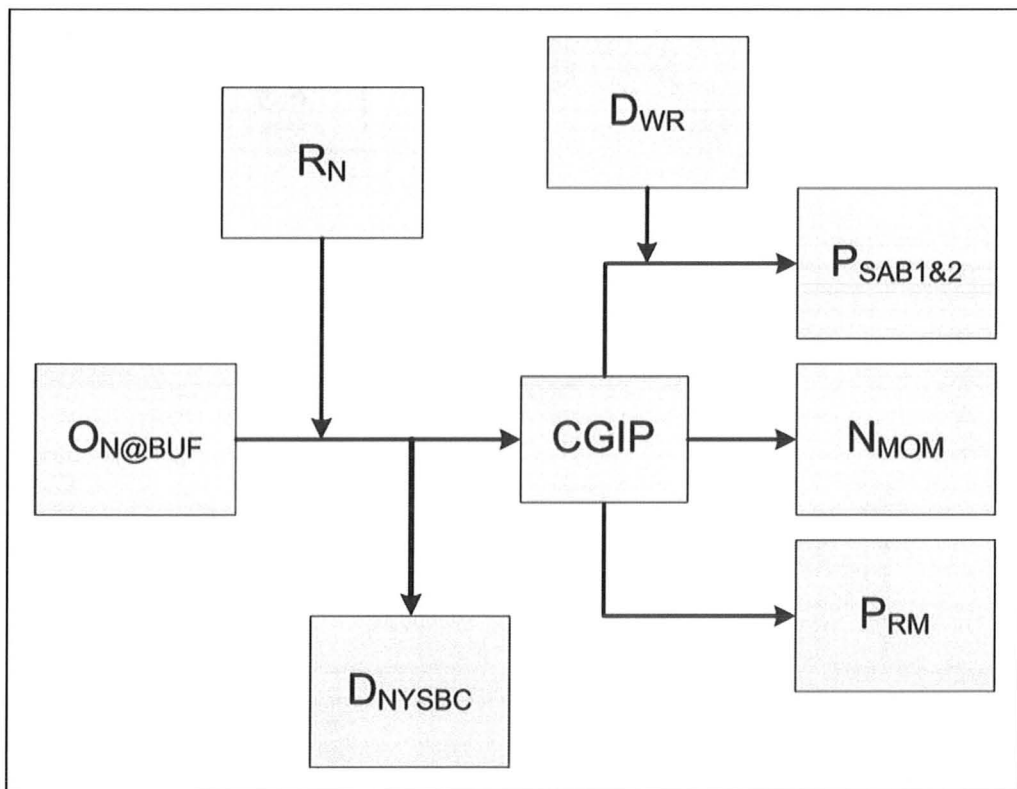


Figure 3-3: Niagara River simplified flow schematic

A large proportion (approximately 30-40%) of the total Lake Erie outflow through the Niagara River passes through the MOM pool. The MOM pool flow (N_{MOM}) includes the total flow that passes over Niagara Falls. In the past, an additional portion of the N_{MOM} flow included water diverted from above and returned to the river below Niagara Falls to produce electricity at several low-head hydropower plants. Since early 2006, when the last of these plants ceased

operation, the N_{MOM} flow consists entirely of the total amount passing over Niagara Falls. The amount that must flow over Niagara Falls varies depending on the time of year and time of day according to rules set out in the Niagara Treaty. During tourist hours, which are 8 a.m. to 10 p.m. from April 1st to September 15th inclusive, and 8 a.m. to 8 p.m. from September 16th to October 31st inclusive, hydropower companies must ensure that no less than 2,832 m³/s (100,000 ft³/s) passes over the Falls; during all other non-tourist hours, including night-time flows during the tourist season and all hours from November 1st to March 31st inclusive, the hydropower companies must ensure that no less than 1,416 m³/s (50,000 ft³/s) flows over the Falls. These are the minimum amounts required by the Treaty, but the actual amount varies depending on existing river conditions.

The hydropower companies divert nearly all of the remainder of the total Niagara River flow at Buffalo from above Niagara Falls to hydropower plants located downstream. The OPG SAB I and II hydropower plants ($P_{SAB\&2}$) consist of 10 and 16 turbines, respectively, while the NYPA RM plant (P_{RM}) consists of 13 turbines. Water is diverted from the Chippawa-Grass Island Pool (CGIP) above Niagara Falls into tunnels and open channels that carry the water downstream to the hydropower plants. The actual amount diverted from the Niagara River is determined from the measured flow through the hydropower plants, as well as the change in storage in the forebays and storage reservoirs upstream.

The NYSBC is a system of canals that traverse the state of New York, connecting the major water bodies of Lake Erie, Lake Ontario and the Atlantic Ocean, in addition to a few small interior lakes (INWC, 1985; Whitford, 1922). A relatively small amount of water is diverted from the Niagara River into the NYSBC system (D_{NYSBC}). Water was originally diverted into the western end of the canal directly from Lake Erie at Buffalo, NY, but this ended in 1918, when a realignment of the canal was completed and the western end was moved to Tonawanda, NY, downstream (north) of Buffalo on the Niagara River. From 1918 until present, water has been diverted from the Niagara River drainage basin as opposed to Lake Erie. Tonawanda Creek originally flowed into the Niagara River at Tonawanda, but the flow was instead diverted into the NYSBC at Pendleton. Depending on the level of the Niagara River and the discharge from the Tonawanda Creek watershed, water has been known to flow both into and out

of the NYSBC from the Niagara River since this time, but the diversion from the basin is treated the same as the diversion from the river itself.

Since outflow from Lake Erie through the Niagara River at Buffalo is desired, but is estimated based on measurements downstream at the MOM pool and the hydropower plants, the local runoff or inflow to the Niagara River, R_N , is subtracted from the measured flows downstream. A lack of gauging stations for measuring local runoff, particularly historically, has meant that the local inflow has been estimated as constant, average monthly values, based on an analysis of measured flows from the period 1913-1960 for the Grand River, ON, and Genesee River, NY (Coordinating Committee, 1962). These two rivers flow into Lake Erie and Lake Ontario, respectively, but they are two of the largest and best monitored inland rivers near the Niagara River, with each having a relatively long period of recorded discharge data; however, how well these two rivers represent the actual conditions and flows in the local Niagara River basin is not known.

A small additional volume of water diverted from the Welland Canal into the Welland River (D_{WR}) is subtracted from the Niagara River flow at Buffalo in the summation equation. The Welland River flows from this diversion at the Welland Canal towards the Niagara River, but the mouth of the Welland River has been dredged and the flow reversed such that the Welland River now flows from the Niagara River to the SAB hydropower plants. Because the amount of water diverted from the Welland Canal into the Welland River is accounted for in the Welland Canal flow estimate (see below), it would be counted a second time as part of the Niagara River outflow as it passes through the SAB hydropower plants. Therefore, the D_{WR} term is subtracted from the Niagara River flow at Buffalo in equation (13).

In addition to the Niagara River flow at Buffalo, the outflow of Lake Erie also includes a portion diverted to the Welland Canal. The Welland Canal is operated by the St. Lawrence Seaway Management Corporation (SLSMC). The SLSMC collects and manages the Welland Canal flow data and provides the data to the INC, but the actual flow estimates come from a number of sources, including the SLSMC itself, OPG, and municipal and industrial users. The Welland Canal flow (O_{WC}) is currently computed by averaging the measured flow into the canal (WC_{IN}) with the total measured flow as it is distributed along the length of the canal at various locations (WC_{DIST}). That is:

$$O_{WC} = \frac{WC_{IN} + WC_{DIST}}{2} \tag{14}$$

Similar to the Niagara River flows, the Welland Canal flows are determined by summing a number of flow estimates as the water passes through various hydraulic control structures and intake/discharge facilities located along the canal system. Figure 3-4 shows a map of the Welland Canal with the major flows indicated. The flow into the Welland Canal is computed as the sum of flows through the Welland Canal supply weir (SW_{WC}) and through the lock located closest to Lake Erie, Lock 8 ($L8$), such that:

$$WC_{IN} = SW_{WC} + L8 \tag{15}$$

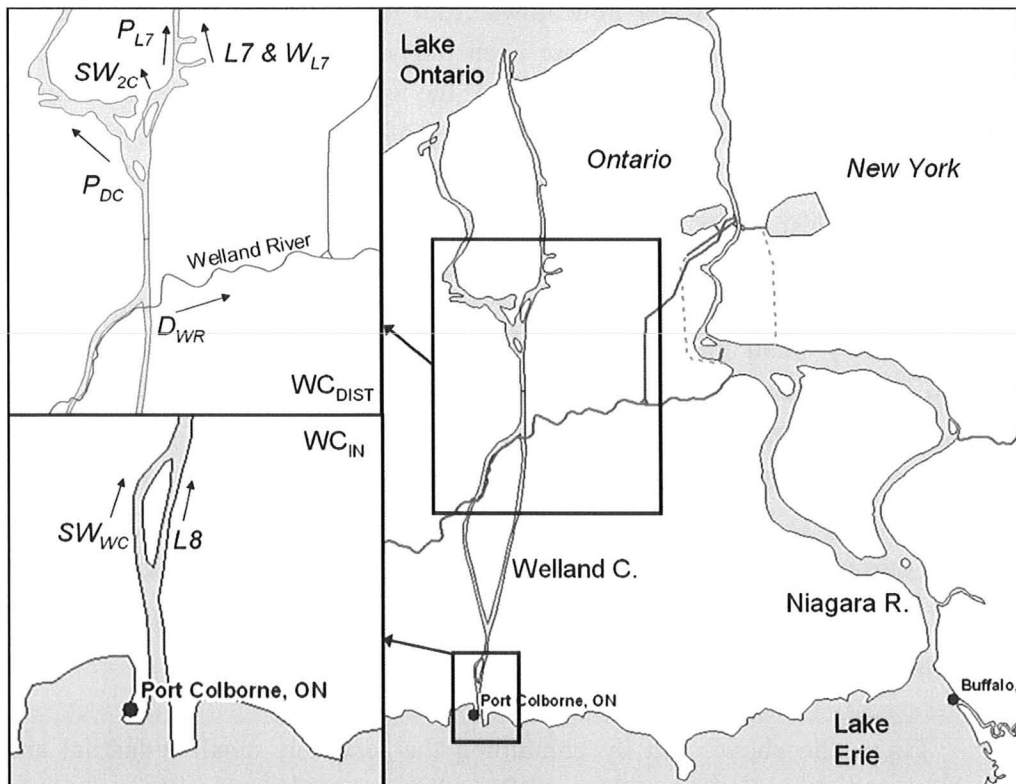


Figure 3-4: Map of Welland Canal flow inputs

For accounting purposes, the distribution of flow along the Welland Canal, WC_{DIST} , is divided into four lettered groups, A, B, C and D:

$$WC_{DIST} = WC_A + WC_B + WC_C + WC_D \quad (16)$$

The Group A flow includes all flows diverted from the Welland Canal into the Welland River, which is also the amount subtracted from the Niagara River flows (i.e. D_{WR}), as discussed previously. Most of this amount comes from both the Welland Water Works, which withdraws water from the Canal and flushes outputs to the Welland River, and from the Welland Canal syphon culvert roof drains. In regards to the latter, the Welland River flows through a syphon culvert that passes below an arm of a previous alignment of the Welland Canal. This older stretch of canal is disconnected and water no longer flows freely through it. For water quality purposes, six small drain holes were cut in the bottom of the old stretch of canal and through the roof of the Welland River syphon culvert, such that a small amount of water now flows from the old canal into the Welland River. Only three of these holes are open today. Two smaller municipal and industrial users account for the remainder of the water diverted from the Welland Canal to the Welland River. The vast majority of Group B discharge is diverted to the De Cew power plants (P_{DC}), which are owned and operated by OPG. The De Cew flows also make up the majority of the total flow distributed along the length of Welland Canal. The remainder of Group B is a small proportion and is divided among a number of industrial and municipal users. Group C flows make up a relatively small proportion of the total Welland Canal flow, with flows divided between the Supply Weir for the second alignment of the Welland Canal (SW_{2C}), which is another discontinued section of canal not used in the current alignment, and industrial users, some of which are obsolete or currently out of service. Group D flows include water passing through Lock 7 ($L7$), or around Lock 7 through the weir (W_{L7}) and the SLSMC power house at this location (P_{L7}). General Motors currently uses a small additional amount, and is the only industrial user in this group.

Given the above, and by combining the relatively small industrial and municipal withdrawals as one, the total flow distributed along the Welland Canal can be summarized as follows:

$$WC_{DIST} = D_{WR} + P_{DC} + SW_{2C} + L7 + W_{L7} + P_{L7} + \sum IM \quad (17)$$

where D_{WR} is the Welland River diversion; P_{DC} is the hydropower diversion to the OPG De Cew generating station; SW_{2C} is the flow through the supply weir for the discontinued Second Canal alignment; $L7$ is the flow through Lock 7; W_{L7} is the flow through the weir at Lock 7; P_{L7} is the flow through the SLSMC powerhouse at Lock 7; and $\sum IM$ is sum of all other industrial and municipal withdrawals. Substituting equations (15) and (17) into equation (14) gives the full equation for the Welland Canal flow as it is currently computed:

$$WC = \frac{(SW_{WC} + L8) + (D_{WR} + P_{DC} + SW_{2C} + L7 + W7 + P_{L7} + \sum IM)}{2} \quad (18)$$

3.3.4 Additional Diversions

Other than the Welland Canal and NYSBC diversions already accounted for, no other diversions are included in the Lake Erie NBS calculations. According to Quinn and Edstrom (2000) there are at least five other minor diversions involving Lake Erie. Two of these are interbasin diversions (i.e. water is diverted into or out of the Great Lakes basin): the Ohio and Erie Canal diverts water from the Ohio River basin to Lake Erie by way of the Cuyahoga River; and the City of Akron, OH, diverts water to communities outside the Lake Erie basin, but is required by the U.S. Water Resources Development Act of 1986 to return the equivalent amount of flow back to the Lake Erie basin. The remaining three diversions are intrabasin diversions (i.e. water is diverted within the Great Lake basin): the City of London, ON, diverts water from both Lake Huron and Lake Erie to the Thames River, which flows into Lake St. Clair; the City of Detroit, MI, diverts water from Lake Huron to the Detroit River downstream; and the City of Hamilton, ON, diverts a small amount of water from Lake Ontario to communities in Haldimand County, within the Lake Erie watershed. The largest of any of these are the Detroit and London diversions at approximately $4 \text{ m}^3/\text{s}$ and $3 \text{ m}^3/\text{s}$, respectively, but even these have no measurable effect on lake levels (Quinn and Edstrom, 2000). The remaining diversions are all less than $1 \text{ m}^3/\text{s}$,

and therefore, the assumption that these minor diversions have a negligible effect on the water balance and the computed NBS and its associated uncertainty is acceptable.

3.3.5 Consumptive Use

There is no agreed upon definition of consumptive use in the Great Lakes basin; rather the definition has varied over time, and by agency and jurisdiction (GLC, 2003a). Consumptive use is defined in the Great Lakes region by the Great Lakes Commission (GLC) in the Regional Water Use Database annual reports as “that portion of water withdrawn or withheld from the Great Lakes Basin and assumed to be lost or otherwise not returned to the Great Lakes Basin due to evapotranspiration, incorporation into products, or other processes” (GLC, 2003a). In the context of NBS estimates, consumptive use can be defined alternatively as that portion of the water balance that is supplied to a basin but is frequently removed before it can be accounted for by other terms of the water balance (Neff and Nicholas, 2005).

The difficulty of defining consumptive use is outweighed by the difficulty of quantifying it. Consumptive use in Lake Erie (C_E) and in the Great Lakes basin in general makes up a very small component of the water balance, and is often omitted from the residual NBS computations. An assessment of the uncertainty caused by this omission is discussed below in Section 10.

3.3.6 NBS Summary for Lake Erie

Substituting each of the individual equations derived above into equation (4) gives the complete equation for Lake Erie NBS (NBS_E) as computed using the residual method:

$$\begin{aligned}
NBS_E = & \\
& \left(\frac{(h_{CLE,t+1} + h_{PS,t+1}) + (h_{TOL,t+1} + h_{PC,t+1})}{4} - \frac{(h_{CLE,t} + h_{PS,t}) + (h_{TOL,t} + h_{PC,t})}{4} \right) \cdot \frac{A_E}{d_i \cdot 86400} \\
& \pm \Delta S_{Th} \\
& - I_{Det} \\
& + (N_{MOM} + P_{SAB\&2} + P_{RM} + D_{NYSBC} - R_N - D_{WR}) \\
& + \frac{(SW_{WC} + L8) + (D_{WR} + P_{DC} + SW_{2C} + L7 + W_{L7} + P_{L7} + \sum IM)}{2} \\
& + C_E
\end{aligned} \tag{19}$$

The complete equation for Lake Erie residual NBS involves a large number of variables, but is mathematically simple. To determine the overall uncertainty in Lake Erie NBS, the uncertainty in each of these variables must first be estimated, and then the individual estimates must be combined using appropriate methods.

4 Uncertainty Analysis Concepts and Methods

4.1 Statistical Terms and Concepts

Prior to presenting the uncertainty analysis, a brief introduction to some of the statistical terms and concepts used in this research is provided. Much of the terminology and many of the concepts used in this research are based on the ISO's *Guide to the Expression of Uncertainty in Measurement* (ISO, 1995). Also known as GUM for short, this document is an internationally recognized standard that describes general rules and guidelines for evaluating and expressing uncertainty estimates, and is generally applicable to a broad range of scientific and engineering disciplines. Other general texts on uncertainty analysis were also found useful in developing and understanding the basic concepts, notably Ang and Tang (1984) and Tung and Yen (2005).

The term uncertainty was defined previously in Section 2.1. Uncertainty analysis involves deriving a quantitative description of how accurate an output of interest is believed to be. This normally involves estimating the probability that a certain output of interest takes on a particular value. In this research, the term *standard uncertainty* is used to describe the uncertainty of a variable when it is expressed as a standard deviation (ISO, 1995). The *combined standard uncertainty* is the standard uncertainty of an output obtained from the combination of a number of other quantities. For example, if a model output is a function of two variables or inputs, and the standard uncertainty of each is known, the combined standard uncertainty is the uncertainty of the output resulting from the standard uncertainty in each of the inputs together.

The standard uncertainty of any variable can be multiplied by a coverage factor to estimate the *expanded uncertainty* of the variable of interest (ISO, 1995). The expanded uncertainty provides an interval within which the true value of the variable of interest is expected to lie with a defined level of confidence. This is also known as the *confidence interval*. For example, the expanded uncertainty estimate can describe the confidence interval within which the value of the variable in question is expected to lie 95% of the time.

The ISO (1995) defines two types of evaluations of uncertainty, Type A and Type B. In Type A evaluations of uncertainty, the uncertainty in an output is evaluated through a statistical analysis of a series of observations. For example, the standard deviation of a series of repeated observations of a quantity can be viewed as a Type A standard uncertainty estimate. In Type B evaluations, other means of evaluating uncertainty are used. Type B uncertainty can be evaluated by pooling together all known information on the possible variability of the variable in question and using engineering judgement to estimate the uncertainty of the variable. It can be based on previous experience, knowledge of the system, previous measurements, incomplete data, and manufacturer specifications among other sources of information. It was found necessary in this research to employ both Type A and Type B methods of evaluating uncertainty.

In some cases, it is helpful to know not only the standard or expanded uncertainty of the variable of interest, but also the *probability distribution*. The probability distribution identifies the likelihood that the variable of interest will take a particular value or fall within a particular interval. For some methods of evaluating uncertainty, such as the Monte Carlo method used in this research, knowledge of the probability distributions of the model inputs are required to evaluate the probability distribution or uncertainty of the model output. A probability distribution can often be described by a mathematical equation known as a probability distribution function (PDF). Also related to this is the cumulative distribution function (CDF), which is a function that describes for any value of a given variable the probability that the variable takes on a value less than or equal to the value specified. A number of well-known probability distributions were used in this research, including the normal, log-normal, uniform, triangular, logistic, and Weibull distribution functions. Descriptions of these can be found in a number of texts and other documents (e.g. Tsokos, 1972; Cooper and Weekes, 1983; ISO, 1995; Haan, 2002).

4.2 First-Order Second Moment (FOSM) Method

The FOSM method was one of two uncertainty analysis methods used in this research. With the FOSM method, the output or model, y , is represented by a function $f(x_1, x_2, \dots, x_n)$, where the set of n input variables (x_1, x_2, \dots, x_n) are used to evaluate the output. This function can be approximated using a Taylor series expansion of the input variables about their means. Evaluating the first

order terms of the Taylor series, one can find the expected or mean value of the output variable given as $E(y)$, as well as the variance of the output variable given as $u^2(y)$, from:

$$E(y) = f(\bar{x}_1, \bar{x}_2, \dots, \bar{x}_n) \quad (20)$$

$$u^2(y) = \sum_{i=1}^n c_i^2 u^2(x_i) + 2 \cdot \sum_{i=1}^{n-1} \sum_{j=i+1}^n c_i \cdot c_j \cdot u(x_i) \cdot u(x_j) \cdot r(x_i, x_j) \quad (21)$$

where \bar{x}_i are the mean values of x_i ; $u^2(x_i)$ are the variances of each input variable x_i ; c_i are the sensitivity coefficients computed for each input variable x_i ; and $r(x_i, x_j)$ are the correlation coefficients computed for each pair of input variables x_i and x_j . The sensitivity coefficients are determined as the partial derivatives of the model output with respect to the input variables, and can be represented by:

$$c_i = \frac{\partial y}{\partial x_i} \quad (22)$$

When the input variables are uncorrelated, the values of $r(x_i, x_j)$ can be assumed equal to zero, and equation (21) can be simplified to:

$$u^2(y) = \sum_{i=1}^n c_i^2 u^2(x_i) \quad (23)$$

The FOSM method of estimating uncertainty as described by equations (21) and (23) is termed the *law of propagation of uncertainty* by the ISO (1995). The FOSM method is relatively simple to apply in that it requires only knowledge of the mean and variance of the input variables. The method allows estimation of the mean and variance of the output, but cannot provide information on the output's probability distribution. Furthermore, the accuracy of the FOSM method can be compromised when the model is highly non-linear, or when the uncertainty in the input variables is non-symmetric and varies significantly from the normal distribution (Tung and Yen, 2005). In such cases the variance may not provide a good estimate of the uncertainty in the model inputs, and the accuracy of the

combined uncertainty estimate can be compromised. In order to determine the full probability distribution of the output, and to deal with highly non-linear problems, a more sophisticated approach is required.

4.3 Monte Carlo Simulation Method

The second uncertainty analysis method used in this research was the Monte Carlo simulation approach. A Monte Carlo simulation involves repeatedly simulating the output variable, y , using randomly generated subsets of input variable values, (x_1, x_2, \dots, x_n) , according to their respective probability distributions in order to derive the probability distribution of the model output.

To apply this approach, knowledge about the probability distributions of the stochastic input variables must be known. The probability distribution of an input variable can be determined by reviewing the data graphically or using statistical means, or in some cases a probability distribution can be assumed based on knowledge of the variable itself. In many cases a probability distribution that can be described mathematically can approximate the data and be fit to the data using various methods. If the input variable is not easily represented by a known probability distribution, another approach is to develop an empirical distribution from data describing the input variable and to randomly sample directly from this. This approach is known as random sampling with replacement, or the bootstrapping technique.

Once the probability distributions of the input variables are defined, a set of input variables are then randomly sampled from the distributions. The model output is then simulated for each set of randomly sampled input variables. A set of simulated model outputs is combined to produce a probability distribution for the model output, which then provides the model output's uncertainty estimate.

The Monte Carlo method becomes much more complicated if model input variables are correlated. Special care must be taken to ensure that the correlation of the input variables is preserved in developing the subset of input variables used to evaluate the model output. In such cases, joint PDFs must be developed for the correlated inputs and sampled accordingly.

The Monte Carlo simulation approach is computationally more demanding than the FOSM method, as it requires significantly more evaluations of the model output. To reduce the computational burden of this approach, some researchers have proposed adding simplifying assumptions or more sophisticated sampling techniques, including response surface replacement of the model and Latin Hypercube sampling (Iman and Helton, 1988). In this research the input and output variables and the relationships between them are already mathematically quite simple, so it was unnecessary to use such methods.

5 Discussion of Open-Channel Flow Measurement Uncertainty

5.1 Overview

Due to the large magnitudes of the inflows and outflows relative to Lake Erie's NBS, uncertainty in these flow estimates can cause relatively high uncertainty in the overall Lake Erie NBS computed using the residual method. For example, Lee (1992) suggested that flows were normally considered accurate to within 5%, but as noted by Quinn and Guerra (1986), a 5% error in Detroit or Niagara River flows can result in a 34% error in residual Lake Erie NBS. Neff and Nicholas (2005) came to similar conclusions, indicating that uncertainty in the inflow and outflow contributed the most uncertainty to the residual NBS for Lake Erie. Therefore, accurate estimates of flow uncertainty are required.

Determining the uncertainty in Lake Erie inflows and outflows requires determining the uncertainty in the data and models used to compute them. The data includes gauged flow measurements, measured water levels and channel velocities, while the models used are primarily linear or linear-transformed mathematical relationships between certain measured input variables and the continuous flow in the channels. There are many methods proposed in the literature for estimating uncertainty in linear discharge models such as stage-discharge relationships. Of these, statistical methods involving a comparison of gauged flow measurements to modelled discharge were primarily chosen for this study. Given that these methods have been subject to some debate (Dymond and Christian, 1982; Clarke et al., 2000) and in the case of Lake Erie are applied to flows obtained using different models (i.e. stage-discharge, stage-fall-discharge and index-velocity methods), a more detailed general discussion is provided below prior to specific application to the Lake Erie inflows and outflows.

5.2 Uncertainty in Gauged Discharge Measurements

Gauged discharge measurements provide a snapshot of the flow in a channel at any point in time, but continuously collecting gauged flow

measurements is not practical. Instead, the gauged flow measurements are used to establish discharge models that relate a continuously measured variable, such as water level or velocity, to the channel discharge. Gauged discharge measurements are subject to uncertainty and this translates to uncertainty in the calibrated discharge models. Therefore, the uncertainty in the gauged flows must be estimated in order to determine the combined standard uncertainty in the Lake Erie inflows and outflows.

As discussed in Section 2.3, many researchers have investigated the uncertainty in gauged flow measurements. The total uncertainty in a gauged discharge measurement varies depending not only on the method used to collect the measurement, but also on the conditions under which the measurement was performed. For example, ice, flow obstructions, wind, and changes in stage occurring during the measurement can all affect measurement accuracy. According to Sauer and Meyer (1992), under good conditions the standard error in gauged discharge likely ranges between around 3 and 6%, but could be as great as 20% under overall poor conditions. Herschy (2009) also noted these variations in uncertainty, and estimated that the attainable level of uncertainty in a single measurement of discharge given good measurement practice was between 5 and 20% at a 95% confidence level, depending on the measurement method used. The attainable level of uncertainty for both conventional current meter and ADCP discharge measurements was given as 5%.

In the Great Lakes specifically, Quinn (1979a) applied the methods of Carter (1970) and Herschy (1970) to investigate the uncertainty in gauged flows collected in the Niagara and St. Lawrence rivers using the velocity-area method with conventional current meters and found the standard errors to be on the order of 3 to 5%, or approximately 6 to 10% at the 95% confidence level. Schmidt et al. (2009) noted that the methods used to collect discharge measurements in the St. Clair and Detroit rivers have varied over time, and that the data available to describe these methods was insufficient to allow for a full uncertainty analysis. Nonetheless, the authors estimated the minimum standard error in conventional measurements taken on the St. Clair and Detroit rivers to be 3.2 to 6.9%, depending on the number of velocity panels used for each specific measurement. Schmidt et al. (2009) also noted similar issues in terms of data limitations for the more recent ADCP measurements on the St. Clair and Detroit rivers, and based in part on a study by Mueller (2003), estimated uncertainty in these measurements to be at least 5%. On the other hand, Espey et al. (2001) examined errors in ADCP

gauged measurements for the Lake Michigan diversion at Chicago, and estimated the random error to be 0.9%, with systematic errors between 0.2 and 0.7%. From this it was estimated that the overall uncertainty in the ADCP measurements could be as low as 0.5%; however, Espey et al. (2001) also noted that some sources of uncertainty were likely unaccounted for, and based on their own professional judgement and reports by Lipscomb (1995) and Morlock (1996), a more conservative uncertainty estimate of 5% was used. Espey et al. (2001) also noted that systematic errors were more likely to affect flow models developed from ADCP measurements than from conventional current meter measurements, since typically a single ADCP is used for all gauged discharge measurements, and since calibration procedures for ADCPs were not yet well-documented.

Given the limited data available to describe the discharge measurement methods used as noted by Schmidt et al. (2009), a more detailed analysis of uncertainty in individual discharge measurements was not pursued in this research. Instead, based on the combined results described above, an uncertainty estimate of 5% at the 95% confidence level, or a standard uncertainty of 2.5%, was assumed for all gauged discharge measurements used to evaluate flow models in this study.

5.3 Uncertainty in Discharge Determined from a Linear Model

One of the methods or models most frequently used to measure streamflow in an open-channel is to relate measured water level(s) to channel discharge through the use of a rating equation. The simple case of relating discharge to a single water level measurement is known as a stage-discharge equation. The stage-discharge equation can be given in the form

$$Q_c = C \cdot h^\beta \quad (24)$$

where Q_c is the rating curve discharge; C is a coefficient; h is the stage; and β is an exponent. Normally h is replaced by $h - a$ (Herschy, 2009), where a is the elevation of zero flow, such that:

$$Q_c = C \cdot (h - a)^\beta \quad (25)$$

The stage-discharge relation is normally calibrated by fitting a linear version of the equation to measured flows and water levels. The stage-discharge equation can be linearized by taking the natural logarithm of both sides.

$$\ln(Q_c) = \ln(C) + \beta \cdot \ln(h - a) \quad (26)$$

If we let the dependant variable $\ln(Q_c) = Y$, and the predictor variable $\ln(h - a) = X$, the equation can be written in the familiar form of a straight line with intercept $\ln(C) = b_0$ and slope $\beta = b_1$.

$$Y = b_0 + b_1 X \quad (27)$$

In practice, when establishing a stage-discharge curve the value of a is often given an initial assumed value prior to fitting the other model parameters; it is then varied until a curve having best fit is found (INBC, 2009; Herschy, 2009). If a value of a is assumed, measured pairs of Y_i and X_i can be used to calibrate this equation, a solution of which can be found using least squares regression theory (e.g. Draper and Smith, 1998), such that:

$$b_1 = \frac{\sum_{i=1}^n (X_i - \bar{X}) \cdot (Y_i - \bar{Y})}{\sum_{i=1}^n (X_i - \bar{X})^2} \quad (28)$$

$$b_0 = \bar{Y} - b_1 \bar{X} \quad (29)$$

where Y_i are the n measured log-transformed gauged discharge measurements, $\ln(Q_g)$; X_i are the log-transformed gauged water levels converted to depths, $\ln(h_g - a)$; and \bar{Y} and \bar{X} are the mean values of these variables. The model parameters b_0 and b_1 are subject to uncertainty. Equations for the sample variance of each parameter, as adapted from Draper and Smith (1998), are given as:

$$Var(b_0) = \left(\frac{\sum_{i=1}^n X_i^2}{n \sum_{i=1}^n (X_i - \bar{X})^2} \right) \cdot s^2 \quad (30)$$

$$Var(b_1) = \frac{s^2}{\sum_{i=1}^n (X_i - \bar{X})^2} \quad (31)$$

The sample variance, s^2 , or the mean squared residual, is an estimate of the true variance σ^2 based on the sample of measured values. It is defined by:

$$s^2 = \frac{\sum_{i=1}^n (Y_i - \hat{Y})^2}{(n-2)} \quad (32)$$

where \hat{Y} is the log-transformed discharge obtained from the linear model, $\ln(Q_m)$. It follows that the sample standard deviation of the model parameters are then:

$$sd(b_0) = \left(\frac{\sum_{i=1}^n X_i^2}{n \sum_{i=1}^n (X_i - \bar{X})^2} \right)^{1/2} \cdot s \quad (33)$$

$$sd(b_1) = \frac{s}{\left(\sum_{i=1}^n (X_i - \bar{X})^2 \right)^{1/2}} \quad (34)$$

Furthermore, taking the square root of the sample variance gives s , which is known as the residual standard error or standard error of estimate. As explained by Herschy (2009), the standard error of estimate defines the spread or dispersion of measured discharge values about the fitted relationship. It can be expressed as

a percentage, and can be multiplied by an appropriate Student's t -value to give the error estimate at a desired level of confidence.

Returning to equation (27), by substituting equation (29) we obtain:

$$Y = \bar{Y} + b_1(X - \bar{X}) \quad (35)$$

Using this equation, for any value of $X = X_0$ we can predict the mean response $Y = \hat{Y}_0$ from the fitted model. Furthermore, the variance of the mean response can be given by:

$$Var(\hat{Y}_0) = Var(\bar{Y}) + Var(b_1)(X_0 - \bar{X})^2 \quad (36)$$

The $Var(\bar{Y})$ can be represented by the sample variance of the mean equal to s^2 / n , and substituting equation (31) for $Var(b_1)$ and simplifying gives:

$$Var(\hat{Y}_0) = s^2 \cdot \left[\frac{1}{n} + \frac{(X_0 - \bar{X})^2}{\sum_{i=1}^n (X_i - \bar{X})^2} \right] \quad (37)$$

The sample standard deviation of the mean response is then:

$$sd(\hat{Y}_0) = s \cdot \left[\frac{1}{n} + \frac{(X_0 - \bar{X})^2}{\sum_{i=1}^n (X_i - \bar{X})^2} \right]^{1/2} \quad (38)$$

This equation represents the standard deviation of the mean predicted value of \hat{Y}_0 , and is also known as the standard error of the mean relation. The standard error of the mean relation gives curved uncertainty limits which are smaller than the standard error of the estimate, and are at a minimum at the mean stage and corresponding discharge values, and increase towards the extreme high and low stage and discharge values. The minimum value for the standard error of the

mean occurs when $X_0 = \bar{X}$ (i.e. $\ln(h+a) = \overline{\ln(h+a)}$), such that the above equation is reduced to:

$$sd(\hat{Y}_0) = \frac{s}{\sqrt{n}} \quad (39)$$

The curved limits given by equation (38) are more acceptable, given that error is likely to increase as one moves further from the mean value.

However, since the actual observed values of Y_i vary about the true mean value with variance σ^2 , a predicted value \hat{Y}_0 of an individual observation will have variance equal to that of the mean relation plus additional model error (Draper and Smith, 1998; Tung and Yen, 2005), such that the sample variance of the observations is defined as:

$$Var(\hat{Y}_0)_{obs} = s^2 + sd(Y_0)^2 = s^2 \cdot \left\{ 1 + \frac{1}{n} + \frac{(X_0 - \bar{X})^2}{\sum_{i=1}^n (X_i - \bar{X})^2} \right\} \quad (40)$$

The sample standard error of the observations is then:

$$sd(\hat{Y}_0)_{obs} = (s^2 + sd(Y_0)^2)^{1/2} = s \cdot \left\{ 1 + \frac{1}{n} + \frac{(X_0 - \bar{X})^2}{\sum_{i=1}^n (X_i - \bar{X})^2} \right\}^{1/2} \quad (41)$$

Equation (41) provides an estimate of the spread of observations, which can be used to produce an uncertainty interval within which any observed value of Y can be expected to lie. That is, any past or future measurement of Y is expected to be within $sd(\hat{Y}_0)_{obs}$ of the model predicted value, \hat{Y}_0 , approximately two thirds of the time. Contrast this with the standard error of the mean relation, $sd(\hat{Y}_0)$, which can be used to construct an uncertainty interval within which the mean of a set of observations Y_i can be expected to lie approximately two-thirds of the time. Tung and Yen (2005) call the interval constructed with the standard

error of the mean relation, $sd(\hat{Y}_0)$, the confidence interval of the true mean response, while the interval constructed with the standard error of the observations, $sd(\hat{Y}_0)_{obs}$, is called the prediction interval of an observed value. These two definitions differ, and both have been suggested as defining the uncertainty in a discharge measurement taken from a stage-discharge curve. For example, Herschy (1978; 2009) suggests the standard error of the mean relation to represent the uncertainty, whereas Clarke et al. (2000) disagreed, and suggested the standard error of observations as the preferred estimate of uncertainty.

Assuming that $sd(\hat{Y}_0)$ represents the total uncertainty in a stage-discharge measurement, as Herschy (1978; 2009) does, essentially assumes that observed differences between the gauged and modelled flows is primarily the result of error in the gauged discharges, and that the model, being based on a large sample of gauged flow measurements, provides the more accurate estimate of the true discharge. On the other hand, assuming that $sd(\hat{Y}_0)_{obs}$ represents the total uncertainty, as preferred by Clarke et al. (2000), basically assumes that the differences between gauged and modelled discharges result primarily from errors in the model itself. Dymond and Christian (1982) added a term in their assessment of uncertainty in the stage-discharge curve to account for uncertainty in the gauged discharge measurements, essentially implying that the difference between the gauged and modelled discharges is the result of error in both the gauged measurements and the fitted model, providing somewhat of a compromise between the two methods; however, if the standard error of the gauged discharges is greater than the standard error of the estimates, the method proposed by Dymond and Christian (1982) basically gives the same result as Herschy (1978; 2009).

The mean of a number of repeated observations will provide a more accurate estimate of the measured quantity than any individual measurement itself, but only if the errors are random and the measurements are repeated under the same conditions. This is not possible in a dynamic, natural channel, where conditions from one measurement to the next cannot be maintained. The gauged flows, while being subject to error themselves, also account for hydrodynamic processes taking place in the channel that are not accounted for in the simplified stage-discharge model used to estimate discharge. For these reasons the standard

error of the observations, $sd(\hat{Y}_0)_{obs}$, was considered the more appropriate and conservative estimator of the model uncertainty for this study.

Up until this point only linear relationships having one predictor variable have been discussed. However, the more general case of having two or more predictors in a linear relationship can be dealt with using similar methods. This will be necessary for assessing uncertainty in stage-fall-discharge relationships, such as those used to estimate flows in the St. Clair and Detroit rivers.

The case of two or more predictors is better dealt with using matrix notation. However, in order to demonstrate its use, it is easier to first revert back to the two-parameter linear relationship defined by equation (27), i.e. $Y = b_0 + b_1X$. Then, as adapted from Draper and Smith (1998) and Tung and Yen (2005), if we define in matrix notation (identified by **bold** print) the series of observations **Y** and **X**, and the parameters of the linear equation, **b**, as:

$$\mathbf{Y} = \begin{bmatrix} Y_1 \\ Y_2 \\ \cdot \\ \cdot \\ \cdot \\ Y_n \end{bmatrix}; \mathbf{X} = \begin{bmatrix} 1 & X_1 \\ 1 & X_2 \\ \cdot & \cdot \\ \cdot & \cdot \\ \cdot & \cdot \\ 1 & X_n \end{bmatrix}; \mathbf{b} = \begin{bmatrix} b_0 \\ b_1 \end{bmatrix}; \quad (42)$$

Then when written in matrix form, the linear equation becomes:

$$\mathbf{Y} = \mathbf{Xb} \quad (43)$$

This is equivalent to equation (27) in standard notation. Also, for the two parameter case, it can be shown that:

$$\mathbf{X'X} = \begin{bmatrix} n & \sum X_i \\ \sum X_i & \sum X_i^2 \end{bmatrix} \quad (44)$$

$$\mathbf{X'Y} = \begin{bmatrix} \sum Y_i \\ \sum X_i Y_i \end{bmatrix} \quad (45)$$

where \mathbf{X}' is the transpose of \mathbf{X} . Multiplying equation (43) by \mathbf{X}' gives:

$$\mathbf{X}'\mathbf{Y}=\mathbf{X}'\mathbf{X}\mathbf{b} \quad (46)$$

This equation can be solved for the parameters \mathbf{b} in matrix form by:

$$\mathbf{b}=(\mathbf{X}'\mathbf{X})^{-1}\mathbf{X}'\mathbf{Y} \quad (47)$$

The term $(\mathbf{X}'\mathbf{X})^{-1}$ is the inverse of $(\mathbf{X}'\mathbf{X})$ and is given by:

$$(\mathbf{X}'\mathbf{X})^{-1}=\begin{bmatrix} \frac{\sum X_i^2}{n\sum(X_i-\bar{X})^2} & \frac{-\bar{X}}{\sum(X_i-\bar{X})^2} \\ \frac{-\bar{X}}{\sum(X_i-\bar{X})^2} & \frac{1}{\sum(X_i-\bar{X})^2} \end{bmatrix} \quad (48)$$

The matrix $(\mathbf{X}'\mathbf{X})^{-1}$ multiplied by the variance of Y , σ^2 , gives the variance-covariance matrix of the parameters \mathbf{b} :

$$\text{Var}(b)=(\mathbf{X}'\mathbf{X})^{-1}\sigma^2 \quad (49)$$

For any value of $X=\mathbf{X}_0=\begin{bmatrix} 1 \\ X_0 \end{bmatrix}$ we can predict $Y=\hat{Y}_0$ from:

$$\hat{Y}_0=\mathbf{X}_0'\mathbf{b}=(1,X_0)\begin{bmatrix} b_0 \\ b_1 \end{bmatrix} \quad (50)$$

Furthermore, using equations (49) and (50) and substituting the sample variance of Y (i.e. s^2) for σ^2 , an estimate of the variance of the mean predicted value (\hat{Y}_0) can be determined from:

$$\text{Var}(\hat{Y}_0)=\mathbf{X}_0'(\mathbf{X}'\mathbf{X})^{-1}s^2\mathbf{X}_0 \quad (51)$$

This equation, in matrix form, is equivalent to equation (37) given previously in standard notation. It follows that the sample standard deviation, or standard error of the mean relation, can be given by:

$$sd(\hat{Y}_0) = s \cdot \{ \mathbf{X}_0' (\mathbf{X}'\mathbf{X})^{-1} \mathbf{X}_0 \}^{1/2} \quad (52)$$

Similarly, the standard error for an individual observation is:

$$sd(\hat{Y}_0)_{obs} = s \cdot \{ 1 + \mathbf{X}_0' (\mathbf{X}'\mathbf{X})^{-1} \mathbf{X}_0 \}^{1/2} \quad (53)$$

While these definitions were developed using the case of a linear model having one predictor variable, the resulting equations are applicable to the case of a linear model having any number of predictor variables, p . In summary, any set of n observations of a dependant variable, \mathbf{Y} , can be written in matrix notation as:

$$\mathbf{Y} = \begin{bmatrix} Y_1 \\ Y_2 \\ \cdot \\ \cdot \\ \cdot \\ Y_n \end{bmatrix} \quad (54)$$

Similarly, the n sets of p predictor variables, \mathbf{X} , can be written as:

$$\mathbf{X} = \begin{bmatrix} 1 & X_{1,1} & \cdot & \cdot & \cdot & X_{p,1} \\ 1 & X_{1,2} & \cdot & \cdot & \cdot & X_{p,2} \\ \cdot & \cdot & & & & \cdot \\ \cdot & \cdot & & & & \cdot \\ \cdot & \cdot & & & & \cdot \\ 1 & X_{1,n} & \cdot & \cdot & \cdot & X_{p,n} \end{bmatrix} \quad (55)$$

A linear relationship between the predictor variables and the dependant variable can then be written from equation (43) as $\mathbf{Y}=\mathbf{X}\mathbf{b}$, and the relationship parameters, \mathbf{b} , are given as:

$$\mathbf{b} = \begin{bmatrix} b_0 \\ b_1 \\ \cdot \\ \cdot \\ \cdot \\ b_n \end{bmatrix} \quad (56)$$

The linear relationship can be solved in matrix form using equation (47), and the standard error of the mean relation and the standard error of observations can be determined from equations (52) and (53), respectively.

An example of a two-predictor model is any of the stage-fall-discharge equations used in the Detroit River. The stage-fall-discharge equations are derived from Manning's equation, and summarizing Quinn (1979b), Schmidt (2009), and Fay and Noorbakhsh (2010), are given in the form:

$$Q_c = \kappa \cdot (w_1 h_1 + w_2 h_2 - \alpha)^{\beta_1} \cdot (h_1 - h_2)^{\beta_2} \quad (57)$$

where Q_c is the rating discharge; κ is a coefficient accounting for channel roughness, channel width, reach length, and other factors not accounted for elsewhere; the term $(w_1 h_1 + w_2 h_2 - \alpha)^{\beta_1}$ accounts for the area and hydraulic radius of the channel; the term $(h_1 - h_2)^{\beta_2}$ accounts for the water surface slope; h_1 and h_2 are equivalent to the water surface elevation at the upper and lower ends of the reach, respectively; w_1 and w_2 are weights given to h_1 and h_2 , respectively; α is a coefficient representing the mean bottom elevation, and is similar to the value of a from the stage-fall discharge relationship given in equation (25) in that it defines the water level elevation of zero flow; and the exponents β_1 and β_2 are empirical constants.

The water levels h_1 and h_2 in the term $(w_1 h_1 + w_2 h_2 - \alpha)^{\beta_1}$ can be given any weighting, but are often given equal weight, such that w_1 and w_2 both equal 0.5, providing the average of the two gauged water levels; alternatively, the weights can be given values of 1 and 0, or vice versa, such that the water level of only one gauge is employed in this term of the equation (Quinn, 1978; Fay and Noorbakhsh, 2010). The values of κ , α , β_1 and β_2 are the model calibration

parameters. In practice, α is often given an assumed value and then the remaining model parameters are used to fit the model to the observed data (Fay and Noorbakhsh, 2010). For β_1 and β_2 , Quinn (1978) suggested values of 2 and 0.5, respectively, based on Manning's equation, while Schmidt (2009) stated that β_1 has also been given a value of 5/3. The exponents can also be fit empirically during model calibration, and this has been the case most recently for the St. Clair and Detroit rivers (Fay and Noorbakhsh, 2010).

The non-linear stage-fall-discharge equation can be linearized by again using a natural logarithm transformation, such that:

$$\ln(Q_c) = \ln(\kappa) + \beta_1 \cdot \ln(w_1 h_1 + w_2 h_2 - \alpha) + \beta_2 \cdot \ln(h_1 - h_2) \quad (58)$$

Given a set of n observations of gauged flows Q_g and measured water levels h_{1g} and h_{2g} , and working from equations (54), (55) and (56), we can define the set of n dependant variables as:

$$\mathbf{Y} = \begin{bmatrix} Y_1 \\ Y_2 \\ \cdot \\ \cdot \\ \cdot \\ Y_n \end{bmatrix} \quad (59)$$

where $Y_n = \ln(Q_g)_n$. Likewise, the predictor variables are defined as:

$$\mathbf{X} = \begin{bmatrix} 1 & X_{1,1} & X_{2,1} \\ 1 & X_{1,2} & X_{2,2} \\ \cdot & \cdot & \cdot \\ \cdot & \cdot & \cdot \\ \cdot & \cdot & \cdot \\ 1 & X_{1,n} & X_{2,n} \end{bmatrix} \quad (60)$$

where $X_{1,n} = \ln(w_1 h_{1g} + w_2 h_{2g} - \alpha)_n$ and $X_{2,n} = \ln(h_{1g} - h_{2g})_n$. Lastly, the model parameters are defined as:

$$\mathbf{b} = \begin{bmatrix} b_0 \\ b_1 \\ b_2 \end{bmatrix} \quad (61)$$

where $b_0 = \ln(\kappa)$, $b_1 = \beta_1$, and $b_2 = \beta_2$. From these, the two-predictor linear model can be solved and the standard error estimates found using the matrix form of the equations given above. The matrix operations were performed for this research using the open-source statistical software package “R” (<http://www.r-project.org/>).

5.4 Uncertainty in Model Predictor Variables

The methods outlined above for estimating uncertainty in discharge determined from a linear model capture uncertainty resulting from random errors as represented by the differences between gauged and modelled discharge measurements. This is termed the model error. Additional error results from uncertainty in the model variables, which includes error in measured water levels, velocities or other predictor variables. Given the case of n predictor variables, which will be assumed to be water levels denoted as h , from the law of propagation of uncertainty (ISO, 1995), the uncertainty in the discharge Q as a function of the uncertainty in each predictor variable is given as:

$$u^2(Q)_h = \sum_{i=1}^n \left(\frac{\partial Q}{\partial h_i} \right)^2 u^2(h_i) + 2 \sum_{i=1}^{n-1} \sum_{j=i+1}^n \left(\frac{\partial Q}{\partial h_i} \right) \left(\frac{\partial Q}{\partial h_j} \right) \cdot u(h_i) \cdot u(h_j) \cdot r(h_i, h_j) \quad (62)$$

where $u(Q)_h$ is the standard uncertainty in the measured discharge Q due to uncertainty in the measured water levels; $u^2(Q)_h$ is the variance of Q ; $\partial Q / \partial h_i$ is the rate of change of Q due to a change in each predictor variable h_i , and is known as the sensitivity coefficient for each h_i ; $u(h_i)$ is the standard uncertainty in predictor variable h_i ; and $r(h_i, h_j)$ is the correlation coefficient of any two

predictor variables h_i and h_j . If errors in the predictor variables are assumed uncorrelated, the equation is reduced to:

$$u^2(Q)_h = \sum_{i=1}^n \left(\frac{\partial Q}{\partial h_i} \right)^2 u^2(h_i) \quad (63)$$

The different flow models used in computing inflows and outflows for the Lake Erie residual NBS require different combinations of predictor variables, and therefore, the uncertainty that results is considered separately for each flow model.

5.5 Combined Uncertainty in Modelled Flows

In determining the overall uncertainty in a single determination of discharge from a rating curve or other flow model, the uncertainties in the gauged discharge measurements, in the model, and in the model predictor variables must all be considered. As described in the previous sections, a number of researchers have defined the overall uncertainty in modelled discharge as either the standard error of the mean relation or the standard error of observations. They have combined this with a term quantifying the uncertainty in flow due to uncertainty in the predictor variables, normally water level, to determine the overall uncertainty in a modelled discharge measurement. The uncertainty in the gauged discharge measurements has normally been ignored, or assumed to be accounted for in the deviations of the gauged measurements from the best-fit model.

A somewhat modified approach for quantifying the overall uncertainty was taken in this research. Assuming that the errors in the gauged discharge measurements, the errors in the model, and the errors in the model predictor variables are uncorrelated, the combined standard uncertainty of any individual discharge measurement taken from a rating curve, $u(Q)$, can be expressed as:

$$u^2(Q) = u^2(Q_g) + u^2(Q_m) + u^2(Q_v) \quad (64)$$

where $u(Q_g)$ is the standard uncertainty in the gauged discharge (assumed to be approximately 2.5%); $u(Q_m)$ is the model uncertainty, taken as the standard error

of observations, $sd(\hat{Y}_0)_{obs}$, or equivalently, the combined standard error of estimate, s , and standard error of the mean relation, $sd(\hat{Y}_0)$; and $u(Q_v)$ is the uncertainty in the measured discharge resulting from uncertainty in the model predictor variables. That is:

$$u^2(Q) = (0.025)^2 + (s^2 + sd(\hat{Y}_0)^2) + u^2(Q_v) \quad (65)$$

Inclusion of the term for gauged discharge uncertainty increases the uncertainty estimate over that suggested by most other studies. This effectively errs on the side of caution, and provides a conservative uncertainty estimate. As will be shown in subsequent sections, if the gauged discharge error term is not included, the overall uncertainty in a single determination of discharge from a rating curve may be underestimated.

5.6 Combined Uncertainty in the Average Discharge in a Period

The preceding section described the uncertainty in a single determination of discharge from a rating curve model. In most water balance studies, including computations of NBS, the average discharge in a period, \bar{Q} , is required. The law of propagation of uncertainty can also be used to determine the combined standard uncertainty of the average discharge in a period. The full equation is given as:

$$u^2(\bar{Q}) = \sum_{i=1}^n \left(\frac{\partial \bar{Q}}{\partial Q_i} \right)^2 u^2(Q_i) + 2 \sum_{i=1}^{n-1} \sum_{j=i+1}^n \left(\frac{\partial \bar{Q}}{\partial Q_i} \right) \left(\frac{\partial \bar{Q}}{\partial Q_j} \right) \cdot u(Q_i) \cdot u(Q_j) \cdot r(Q_i, Q_j) \quad (66)$$

where $u(\bar{Q})$ is the standard uncertainty of the mean discharge for a given period; $u(Q_i)$ is the uncertainty in one of n individual discharge measurements used to compute the mean discharge; $r(Q_i, Q_j)$ is the correlation coefficient for discharge measurements i and j ; and $\partial \bar{Q} / \partial Q_i = 1/n$, since the average of a set of n measurements is being determined, with each measurement given equal weight.

If the error in each individual discharge measurement is assumed random and uncorrelated, $r(Q_i, Q_j)$ is equal to zero, and the equation simplifies to:

$$u^2(\bar{Q}) = \sum_{i=1}^n \left(\frac{1}{n}\right)^2 u^2(Q_i) \quad (67)$$

Furthermore, if $u(Q_i)$ is assumed constant for all Q_i , the equation can be simplified further to:

$$u(\bar{Q}) = \frac{u(Q_i)}{\sqrt{n}} \quad (68)$$

This is the well known equation for the standard error of the mean of a set of observations.

Conversely, if the errors in the discharge values are assumed to be systematic or fully correlated, then $r(Q_i, Q_j)$ is equal to one, and the equation simplifies to:

$$u^2(\bar{Q}) = \left(\frac{1}{n} \sum_{i=1}^n u(Q_i)\right)^2 \quad (69)$$

Again, if $u(Q_i)$ is assumed constant for all Q_i , this equation can be simplified further to:

$$u(\bar{Q}) = u(Q_i) \quad (70)$$

That is, the uncertainty in the mean discharge is equal to the uncertainty in any single discharge estimate.

It is exceedingly difficult to determine whether the sources of error that cause each of the various sources of uncertainty in the modelled discharge are correlated, and if so, to what degree. This is especially true since the true discharge can never be determined. Not knowing whether the errors are correlated or not makes evaluating the combined uncertainty in the average

discharge in a period difficult as well. The result is that the combined uncertainty could be either over or underestimated, depending on how well the assumptions made reflect reality.

In this study, it was assumed that the errors in the gauged discharge measurements were fully correlated. This implies that the errors in ADCP discharge measurements are systematic, and therefore they cannot be reduced by averaging repeated samples. Since normally a large number of measurements are used to define the rating curve, if the errors in gauged discharge were assumed random and entirely uncorrelated, they would effectively cancel out. However, often the same instruments, crews and methods have been used to collect the data. Gauged discharge measurements evaluated in this study were primarily conducted using ADCPs. Simpson (2001) noted a number of sources of both random and systematic errors in ADCP measurements. Espey et al. (2001) has suggested that errors in ADCP discharge measurements are more likely to be systematic than conventional measurements. Unlike conventional current meter measurements, ADCP measurements are often conducted with the same instruments due to their higher costs, so any systematic error, such as that caused by the instrument calibration, for example, will affect each measurement in a similar manner. As another example, due to signal interference caused by channel boundaries (i.e. the bed surface and channel banks) or the instrument itself, ADCPs are unable to measure the velocity and flow near these boundaries or just below the receiver (Simpson, 2001). Instead the velocities in these portions of the cross-section are estimated based on a mathematical relationship. Any error caused by these relationships will affect each ADCP measurement in a similar manner, and these errors will not be reduced by averaging. Also, as will be shown in the Niagara River MOM pool flow evaluation, conditions in the river and limitations of the instrumentation were found to have caused a systematic error in the conventional measurements collected prior to 2001 that was not detected until more recent ADCP measurements became available. It is likely that some of the error in gauged discharge measurements is random, and given enough measurements, these random errors will effectively cancel out; however, determining what portion of the error is random and what portion is not was found to be difficult and beyond the scope of this study. For these reasons, the safer assumption was made, and errors in gauged discharge measurements were assumed to be fully correlated, and therefore not reduced by averaging, in order to provide a conservative uncertainty estimate.

Determining whether the uncertainty terms accounting for model error are correlated is also difficult to determine. The standard error of the mean relation and the standard error of estimates were each considered separately. Since each measurement is obtained from the same flow model, the uncertainty in the model relationship, namely the standard error of the mean relation, was assumed fully correlated, since averaging a series of measurements will not reduce the error that results from differences between the estimated mean relation and the true mean.

On the other hand, it is assumed that natural variability in the channel flow is captured in the gauged discharge measurements used to construct the rating equations, and that this natural variability is represented by the spread of the measurements around the best fit flow model (i.e. the standard error of estimate). This natural variability could be assumed random and the errors that result could be assumed uncorrelated. Likewise, the uncertainty in the model predictor variables, namely the measured water level and/or velocity, could also be assumed to be random in nature. Assuming these errors to be uncorrelated, they would be reduced by averaging consecutive measurements to obtain the mean discharge in a period. This may be true or partly true in some cases; however, it is also possible that the same conditions causing the errors observed are persistent, causing the errors to be correlated to a certain degree. For example, it is possible that part of the spread of the observed measurements is caused by hysteresis effects resulting from variable slope during periods of rising and falling discharge; or perhaps a persistent wind causes super-elevation of the water surface and a systematic error for a long enough period of time that the errors should not be assumed random in nature. The conservative approach would be to assume that, as with the gauged discharge measurement errors, the model errors in repeated measurements are fully correlated; however, this likely overestimates the combined uncertainty since the random variability would in reality average out.

In light of the difficulties in determining whether errors should be assumed correlated or not, the analysis of uncertainty in inflows and outflows that follows deals with this aspect on a case-by-case basis.

5.7 Additional Sources of Uncertainty and Systematic Errors

Using a model to determine discharge requires the assumption that the flow model used, which is derived from gauged discharge measurements

collected previously, continues to represent the existing conditions in the river. Additional systematic errors, such as those caused by changing channel conditions possibly arising from erosion, deposition, aquatic vegetation/weed growth, ice or other obstructions, for example, can cause the model to not accurately represent the actual channel conditions existing at the time of the flow measurement. This can result in errors which are often much larger than the errors determined using the methods described above, and these must be dealt with separately.

6 Sources and Estimates of Uncertainty in Niagara River Flow

6.1 Niagara River Flow Overview

As discussed, the current accounting of Lake Erie outflow through the Niagara River is quite complicated. The summation equation includes the MOM pool flow, the flow through the hydropower plants, the flow through the NYSBC, local runoff to the upper Niagara River, and the Welland River diversion from the Welland Canal. Determining the total uncertainty in the Lake Erie outflow through the Niagara River requires assessing the uncertainty in each of these different subcomponents, and since these are each measured or estimated using different methods, the uncertainty analysis requires a variety of techniques. The total combined uncertainty in the Niagara River flows can then be determined by combining the uncertainty from each of the different subcomponents. An alternative method for determining Niagara River flows involves measuring discharge at the actual outlet of Lake Erie using a stage-discharge relationship. This method is discussed, as well as its limitations, at the end of this section.

6.2 Niagara Maid-of-the-Mist (MOM) Pool Flow

The flow through the Niagara River MOM pool (N_{MOM}) is currently modelled using a stage-discharge rating equation based on measured water levels at the Ashland Avenue water level gauge located in Niagara Falls, NY, just downstream of Niagara Falls at the MOM pool. Near-instantaneous hourly water level readings are used to determine 24 hourly discharge estimates each day, which are averaged to determine the daily mean discharge. The daily mean discharges are then averaged to determine the mean monthly discharge.

The International Niagara Board of Control (INBC) is responsible for developing and maintaining the Ashland Avenue stage-discharge relationship. The Ashland Avenue gauge was established in 1957. Prior to this, the stage-discharge equation was based on water levels measured at the discontinued Morrison Street gauge, located on the Canadian side of the MOM pool. The

Ashland Avenue gauge station has been used to establish the stage-discharge rating for determining flow through the MOM pool since this time. The first rating was the 1964 Ashland Avenue equation, and since then there have been two revisions of this equation, one in 1981, and the most recent in 2009 (INBC, 2009). The current Ashland Avenue equation is given by:

$$N_{MOM} = 0.6429 \cdot (h_{AA} - 82.814)^{3.0} \quad (71)$$

where h_{AA} is the water level measured at Ashland Avenue. This equation was developed using concurrent gauged Ashland Avenue water levels and a total of 281 ADCP discharge measurements collected from 2001 to 2007 by the INBC at what is known as the cableway section located downstream of the MOM pool, just upstream of the hydropower plants.

The model uncertainty in the Niagara MOM pool flows determined from the Ashland Avenue equation was estimated using the statistical methods outlined in Section 5. The standard error of estimate, standard error of the mean relation, and standard error of observations were all computed. Using the 281 ADCP discharge measurements, the standard error of estimate was found to be 2.1%. A range of realistic Ashland Avenue water levels from 95 to 104 metres was used to compute a range of standard errors of the mean and standard errors of the observations. The standard errors of the mean relation for the Niagara River MOM flows were extremely low, ranging from only 0.1 to 0.4% for the range of water levels investigated. This is in part the result of the large number of measurements used to define the rating curve. The standard errors of the observations are larger than the standard errors of the mean, and are all fairly similar, ranging from 2.1 to 2.2% for the range of Ashland Avenue water levels examined. These values are very similar to the standard error of estimate as well, as would be expected due to the small standard errors of the mean computed.

Despite the fact that the hydropower companies divert a large amount of water for power production purposes, with exact volumes varying throughout the year and throughout the day during the tourist season, the water levels and flows in the Niagara River do not show significant variation due to the regulating effects of Lake Erie. That is, water levels of Lake Erie have a relatively narrow range due to the lake's large surface area. Lake Erie water levels can show greater variation during storm-setup, but in general the flow conditions in the Niagara River are relatively steady. Furthermore, gauged flow measurements have been

collected at a range covering much of the range of water levels and flows that may reasonably be expected at the Niagara River below Niagara Falls. This is in contrast to rating equations developed for many inland rivers and streams, where during large floods flow measurements are rarely collected, and flow estimates must be determined by extrapolating the rating curve well beyond the range of actual gauged flow measurements used to calibrate the relationship, or using alternative flow estimation methods.

A plot of the Ashland Avenue rating curve, the ADCP measurements, and the 95% confidence level as obtained from the standard error of the observations is shown below in Figure 6-1. To simplify the uncertainty analysis, a constant value of 0.5% was used for the standard error of the mean relation, along with the 2.1% standard error of estimate, such that the combined standard error of observation was approximately 2.2%. This represents the total model uncertainty, or the uncertainty in an instantaneous discharge estimate due to errors in the model used.

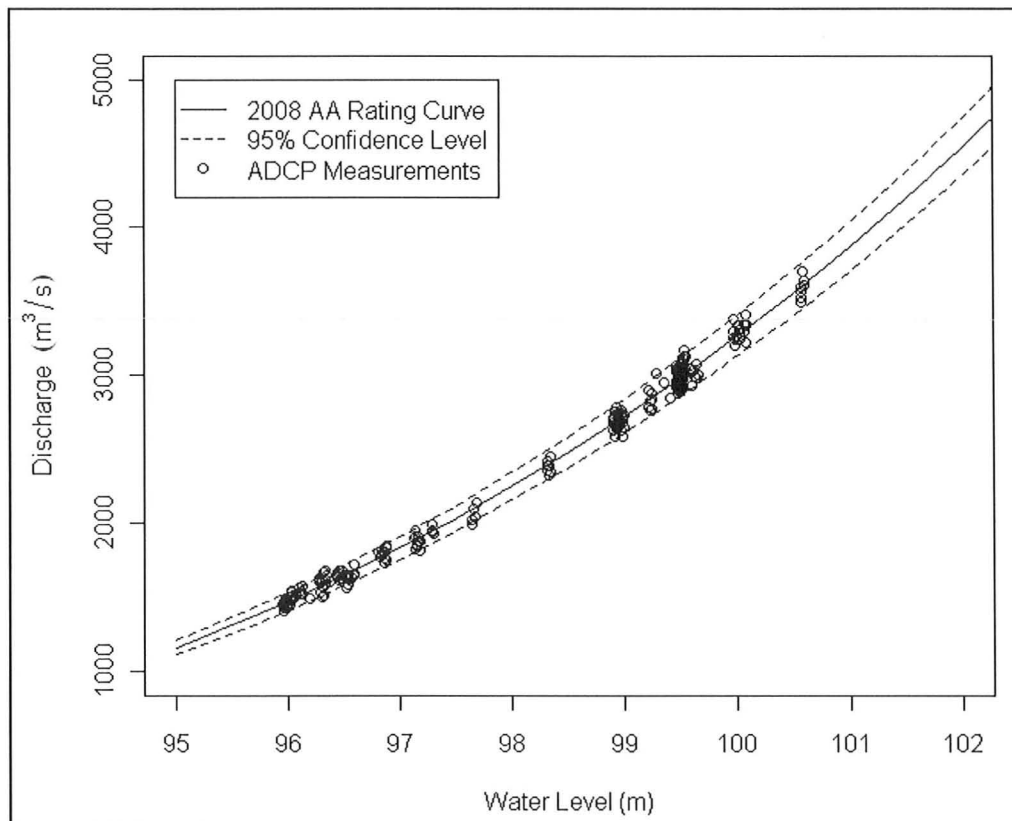


Figure 6-1: Ashland Ave. rating compared to ADCP measurements

The Ashland Avenue rating is rarely affected by ice and weeds due to the steep slope and strong current in this stretch of the Niagara River. Furthermore, the channel bed at this location is rock and is believed to be stable, such that changes to the channel cross-section are unlikely to occur. Therefore, additional error caused by these sources was assumed to be negligible.

The Niagara River does, however, provide a good example of the systematic errors that can exist in gauged flow measurements. Prior to 2001, when ADCP measurements began to be collected, the cableway section was used to measure discharge out of the MOM pool using conventional current meters and the velocity-area method. Upon comparing the conventional and ADCP discharge measurements, the INBC (2009) found that the ADCP-measured flows were consistently higher than the previous Ashland Avenue rating equation and the conventional flow measurements collected between 1973 and 2001. This discrepancy was investigated using detailed soundings of the cableway cross-section and it was concluded that changes in the channel itself had not occurred, but rather increased resolution of the ADCP measurements had caused them to have a cross-sectional area approximately 4% greater in size than that measured during the lower resolution conventional measurements, which subsequently resulted in the greater flows computed from the ADCP. The current Ashland Avenue rating equation was therefore calibrated using only the most recently collected ADCP measurements, since these were believed to be more accurate than the older conventional measurements.

In this research, the conventional measurements were compared to the new rating (Figure 6-2), and the standard error was found to be approximately 4.6%. Therefore, for discharge taken from the old rating there would have been an unknown systematic error of approximately 4.6%. This would be in addition to the uncertainty in the rating curve described by the spread of measurements around the curve (i.e. the model error). A similar unaccounted for or unknown bias could exist for any flow model. This analysis shows the importance of including the uncertainty in the gauged discharge measurements in addition to the model and predictor variable uncertainty. If uncertainty in the gauged discharge measurements was not included in the previous Ashland Avenue rating equation, the uncertainty in the MOM pool flow would be underestimated. This also provides an additional example of systematic errors in gauged discharge measurements, giving further evidence of the need to treat these errors as fully correlated.

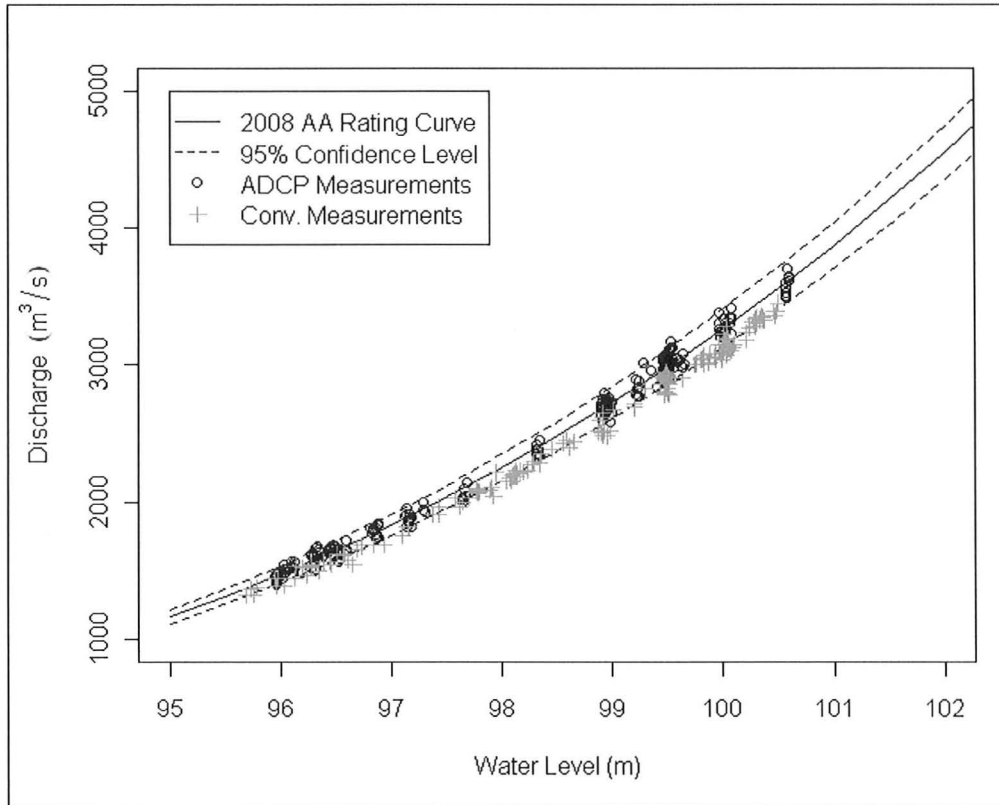


Figure 6-2: Ashland Ave. rating compared to conventional flow measurements (pre-2001) and ADCP measurements (post-2001)

In addition to uncertainty in the gauged discharge measurements and model uncertainty, the uncertainty in discharge resulting from uncertainty in the model variables must also be considered. In the case of a stage-discharge equation, the only predictor variable is the measured water level. Uncertainty in water levels actually affects the modelled discharge in two ways: first, the gauged discharge measurements used to calibrate the model require corresponding water level measurements; second, measured water levels are used as an input variable in the model itself. The uncertainty resulting from the first source was assumed to be small, and is likely captured in the analysis of model uncertainty.

In regards to the second source, the MOM pool flow equation is evaluated using instantaneous hourly water levels measured at Ashland Avenue by the hydropower companies, and the uncertainty in an instantaneous measured water level is small, being 3 mm according to NOAA (2009). Other unaccounted for sources of error in the water level measurements may cause the uncertainty to be

somewhat greater. Nonetheless, given the large depths and the range of water levels observed, this source of uncertainty has a relatively small effect on the Niagara River flows. For example, taking the derivative of equation (71), the sensitivity coefficient, or the change in flow with respect to a change in water level, is:

$$\frac{\partial N_{MOM}}{\partial h_{AA}} = 1.9287 \cdot (h_{AA} - 82.814)^{2.0} \quad (72)$$

Applying the law of propagation of uncertainty, the uncertainty in discharge due to uncertainty in the Ashland Avenue water level can be found from:

$$u^2(N_{MOM})_h = \sum_{i=1}^n \left(\frac{\partial N_{MOM}}{\partial h_{AA}} \right)^2 u^2(h_{AA}) \quad (73)$$

Assuming a relatively high Ashland Avenue water level of 101 metres to evaluate equation (72), the change in discharge with respect to a change in water level is approximately 640 m³/s per metre. Assuming a conservative estimate of 1 cm for the uncertainty in the measured water level, this corresponds to an error in discharge of less than 7 m³/s, a negligible amount. Furthermore, assuming that errors in the measured water levels are random and uncorrelated, by averaging the instantaneous discharge measurements these errors will effectively cancel out over the course of a month.

On the other hand, since the hourly water levels are actually instantaneous water levels taken at the top of each hour, they do not necessarily represent the true continuous water level or the true average hourly water level. As a result, the instantaneous modelled flows will not necessarily represent the continuous and true average flow, and this will result in additional uncertainty in the mean daily and monthly flow estimates. To evaluate the magnitude of this source of uncertainty, 6-minute water level data (the highest resolution data available at Ashland Avenue) for the months of January through July 2010 were used to compute 6-minute flow estimates, and the average of these were compared to average flows computed using hourly data. For the non-tourist season months of January through March, a comparison of the 6-minute and hourly results showed absolute differences of less than 20 m³/s for all daily means, and these errors

cancelled out over the course of a month such that the monthly means were found to be no greater than $1 \text{ m}^3/\text{s}$ different.

The same comparison was performed for the tourist season months. Figure 6-3 shows an example comparison of the 6-minute and hourly flows for one day during the tourist season. Similar to the non-tourist season, for the tourist season months of April through July, the absolute differences were small, being less than a maximum of $23 \text{ m}^3/\text{s}$ for the daily means. However, the flows determined from the hourly data appeared to be biased, almost always being slightly higher on average than the flows determined from the 6-minute data for both the daily and monthly means. The monthly means determined from the hourly data for the tourist season months were 3 to $4 \text{ m}^3/\text{s}$ greater than the means determined from the 6-minute data. The cause of this small bias is not entirely clear, but appears to be related to a combination of the rise and fall of the flows during the transition to and from tourist hours, the non-linearity of the 6-minute flow estimates between the top of each hour (see Figure 6-3), and the starting and ending elevation of each day. The discrepancy between 6-minute and hourly data should be investigated further, but the uncertainty caused by using instantaneous hourly water level readings as opposed to higher resolution data was considered negligible given this analysis.

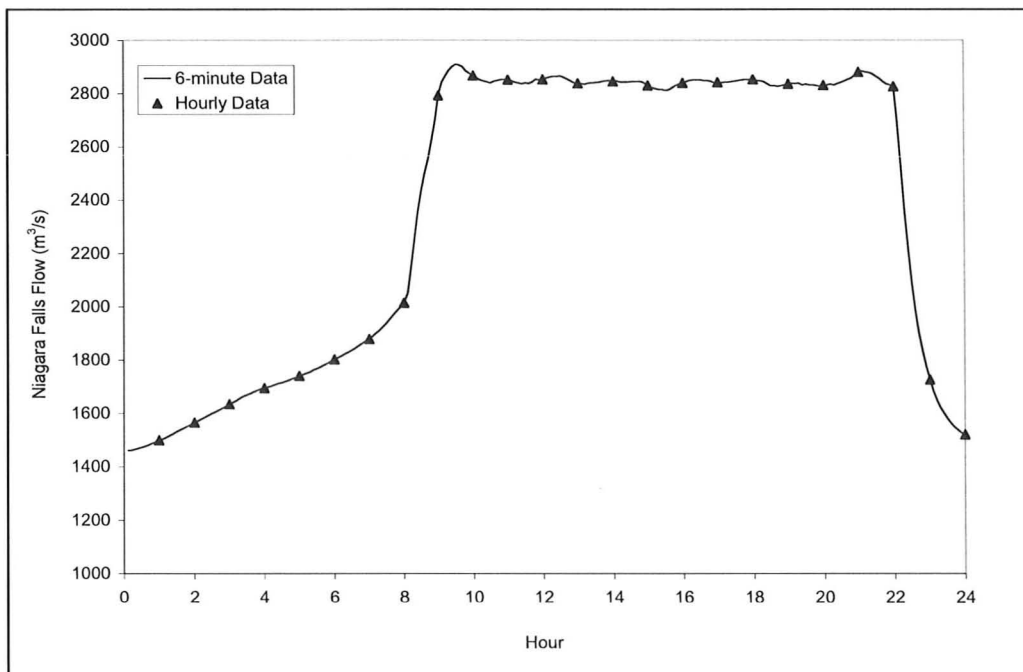


Figure 6-3: Six-minute vs. hourly Ashland Ave. water level data (1 April, 2010)

The combined uncertainty in the monthly MOM pool flow can be estimated using the methods outlined in Section 5.6. Equation (65) can be applied to determine the uncertainty in a single determination of the MOM pool flow, but to determine the combined uncertainty in the monthly flow estimates, assumptions about whether the errors are correlated or not must also be made. As stated, the errors in the gauged discharge measurements were assumed to be fully correlated. Furthermore, the uncertainty in the fitted relation, i.e. $sd(\hat{Y}_0)$, is assumed fully correlated since the same rating is used for each hourly measurement. Assuming the errors in the remaining components of equation (65) (i.e. the standard error of estimate and the uncertainty caused by the measured water levels used as the model predictor variables) are fully correlated as well gives the maximum standard uncertainty estimate of 3.4%. That is:

$$u(N_{MOM}) = (0.025^2 + 0.021^2 + 0.005^2 + 0.005^2)^{0.5} = 3.4\%$$

Alternatively, if the errors in the remaining components are assumed uncorrelated, the minimum uncertainty estimate can be obtained. Since 24 hourly flow measurements are obtained from the model each day and then averaged for the entire month (approximately 30 days), the minimum uncertainty estimate is 2.6%. That is:

$$u(N_{MOM}) = \sqrt{0.025^2 + \left(\frac{0.021}{\sqrt{24 \cdot 30}}\right)^2 + 0.005^2 + \left(\frac{0.005}{\sqrt{24 \cdot 30}}\right)^2} = 2.6\%$$

Essentially the random uncertainty in the model and in the predictor variables cancels out due to the large number of measurements that are averaged, and the overall uncertainty results primarily from the uncertainty from the ADCP measurements used to calibrate the equation. It seems unlikely that there would not be at least some residual random error in the monthly flow estimates. Also, given that the flows over Niagara Falls are managed by the hydropower companies, the assumption that the errors are entirely random and uncorrelated seems unreasonable.

A review of the ADCP discharge measurements used in the Ashland Avenue rating curve calibration further supported the assumption that at least a portion of the model error was correlated and not reduced by averaging. For

example, a total of 93 ADCP measurements were collected on four consecutive days from 30 October to 2 November, 2004. Assuming a standard error of estimate of 2.1%, if the model errors were uncorrelated, the overall error in these measurements would be reduced to $2.1/\sqrt{93} = 0.2\%$. A comparison of the rating flows and the ADCP gauged discharge measurements showed the average difference between the two estimates to be approximately 1%. That is, the uncertainty estimate of 2.1% was reduced by averaging, but not entirely, and not as much as would be expected if the errors were assumed entirely uncorrelated. A similar analysis performed on 43 measurements collected on 8-9 May, 2007, showed similar results, with the average difference being $-9 \text{ m}^3/\text{s}$, or approximately 0.35% of the average flow on the two days. A similar error value of approximately 1.5% or less was observed for a number of other consecutive days of measurements where ADCP and rating curve discharge estimates were compared. If an estimate of 1.5% is used and assumed fully correlated, the combined uncertainty would be approximately 3%. That is:

$$u(N_{MOM}) = \sqrt{0.025^2 + 0.015^2 + 0.005^2} = 3\%$$

This estimate seems reasonable, but is again dominated by the uncertainty in the ADCP discharge measurements. Given the difficulty in determining whether errors are correlated or not, and given that additional unaccounted for sources of error may exist (for example, these results are based on the gauged discharge measurements used to calibrate the flow model, whereas additional measurements may show slightly different results), the maximum standard uncertainty estimate of 3.4% was used in this analysis in order to provide a conservative estimate; however, it should be noted that this is likely somewhat over-estimated, and this analysis shows that the actual uncertainty could be much lower.

6.3 *Hydropower Diversions*

The discharge through the OPG and NYPA hydropower plants on the Niagara River is determined from rating tables, which relate turbine unit discharge to the combination of power output measured for each unit and the gross head difference between the penstock intake and the tailrace (Mikhail, 2006). The rating tables themselves are derived from field test results. Relatively

recent field testing for the Niagara hydropower plants was conducted during unit upgrades, and involved determining discharge through selected turbine units using the Gibson test method. The Gibson test method (also known as the pressure-time method) of estimating flow in a closed conduit is rather involved, but essentially entails application of the energy balance equation to two sections of a closed conduit (the penstock), and accounting for the static pressure difference that arises between the two sections as a result of a change of momentum induced when the flow through the penstock is stopped suddenly (Adamkowski et al., 2006). The full Gibson test was performed on about one in every four of the turbine units on the Niagara River, with less extensive Index testing using what is known as the Winter-Kennedy flow relationship performed on the remaining units to ensure a similar performance as those tested with the absolute Gibson test method (Mikhail and Knowlton, 2006).

The accuracy of the hydropower flow measurements has been estimated by a number of sources. According to test reports for the Niagara hydropower plants (e.g. Mikhail, 2007; Mikhail and Knowlton, undated), while the accuracy of each Gibson test varies, the expected accuracy of the flows measured using the Gibson test is quoted as 2.25%. This agrees with estimates given in international standards, where the accuracy of the Gibson test is reported as being within the range of 1.5 to 2.3% (IEC, 1991, as reported by Adamkowski et al., 2006). Uncertainty estimates in the Index test reports for the Niagara River (e.g. Mikhail, 2007) give the total uncertainty as around 2% at a 95% confidence level, though it is unclear whether this refers to the turbine flows or the combined test results. Regardless, these results agree with Adamkowski et al. (2006), who state that the accuracy of flows determined using the Winter-Kennedy method is close to the accuracy of the flows determined using the absolute Gibson method.

It seems that other researchers have accepted these estimates of uncertainty in the measured flow as the total uncertainty estimate for the hydropower diversion. For example, Neff and Nicholas (2005), in close agreement with the estimates given above, gave an uncertainty estimate for the Niagara hydropower flows of 2.33%, which according to the authors was based on a written communication with OPG. Likewise, Metcalfe (2002) gave the “overall uncertainty” as +/- 2.1% at the 95% confidence level for the Niagara hydropower flows. Additional information on how these flow uncertainty estimates were obtained and the probability distribution of the error estimates

could not be obtained from the hydropower companies, and was not found in the literature or test reports.

While these estimates are all fairly consistent, they are likely based in part on the same assumptions and estimation methods. The fact that they are in such good agreement with the Gibson test uncertainty estimates indicates that other sources of uncertainty (i.e. in addition to uncertainty in the measured flows from the Gibson test) may not be properly accounted for. For example, the discharge through the hydropower turbines is determined from rating tables that relate the measured flows as determined from the Gibson tests to the power output and gross head. Uncertainty in the measured power output and gross head, as well as uncertainty in the relationship between these variables and the rated discharge, must also be accounted for in the uncertainty estimate of the Niagara hydropower diversions. Furthermore, the actual discharge diverted from the Niagara River is calculated on an hourly basis not from the flow through the hydropower plants alone, but rather it also includes the change in storage in the forebays and storage reservoirs upstream. Over the course of a month or longer, the effects of storage on the mean monthly power diversion are small, but this would also provide a source of uncertainty. Losses due to evaporation and leakage provide another source of uncertainty, though again, the amount may be negligible.

According to OPG (K.C. Chan, OPG, written communication, 24 August, 2010), the combined uncertainty of the rating table flows for the SAB II units would consist of three components, including: uncertainty resulting from performance testing on units tested by the absolute method (Gibson test); uncertainty due to variation of the other units tested for similarity by the Index method; and extrapolation of the results to other heads from the test head. Similar to the estimates given above, the uncertainty in the first two sources, the Gibson and Index tests, were suggested as $\pm 2.0\%$ and $\pm 1.8\%$, respectively. For the third source of uncertainty, there apparently is no estimate available, but it is judged by Mr. Chan to be 0.5% for a medium head plant such as the SAB units. From this, it was estimated that the combined uncertainty level for the derived rating table would be $\pm 2.7\%$; however, this estimate is based on the assumption that all errors are uncorrelated, which seems unlikely given, for example, that only one quarter of the turbine units were tested and that test results are extrapolated from the test head to other heads. Mr. Chan also suggested that other sources of uncertainty in the flow accounting include the accuracy of the station head measurements, the variation of head with time and the flow accounting

software package used. Furthermore, these results are for SAB II, and uncertainty may be somewhat different for the other hydropower plants.

A more detailed investigation of uncertainty in the hydropower flows was deemed to be beyond the scope of this research. Based on the above findings, and assuming full correlation of the uncertainty estimates provided by OPG for the Gibson test, Index test, and extrapolation of results, an uncertainty estimate of approximately 4.0%, having a normal distribution, was assumed at the 95% confidence level for the combined Niagara River hydropower diversion. It is recognized, however, that this may be underestimated, and a more exhaustive uncertainty analysis of the hydropower diversions from the Niagara River may be worthwhile.

6.4 New York State Barge Canal (NYSBC) Diversion

The amount of water diverted to the NYSBC from both Lake Erie prior to 1918 and from the Niagara River since then is not well known. The actual diversion from the Niagara River has been gauged periodically in the past, but has not been measured continuously, and is instead estimated for water balance purposes as a constant value. The estimated amount currently used varies depending on whether the NYSBC is open for navigation or closed during the non-navigation season. When the NYSBC is open, it is assumed that the mean daily flow is $31 \text{ m}^3/\text{s}$; when closed, the flow is assumed to be zero. Since the NYSBC flows are reported monthly, the monthly flows during maintenance periods and during the transition period to and from the navigation season are estimated as the mean discharge times the ratio of days with the canal in operation to the number of days with zero flow in the canal (Len Falkiner, EC, personal communication, 10 August, 2010). For example, if in April during the transition to navigation season conditions the NYSBC is in operation for only 20 days, the mean monthly flow would be $21 \text{ m}^3/\text{s}$ (i.e. 20 days in operation divided by 30 days in April, multiplied by $31 \text{ m}^3/\text{s}$).

Though little documentation is available (and at times the reports are conflicting) according to the Special International Niagara Board (SINB, 1930) and the IJC (1953), the flow estimate when the NYSBC is open appears to have been at least originally based on measurements conducted in the 1920s. Measurements were also made in the 1950s (INWC, 1985; IJC, 1985), possibly in

order to confirm or adjust the earlier estimates. The SINB (1930) gives one of the more detailed reports on the NYSBC diversion. In this report, the results of measurements collected during the summer months from 1923 to 1926 and in the winter of 1927 were given. These are shown here in Tables 6-1 and 6-2, respectively, with the mean and standard deviations also computed. The SINB (1930) noted that during the navigation season, levels at Lockport were carefully maintained, with flow likely the same at night as during the day; however, during winter, when levels were not as carefully maintained, the flow at night was about $40 \text{ ft}^3/\text{s}$ ($1 \text{ m}^3/\text{s}$) less than during the day, and the discharge all day on Sunday was about $275 \text{ ft}^3/\text{s}$ ($8 \text{ m}^3/\text{s}$) less than the weekday day-time flows. From this information and the measurements collected, the average NYSBC diversion from the Niagara River at the time was estimated to be $1,400 \text{ ft}^3/\text{s}$ ($40 \text{ m}^3/\text{s}$) during the navigation season and $1,000 \text{ ft}^3/\text{s}$ ($28 \text{ m}^3/\text{s}$) during winter, with an average of $1,200 \text{ ft}^3/\text{s}$ ($34 \text{ m}^3/\text{s}$) for the year.

Table 6-1: Measured NYSBC flows: 1923-1926 navigation season (SINB, 1930)

Date	Flow (ft^3/s)	Flow (m^3/s)
6/5/1923	1318.7	37.3
8/9/1923	1392.3	39.4
8/13/1923	1341.7	38.0
7/24/1924	1405.4	39.8
10/20/1924	1381.8	39.1
9/11/1925	1458.5	41.3
9/11/1925	1408.6	39.9
9/14/1925	1341.6	38.0
9/14/1925	1330.6	37.7
9/24/1925	1461.6	41.4
9/24/1925	1465.7	41.5
8/31/1926	1463.4	41.4
8/31/1926	1469.0	41.6
Mean	1403.0	39.7
Std. Dev.	57.0	1.6

Table 6-2: Measured NYSBC flows: 1927 non-navigation season (SINB, 1930)

Date	Flow (ft ³ /s)	Flow (m ³ /s)
2/24/1927	1025	29.0
2/24/1927	1049	29.7
3/10/1927	1080	30.6
3/10/1927	1085	30.7
Mean	1060	30.0
Std. Dev.	28	0.8

A report by the IJC (1953) noted that until October 1928, approximately 275 ft³/s (8 m³/s) of the total diversion was diverted for power purposes. This was discontinued after this year, such that the total diversion during the navigation season would have been 275 ft³/s (8 m³/s) less than the 1400 ft³/s (40 m³/s) measured in the 1920s, or approximately 1125 ft³/s (32 m³/s). When rounded to the nearest 100 ft³/s, this is equivalent to the constant amount of 31 m³/s currently used.

Occasional field measurements have been collected since this time, including some in the 1950s, with some reports stating that these were used to provide the current estimated amount of the diversion (INWC, 1985; IJC, 1985). For example, according to the International Niagara Working Committee (INWC, 1985), just prior to field tests conducted in 1957, flow measurements made by current metering estimated the NYSBC flow reaching Lockport to be 1120 ft³/s (32 m³/s). The 1957 field tests after this were conducted to determine the possibility of passing additional flow through the NYSBC for the purposes of agriculture. Actual data for these tests was not found, but it was noted by Stellato (1981) and the INWC (1985) that these tests showed that increases in the discharge of greater than approximately 100 ft³/s (3 m³/s) resulted in increased levels of seepage and leakage, and as such, no further work has been conducted in this regard (INWC, 1985).

Regardless of the actual source, the NYSBC diversion reported by the INBC is today based on these past studies and estimates, and is given as 31 m³/s during the navigation season and zero during the non-navigation season. The uncertainty in the NYSBC flows was determined from the above information. The 1923-1927 measurements and additional findings reported by the SINB (1930) are assumed to be the best available. Using the measurements from Table 6-1, and removing the additional 275 ft³/s (8 m³/s) diverted for power

production prior to 1928, the mean measured discharge was found to be $31.9 \text{ m}^3/\text{s}$ with standard deviation of approximately $1.6 \text{ m}^3/\text{s}$. The mean is slightly greater than the $31 \text{ m}^3/\text{s}$ currently used in NYSBC flow accounting. Also, since only 13 measurements were collected, multiplying the standard deviation by a Student's *t*-value of 2.18 for 12 degrees of freedom gives the error as $3.5 \text{ m}^3/\text{s}$ (or approximately 10%) at the 95% confidence level. This compares well with results reported by Stellato (1981) as discussed above, which explained that field measurements had showed that increases in NYSBC discharge of greater than $3 \text{ m}^3/\text{s}$ could not be accommodated without increased seepage and leakage. It is assumed that conditions in the NYSBC have not changed significantly since these measurements were first collected. Therefore, given the difference in the mean and the standard deviation computed above, and the fact that discharge likely varies to a small degree due to the Niagara River water level, for this study the NYSBC discharge was assumed to be $31 \text{ m}^3/\text{s}$, with an uncertainty estimate of $\pm 15\%$ at the 95% confidence level during the navigation season. During the non-navigation season, with the canal dewatered, it is assumed that the amount of zero used for reporting purposes is correct, with any leakage assumed negligible.

6.5 Upper Niagara River Local Runoff

The local runoff, or local inflow, to the upper Niagara River between Niagara Falls and Buffalo (R_N) is not measured directly. Instead, 12 constant monthly values are traditionally used. These monthly values were determined from an analysis of measured flows from the Grand River, ON, and Genesee River, NY, based on the period of record from August 1913 through December 1960 (Coordinating Committee, 1962). In the original analysis, drainage area ratios were used to extrapolate the Grand and Genesee River flows to the local upper Niagara River basin. That is, the monthly mean discharge per unit area for the combined Grand and Genesee rivers were multiplied by the local drainage area of the upper Niagara River and then averaged by month to estimate the mean monthly local inflows. The mean monthly values currently used as determined from the original analysis are given in Table 6-3.

Table 6-3: Niagara River local runoff values (Coordinating Committee, 1976)

Month	Jan	Feb	Mar	Apr	May	Jun	Jul	Aug	Sep	Oct	Nov	Dec
Flow (m^3/s)	37	37	91	93	45	23	14	8	8	14	25	31

There are three major sources of uncertainty in these estimates of local runoff to the upper Niagara River. The first is the uncertainty in the measured flows from the Grand and Genesee rivers. De Marchi et al. (2009) discussed uncertainty in runoff estimates to the Great Lakes. The second source of uncertainty results from the use of Grand and Genesee River flows as surrogates for Niagara River tributary inflows. The Grand and Genesee rivers flow into Lake Erie and Lake Ontario, respectively. They are the two major inland rivers located closest to the Niagara River, but how well these two rivers represent the actual conditions and flows in the upper Niagara River basin is not known. The last source of uncertainty results from the use of a constant mean flow value based on a short historic record to represent a time-varying quantity. Local runoff varies seasonally and annually, so the deviation of flows about their mean will provide a source of error given that constant mean values are used.

To quantify the uncertainty in the local inflow to the upper Niagara River for this study, revised local inflow estimates were derived using a similar area ratio method as used by the Coordinating Committee (1962), but based on measured discharges from actual tributaries to the upper Niagara River basin. Currently approximately 1434 km² of the upper Niagara River drainage basin is gauged, which corresponds to approximately 44% of the 3250 km² total drainage area of the basin as estimated by the Coordinating Committee (1962). This includes gauges operated by Water Survey of Canada (WSC) at the Welland River at Caistor Corners, ON (238 km²), and Oswego Creek at Canboro, ON (80.7 km²), in addition to gauges operated by the United States Geological Survey (USGS) at the Tonawanda Creek at Rapids, NY (904 km²) and Ellicott Creek below Williamsville, NY (211 km²). The Ellicott Creek gauge was originally located at Williamsville (Ellicott Creek at Williamsville, NY); this gauge was relocated downstream in 1972, which increased the measured drainage area. An additional gauge station, Tonawanda Creek at Batavia, NY (443 km²), is located upstream of the Tonawanda Creek at Rapids gauge station. A summary of these gauge stations and their periods of record is given in Table 6-4.

Table 6-4: Upper Niagara River tributary gauge information

Agency	Station Number	Station Name	Drainage Area (km ²)	Start Year	End Year
EC	02HA007	Welland River below Caistor Corners	238	1957	2008
EC	02HA024	Oswego Creek at Canboro	80.7	1988	2008
USGS	04217000	Tonawanda Creek at Batavia NY	443	1944	2009
USGS	04218000	Tonawanda Creek at Rapids NY	904	1955	2009
USGS	04218500	Ellicott Creek at Williamsville NY	197	1955	1972
USGS	04218518	Ellicott Creek below Williamsville NY	211	1972	2009

When the Coordinating Committee (1962) conducted its local inflow analysis some of these stations did not exist, while others had too short a period of record to be used for such an analysis. As such, the Grand and Genesee rivers, each with long established periods of record, were used instead of the actual local tributaries. The Coordinating Committee (1962) did, however, compare the mean local flows derived for the upper Niagara River from the Grand and Genesee River data to flows determined from the existing tributary gauges for the 1955-1960 period and found that the use of the local inflows determined from the Grand and Genesee records would generally underestimate actual tributary flow from December through March, and overestimate it from April through November. Since there are longer periods of record available today for the local tributaries, it is possible to obtain better estimates of local runoff from these.

Similar to what was done for the Grand and Genesee rivers, the monthly mean measured flows were obtained for the local tributary gauges and multiplied by area ratios to estimate the mean and standard deviations for the Niagara River local inflows. The general equation can be written as

$$R_N = \sum R_{Gauged} \cdot \frac{A_{Total}}{\sum A_{Gauged}} \quad (74)$$

where R_N is the estimated local runoff to the upper Niagara River; R_{Gauged} is the sum of measured runoff from the gauged portion of the basin; A_{Total} is the total upper Niagara River drainage basin area; and A_{Gauged} is the sum of the areas of the gauged portion of the basin. The period of record used started in July 1957, which corresponds to the installation of the Welland River gauge, and ended in December 2008. The combination of gauges used was chosen to maximize the gauged portion of the basin without overlap. For example, if data at Tonawanda Creek at Rapids, NY, were available, then Tonawanda Creek at Batavia, NY, was not used, as it is located upstream; however, Tonawanda Creek at Batavia, NY, was used when the downstream gauge data were unavailable, with the areas adjusted accordingly.

A comparison of the results is given below. Table 6-5 shows that the currently used values based on the Coordinating Committee (1962) analysis underestimate the local tributary flows for the months of August to March by an average of -2 to -29 m³/s, with the largest discrepancies occurring in the winter months. On the other hand, the Coordinating Committee (1962) values overestimate the flows by an average of 3 to 9 m³/s for the remaining months. This agrees fairly well with the Coordinating Committee (1962) findings.

Table 6-5: Comparison of upper Niagara River local runoff estimates

Statistic	Upper Niagara River Local Inflows (m ³ /s)											
	Jan	Feb	Mar	Apr	May	Jun	Jul	Aug	Sep	Oct	Nov	Dec
Grand and Genesee rivers, Coordinating Committee (CC), 1962												
Mean	37	37	91	93	45	23	14	8	8	14	25	31
Local Tributaries (LT)												
Mean	56	65	104	84	37	20	11	10	14	19	39	60
Median	53	66	104	81	29	14	7	6	6	13	30	57
StDev	33	38	37	29	22	18	10	14	25	25	29	36
Max	148	167	181	151	97	108	45	90	162	162	141	166
Min	3	9	41	31	13	4	2	2	2	1	2	2
Mean Difference												
CC – LT	-19	-28	-13	9	8	3	3	-2	-6	-5	-14	-29

Figure 6-4 shows a boxplot of the results. The boxplot indicates that the spread of local inflows varies significantly about the mean, such that for any given month the Coordinating Committee (1962) estimates could be in error by more than $100 \text{ m}^3/\text{s}$. The mean (grey dashed line) and median (horizontal solid black line within the boxes) of the local tributary flow estimates also can be seen to differ, due to the non-symmetric distribution of the estimated local inflows.

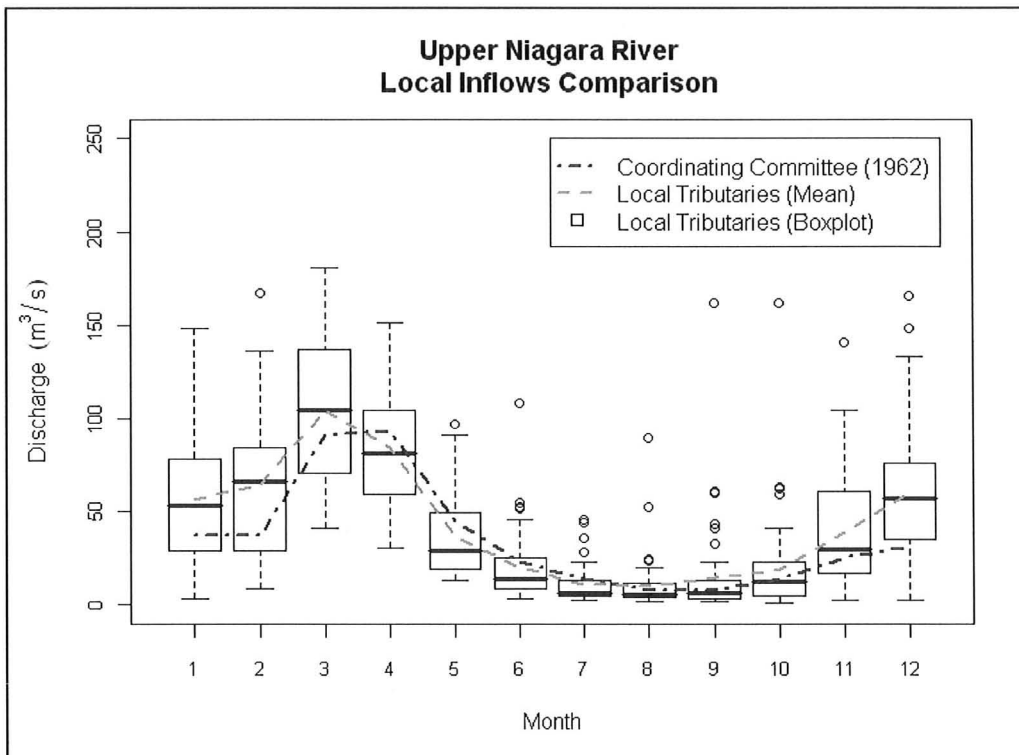


Figure 6-4: Boxplot comparison of upper Niagara River local runoff estimates

The differences between the mean Grand and Genesee River based flow estimates and the mean local tributary based flow estimates were used as the mean error in the local runoff, while the standard deviations of the local tributary based runoff estimates were used as the standard uncertainty estimate in the FOSM uncertainty analysis. For the Monte Carlo analysis, probability distributions were fit to the local tributary runoff data for each month using the “R” statistical software package. Empirical CDFs were plotted against fitted distributions until a distribution that looked to provide an acceptable fit to the data was found. The results of this exercise are provided in Appendix A. The type of

PDFs found to provide the best fit varied depending on the month. A list of the distributions used and their parameters are given in Table 6-6. These distributions were randomly sampled using “R” to obtain a probabilistic estimate of the local tributary runoff for any month for input into the Monte Carlo analysis.

Table 6-6: Probability distributions used for local runoff uncertainty estimation

Month	Distribution	Parameter 1	Value	Parameter 2	Value
Jan	Weibull	Shape	1.73	Scale	62.77
Feb	Weibull	Shape	1.78	Scale	72.80
Mar	Log-Normal	Mean-Log	4.58	StDev-Log	0.37
Apr	Normal	Mean	83.81	StDev	28.89
May	Log-Normal	Mean-Log	3.45	StDev-Log	0.56
Jun	Log-Normal	Mean-Log	2.70	StDev-Log	0.75
Jul	Log-Normal	Mean-Log	2.06	StDev-Log	0.73
Aug	Log-Normal	Mean-Log	1.90	StDev-Log	0.82
Sep	Log-Normal	Mean-Log	2.00	StDev-Log	1.05
Oct	Log-Normal	Mean-Log	2.40	StDev-Log	1.06
Nov	Weibull	Shape	1.35	Scale	42.16
Dec	Weibull	Shape	1.73	Scale	67.08

The preceding results provide an estimate of the uncertainty that results from using mean local inflows determined from historic Grand and Genesee River data instead of actual tributary flows. Additional uncertainty results from the uncertainty in the measured local tributary flows themselves, and the use of area ratios to extrapolate the gauged portion of the tributary basins to the ungauged portions. De Marchi et al. (2009) estimated the uncertainty in runoff estimates for the entire Great Lakes region as determined using a similar area ratio method as was used in this study. They assumed that the uncertainty in the actual measured flows was 10% at the 95% confidence level, and represented this by a normal distribution. In addition, for Lake Erie runoff they showed that the uncertainty resulting from extrapolating measured flows from gauged basins to ungauged portions of the basin when between 40 and 60% of the basin is gauged (which is approximately the proportion of the upper Niagara River basin that is gauged) could be fitted with a logistic distribution having parameters of approximately -0.038 and 0.086. This means the ungauged basin runoff for Lake Erie was underestimated by approximately 4%, with standard error of approximately 9%.

However, these results depend on the actual gauged basins used in the analysis, and may not apply exactly to the upper Niagara River basin. The bias identified by De Marchi et al. (2009) was instead assumed to be an unknown source of error, and therefore the combined uncertainty due to both the uncertainty in the gauged flows and the uncertainty due to extrapolating to ungauged portions of the basin was computed as $\sqrt{5^2 + 4^2 + 9^2} = 11\%$, with mean error of zero. This source of uncertainty is essentially negligible compared to the uncertainty that results from using a constant monthly value for the local runoff instead of an actual estimate of the tributary flows, and therefore it was omitted from the remainder of this analysis; however, if a new approach to estimating local inflow were to be employed, such as the one suggested in this research, this additional source of uncertainty would need consideration.

6.6 Welland River Diversion

As discussed, a small additional volume of water is diverted from the Welland Canal to the Welland River (D_{WR}). The Welland River has been routed to pass below an old stretch of the Welland Canal through a set of six syphon culverts, and flows from here to the Sir Adam Beck hydropower plants, where the total Welland River flow is measured as part of the hydropower plant flows. Since flow diverted to the Welland River is measured at both the Welland Canal and at the hydropower plants, it must be subtracted from the total Lake Erie outflow to avoid accounting for this volume twice.

The water diverted from the Welland Canal enters the Welland River from a number of sources. The largest source is the flow that passes through a set of holes cut into the bottom of the old stretch of canal and through the roof of the syphon culverts. This flow currently makes up approximately 50% of the total Welland River diversion, but in the past was even greater, making up approximately 70% of the diversion. The next largest amount comes from the Welland Water Works, which takes water from the Canal and flushes it to the Welland River. This currently makes up approximately 40% of the total diversion, and in the past made up approximately 20% of the total. The remaining 10% comes from smaller domestic and municipal sources, which also take water from the Welland Canal and return it to the Welland River.

The flow through the syphon culvert drain holes into the Welland River syphon culverts is estimated by treating each of the holes as a simple submerged orifice. The theoretical equation of flow through an orifice (Olson, 1966) results from the continuity equation, $Q = VA$, where A equals area, and the velocity, V , is determined from $V = \sqrt{2gh}$, where g is gravitational acceleration and h is the head difference. In this case the continuity equation is multiplied by a coefficient, K , which results from the fact that in practice theoretical flow is different than actual flow, due primarily to different orifice shapes. The flow through the three syphon culvert drains (WR_{SD}) can therefore be determined from:

$$WR_{SD} = 3 \cdot (K \cdot \sqrt{2gh} \cdot A) \quad (75)$$

Assuming that errors in determining A and h are small, uncertainty results primarily from the coefficient chosen, and the fact that the equation is theoretically based and may not accurately represent the true flow. The coefficient used by the SLSMC is 0.934, and was determined based on flow measurements taken in September 1973 (Fraser Johnston, SLSMC, letter to the INC, undated). Theoretical values of the coefficient normally range from approximately 0.6 to 1.00 according to Olson (1966). This gives a range of 0.4. A range of 0.6 was used in this analysis to be conservative. Given a range of 0.6 in the coefficients, flow error could range from 0 to 60% of flow. If these are assumed to be the lower and upper 95% confidence limits, then the standard error is approximately 15%.

Data and information for the Welland Water Works and the other flows that make up the total Welland River diversion was not available. It seems unlikely that these flows would be less accurate than the flow through the syphon culvert drains. Assuming a standard error of 5% for this remaining 50% of the total diversion and combining with the uncertainty determined for the syphon culvert drains, the total standard uncertainty would be less than 10%. A conservative estimate of 10% for the standard uncertainty in the Welland River diversion was assumed, and it was assumed that this was normally distributed.

6.7 Combined Uncertainty in Niagara River Flow at Buffalo

The combined uncertainty in the Niagara River flows was estimated using both the FOSM and the Monte Carlo approach. Archived monthly estimates of the total Niagara River flow at Buffalo are available from 1900 to 2008, as is data for the NYSBC and the constant monthly local runoff estimates; however, monthly estimates of the Niagara River MOM pool flows were only readily available for the period 1962 to 2008, and monthly estimates of the combined hydropower diversions were only readily available for the period of August 1999 to December 2008. As a result, an uncertainty analysis on the Niagara River flows for the full period of record could not be performed. Instead, only the 1962 to 2008 period was investigated. The hydropower flows for 1962 to July 1999 were estimated from equation (13) by subtracting the MOM and NYSBC flows from the total Niagara River flow at Buffalo, and then adding the coordinated local runoff values for each month and an estimate of the Welland River diversion. Due to rounding errors the results are not likely exact, but they provide a good estimate of the magnitude of the hydropower flows in comparison to the remainder of the Niagara River flow components, and are sufficient for the purposes of this analysis. The results of this analysis were applied to the overall uncertainty analysis in Lake Erie NBS for the full period of record (1900 to 2008) as will be described in subsequent sections.

Table 6-7 provides a summary of the mean magnitude of each of the inputs to the Niagara River flow at Buffalo as computed using the summation method, as well as the computed uncertainty of each input as used in the FOSM method. Note that the local inflow uncertainty estimates were the only inputs treated differently for the FOSM and Monte Carlo methods, with the FOSM method using the mean and standard deviations of the local tributary results, and the Monte Carlo method using the probability distributions as described in Section 6.5. The mean flow in the case of the FOSM method is simply the mean Coordinating Committee (1962) values, and in addition to the uncertainty estimates provided, there is also a mean error caused by the mean difference between these currently used estimates and the local tributary estimates determined in this research, as shown in Table 6-5.

Table 6-7: Niagara River mean input flows (1962-2008) and uncertainty estimates

Month	N_{MOM}			$P_{SAB\&2+RM}$			D_{NYSBC}			R_N			D_{WR}			$O_{N@Buf}$
	\bar{Q} (m ³ /s)	u (%)	u (m ³ /s)	\bar{Q} (m ³ /s)	u (%)	u (m ³ /s)	\bar{Q} (m ³ /s)	u (%)	u (m ³ /s)	\bar{Q} (m ³ /s)	u (%)	u (m ³ /s)	\bar{Q} (m ³ /s)	u (%)	u (m ³ /s)	\bar{Q} (m ³ /s)
Jan	2016	3.4	69	3932	2.0	79	1	7.5	0	37	89	33	19	10.0	2	5894
Feb	1949	3.4	66	3943	2.0	79	0	7.5	0	37	103	38	19	10.0	2	5837
Mar	2000	3.4	68	4146	2.0	83	1	7.5	0	91	41	37	19	10.0	2	6037
Apr	2620	3.4	89	3749	2.0	75	7	7.5	1	93	31	29	19	10.0	2	6264
May	2634	3.4	90	3847	2.0	77	29	7.5	2	45	49	22	19	10.0	2	6445
Jun	2603	3.4	89	3769	2.0	75	31	7.5	2	23	78	18	19	10.0	2	6361
Jul	2560	3.4	87	3710	2.0	74	31	7.5	2	14	71	10	19	10.0	2	6267
Aug	2532	3.4	86	3625	2.0	73	31	7.5	2	8	175	14	19	10.0	2	6160
Sep	2463	3.4	84	3567	2.0	71	31	7.5	2	8	313	25	19	10.0	2	6033
Oct	2398	3.4	82	3556	2.0	71	31	7.5	2	14	179	25	19	10.0	2	5951
Nov	1887	3.4	64	4072	2.0	81	21	7.5	2	25	116	29	19	10.0	2	5935
Dec	1965	3.4	67	4095	2.0	82	3	7.5	0	31	116	36	19	10.0	2	6013

As expected, the largest sources of uncertainty are the MOM pool flows and the combined hydropower diversions, owing to their large magnitude in comparison to the other inputs used to compute the Niagara River flow at Buffalo. The local runoff, though somewhat smaller in magnitude, is also a notable source of uncertainty. Despite having large uncertainties in a relative sense, the uncertainties in the Niagara River flow resulting from the NYSBC and Welland River diversions are small in comparison due to the smaller volumes of water diverted at these locations. In terms of NBS and Niagara River flow computations, the uncertainty from these sources could have been assumed negligible and omitted from the analysis.

The combined uncertainty in the Niagara River flow at Buffalo can be computed using the FOSM method and the uncertainty estimates shown in Table 6-7. Assuming the different flow estimates to be uncorrelated, from equation (23), the combined standard uncertainty is simply the root sum of squares of each of the different standard uncertainty estimates provided, since in the summation model used to compute the Niagara River flow at Buffalo the sensitivity coefficients are all equal to one. That is:

$$u(O_{N@Buf}) = \sqrt{u^2(N_{MOM}) + u^2(P_{SAB\&2+RM}) + u^2(D_{NYSBC}) + u^2(R_N) + u^2(D_{WR})}$$

where $u(P_{SAB\&2+RM})$ is the uncertainty in the combined hydropower diversions, and all other variables are as previously defined.

The Monte Carlo method was computed by sampling from each of the different probability distributions identified for each input, a summary of which is provided in Table 6-8. For each month from 1962 to 2008, the statistical software package “R” was used to create stochastic representations of each input by randomly sampling from each probability distribution. A total of 2500 realizations were computed for each month. The mean value for each of the MOM pool, combined hydropower, NYSBC and Welland River diversion flows was assumed to be the deterministic value obtained from the USACE, and these were perturbed by the normal distributions defined by their standard deviations in Table 6-8. For the local runoff, values were sampled directly from the distributions listed in Table 6-8. The randomly generated input variables were then combined to produce a total of 2500 estimates of the Niagara River flow at Buffalo for each month in the period of record, the probability distribution of

which defined the uncertainty in the Niagara River flow. The results were checked for convergence by using a subset of 1000, 1500, and 2000 of the 2500 Monte Carlo simulated values, and the results were found to be nearly identical to those determined from the full dataset.

Table 6-8: Niagara River Monte Carlo analysis input distributions and parameters

Input	Month	Distribution	Parameter 1	Value	Parameter 2	Value
N_{MOM}	All	Normal	Mean	monthly estimates	StDev	3.4
$P_{SAB\&2+RM}$	All	Normal	Mean	monthly estimates	StDev	2.0
D_{NYSBC}	All	Normal	Mean	monthly estimates	StDev	7.5
R_N	Jan	Weibull	Shape	1.73	Scale	62.77
	Feb	Weibull	Shape	1.78	Scale	72.80
	Mar	Log-Normal	Mean-Log	4.58	StDev-Log	0.37
	Apr	Normal	Mean	83.81	StDev	28.89
	May	Log-Normal	Mean-Log	3.45	StDev-Log	0.56
	Jun	Log-Normal	Mean-Log	2.7	StDev-Log	0.75
	Jul	Log-Normal	Mean-Log	2.06	StDev-Log	0.73
	Aug	Log-Normal	Mean-Log	1.9	StDev-Log	0.82
	Sep	Log-Normal	Mean-Log	2.0	StDev-Log	1.05
	Oct	Log-Normal	Mean-Log	2.4	StDev-Log	1.06
	Nov	Weibull	Shape	1.35	Scale	42.16
	Dec	Weibull	Shape	1.73	Scale	67.08
D_{WR}	All	Normal	Mean	monthly estimates	StDev	10

A summary of the uncertainty analysis results from the FOSM and Monte Carlo methods for the Niagara River flow are provided in Table 6-9. Of note is that the two methods gave almost identical results, even despite the fact that the uncertainty in the local runoff was treated slightly differently in each case. The reason for this is that the output (in this case, the total Niagara River flow at Buffalo) is a linear function of the model inputs (i.e. the summation equation). If a model is highly non-linear, the FOSM method will not accurately represent the uncertainty in the model output, since only the first-order terms of the Taylor series expansion are used to represent the model. Including higher-order terms of the Taylor series expansion can improve this, but would also require additional and more difficult computations of the higher-order moments of the input error

distributions. As stated, in the case of the Niagara River flows, inclusion of the higher-order terms was not necessary, and this is reflected in the similarity between the FOSM and Monte Carlo method results. Monthly differences in the uncertainty estimates is partly the result of the difference in the MOM pool flows during tourist and non-tourist seasons, since the relative uncertainty in the MOM pool flows is somewhat greater than in the hydropower diversions. The difference is also partly the result of differences between the local runoff estimates. Lastly, histograms of the Monte Carlo analysis results for 2008 were plotted (see Appendix B) and were found to be normally distributed, a result of the central limit theorem. According to this theorem, the sum of a large number of statistically independent random variables, such as the inputs to the Niagara River flow equation, will tend towards a normal distribution, even if the random variables themselves are not normally distributed, so long as none of them dominates in terms of magnitude.

Table 6-9: Niagara River FOSM and Monte Carlo analysis results comparison

Month	Mean $O_{N@Buf}$	Uncertainty (m^3/s)			Uncertainty (% of $O_{N@Buf}$)		
		FOSM	MC	DIFF.	FOSM	MC	DIFF.
Jan	5894	109	110	0	1.86	1.86	0
Feb	5837	110	110	0	1.88	1.88	0
Mar	6037	113	115	-2	1.88	1.91	-0.03
Apr	6264	120	120	0	1.92	1.92	0
May	6445	120	121	-1	1.86	1.87	-0.01
Jun	6361	118	118	0	1.85	1.85	0
Jul	6267	115	115	0	1.83	1.83	0
Aug	6160	113	113	0	1.84	1.84	0
Sep	6033	113	111	1	1.87	1.85	0.02
Oct	5951	111	112	-1	1.87	1.88	-0.01
Nov	5935	108	108	0	1.81	1.81	0
Dec	6013	112	112	0	1.86	1.86	0

6.8 Alternative Niagara River Flow Estimation Methods

The current method of determining the total Niagara River flow involves the summation of a number of smaller flow estimates. Each of these flow estimates could be measured using alternative methods or models, and these could

provide an alternative or supplemental estimate of the different flows used to compute the summation equation. While it is unclear whether such methods would provide a more accurate estimate, at the very least they could provide a check on the existing estimates, and may help identify unaccounted for sources of error. As an example, a number of the subcomponent flows could be measured using an Acoustic Velocity Meter (AVM). For instance, as an alternative to determining the hydropower diversions from the flow through the power plants and the change in storage upstream, the diversions could be measured directly at points between the Chippawa Grass Island Pool and the power plants themselves using acoustic velocity methods. Similarly, the diversion to the NYSBC could also benefit from the use of acoustic velocity instruments. In fact, in 1989, a trial attempt was made to measure the NYSBC diversion using an AVM and index-velocity relationship in combination with a simple hydrologic model (INC, 1990). Unfortunately, the results of this trial were quite poor, with the AVM providing flow estimates that were erratic and generally too high, possibly due to inexperience with the equipment and a less than ideal location for the instrument installation. As such, the project was terminated, and no direct field measurements have been taken since that time. However, given the more modern instrumentation and software now available, in combination with more experienced technicians and a better location for the instrument than was used in 1989, it seems likely that acoustic technology could be a useful tool to measure flow at this location.

The estimation of local inflows could be improved by using estimates from actual gauged tributary flows extrapolated to ungauged portions of the basin as opposed to the constant mean values based on historic Grand and Genesee River flows as is currently used. Though the measured tributary flows are subject to uncertainty and extrapolation of these to the ungauged areas of the basin adds additional uncertainty, this method would provide a time varying estimate that should at least be more representative than the current estimates since the flows would be based on measurements from the tributaries themselves.

An alternative method for determining the total outflow from Lake Erie would be to measure it directly at Buffalo using any number of models, such as a stage-discharge or index velocity relationship, for example. The hydropower companies currently use a rating equation for their operations, which is based on water levels measured at one of their own gauges located at Fort Erie. The NOAA water level gauge at Buffalo, NY, has also been used to establish a stage-

discharge relationship in the upper Niagara River. This equation is used primarily for Great Lakes routing model purposes, since the Buffalo gauge, being located on Lake Erie, allows the Lake Erie outflow through the Niagara River to be estimated based on the water level of the lake (Quinn and Noorbakhsh, 2001). The stage-discharge relationship developed from the Buffalo water level gauge has been found to be sufficiently accurate for many purposes; however, since the factors affecting water levels can differ between the lake and the connecting channels, flow in the Niagara River may be better represented by a gauge on the river itself. Furthermore, the Buffalo stage-discharge relationship is affected by weeds in the summer months and by ice in the winter months, both of which retard flow. The average monthly flow retardation at this location was found to range from 50 to 300 m³/s according to Fan and Fay (2003). Constant monthly mean flow retardation values are used for Great Lakes routing model purposes, and in addition to including the effects of ice and weeds, these also account for the fact that the Buffalo water level does not necessarily represent the mean Lake Erie water level. Therefore, the Buffalo rating is assumed only reliable for estimating the actual Lake Erie outflow during the relatively weed and ice free months of May and November.

Recently, WSC re-established a water level gauge at Fort Erie. This will be used to establish another stage-discharge relationship in the upper Niagara River, although it may take several years to obtain a wide enough range of water levels and flows to properly define the curve. The gauge is expected to be designated as an International Gauge, which will ensure that agencies from both Canada and the United States are involved in the development, validation and review of the flow model used and the resulting flow estimates. The location of this gauge station is on the river itself, which may allow it to more accurately reflect the variation in flows occurring in the river than the Buffalo gauge; however, this relationship may also be affected by weeds and ice, and if this is determined to be the case, then additional flow measurements during the summer and winter months and ongoing adjustments to the rating curve may be necessary (Jeanette Fooks, WSC, personal communication, 13 October, 2010).

Additional methods for estimating flows, such as a stage-fall-discharge equation, acoustic velocity measurement and index velocity relationships, or hydrodynamic models, for example, could be used to provide additional estimates of flow out of Lake Erie through the Niagara River, and these could potentially increase the accuracy of the total Lake Erie outflow estimates.

7 Sources and Estimates of Uncertainty in Welland Canal Flow

7.1 Welland Canal Overview

As stated and shown in equation (14) the total outflow through the Welland Canal (O_{WC}) is currently determined by averaging the flow entering the canal from Lake Erie at the far southern end (WC_{IN}) with the flow measured as it is distributed along the canals' length (WC_{DIST}). Similar to the Niagara River flows, the total Welland Canal flow is determined by summing a number of smaller flows that are distributed along different paths (see Section 3.3.3).

There are sources of error in each of the different subcomponents, and the uncertainty caused by each of these is evaluated in this section. The uncertainty from each of the different subcomponents is then combined to estimate the uncertainty in the estimated flow into the Welland Canal, and the uncertainty in the estimated flow distributed along the length of the Welland Canal. These flow estimates are also compared, and an assessment of the uncertainty in the total Welland Canal flow used in Lake Erie NBS computations as estimated from the average of the two is made.

7.2 Welland Canal Supply Weir Flow

The flow into the Welland Canal is determined from equation (15) as the flow through the Welland Canal supply weir and the flow through Lock 8, with the supply weir controlling the total discharge entering the Welland Canal and making up the greatest proportion of the total flow. The flow through the supply weir is currently measured using a SonTek Argonaut-SL side-looking ADCP and an index-velocity rating. Prior to the SonTek installation, a set of two rating equations relating discharge to head difference above and below the weir and the weir gate opening was used to measure flow through the supply weir. The choice of which equation to use depended on the Lake Erie water levels at the time, as verified by the INBC. The current use of the SonTek is believed to provide a more accurate estimate of the supply weir flows.

The SonTek ADCP measures the velocity of a relatively small area of the channel cross-section. An index-velocity rating is used to relate the measured velocity to the mean velocity in the channel, which is then multiplied by the measured channel cross-section area to get discharge. The channel area is determined from a stage-area rating, which relates measured stage to area of the cross-section. The Welland Canal stage-area rating was developed in 2004 from depths obtained from ADCP measurements of the channel flow. Stage is measured using a pressure transducer located inside a well immediately adjacent to the SonTek instrument.

The SLSMC owns and operates the equipment, and is responsible for measuring and providing discharge records to the INC. The INBC supports the SLSMC and INC in this regard, and is responsible for developing and validating the supply weir index-velocity and stage-area ratings. To calibrate and validate the index-velocity rating, gauged discharge measurements are required at a section near the instrument. For the Welland Canal, gauged discharge measurements are collected by the INBC using another ADCP, this one mounted to a tethered boat and operated from a bridge located upstream of the supply weir and the SonTek horizontal ADCP and related instrumentation. The gauged discharge measurements are divided by the cross-sectional area of the channel determined from the stage-area rating to estimate the mean channel velocity. The mean velocity from each gauged discharge measurement is then related to the corresponding measured SonTek velocity, and a linear regression relationship is used to develop the index-velocity rating.

Since the discharge obtained from an index-velocity relationship is determined as the estimated mean velocity times the measured cross-sectional area, the uncertainty in the discharge is determined by first estimating the uncertainty in the velocity and area separately, and then combining the results. The uncertainty in the mean velocity obtained from the index-velocity rating was determined using the statistical methods outlined in Section 5. In this case, instead of discharge, the mean velocity is the dependant variable in the linear relationship; instead of stage, the measured velocity from the SonTek is the independent variable. The standard error of estimate was found to be 3.1%. Depending on the magnitude of the measured velocity the standard error of the mean relation ranged from 1.0 to 2.1%, and the standard error of the observations ranged from 3.2 to 3.7%. The minimum relative error values occur near the mean

measured velocity, whereas the highest errors occur at the extreme maximum and minimum velocities. A comparison of the Welland Canal supply weir index-velocity relationship and the ADCP measured velocities are given in Figure 7-1.

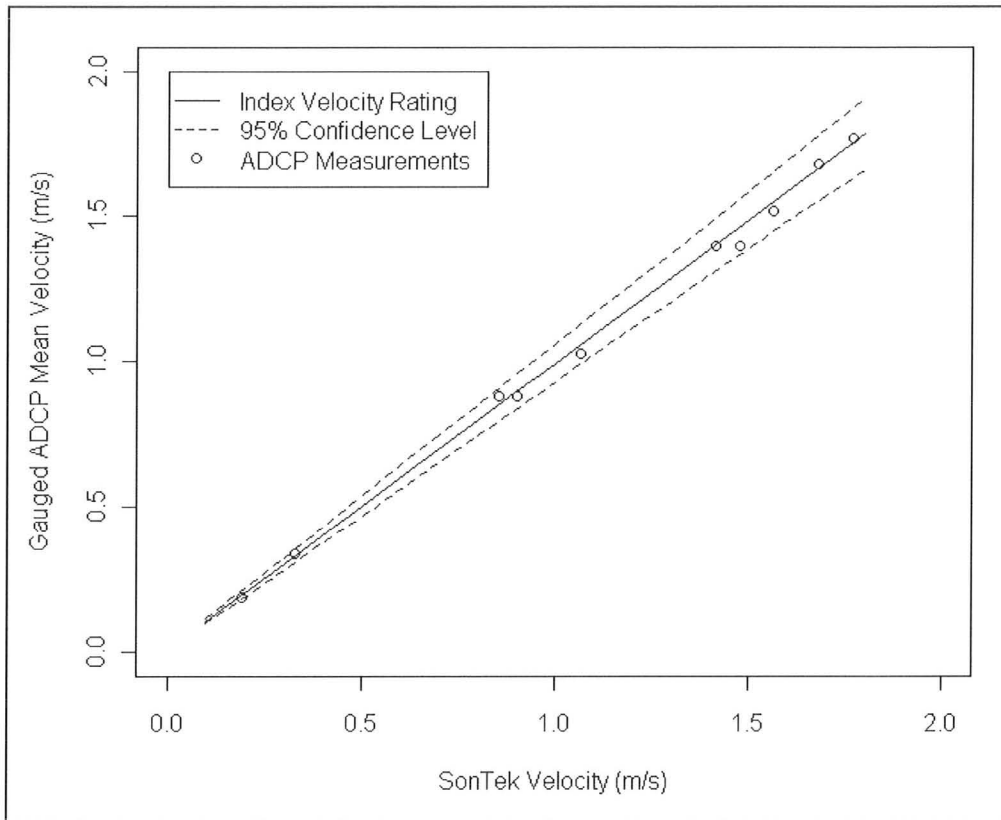


Figure 7-1: Welland Canal supply weir index-velocity rating vs. mean velocities from ADCP measurements

The uncertainty in the supply weir flows due to error in the mean channel velocity can be determined from

$$u(SW_{WC}) = \sqrt{A_{XS}^2 \cdot u(V)^2} \tag{76}$$

where $u(SW_{WC})$ is the uncertainty in the flow through the supply weir; A_{XS} is the cross-sectional area; and $u(V)$ is the uncertainty in mean channel velocity. Errors in the measured velocity result from both errors in the index-velocity rating, as

described above, and errors in the model predictor variable, i.e. the measured velocity itself. These two sources are assumed uncorrelated and treated separately. The uncertainty in the supply weir flows due to error in the index-velocity rating alone can be determined from the standard error of estimate (3.1%) and by assuming a constant standard error of the mean relation value of 2.0% to simplify the computations. Assuming an approximate average cross-sectional area of 200 m² and using a conservative (i.e. high) estimate of the mean velocity of 2 m/s, the combined standard uncertainty in discharge due to model error would be approximately 15 m³/s. That is:

$$u(SW_{WC}) = \sqrt{200^2 \cdot (2 \cdot 0.031)^2 + 200^2 \cdot (2 \cdot 0.020)^2} = 15 \text{ m}^3/\text{s}$$

Additional uncertainty results from uncertainty in the measured velocity used to evaluate the index-velocity rating. According to brochures on the SonTek company website (<http://www.sontek.com/>), the accuracy of the measured velocity is 1% plus an additional 0.5 cm/s due to resolution of the instrument. A confidence level is not stated, but it was assumed that this was the expanded uncertainty estimated at the 95% confidence level, such that the standard uncertainty was assumed to be 0.5%. Using the same method as before and the same assumptions of a 2 m/s average velocity and 200 m² average cross-section area, the combined standard uncertainty due to the measured velocity was found to be approximately 2 m³/s. That is:

$$u(SW_{WC}) = \sqrt{200^2 \cdot (2 \cdot 0.005)^2 + 200^2 \cdot 0.005^2} = 2 \text{ m}^3/\text{s}$$

The uncertainty in the cross-sectional area of the channel must also be determined. As explained by Duncker et al. (2006) in regards to the Lake Michigan Diversion at Chicago, errors in the stage-area rating effectively cancel out. The reasoning for this is as follows. In developing the index-velocity rating, the cross-sectional area from the stage-area rating (A_{XS}) is first used to determine the mean velocities (\bar{V}_{gauged}) from the gauged discharge measurements (Q_{gauged}) using:

$$\bar{V}_{gauged} = \frac{Q_{gauged}}{A_{XS}} \quad (77)$$

Subsequently, when determining the modelled supply weir flow from the index-velocity rating, the mean cross-sectional velocity determined from the rating (\bar{V}_{rating}) is multiplied by the cross-sectional area determined from the same stage-area rating. That is:

$$SW_{WC} = \bar{V}_{rating} \cdot A_{XS} \quad (78)$$

Therefore, any errors in A_{XS} effectively cancel out, and as such, only the error in cross-sectional area resulting from errors in the measured water levels needs consideration in this analysis.

The SLSMC does not provide an estimate of the accuracy of the water level gauge at this location. Instead, a conservative standard uncertainty estimate of +/-1 cm was assumed. The stage-area rating is given as:

$$A_{XS} = 138.27 + 34.35 \cdot (h_{sw} - 172.37) \quad (79)$$

The area of the cross-section is determined from the measured water level (h_{sw}) and the area below and above the SonTek instrument. The area below the SonTek instrument is given as a constant 138.27 m²; the area above is equal to the measured water level minus the SonTek elevation (172.37 m) times the width of the channel (34.45 m). Assuming a conservative water level uncertainty estimate of 1 cm, the uncertainty in the cross-sectional area from the rating, $u(A_{XS})$, is equal to $34.35 \cdot 0.01 = 0.345$ m². Given that the average velocity in the channel is less than 2 m/s, it can be shown that the uncertainty in area would correspond to an uncertainty in discharge of no more than $\sqrt{2^2 \cdot 0.345^2} = 0.7$ m³/s. This is a negligible amount when compared to the uncertainty in the mean velocity, and as a result uncertainty in the cross-sectional area was considered negligible.

The overall uncertainty in the supply weir flows can therefore be taken as the uncertainty in the gauged discharge measurements (assumed standard uncertainty of 2.5%) plus the model uncertainty and the predictor variable uncertainty due to velocity alone. As was done for the MOM pool flow, all errors were assumed fully correlated, and therefore not reduced by averaging. Given an average supply weir discharge of approximately 200 m³/s (as determined from INC records for the period 1999-2009), the combined standard uncertainty for any

individual estimate is approximately $\sqrt{(200 \cdot 0.025)^2 + 15^2 + 2^2} = 16 \text{ m}^3/\text{s}$, or approximately $32 \text{ m}^3/\text{s}$ at a 95% confidence level. This corresponds to a relative standard uncertainty of 8%, or 16% at the 95% confidence level.

7.3 Uncertainty in Flows into the Welland Canal

Lock 8 is the lock located furthest south and closest to Lake Erie, and flow through Lock 8 makes up the remainder of the total flow into the Welland Canal. The flow through Lock 8 is generally much less than that which flows through the supply weir. For example, a review of data from the SLSMC for the period of 2000-2009 showed that the flow through Lock 8 made up a maximum of 36% of the total flow into the Welland Canal for any month (this occurred in March 2007), but on average the flow through Lock 8 makes up much less of the total Welland Canal flow, being less than 7% for the month of March, and less than 4% on average for all other months. The higher proportion occurring in March is a result of the need to flush ice from the lock chamber. Other months at the end of the navigation season also see a slightly greater proportion of the flow into the Welland Canal pass through Lock 8 as a result of ice flushing and also due to larger volumes of shipping occurring just prior to the close of the navigation season.

The flow through Lock 8 is divided between flow due to lockages and flow due to hydraulic assists. Flow due to lockages is computed from the number of lock cycles times the capacity of the lock relative to the head differential. The lock dimensions are all that are needed, because the water moves from one lock to the other through the bottom of the lock chamber, and therefore ship displacement does not need to be considered. The flow due to lockages is normally quite small, amounting to only approximately $1 \text{ m}^3/\text{s}$ or less in a given month. Hydraulic assists involve allowing additional water to enter one end of the lock chamber to assist the ships in exiting the lock. Hydraulic assists are measured by fixed intake valve opening flow rates multiplied by the time they are open. The flow due to hydraulic assists is larger than the flow due to lockages at Lock 8, but is also normally quite small compared to the flow that passes through the supply weir.

Data to compute uncertainty in Lock 8 flows were not available. Given that the flows are computed primarily from measurements of water levels and the dimensions of the lock and valve openings, it seems unlikely that the relative

uncertainty in Lock 8 flows is greater than the supply weir flows. Therefore, as a conservative estimate, the total uncertainty in the flow into the Welland Canal was assumed to be equal to the relative uncertainty computed for the supply weir flows, which was found in Section 7.2 to be equal to 8%, or 16% at the 95% confidence level.

7.4 Uncertainty in Flows Distributed Along the Welland Canal

Equation (17) was given in Section 3.3.3 to describe the flow distributed along the length of the Welland Canal. The information and data available for the flows distributed along the length of the Welland Canal to the various hydraulic control structures, intake and discharge facilities, and industrial and municipal users was insufficient to directly evaluate the uncertainty. Instead, indirect means and inferences from other analyses were used.

Approximately 6 to 8% of the total flow distributed along the length of the Welland Canal comes from the Welland River diversion (D_{WR}). The uncertainty of this was estimated to be 10% in Section 6.6.

The OPG diversion to the De Cew power plants (P_{DC}) makes up by far the greatest proportion of the total Welland Canal flow at approximately 75-85%. The diversion is determined in a similar manner as the diversions to the power plants on the Niagara River, in that the total flow is determined from the flows through the power plants, which are measured using rating tables that relate water level head differences and power output to discharge, as well as the measured change in storage on Lake Gibson and Lake Moodie upstream of the De Cew power plants. The rating tables are based on performance testing results, but performance testing has not been conducted at De Cew since at least the early 1980s, and possibly longer than this for some units (Joan Frain, OPG, personal communication, 20 September, 2010). Given improvements in flow measurement technology and changes in plant efficiency that may have occurred since the plants were last rated, it seems that the relative uncertainty in this diversion estimate should be somewhat greater than the uncertainty in the total Niagara River hydropower diversion, which was estimated to be approximately 4% at the 95% confidence level in Section 6.3. Therefore, it was assumed that the uncertainty in the OPG De Cew diversion from the Welland Canal was normally

distributed, having an uncertainty of 5% at the 95% confidence level, or 2.5% standard uncertainty.

Depending on the time of year, anywhere from about zero to 5% of the total Welland Canal flow passes through Lock 7 due to lockages ($L7$). Since Lock 7 flows require only the measurement of water levels and the lock dimensions, which are unlikely to be subject to significant errors, the standard uncertainty in Lock 7 flows is likely small, and was assumed to be 5%. A much smaller proportion of the Lock 7 flows is assumed to be leakage, and this error was considered negligible.

Similarly, an additional zero to 4% of the total Welland Canal flow passes through the weir at Lock 7 (W_{L7}). The flow through the weir at Lock 7 is measured using a rating table similar to what was used at the supply weir prior to the installation of the SonTek. The relative standard uncertainty in this flow estimate is likely to be greater than the Welland Canal supply weir flow estimate measured using the SonTek, and therefore it was assumed to be 10%.

Another approximately 5 to 6% of the Welland Canal flow passes through the SLSMC powerhouse at Lock 7 (P_{L7}). The powerhouse flow is measured using a rating table similar to those used at De Cew and on the Niagara River. The P_{L7} rating tables were recently revised due to the installation of new equipment. The verification flows were measured using a dye dilution method. It seems reasonable to assume that uncertainty in the powerhouse flows would be similar to what it is at the hydropower plants at De Cew, i.e. 5% at the 95% confidence level, or standard uncertainty of 2.5%.

The remaining flows distributed along the length of the Welland Canal, namely the flow through the second canal supply weir (SW_{2C}) and the sum of the small industrial and municipal users ($\sum IM$) is quite small, and uncertainty from these components was assumed negligible.

If we assume that 80% of the flow passes through the De Cew hydropower plants, and the remaining 20% is divided evenly between the Welland River diversion, Lock 7, the weir at Lock 7, and the powerhouse at Lock 7 (i.e. 5% of the total flow to each), then, assuming that errors in each of the different flow estimates are uncorrelated, the relative uncertainty in the total flow distributed

along the length of the Welland Canal can be estimated as approximately 2.1%. That is:

$$\begin{aligned}
 u(WC_{DIST}) &= \sqrt{u(D_{WR})^2 + u(P_{DC})^2 + u(L7)^2 + u(W_{L7})^2 + u(P_{L7})^2} \\
 &= \sqrt{(0.05 \cdot 0.10)^2 + (0.8 \cdot 0.025)^2 + (0.05 \cdot 0.05)^2 + (0.05 \cdot 0.10)^2 + (0.05 \cdot 0.025)^2} \\
 &= 2.1\%
 \end{aligned}$$

This estimate is much less than the estimated standard uncertainty of the flow into the Welland Canal, which was given as approximately 8%. This is primarily the result of the large percentage of the total flow that passes through the De Cew power plants, which is assumed to be relatively accurate.

7.5 Comparison of Flows Into and Distributed Along Welland Canal

Since the proportion of the total Lake Erie outflow that passes through the Welland Canal is estimated as the average of the flows into and flows distributed along the Welland Canal, if the two estimates are assumed to be free from systematic errors and the errors in the estimates are assumed uncorrelated, the total uncertainty in the estimated Welland Canal flow can be found from:

$$u(O_{WC}) = \sqrt{0.5^2 \cdot u(WC_{IN})^2 + 0.5^2 \cdot u(WC_{DIST})^2} \quad (80)$$

Using the uncertainty estimates determined for WC_{IN} and WC_{DIST} of 8% and 2.1%, respectively, the total standard uncertainty in the estimated Welland Canal flow is approximately 4%, or approximately 8% at the 95% confidence level. What remains to be determined is whether the assumption that neither flow estimate is subject to systematic errors is indeed correct.

The measured flows into the Welland Canal were compared to the measured flows distributed along the length of the Welland Canal for the period April 2005 (when the flows through the supply weir began being measured using the SonTek ADCP) to April 2010. Five months of data were missing in the records for the flows into the Welland Canal, likely the result of equipment issues

or maintenance requirements, resulting in 56 months of data used for this analysis. Since both WC_{IN} and WC_{DIST} are believed to be equally valid estimates of the actual Welland Canal flow, the differences between them provide an additional estimate of the uncertainty.

A plot of the differences is shown in Figure 7-2. The mean and standard deviation of the two estimates are provided in Table 7-1. The maximum absolute difference between the two estimates was found to be $39.7 \text{ m}^3/\text{s}$. This is larger than the 95% confidence level estimated for either of the individual flow estimates individually. However, the root mean squared difference was found to be $14 \text{ m}^3/\text{s}$, or approximately 7% of the average Welland Canal flow. Using this as the standard error, the standard error of the mean of the two estimates is equal to $14/\sqrt{2} = 10 \text{ m}^3/\text{s}$, or approximately 4% of the Welland Canal flow, which is the same as the estimated uncertainty calculated above and helps confirm the results.

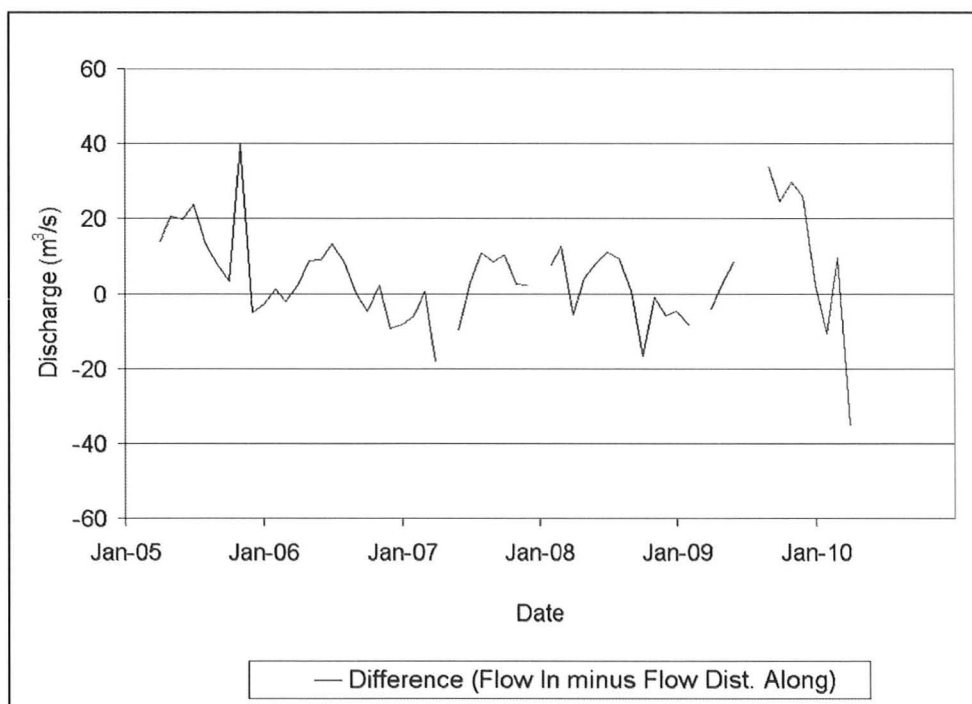


Figure 7-2: Difference in Welland Canal flow estimates (Apr. 2005 – Apr. 2010)

Table 7-1: Comparison of Welland Canal flow estimates (Apr. 2005 - Apr. 2010)

Flow Estimate	Mean (m ³ /s)	Standard Deviation (m ³ /s)
WC_{IN}	218	41
WC_{DIST}	214	36

7.6 Combined Uncertainty in Welland Canal Flows

The individual uncertainty estimates given for WC_{IN} and WC_{DIST} of 8% and 2%, respectively, might suggest that inclusion of the estimated flow into the Welland Canal increases the level of uncertainty in the total estimated Welland Canal flow. However, the previous analysis showed that the differences between the two estimates are greater than the uncertainty of either estimate individually. It is unclear what causes the differences. For example, it is known that local inflows along the length of the Welland Canal (from stormwater drainage, for example) will be accounted for in WC_{DIST} , but there may also be an unknown amount of leakage along the length of the canal. There may also be a small time lag between the flows measured as they enter the Welland Canal, and flows measured as they are distributed along the Welland Canal's length. These are just two examples, but regardless of the many possible causes, their effect on either flow estimate is unknown. The differences between the two Welland Canal flow estimates indicate that unknown systematic errors may exist at times. Furthermore, these errors may not be properly captured in the uncertainty estimates for the two flow estimates individually. By averaging the two estimates, the effects of any such errors are reduced. Therefore, unless these systematic errors can be identified, the two flow estimates should continue to be averaged to obtain the estimated total Welland Canal flow. From the previous analysis, a standard uncertainty estimate of 4% was determined to be reasonable for the estimated Welland Canal flow.

7.7 Alternative Welland Canal Flow Estimation Methods

In addition to the need to reduce errors in either Welland Canal flow estimate, it is useful to have both estimates available in order to reduce the chance of having periods of missing data. Recently this has occurred more often with the

flows into the Welland Canal, due to power interruptions, equipment failures or maintenance requirements of the supply weir SonTek ADCP. The two flow estimates also make it possible to make comparisons of flows into and distributed along the Welland Canal, often allowing potential problems with one or both datasets to be more easily identified.

Additional flow models could also be used to estimate the flow in the Welland Canal, and could again provide a check of the current estimates. For example, a rating equation, such as that which was used in the past, could still be used today and compared to the index-velocity rating. Furthermore, ADCPs and index-velocity ratings could be installed at a number of other locations, such as downstream of Lock 8 and the supply weir to measure the total flow into the Welland Canal, or at the actual diversion to the OPG De Cew power plants in order to provide an additional estimate of the true amount of water diverted from the canal at this location.

8 Sources and Estimates of Uncertainty in Detroit River Flow

8.1 Detroit River Overview

The Detroit River flow (I_{Det}) is determined using a combination of flow models, including a collection of rating equations and hydrodynamic models of the Detroit River, as well as using flow estimates determined for the St. Clair River by adjusting them for the monthly NBS and change in storage of Lake St. Clair (these adjustments are known as transfer factors). The actual combination of models used for any given month is complicated, and depends in part on the time period and conditions at the time of measurement. For example, only certain stage-fall-discharge equations can be used when ice is present in the Detroit River. The water resources engineers at the USACE and EC that are responsible for determining what they believe to be the best monthly flow estimates also use a considerable amount of judgement based on the data and information available to them. To simplify the uncertainty analysis for this study, only the uncertainty in stage-fall-discharge equations derived for both the Detroit and St. Clair rivers were estimated, as well as the uncertainty in the Lake St. Clair transfer factors. The overall uncertainty in the monthly Detroit River flows was inferred from these results.

8.2 Stage-Fall-Discharge Equations

Compared to the Niagara River, the Detroit River has a much more gradual slope. There is no specific control section in the Detroit River, but rather the flow is controlled by the characteristics of the entire channel reach. For this reason, a traditional stage-discharge equation relating water level to flow is inappropriate, and more complex techniques are required. Stage-fall-discharge equations are one such method.

Quinn (1979b) derived stage-fall-discharge equations and outlined methods of calibrating them for the Great Lakes connecting channels. Schmidt (2009) also examined the form of stage-fall-discharge equations used in the Great

Lakes. A number of stage-fall-discharge equations have been developed for the Detroit River using various water level gauges and gauge pairs. Figure 8-1 shows the location of available water level gauges on the Detroit River. The most recent equations were developed by the Coordinating Committee (Fay and Noorbakhsh, 2010) from a total of 212 ADCP discharge measurements collected from 1996 to 2006, and concurrent water level measurements collected at gauging stations along the Detroit River. These equations are given in Table 8-1. It should be noted that at the time of this research the stage-fall-discharge equations provided were designated as preliminary and are subject to change. In fact, these caveats are often applied to the flow equations and flow estimates determined by the Coordinating Committee, since both the equations and estimates themselves have been and continue to be revised as additional data and analyses are made available. Regardless, the equations presented here are the best available at the time of this research, and they provide a model for estimating the uncertainty in the Detroit River flows as they are currently computed.

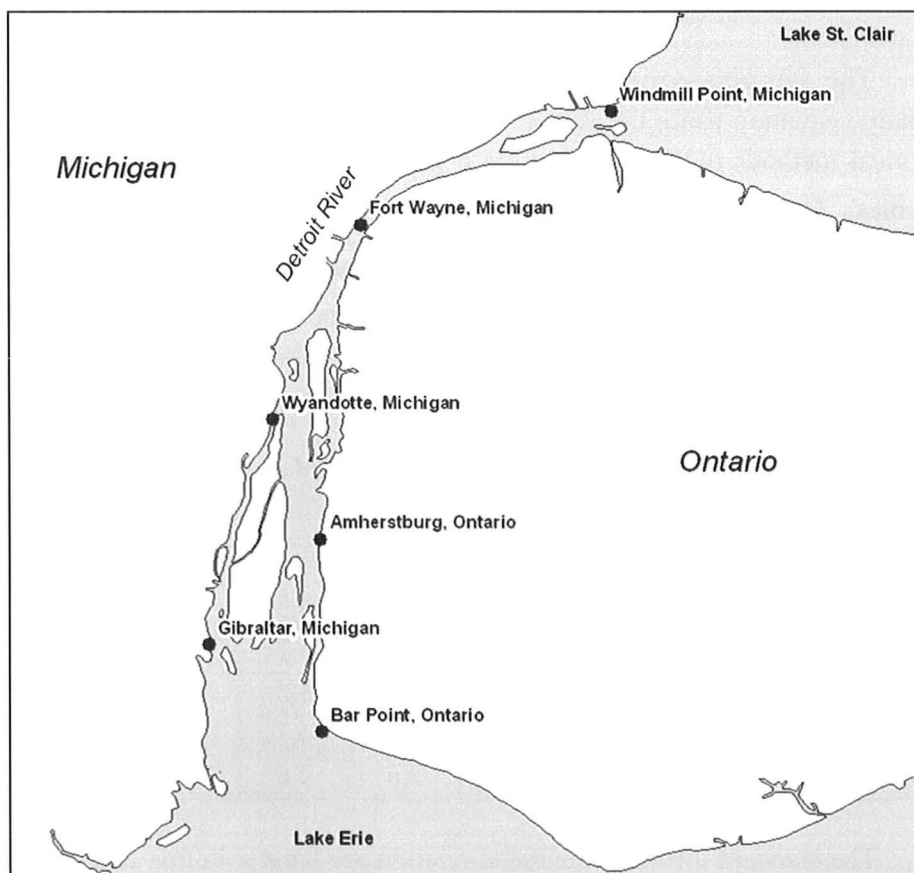


Figure 8-1: Detroit River water level gauges

Table 8-1: Detroit River stage-fall-discharge rating equations

Eqn	Gauge 1	Gauge 2	Equation
D.1	Windmill Point (h_{WP})	Fort Wayne (h_{FW})	$Q = 118.1081 \cdot (h_{WP} - 164)^{1.8364} \cdot (h_{WP} - h_{FW})^{0.3624}$
D.2	Windmill Point (h_{WP})	Wyandotte (h_{WY})	$Q = 99.1367 \cdot (h_{WP} - 164)^{1.8474} \cdot (h_{WP} - h_{WY})^{0.3718}$
D.3	Windmill Point (h_{WP})	Amherstburg (h_{AM})	$Q = 51.3625 \cdot (h_{WP} - 164)^{2.0851} \cdot (h_{WP} - h_{AM})^{0.3698}$
D.4	Fort Wayne (h_{FW})	Wyandotte (h_{WY})	$Q = 66.2808 \cdot (h_{FW} - 164)^{2.122} \cdot (h_{FW} - h_{WY})^{0.2943}$
D.5	Fort Wayne (h_{FW})	Amherstburg (h_{AM})	$Q = 23.5558 \cdot (h_{FW} - 164)^{2.4866} \cdot (h_{FW} - h_{AM})^{0.2906}$

The standard error of estimate (s) was calculated for each stage-fall-discharge equation using the ADCP data and corresponding water levels, and the statistical methods outlined in Section 5 for linear models having two predictor variables. The standard error of the mean relation ($sd(\hat{Y}_0)$) and standard error of observations ($sd(\hat{Y}_0)_{obs}$) were calculated for observed daily water levels at each gauge pair from 1994 to 2009, and the minimum and maximum of each are given along with the standard error of estimate in Table 8-2 below.

Table 8-2: Detroit River rating equation standard error estimates (%)

Eqn.	s	$sd(\hat{Y}_0)$			$sd(\hat{Y}_0)_{obs}$		
		Min	Mean	Max	Min	Mean	Max
D.1	3.3	0.2	0.4	2.5	3.3	3.3	4.1
D.2	3.2	0.2	0.4	2.0	3.2	3.2	3.8
D.3	3.5	0.2	0.4	2.1	3.5	3.5	4.0
D.4	4.1	0.3	0.5	2.6	4.1	4.2	4.9
D.5	4.6	0.3	0.5	2.6	4.6	4.6	5.3

The standard errors of the mean relation are greater in this case than those computed for the MOM pool flows. They also show a greater range, which is the

result of the second variable in the stage-fall-discharge equation being a measured fall (i.e. the water level upstream minus the water level downstream), which varies significantly about the mean, unlike the water levels themselves in the connecting channels, which have relatively less variability. For example, the coefficient of variation computed for the difference between water levels measured at Windmill Point and Fort Wayne during the ADCP gauged discharge measurements was approximately 15.2%, whereas the coefficient of variation for the measured water levels themselves at Windmill Point and Fort Wayne were each approximately 0.2%. For the same reason, the standard error of the observations also showed a greater range than those seen in the Niagara River. In determining the actual Detroit River flow, the current practice is to average the flows determined from the two best flow equations, which are assumed to be equations D.1 and D.2 based on their estimated standard errors and standard error of observations; regardless, averaging the flow equations will not reduce the uncertainty since the equations are likely highly correlated since they are based in part on the same water levels, and also on the same flows used for calibration. As proof of this, the standard error of estimate of the two-equation average was computed separately, and was found to be 3.1%, which is only slightly less than the standard errors of estimate computed for equations D.1 and D.2 individually.

Similar to the Niagara River MOM pool flow discussions already presented, in addition to model uncertainty, the uncertainty in Detroit River discharge resulting from uncertainty in the model's input variables must also be considered. In the case of a stage-fall-discharge equation, the model's input variables are the two water levels measured upstream and downstream. The uncertainty in discharge resulting from uncertainty in water levels was assessed for each equation. In the case of a stage-fall-discharge equation, uncertainty in water levels affects both the water level and slope portion of the equation. The Detroit River flows are determined from mean daily water levels rounded to the centimetre. The daily flows are then averaged for a month to obtain the monthly mean Detroit River flow used in the Lake Erie NBS computations. The uncertainty in the measured water levels was assumed to be equal to the uncertainty due to gauge accuracy, uncertainty due to rounding the daily water levels to the centimetre, and uncertainty in computing the mean of 24 hourly water levels. These errors were assumed to be uncorrelated. The error due to gauge accuracy is likely smaller than 1 cm, and since it can be assumed to be random, it would be reduced to a negligible level by averaging the 24 hourly readings. On the other hand, the daily mean water level is rounded to the

centimetre, not the hourly levels, so this error in the daily means level is not reduced by averaging, and can be represented by a uniformly distributed uncertainty estimate of +/- 0.5 cm, which corresponds to a standard uncertainty of $0.5/\sqrt{3} = 0.3$ cm. The uncertainty in the computed mean of the 24 hourly levels was determined for each gauge as the standard deviation of the hourly water levels, sd_{24-hr} , divided by the square root of 24 hours in a day. That is:

$$u(\bar{h}_d) = \frac{sd_{24-hr}}{\sqrt{24}} \quad (81)$$

The uncertainty in the mean daily water level was computed for each gauge using equation (81) and hourly water levels from the years 2000 to 2005. The results are provided in Table 8-3. The results varied by month, with the largest errors occurring in the fall and winter. It can also be noted that the errors increase moving downstream, with the largest errors observed at the Amherstburg gauge, which is likely a reflection of water level variability caused by backwater effects resulting from the water level of Lake Erie.

Table 8-3: Standard uncertainty in 24-hour mean Detroit River water levels

Month	Standard Uncertainty in Mean Water Level (m)			
	Windmill Point (WIPO)	Fort Wayne (FOWA)	Wyandotte (WYAN)	Amherstburg (AMHE)
1	0.003	0.004	0.006	0.006
2	0.003	0.005	0.006	0.007
3	0.005	0.006	0.007	0.008
4	0.004	0.005	0.006	0.006
5	0.003	0.005	0.005	0.006
6	0.002	0.003	0.003	0.004
7	0.002	0.003	0.003	0.003
8	0.002	0.002	0.003	0.003
9	0.002	0.003	0.004	0.005
10	0.004	0.005	0.007	0.007
11	0.004	0.006	0.007	0.008
12	0.004	0.006	0.008	0.009

The overall uncertainty in the daily flows resulting from all three sources can be determined by first computing the derivative of each stage-fall-discharge

equation. An example is provided for equation D.1, where the change in flow with respect to a change in Windmill Point (h_{WP}) water level is:

$$\frac{\partial Q}{\partial h_{WP}} = \frac{42.802 \cdot (h_{WP} - 164)^{1.8364}}{(h_{WP} - h_{FW})^{0.6376}} + 216.89 \cdot (h_{WP} - 164)^{0.8364} (h_{WP} - h_{FW})^{0.3624} \quad (82)$$

Furthermore, the change in flow with respect to a change in Fort Wayne (h_{FW}) water level is:

$$\frac{\partial Q}{\partial h_{FW}} = -\frac{42.802 \cdot (h_{WP} - 164)^{1.8364}}{(h_{WP} - h_{FW})^{0.6376}} \quad (83)$$

Based on a review of monthly data from 1960 to 2006, the approximate average water levels for Windmill Point and Fort Wayne were found to be approximately 175.10 m and 174.87 m, respectively. Substituting these values into equations (82) and (83), the rate of change in flow as a result of a change in Windmill Point water level is approximately 10,030 m³/s per metre, and the rate of change in flow as a result of a change in Fort Wayne water level is approximately -9080 m³/s per metre. These are the sensitivity coefficients for the upstream and downstream water levels, respectively. The sensitivity coefficients computed for the other equations are given in Table 8-4. Of note is that the coefficients are nearly equivalent in magnitude, but opposite in sign, a result of the form of the stage-fall-discharge equations used.

Table 8-4: Detroit River rating equation sensitivity coefficients

Water Level Gauge	Sensitivity Coefficient (m ³ /s per metre)				
	D.1: WIPO- FOWA	D.2: WIPO- WYAN	D.3: WIPO- AMHE	D.4: FOWA- WYAN	D.5: FOWA- AMHE
Upstream Gauge	10049	6955	5926	14200	9212
Downstream Gauge	-9096	-5992	-4852	-13078	-7925

The rounding errors affecting each daily water level can be assumed uncorrelated. However, the errors in the mean 24-hour water levels, as shown in Table 8-3, affect each gauge and were found to be highly correlated, with correlation coefficients found to be greater than 0.8 in all cases (Table 8-5). This is to be expected given that the same factors affecting water level and flow in the river affect each of the water level gauges. Using the correlation coefficients given, the combined standard uncertainty in discharge resulting from the uncertainty in water levels, $u(Q)_h$, can be computed from the simplified equation:

$$\begin{aligned}
 u^2(Q)_h &= \left(\frac{\partial Q}{\partial h_{u/s}} \right)^2 \cdot \left[\left(\frac{0.3}{100} \right)^2 + u^2(\bar{h}_{d,u/s}) \right] \\
 &+ \left(\frac{\partial Q}{\partial h_{d/s}} \right)^2 \cdot \left[\left(\frac{0.3}{100} \right)^2 + u^2(\bar{h}_{d,d/s}) \right] \\
 &+ 2 \cdot \left(\frac{\partial Q}{\partial h_{u/s}} \right) \left(\frac{\partial Q}{\partial h_{d/s}} \right) \cdot u(\bar{h}_{d,u/s}) \cdot u(\bar{h}_{d,d/s}) \cdot r(h_{u/s}, h_{d/s})
 \end{aligned} \tag{84}$$

where $\partial Q / \partial h_{u/s}$ and $\partial Q / \partial h_{d/s}$ are the sensitivity coefficients computed for the upstream and downstream water levels, respectively; $(0.3/100)^2$ represents the rounding error; $u(\bar{h}_{d,u/s})$ and $u(\bar{h}_{d,d/s})$ are the standard uncertainty in the mean 24-hour (daily) upstream and downstream water levels, respectively; and $r(\bar{h}_{u/s}, \bar{h}_{d/s})$ is the correlation coefficient. Using the results in Tables 8-3, 8-4 and 8-5, the uncertainty in discharge due to uncertainty in water levels was computed and is shown in Table 8-6. These uncertainty estimates are larger than that estimated to be due to uncertainty in the Ashland Avenue water level computed for the Niagara River MOM pool flow equation, a result of the greater uncertainty in the daily mean water levels than the hourly water levels, and relatively larger uncertainty in computing the difference between water levels than in computing the water levels individually. The uncertainty values are also fairly constant, reflecting the fact that the uncertainties in the upstream and downstream daily mean water levels have the effect of cancelling out to a large degree due to the correlation between these errors and the positive and negative sensitivity coefficients computed for the upstream and downstream gauges, respectively.

Table 8-5: Detroit River mean daily water level correlation coefficients

Gauge	WIPO	FOWA	WYAN	AMHE
WIPO	1.00	0.90	0.86	0.82
FOWA	0.90	1.00	0.99	0.97
WYAN	0.86	0.99	1.00	0.99
AMHE	0.82	0.97	0.99	1.00

Table 8-6: Detroit River combined standard uncertainty due to uncertainty in measured water levels

Month	Standard Uncertainty due to Uncertainty in WLs (m ³ /s)				
	D.1: WIPO- FOWA	D.2: WIPO- WYAN	D.3: WIPO- AMHE	D.4: FOWA- WYAN	D.5: FOWA- AMHE
Jan	44	33	30	58	38
Feb	46	35	32	58	38
Mar	47	36	32	58	38
Apr	45	34	29	57	37
May	44	32	28	57	37
Jun	42	30	26	56	36
Jul	42	30	25	56	36
Aug	42	29	25	56	36
Sep	42	30	27	57	36
Oct	46	35	31	58	38
Nov	47	36	32	58	39
Dec	48	39	36	59	41

In addition to the uncertainty that results from the water level measurement errors, the error that results from using daily water levels as opposed to a shorter time step was also assessed. Hourly water levels are more representative of the continuous flow fluctuations that occur in the Detroit River. They are also more representative of the time it takes to conduct a gauged flow measurement. Since gauged flow measurements are used to calibrate the stage-fall-discharge equations, it seems logical that the discharge equations developed from them are more representative of hourly flows than daily flows.

A comparison was made between monthly flows determined from daily water levels and those determined from hourly water levels for the 5-year period of 2000 to 2004. Uncertainty caused by using daily water levels instead of a shorter time period was found to cause an average bias of approximately $9 \text{ m}^3/\text{s}$ for equation D.1. That is, on average, the monthly flows determined from average daily water levels were found to be $9 \text{ m}^3/\text{s}$ greater than those determined from hourly water levels. The standard deviation of the differences was $4 \text{ m}^3/\text{s}$. The results were similar for equation D.2 and for the average of the two equations, with a bias of approximately $8 \text{ m}^3/\text{s}$ observed, having standard deviation of $4 \text{ m}^3/\text{s}$. The cause of these biases is the non-linearity of the stage-fall discharge model. As a simple example, given a non-linear function $y = f(x)$ having x to some exponent λ , it can be shown that $y = \sum x^\lambda$ is not equivalent to $y = (\sum x)^\lambda$. Again, since the gauged flows used to calibrate the model are collected in a much shorter time period than 24 hours, and usually closer to one hour, the stage-fall-discharge relationships will be more representative of hourly flows, and therefore the bias should be regarded as real and should be considered in addition to the random uncertainty caused by the deviations of the flow measurements from the model.

Similar to the Niagara River MOM pool flows, the combined uncertainty in the Detroit River flows estimated from stage-fall-discharge equations can be estimated using the methods outlined in Section 5.6. To determine the combined uncertainty, assumptions about whether the different sources of error are correlated or not need to be made. As stated the errors in the gauged discharge measurements were assumed to be fully correlated. Furthermore, the uncertainty in the mean relation (i.e. $sd(\hat{Y}_0)$), was assumed to be a constant value of 1%, which is a conservative estimate based on the average results shown in Table 8-2. As was done for the Niagara River MOM pool flow, this value was assumed fully correlated since the same stage-fall-discharge equations are used for each measurement. Furthermore, the standard error of estimate, s , was assumed to be a constant 3.2% for each equation and the average of equations D.1 and D.2. Assuming this error and the errors in the predictor variables to be fully correlated gives the maximum standard uncertainty estimates for each equation. As an example, the uncertainty due to water levels determined from equation D.1 was found to be a maximum during December when it was found to be $48 \text{ m}^3/\text{s}$, which is approximately 1% of the average Detroit River discharge. The combined

standard uncertainty for this month for equation D.1 would therefore be computed as:

$$u(Q_{D,1}) = (0.025^2 + 0.032^2 + 0.01^2 + 0.01^2)^{0.5} = 4.3\%$$

Alternatively, if the errors are assumed uncorrelated, the minimum uncertainty estimate is obtained, since random model errors represented by the standard error of estimate and uncertainties due to model variables are reduced by averaging. Since daily water levels are used to estimate daily flows, which are then averaged for the entire month (approximately 30 days), the minimum uncertainty estimate for the month of December for equation D.1 is 2.8%. That is:

$$u(Q_{D,1}) = \sqrt{0.025^2 + \left(\frac{0.032}{\sqrt{30}}\right)^2 + 0.01^2 + \left(\frac{0.01}{\sqrt{30}}\right)^2} = 2.8\%$$

Essentially the random uncertainties in the model and in the predictor variables cancel out due to the daily measurements being averaged for each month. The overall uncertainty is dominated by the uncertainty from the ADCP measurements used to calibrate the equation. The random component of the uncertainty in this case (i.e. the combined random model uncertainty and predictor variable uncertainty) would be less than 1%. Again, it seems unlikely that there would be so little residual random error in the monthly flow estimates, although, unlike the Niagara River MOM pool flows, the Detroit River flows are not managed in any way, and therefore all scatter could be assumed the result of natural variability. Nonetheless, the estimate for the random component of less than 1% intuitively seems too small, and calls into question the assumption that the errors are entirely random and uncorrelated.

The discharge measurements on the Detroit River are not collected consecutively as at the cableway on the Niagara River: on the Niagara River, the flow that currently passes over Niagara Falls and through the MOM pool can be adjusted, whereas on the Detroit River, the flow is relatively steady and consecutive measurements would give similar flow estimates. Therefore, a review of consecutive ADCP discharge measurements used to calibrate the Detroit River equations as was performed for the MOM pool was not possible.

Instead, the flows estimated from each of the different stage-fall-discharge rating equations were compared to each other. Since it has been assumed that errors in the ADCP gauged discharge measurements are fully correlated, they will affect each rating equation approximately equally, since each equation was calibrated using the same discharge measurements. Also, any random error in the ADCP discharge measurements should cancel out due to the large number of measurements used in the calibration process. Therefore, any differences in flow estimated from the different rating equations should be entirely the result of errors in the models and the predictor variables.

Monthly flows were computed from daily water levels for the period of 1994-2009 for each of the five Detroit River rating equations. Flows computed in the winter months can differ significantly due to ice effects in the Detroit River, and this is dealt with differently, so only the non-winter months were considered in this analysis. The average difference and root mean squared deviation found for each pair of equations was computed for each month of April to November. The results are given in Tables 8-7 and 8-8, respectively.

Table 8-7: Mean difference in Detroit River flow estimates (1994-2009)

Month	Average Difference (%)									
	D.1 - D.2	D.1 - D.3	D.1 - D.4	D.1 - D.5	D.2 - D.3	D.2 - D.4	D.2 - D.5	D.3 - D.4	D.3 - D.5	D.4 - D.5
Apr	0.5	1.1	0.3	0.9	0.6	-0.3	0.4	-0.8	-0.2	0.6
May	0.4	0.7	0.2	0.4	0.3	-0.3	-0.1	-0.5	-0.3	0.2
Jun	0.3	0.1	-0.2	-0.5	-0.1	-0.4	-0.7	-0.3	-0.6	-0.3
Jul	0.0	-0.4	-0.6	-1.3	-0.4	-0.7	-1.4	-0.3	-0.9	-0.7
Aug	0.2	-0.7	-0.1	-1.6	-0.9	-0.3	-1.8	0.6	-1.0	-1.6
Sep	0.0	-0.8	-0.2	-1.5	-0.8	-0.2	-1.5	0.6	-0.7	-1.3
Oct	-0.3	-0.3	-0.1	0.1	0.0	0.2	0.4	0.2	0.4	0.2
Nov	-0.3	0.3	0.6	1.9	0.7	0.9	2.2	0.2	1.5	1.3

Table 8-8: Root mean squared deviation in Detroit River flow estimates (1994-2009)

Month	Root Mean Square Deviation (%)									
	D.1 - D.2	D.1 - D.3	D.1 - D.4	D.1 - D.5	D.2 - D.3	D.2 - D.4	D.2 - D.5	D.3 - D.4	D.3 - D.5	D.1 - D.2
Apr	0.8	1.3	1.6	1.8	0.7	1.2	1.4	1.4	1.2	0.9
May	0.7	0.8	1.6	1.5	0.4	1.2	1.4	1.3	1.3	0.7
Jun	0.5	0.5	1.4	1.4	0.4	1.1	1.3	1.1	1.1	0.8
Jul	0.5	0.6	1.3	1.7	0.5	1.1	1.7	0.9	1.3	1.0
Aug	0.6	0.9	1.4	2.1	1.0	1.0	2.2	1.1	1.3	1.8
Sep	0.6	1.0	1.5	2.0	0.9	1.1	2.0	1.3	1.2	1.6
Oct	0.7	0.8	1.4	1.1	0.4	0.9	0.9	1.1	0.8	0.9
Nov	0.7	0.7	1.5	2.2	0.8	1.3	2.4	1.1	1.7	1.4

Table 8-7 shows that the ratings are biased to a certain degree, depending on the month, with the average differences between ratings being less than 2% in all cases. Furthermore, there also appears to be a seasonal component to the bias, with the average differences being positive or negative for consecutive months. These biases will be partly accounted for by the standard errors of the mean relation, lending further proof that this component of the uncertainty estimate should be considered fully correlated. Also, the largest differences involve equation D.5, which is not normally used in computing the Detroit River flow. Table 8-8 indicates that the root mean squared difference between ratings is also normally less than 2%, with only six months having values greater than this, and all of these involved equation D.5.

If the random component of the uncertainty in the stage-discharge equations is assumed to be 1% after averaging, the uncertainty in the difference between equations would be $\sqrt{0.01^2 + 0.01^2} = 1.4\%$. This is close to the root mean squared deviations calculated in Table 8-8, and would seem to support the assumption that model errors caused by natural variability of the channel flow are random and uncorrelated, and therefore reduced by averaging over the course of a month.

However, this assumption also implies that further reduction in error could be gained by computing the flows on a smaller time-scale, e.g. hourly as opposed to daily. A similar analysis as that performed on the daily flows was performed on a shorter period of 5 years of hourly data (2000-2004). The monthly flows

determined from hourly data for each of the different equations were compared. The results were fairly similar to the daily analysis. The values of the root mean squared deviations for the different equations were approximately 1%, and therefore did not appear to be reduced below the values computed from the daily water levels and flows. It is possible that on a shorter term basis some of the errors are correlated: for example, during a wind event on Lake Erie, backwater effects may cause persistent errors in water levels and flows that would be correlated such that if the wind event lasted for a sufficiently long period of time, the errors in discharge estimated from the rating during that period would be correlated and would not be reduced by averaging.

Nonetheless, overall this analysis indicates that while the error in discharge may be uncorrelated and reduced in part by averaging flows measured over a month, it may be unsafe to assume this in all cases. Therefore, for the two-equation average discharge determined from equations D.1 and D.2, the maximum standard uncertainty estimate determined for equation D.1 of approximately 4.3% was used, which corresponds to approximately 8.6% at the 95% confidence level.

8.3 Flow Transfers

In addition to the Detroit River stage-fall-discharge equations, the total Detroit River flow is also estimated using the monthly St. Clair River flows transferred to the Detroit River using what are known as transfer factors (TF). The transfer factors are determined from the Lake St. Clair water balance, and can be computed as:

$$TF = P + R - E - \Delta S \quad (85)$$

where P , R and E are the monthly precipitation, runoff and evaporation to Lake St. Clair, respectively; and ΔS is the monthly Lake St. Clair change in storage. Since $P + R - E = NBS$, this equation can also be written as:

$$TF = NBS - \Delta S \quad (86)$$

The monthly Detroit River flow (Q_{DET}) is then estimated from:

$$Q_{DET} = Q_{SC} + TF \quad (87)$$

where Q_{SC} is the monthly St. Clair River flow. In order to determine the uncertainty in this estimate of Detroit River flow, the uncertainty in each component must be computed.

Similar to the Detroit River, the St. Clair River flows are determined from a combination of flow models. This includes the use of stage-fall-discharge equations, which have been developed for a number of gauge pairs on the St. Clair River. A map of the St. Clair River gauge locations is shown in Figure 8-2. The most recently coordinated stage-fall-discharge equations were developed by Fay and Noorbakhsh (2010). There are a total of 18 equations for the St. Clair River (Table 8-9), with the choice of which to use depending on data availability and ice conditions in the river. Specifically, for the most recent flow estimates on the St. Clair River, equations S.1 and S.2 (Group A) were averaged during ice-free conditions whenever data were available; equations S.3 through S.10 (Group B) were averaged during ice-free conditions whenever data were unavailable to compute S.1 or S.2; equations S.11 through S.15 (Group C) were averaged whenever ice occurred between Algonac and St. Clair State Police gauges; and equations S.16 through S.18 (Group D) were averaged whenever ice occurred at or above the St. Clair State Police gauge (Fay and Noorbakhsh, 2010). Due to the higher velocities in the channel, ice effects do not normally impact upstream water levels in the St. Clair River, which explains the use of the upstream water levels only in equations S.11 through S.18.

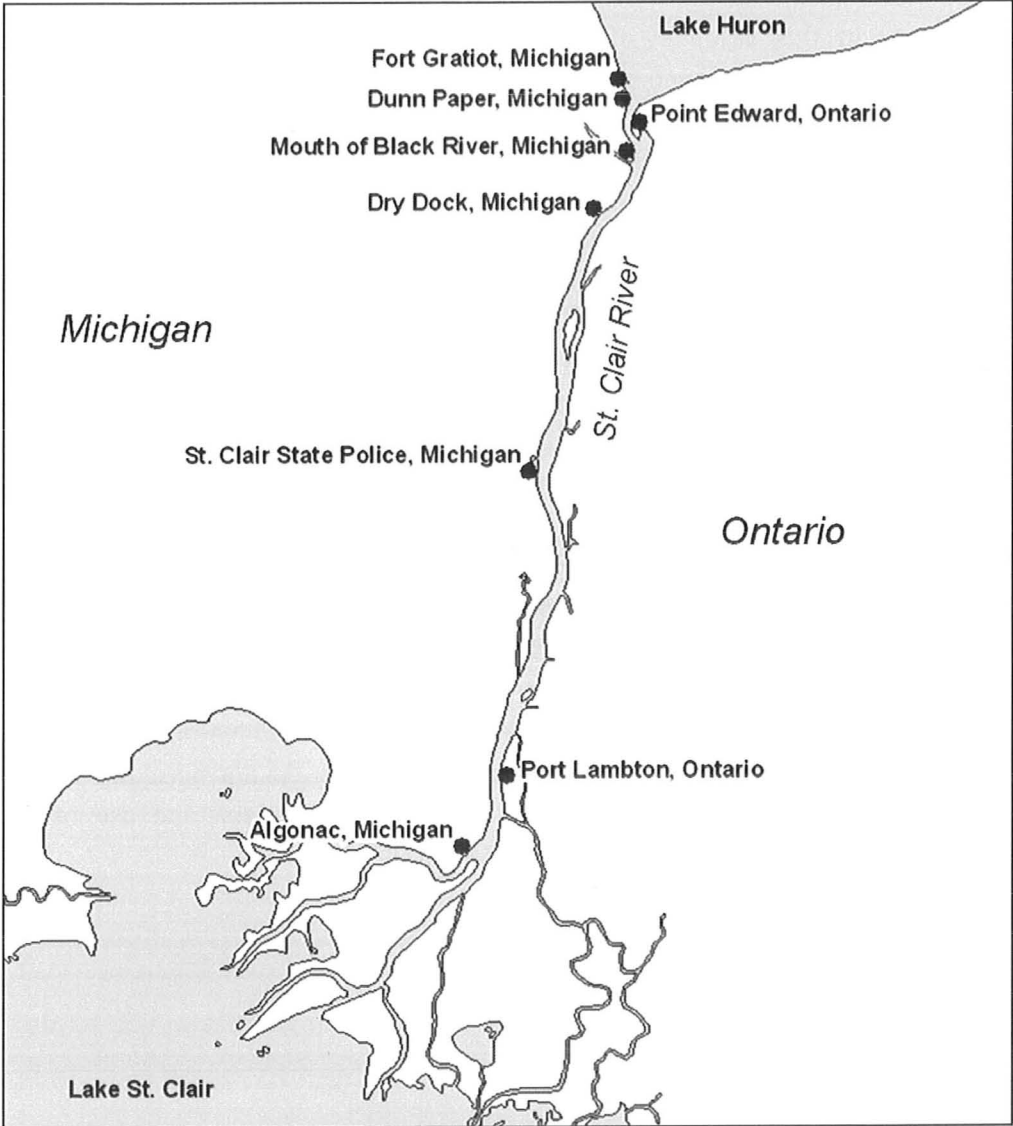


Figure 8-2: St. Clair River water level gauges

Table 8-9: St. Clair River stage-fall-discharge rating equations

Eqn.	Group	Gauge 1	Gauge 2	Equation	Usage
S.1	A	Fort Gratiot (h_{FG})	Port Lambton (h_{PL})	$Q = 497.5476 \cdot (h_{PL} - 167)^{1.1244} \cdot (h_{FG} - h_{PL})^{0.5072}$	Averaged during ice-free conditions when data were available
S.2		Fort Gratiot (h_{FG})	Algonac (h_{AL})	$Q = 478.3803 \cdot (h_{AL} - 167)^{1.1342} \cdot (h_{FG} - h_{AL})^{0.5187}$	
S.3	B	Dunn Paper (h_{DP})	Port Lambton (h_{PL})	$Q = 429.7046 \cdot (h_{PL} - 167)^{1.2242} \cdot (h_{DP} - h_{PL})^{0.5173}$	Averaged during ice-free conditions when data were unavailable to compute S.1 or S.2
S.4		Dunn Paper (h_{DP})	Algonac (h_{AL})	$Q = 401.7882 \cdot (h_{AL} - 167)^{1.2461} \cdot (h_{DP} - h_{AL})^{0.5240}$	
S.5		Mouth Black R. (h_{MBR})	Port Lambton (h_{PL})	$Q = 392.4165 \cdot (h_{PL} - 167)^{1.2945} \cdot (h_{MBR} - h_{PL})^{0.5295}$	
S.6		Mouth Black R. (h_{MBR})	Algonac (h_{AL})	$Q = 367.8937 \cdot (h_{AL} - 167)^{1.3141} \cdot (h_{MBR} - h_{AL})^{0.5392}$	
S.7		Dry Dock (h_{DD})	Port Lambton (h_{PL})	$Q = 454.7937 \cdot (h_{PL} - 167)^{1.2580} \cdot (h_{DD} - h_{PL})^{0.5148}$	
S.8		Dry Dock (h_{DD})	Algonac (h_{AL})	$Q = 408.6712 \cdot (h_{AL} - 167)^{1.2951} \cdot (h_{DD} - h_{AL})^{0.5162}$	
S.9		Point Edward (h_{PE})	Port Lambton (h_{PL})	$Q = 334.5477 \cdot (h_{PL} - 167)^{1.3619} \cdot (h_{PE} - h_{PL})^{0.5362}$	
S.10		Point Edward (h_{PE})	Algonac (h_{AL})	$Q = 323.1508 \cdot (h_{AL} - 167)^{1.3680} \cdot (h_{PE} - h_{AL})^{0.5497}$	
S.11	C	Fort Gratiot (h_{FG})	St. Clair St. Police (h_{SCP})	$Q = 511.0261 \cdot (h_{SCP} - 167)^{1.1792} \cdot (h_{FG} - h_{SCP})^{0.4557}$	Averaged whenever ice occurred between Algonac and St. Clair State Police gauges
S.12		Fort Gratiot (h_{FG})	St. Clair St. Police (h_{SCP})	$Q = 371.8869 \cdot (h_{FG} - 167)^{1.2663} \cdot (h_{FG} - h_{SCP})^{0.3673}$	
S.13		Dunn Paper (h_{DP})	St. Clair St. Police (h_{SCP})	$Q = 292.1239 \cdot (h_{SCP} - 167)^{1.4495} \cdot (h_{DP} - h_{SCP})^{0.3556}$	
S.14		Mouth Black R. (h_{MBR})	St. Clair St. Police (h_{SCP})	$Q = 375.9090 \cdot (h_{SCP} - 167)^{1.4024} \cdot (h_{MBR} - h_{SCP})^{0.4532}$	
S.15		Point Edward (h_{PE})	St. Clair St. Police (h_{SCP})	$Q = 260.6836 \cdot (h_{PE} - 167)^{1.5509} \cdot (h_{PE} - h_{SCP})^{0.4279}$	
S.16	D	Fort Gratiot (h_{FG})	Mouth Black R. (h_{MBR})	$Q = 340.4156 \cdot (h_{MBR} - 167)^{1.4123} \cdot (h_{FG} - h_{MBR})^{0.2322}$	Averaged whenever ice occurred at or above St. Clair State Police gauge
S.17		Fort Gratiot (h_{FG})	Dry Dock (h_{DD})	$Q = 458.5184 \cdot (h_{DD} - 167)^{1.2932} \cdot (h_{FG} - h_{DD})^{0.3295}$	
S.18		Fort Gratiot (h_{FG})	Dry Dock (h_{DD})	$Q = 378.2970 \cdot (h_{FG} - 167)^{1.3363} \cdot (h_{FG} - h_{DD})^{0.2849}$	

The uncertainty in each of the St. Clair River stage-fall-discharge equations was determined in a similar manner as was done for the Detroit River, with ADCP gauged discharge measurements collected from 1996 to 2006 in the St. Clair River used to evaluate the standard error, and daily water levels from 1994-2009 used to evaluate the standard error of the mean relation and standard error of observations. The results are given in Table 8-10.

Table 8-10: St. Clair River rating equation standard error estimates (%)

Eqn.	Group	s	$sd(\hat{Y}_0)$			$sd(\hat{Y}_0)_{obs}$		
			Min	Mean	Max	Min	Mean	Max
S.1	A	3.14	0.21	0.42	2.56	3.15	3.18	4.05
S.2		3.63	0.24	0.45	2.17	3.64	3.66	4.23
S.3	B	3.01	0.20	0.40	2.36	3.01	3.04	3.82
S.4		3.51	0.23	0.44	2.17	3.51	3.54	4.13
S.5		3.13	0.21	0.41	2.39	3.14	3.17	3.94
S.6		3.64	0.24	0.45	2.47	3.65	3.68	4.40
S.7		2.92	0.19	0.39	2.23	2.93	2.95	3.67
S.8		3.41	0.23	0.44	2.55	3.42	3.44	4.26
S.9		3.59	0.23	0.47	2.76	3.60	3.63	4.53
S.10		3.52	0.23	0.44	2.42	3.53	3.56	4.28
S.11	C	3.74	0.25	0.53	5.46	3.74	3.80	6.61
S.12		3.74	0.25	0.54	5.81	3.74	3.80	6.91
S.13		3.72	0.24	0.52	5.28	3.73	3.78	6.46
S.14		3.84	0.25	0.54	5.60	3.85	3.90	6.79
S.15		4.06	0.26	0.56	5.87	4.07	4.12	7.14
S.16	D	3.88	0.26	0.52	6.92	3.89	3.94	7.94
S.17		3.61	0.24	0.50	6.34	3.62	3.67	7.30
S.18		3.62	0.24	0.51	6.63	3.63	3.68	7.56

A number of important points can be noted. First the standard errors of estimate (s) were for the most part between approximately 3 and 4%, which is similar to the Detroit River standard error estimates. Furthermore, the standard errors of the mean relation ($sd(\hat{Y}_0)$) and standard errors of observations ($sd(\hat{Y}_0)_{obs}$) were also of a similar magnitude for all equations. It can be noted, however, that all of the standard errors tended to be greater for the equations used

only during ice effects (i.e. equations S.11 through S.18), which is the result of the slope estimate being more uncertain due to the smaller distance between gauge pairs used in these equations. This is especially true for the maximum $sd(\hat{Y}_0)_{obs}$ computed for each equation, which were found to be greater than 7% in some cases. Nonetheless, overall the differences in the mean $sd(\hat{Y}_0)_{obs}$ were not very large, ranging from about 3 to 4%, regardless of the equation used. Also of note is that those equations using Port Lambton as the downstream gauge (such as S.1 for example) tended to have smaller error estimates than those using Algonac (such as S.2 for example). This might be a reflection of backwater effects from Lake St. Clair and the St. Clair Delta at Algonac. Overall, the results were quite similar to the Detroit River stage-fall-discharge equations, and a standard uncertainty estimate of 4.3% was used for the St. Clair River flows for the remainder of this analysis.

Transfer factors have been computed in the past by Quinn (1976) and more recently under the auspices of the Coordinating Committee. The more recent coordinated flow transfer factors are computed using Lake St. Clair monthly NBS estimates determined from a revised version of the component method (Rob Caldwell, EC, written communication, 13 August, 2010). Precipitation has been determined from basin gauge averages or from NOAA GLERL estimates. Runoff is calculated from Lake St. Clair tributaries in Canada (Thames River at Thamesville and Sydenham River at Florence) and the United States (Clinton River at Mt. Clemens), with the runoff from these gauged portions of the basin extrapolated to the ungauged portion using area ratios. Additionally, the Rouge River, which is a tributary to the Detroit River, has been included in some transfer factor computations to account for backwater effects on Lake St. Clair that affect the recorded change in storage. Evaporation has been computed using a simplified mass transfer method adapted from Derecki (1976), which relates lake evaporation to surface water temperature, vapour pressure, and wind speed.

Alternatively, GLERL component NBS estimates have been used to compute the transfer factors (Nanette Noorbakhsh, USACE, personal communication, 6 July, 2010). According to De Marchi et al. (2009), uncertainty in GLERL component monthly NBS estimates for Lake St. Clair ranges from approximately -22% to 31% on average at the 95% confidence level, which corresponds to approximately -30 to 50 m³/s for an average Lake St. Clair NBS

estimate of approximately 150 m³/s. De Marchi et al. (2009) also identified a bias of approximately 8.3%, which corresponds to about 12 m³/s, indicating that the GLERL component NBS may be underestimated. These results are specific to the GLERL NBS model, and do not necessarily apply to the coordinated transfer factors described above; however, a comparison of the transfer factors determined using the GLERL NBS and the NBS used in the coordinated transfer factors for the period 1987-2005 showed the coordinated values to be 21 m³/s less than the GLERL values on average, and the root mean squared deviation was calculated as 50 m³/s. Since the uncertainty analysis results presented by De Marchi et al. (2009) were greater than the GLERL deterministic results, the coordinated values would appear to be even further underestimated. The sum of the 12 m³/s found by De Marchi et al. (2009) and the 21 m³/s found by comparing the GLERL and coordinated transfer factors is approximately 30 m³/s, or 20% of the assumed average. Furthermore, an uncertainty estimate of 30% at the 95% confidence level in either NBS estimate used to compute the transfer factors seems like a reasonable assumption given the results presented.

A full analysis of the uncertainty in Lake St. Clair change in storage was not performed; however, based on the analysis of uncertainty in Lake Erie change in storage presented in Section 9, the total standard uncertainty in the monthly Lake St. Clair change in storage was assumed to be 2 cm, or 4 cm at the 95% confidence level, which corresponds to about 10 and 20 m³/s, respectively, when the area of Lake St. Clair and the number of days in a month are included.

Assuming the errors are uncorrelated, the total uncertainty in the Detroit River flows determined from the St. Clair River flows and the Lake St. Clair transfer factors can be found from:

$$u^2(Q_{DET}) = u^2(Q_{SC}) + u^2(NBS_{LSC}) + u^2(\Delta S_{LSC}) \quad (88)$$

where $u(Q_{DET})$ is the standard uncertainty in the Detroit River flow estimates; $u(Q_{SC})$ is the standard uncertainty in the St. Clair River flow estimates; $u(NBS_{LSC})$ is the standard uncertainty in the Lake St. Clair NBS; and $u(\Delta S_{LSC})$ is the standard uncertainty in the Lake St. Clair change in storage. Given that the average St. Clair River flow is approximately 5000 m³/s, the value of $u(Q_{SC})$ in discharge units is approximately 400 m³/s at the 95% confidence level. Even using conservative estimates of 50 m³/s and 20 m³/s for $u(NBS_{LSC})$ and $u(\Delta S_{LSC})$,

respectively, does not significantly increase the overall uncertainty in the Detroit River flows over that of the St. Clair River flow alone. Therefore, it can be assumed that the uncertainty in the Detroit River flows determined from the St. Clair River flows and transfer factors is the same as the Detroit River stage-fall-discharge equation uncertainty estimate of approximately 4.3%. However, the possible bias caused by underestimating the Lake St. Clair NBS should be given consideration in comparisons of the different Detroit River flow estimates.

Lastly, a comparison of the different flow estimates for the 1994-2005 period was made. The flows compared were the flows from the Detroit River stage-fall-discharge equations (D.1 and D.2), and the flows determined from the coordinated St. Clair River flows plus both the coordinated and GLERL transfer factors. The root mean squared difference was approximately 2%, which falls well within the 4.3% uncertainty estimated for each flow estimate individually. This helps confirm that the uncertainty estimate of 4.3% is adequate, and suggests that it may in fact be overestimated.

8.4 Additional Sources of Error

The preceding analysis investigated random errors in estimating flows in the Detroit River stage-fall-discharge equations, as well as the St. Clair River equations and transfer factors. These errors are those that occur due to natural variability and random errors in measuring water level and flow. Additional systematic impacts can cause additional errors, and these are often greater than the random errors described above.

One such source of systematic error is the effect of ice on flows computed with the stage-fall-discharge equations. Ice buildup in the channel retards flow by causing a decrease in the cross-sectional area and increased channel roughness. In the Detroit River, ice normally affects only the lower reaches of the channel. When ice affects the lower reaches, current practice is to only use equation D.1 to estimate the flow, since it only uses water levels from the more upstream gauges. The flows in the St. Clair River are estimated with a similar approach by using only the upper reach equations when ice affects water levels and flows in the lower reaches of the river. The approach of using certain upper reach equations under ice affected conditions should not cause a significant increase in the uncertainty in the measured flow in the Detroit River, since the uncertainty

estimated for equation D.1 was found to be about the same or better than the other equations, and nearly the same as the average of equations D.1 and D.2. This assumes that the gauged discharge measurements collected in the non-winter months would be equally applicable during winter as they are when collected, but unfortunately gauged discharge measurements are not collected in the winter to confirm this assumption. Furthermore, other than in January and February, the number of days that ice affects the flow in the Detroit and St. Clair rivers is small (Table 8-11).

Table 8-11: Number of days flows were affected each month by ice

Month	Detroit River (1994-2009)			St. Clair River (1987-2006)		
	Mean	SD	Max	Mean	SD	Max
Jan	12	10	27	8	9	29
Feb	9	8	24	7	8	28
Mar	1	2	9	2	3	10
Apr	0	0	0	1	4	18
May	0	0	0	0	0	0
Jun	0	0	0	0	0	0
Jul	0	0	0	0	0	0
Aug	0	0	0	0	0	0
Sep	0	0	0	0	0	0
Oct	0	0	0	0	0	0
Nov	0	0	0	0	0	0
Dec	2	4	15	1	3	11

Of greater concern are the occurrences of ice jams which affect the entire river. Under these circumstances, no gauge pairs can be used to accurately estimate flow, and the uncertainty in the flow estimates is likely much greater, possibly even 40 to 50% based on an unpublished analysis of data performed by EC during a recent ice jam that occurred in the St. Clair River in January and February 2010. However, ice jams occur very rarely, and are not known to be a concern in the Detroit River. That said, when an ice jam occurs in the St. Clair River, the water levels and flows in the Detroit River can drop well below the range of flows measured during the establishment of the rating curve. For example, during the January and February 2010 St. Clair River ice jam, Detroit

River flows dropped below the minimum gauged discharge measurement used in the rating calibrations of 4325 m³/s for six days in January, 17 days in February and four days in March. During these extreme flow scenarios it would be expected that the uncertainty would be somewhat greater than during more average conditions. This should be considered during ice jam occurrences, but given the rareness of ice jams the uncertainty estimates for the Detroit and St. Clair River flows were not increased for any month.

Similarly, weed effects can also affect flow. However, like ice effects, in the Detroit River, weeds tend only to be a concern in the shallower lower reaches of the channel. Furthermore, while most flow measurements have been collected in spring and fall, when weeds are unlikely to have a significant effect, some flow measurements have also been collected in the months of June and early September on the Detroit River. The standard error of estimate computed for these measurements alone was similar in magnitude to that computed for the full set of measurements, and therefore the effects of weeds are likely adequately captured in the deviations from the stage-fall-discharge equations and are not of specific concern.

An additional source of systematic error that occurs in the Detroit River is the phenomenon of flow reversals during certain storm events on Lake Erie. Detroit River flows have been known to reverse, but this occurs extremely rarely, normally only during ice jams on the St. Clair River, and the flow reversals appear to last less than 12 hours (Quinn, 1988). Therefore, while on a short term basis the flow in the Detroit River will be subject to considerable error, flow reversals are not a significant source of uncertainty in the monthly Detroit River flow estimates.

A final source of systematic error, and perhaps the greatest source, is the impact of changes to the channel itself. These can result from channel erosion, deposition, dredging, shipwrecks, etc. For the most part, other than recognized dredging for the purposes of navigation, the St. Clair and Detroit River channels have been assumed relatively stable in the past, with natural channel changes and their effects on flows assumed negligible. However, recent studies on the St. Clair River have shown that this assumption may not be valid (IUGLSB, 2009). The analyses presented in this research have assumed that the channel conditions have remained constant. The uncertainty in the estimated flows will increase substantially if channel changes occur and are not identified. If flow

measurements are conducted consistently and on a regular basis, possible channel changes can be identified, and the flows adjusted accordingly; however, channel changes may be overlooked during long periods where no gauged flow measurements are conducted, and furthermore, estimating the flow uncertainty during these periods will be nearly impossible due to the lack of data. Therefore, while uncertainty in flows is likely greater during periods of missing gauged measurements, estimating how much greater is not possible.

8.5 Combined Uncertainty in Detroit River Flows

As stated, determination of the monthly Detroit River flows is quite complicated. Monthly flows are coordinated by engineers from both Canada and the United States, who determine the final estimate based on averaging and comparisons of flows as determined from a number of different flow models, which primarily includes stage-fall-discharge equations and flow transfers as described, as well as whatever additional information is available on ice effects, channel changes and other factors that may be believed to affect flow at any given time (Fay and Noorbakhsh, 2010). As such, determining the combined uncertainty in the Detroit River flows is not straightforward. The maximum standard uncertainty of 4.3% estimated for the stage-fall-discharge equations, which is assumed to be a conservative estimate, was therefore assumed for the uncertainty in the Detroit River flows.

8.6 Alternative Detroit River Flow Estimation Methods

There are a number of alternative models that could be used to determine flows in the Detroit River, and some of these methods are already being applied. In the near future, the most promising alternative may be the use of a horizontal ADCP and associated index-velocity rating. A horizontal ADCP has recently been installed in the Detroit River (IUGLSB, 2009). This will give an additional continuous flow estimate that can be compared to current methods for measuring flow. It will be especially useful for measuring flow during winter and under ice conditions, and for assessing the impacts of weed growth. Furthermore, the ADCP index-velocity flows will provide an estimate of flow at a specific cross-section, which may help separate out the effects of local inflows to the Detroit River entering upstream and downstream.

It must be noted, however, that because the Great Lakes naturally regulate flow in the connecting channels, including the St. Clair and Detroit rivers, the flow does not vary significantly over the course of a year, and can remain relatively similar in magnitude for many years at a time. For this reason it could take a long time to establish the index-velocity rating at a broad range of water levels and flows. Furthermore, if the horizontal ADCP is altered or replaced for any reason, the calibration may be affected, and the process may even need to be started again from the beginning. Once established, the flows determined from the index-velocity rating will of course be subject to uncertainty and errors of their own: they will provide an additional flow estimate, which may or may not be more accurate than the existing methods. Therefore, by no means does the horizontal ADCP and index-velocity rating represent a replacement for the current methods used to determine Detroit River flows. Rather, they provide an additional technique which will compliment the combination of flow measurement methods already in use.

The use of HPGs is also a promising method for measuring connecting channel flow. Being based on the results of hydrodynamic models, HPGs provide a flow estimate using measured water levels as predictors that theoretically should better capture the physics and hydrodynamic processes taking place in the channel. In this way they are believed to reduce the uncertainty resulting from using a model which does not capture these dynamic processes; however, the HPGs will also be subject to the uncertainty resulting from the assumptions and parameters used to develop the hydrodynamic model on which they are based.

Hydrodynamic models themselves may be a promising means of estimating flow in the St. Clair and Detroit rivers. They could also be used to help solve some of the issues in the St. Clair and Detroit rivers regarding continuity and mass balance of flow. Specifically, a hydrodynamic model could be used to perform a sensitivity analysis to estimate the effects of local inflows on measured water levels and flows determined using stage-fall-discharge equations, HPGs or other models. Such an analysis could also determine the effects of local tributary flows on the change in storage on Lake St. Clair, which will help determine what tributary flows to use to compute runoff to Lake St. Clair for determining transfer factors if they are to continue to be used in the future for computing Detroit River flows.

Lastly, no matter what flow model is used, it is important that gauged flow measurements be collected on a set schedule and using best available methods and standards. The various flow models being used or proposed for the Detroit and St. Clair rivers will only be as accurate as the flow measurements they are based on. Furthermore, changes in the channel might not be identified unless flow measurements are collected on a regular basis. This is especially important because channel changes represent one of the greatest sources of uncertainty in flow measurement, and one that cannot be accounted for or reduced unless identified in a timely fashion.

9 Sources and Estimates of Uncertainty in Change in Storage

9.1 Change in Storage Overview

Uncertainty in the computed change in storage results from a number of factors. Quinn (2009) suggested that uncertainty in BOM water levels for Lake Superior was due to three components: uncertainty due to the accuracy of water levels measured at individual gauges; uncertainty resulting from using the two-day average to represent the instantaneous BOM water level; and uncertainty resulting from using the average of the gauged water levels to represent the true lake-wide average water level. A schematic showing the second and third of these sources of error is given in Figure 9-1.

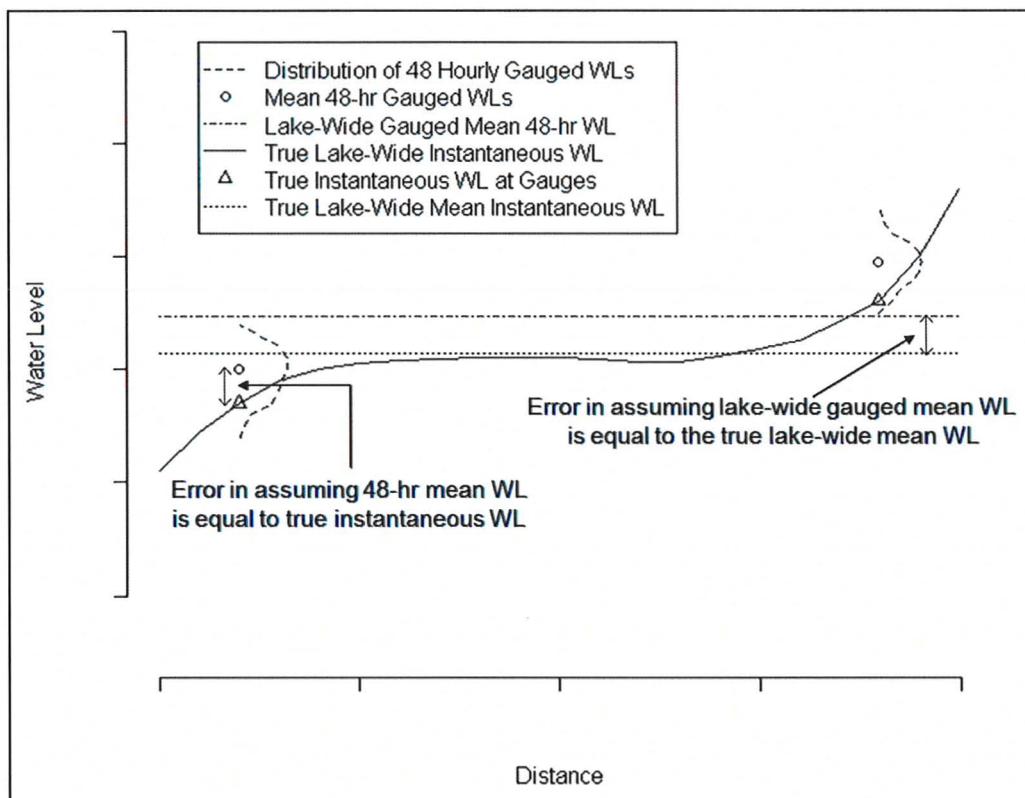


Figure 9-1: BOM lake-wide mean water level error schematic

In addition to these sources, errors resulting from the effects of GIA; from error in the computed area of the lake (and the assumption that it remains constant with changes in water level); and from the effects of thermal expansion and contraction due to heating and cooling of the water volume were also considered in this research. Any other sources of error were considered negligible.

9.2 Accuracy of Gauged Water Levels

The accuracy of individual water level measurements at a gauge station is a function of the precision of the instrument as well as the data collection methodologies and processing algorithms used by the agencies responsible for collecting the data. Water levels on Lake Erie are collected in Canada by the Canadian Hydrographic Service (CHS, a division of DFO) and in the U.S. by the National Ocean Service (NOS, a division of NOAA). Both CHS and NOS use shaft encoders as their primary instrumentation. Secondary instrumentation used by the two countries differs, but these are used only in the event of failure of the primary instrumentation, which is rare (Terese Herron, CHS, personal communication, 31 August, 2010).

The data collection algorithms used by the two countries also differ: in Canada, CHS produces water level data at three-minute increments, with the three-minute reading being the instantaneous value read at the top of every third minute; in the U.S., NOS produces water level data at six-minute increments, with the recorded six-minute instantaneous reading actually being an average of 181 values collected every second, centred on every sixth minute. An analysis by CHS showed that the variation in methods used by the different agencies had little effect on measurement results (Terese Herron, CHS, personal communication, 31 August, 2010).

Canada and the U.S. use the three- and six-minute, respectively, instantaneous water levels at the top of each hour as the hourly water level. The accuracy of the instantaneous hourly water levels will introduce a source of uncertainty into the BOM water level computations. The resolution of the water level gauges is 0.1 cm. According to NOAA (2009), an instantaneous water level determined from the methods outlined above is accurate to within +/- 0.3 cm. Additionally, all measurements are referenced to the survey measuring point, Zero

of the Electric Tape Gauge (ZETG), the accuracy of which, relative to International Great Lakes Datum 1985 (IGLD 85), is ± 0.6 cm. However, because the change in storage computation involves subtracting the BOM water levels from consecutive months, any systematic error from gauge datum accuracy should cancel out. It was assumed for this analysis that the accuracy of the Canadian gauges is equal to that of the U.S. gauges.

To compute the daily mean water level at a gauge, 24 hourly water level readings are averaged. The current practice in Canada is to average the hours of 00:00 to 23:00, whereas U.S. practice is to average the hours of 01:00 to 24:00. If the errors in each hourly reading are assumed to be fully correlated, then the mean of the 24 hourly readings will have an error due to gauge accuracy equivalent to the instantaneous error value of ± 0.3 cm. If the errors are assumed uncorrelated, the error of the 24 hourly readings due to gauge accuracy would be much less due to averaging. Even using the conservative estimate of ± 0.3 cm, the uncertainty due to the accuracy of the gauge instrument is quite small. Additionally, the Coordinating Committee currently rounds daily mean water levels to the centimetre, using engineering rounding, to compute the BOM water levels. Therefore, it is assumed that the total uncertainty of an individual water level reading is determined by the uncertainty caused by gauge reading accuracy (uniform distribution ± 0.3 cm) plus the uncertainty resulting from rounding to the centimetre (uniform distribution ± 0.5 cm). The variance of a uniform distribution can be computed from:

$$Var = \frac{(b - a)^2}{12} \quad (89)$$

where b and a are the maximum and minimum values of the distribution, respectively. The square root of this equation gives the standard error, which was computed as approximately 0.2 cm for the uncertainty caused by gauge accuracy and 0.3 cm for the uncertainty caused by rounding to the centimetre.

9.3 Temporal Variability

The averaging period used in estimating the mean BOM water level has not been studied in detail (Quinn, 2009). The mean BOM water level is theoretically the water level at midnight on the first day of the month; however,

use of the instantaneous water level at midnight would be inappropriate as it would be prone to significant short-term errors caused by meteorological impacts (Quinn, 1976; Croley, 1987). Therefore, it is the current practice to assume that the average of the daily means of the last day of the previous month and the first day of the current month represents the BOM water level (i.e. the true instantaneous level at midnight). Since daily mean water levels are computed regularly by the agencies responsible, the two-day mean may have been chosen originally for the convenience of having to average only two readily available water level values. However, whether the two-day mean actually represents the instantaneous water level at midnight on the first day of the month, or whether a more appropriate averaging period could be chosen, and how much uncertainty the current assumption causes, has not been studied.

Uncertainty in the BOM water levels caused by the averaging period results from differences between the true water level at midnight and the true hourly water levels in the 24 hours before and 24 hours after midnight that are used to estimate the instantaneous water level (i.e. 48 hours total). These differences are caused by short term meteorological impacts on water levels, as well as changes in storage due to actual changes in the mass volume of water over the course of the two days used to compute the mean.

If the difference in method used by Canada and the U.S. is ignored and it is assumed that the same hours are used by both countries to calculate the mean, and if errors resulting from deviations from the planar surface (i.e. due to meteorological impacts, for example) are also ignored, at least for now, then the error due to the averaging period is the result of changes in water levels over the 48 hours due to the actual change in storage resulting from changes in the mass volume of water during this period. That is, the difference between the instantaneous water level at midnight and the water level at any point within the 48 hour period used to compute the mean would be the result solely of changes in the mass volume of water.

Imagining a simple case where the average daily water level is determined as the average of the water level at the beginning of the day (BOD) and the water level at the end of the day (EOD), then:

$$\bar{h}_{daily} = \frac{h_{BOD} + h_{EOD}}{2} \quad (90)$$

where \bar{h}_{daily} is the mean daily water level; h_{BOD} is the instantaneous BOD water level; and h_{EOD} is the instantaneous EOD water level. Then, if the instantaneous BOM water level at midnight (BOM_{12am}) is calculated as the two-day mean (BOM_{2-day}) of the average daily water levels from the day prior (indicated with a subscript of -1) and the day after (indicated with a subscript of +1) midnight, it can be written as:

$$BOM_{2-day} = \frac{\bar{h}_{daily,-1} + \bar{h}_{daily,+1}}{2} = \frac{\left(\frac{h_{BOD,-1} + h_{EOD,-1}}{2}\right) + \left(\frac{h_{BOD,+1} + h_{EOD,+1}}{2}\right)}{2} \quad (91)$$

Furthermore, since $h_{EOD,-1} = h_{BOD,+1} = BOM_{12am}$:

$$BOM_{2-day} = \frac{h_{BOD,-1} + 2 \cdot BOM_{12am} + h_{EOD,+1}}{2 \cdot 2} \quad (92)$$

Furthermore, the water level at the start of the day prior ($h_{BOD,-1}$) is just the difference between the BOM water level and the actual change in storage for the day prior ($\Delta S_{True,-1}$):

$$h_{BOD,-1} = BOM_{12am} - \Delta S_{True,-1} \quad (93)$$

The ΔS_{True} is determined from the water balance as defined in equation (1). Likewise, the water level at the end of the day after ($h_{EOD,+1}$) is:

$$h_{EOD,+1} = BOM_{12am} + \Delta S_{True,+1} \quad (94)$$

Substituting gives:

$$BOM_{2-day} = \frac{(BOM_{12am} - \Delta S_{True,-1}) + 2 \cdot BOM_{12am} + (BOM_{12am} + \Delta S_{True,+1})}{2 \cdot 2} \quad (95)$$

This can be simplified to:

$$BOM_{2\text{-day}} = BOM_{12am} + \frac{\Delta S_{True+1} - \Delta S_{True-1}}{4} \quad (96)$$

Since we assume that the 2-day mean BOM and the true instantaneous BOM are equal, the error in the BOM water level is equal to the second term in equation (96):

$$\varepsilon(BOM_{2\text{-day}}) = \frac{\Delta S_{True+1} - \Delta S_{True-1}}{4} \quad (97)$$

This equation can be easily evaluated for each day if one knows the daily ΔS_{True} . If the ΔS_{True} increases the water level in day one and also increases the water level in day two, the errors in the BOM water level cancel out to some degree. On the other hand, if the ΔS_{True} increases then decreases, or vice versa, the error will be greater. The method could be applied to hourly water levels as well: however, such an equation could not be evaluated unless hourly water balance components were available, and this is not currently the case. Nonetheless, an approximation can be obtained by using the daily water balance components, which are available, and the equations outlined above. That is, the error in the BOM water level due to averaging can be obtained by using daily true change in storage for the day before and the day after each BOM and substituting into equation (97).

Daily component NBS (i.e. precipitation + runoff + evaporation) were obtained from NOAA GLERL. Daily Detroit River and Niagara River flows were obtained from USACE Detroit District. Daily Welland Canal flows were obtained from SLSMC. Data for each of these variables was available for the period 2000-2007. While the daily values are subject to errors proportionally larger than the errors in monthly values, these errors are unlikely to significantly alter the results of this analysis. All other variables (i.e. smaller diversions, groundwater, consumptive use, change in storage due to thermal expansion and contraction, GIA, etc.) were assumed negligible on a daily basis. The true change in storage was therefore determined from:

$$\Delta S_{True} = I - O + P + R - E \quad (98)$$

In addition to errors in the 2-day mean, errors resulting from the 4-, 6-, 8-, 10-, 12-, and 14-day means were also computed. Using a similar procedure to that outlined above to obtain equation (97), it can also be shown that the error from the 4-day mean can be computed from:

$$\varepsilon(BOM_{4\text{-day}}) = \frac{\Delta S_{True,+2} + 3 \cdot \Delta S_{True,+1} - 3 \cdot \Delta S_{True,-1} - \Delta S_{True,-2}}{2 \cdot 4} \quad (99)$$

where $\Delta S_{True,+1}$ and $\Delta S_{True,+2}$ are the daily true change in storage on the first and second day after the BOM, respectively; $\Delta S_{True,-1}$ and $\Delta S_{True,-2}$ are the daily true change in storage in the first and second day before the BOM, respectively. Likewise, the error from the 6-day mean can be computed from:

$$\begin{aligned} \varepsilon(BOM_{6\text{-day}}) \\ = \frac{\Delta S_{True,+3} + 3 \cdot \Delta S_{True,+2} + 5 \cdot \Delta S_{True,+1} - 5 \cdot \Delta S_{True,-1} - 3 \cdot \Delta S_{True,-2} - \Delta S_{True,-3}}{2 \cdot 6} \end{aligned} \quad (100)$$

A pattern can be seen, which can be used to obtain the error equation for any number of days used to compute the mean.

The results of the computations are shown in Table 9-1. The standard error caused by true changes in the mass volume of water resulting from using the 2-day mean was found to be only 0.14 cm, with maximum absolute error of 0.82 cm. Results also showed that even for the 14-day mean, the error in the instantaneous BOM water level was found to be only 0.88 cm, with max error found to be 4.34 cm. Given that even the highest error in the instantaneous BOM water level resulting from using a two-day average as opposed to a true instantaneous water level is less than 1 cm, the uncertainty resulting from true changes in storage during the averaging period used was assumed to be negligible.

Table 9-1: Estimated change in storage error due to true changes in mass volume of water

n-Day Mean	2-Day	4-Day	6-Day	8-Day	10-Day	12-Day	14-Day
Standard Error (cm)	0.14	0.28	0.41	0.54	0.66	0.77	0.88
Max. Absolute Error (cm)	0.82	1.48	2.11	2.72	3.31	3.86	4.34

This analysis indicates that the true instantaneous water level at any given time can be adequately represented by the two-day lake-wide mean water level centred on the instantaneous hour, and that changes in storage due to actual changes in the mass volume of water will not cause significant error in this value. What remains to be determined is the uncertainty of the two-day mean water level determined from the four gauges due to temporal variability, since any deviations from this mean can safely be assumed to be due to meteorological or other short term impacts, as opposed to actual changes in the mass volume of water.

The uncertainty of the four-gauge mean two-day water level was determined by first computing the four-gauge mean hourly water level for each hour from 1984 to 1985, then computing the mean, standard deviation, and standard deviation of the mean for every set of 48 hourly averages. The years 1984 and 1985 were used to minimize the effects of GIA, which causes systematic differences in water levels measured on a given lake over time as a result of differential movement of the earth's crust. GIA has a greater effect on recorded water levels the further they are from 1985, the reference year of IGLD 85, since when IGLD is updated every 25 to 30 years to account for such differential movement, the water level gauge benchmarks on a lake are brought back into harmony, and as a result, so are the recorded water levels (Coordinating Committee, 1995; Coordinating Committee, 1979).

The results of this analysis showed that the average standard deviation of the 48 hourly four-gauge averages was only 2 cm. There was little variation on a monthly basis. This indicates that on average, the hourly mean of the four gauges varied by approximately +/- 4 cm during the 48-hour period, at the 95% confidence level. The standard deviation of the 48-hour mean was then computed as:

$$\bar{s}_{48-hr} = \frac{s_h}{\sqrt{n}} = \frac{2}{\sqrt{48}} = 0.3 \text{ cm} \tag{101}$$

The average standard deviation of the mean was taken as an estimate of the standard uncertainty in the two-day mean, and these errors were assumed to be normally distributed.

Another method for determining the uncertainty in the two-day mean was to calculate the standard deviation and standard deviation of the mean of the 48-hourly water levels for each gauge individually, and then combine the results. The average results for each gauge for each month are given in Table 9-2.

Table 9-2: Average standard deviation of two-day lake-wide mean water levels

Month	Standard Deviation of Two-Day Mean (m)			
	Toledo	Cleveland	Port Stanley	Port Colborne
Jan	0.02	0.01	0.00	0.01
Feb	0.01	0.00	0.00	0.01
Mar	0.02	0.01	0.01	0.01
Apr	0.02	0.00	0.00	0.01
May	0.01	0.00	0.00	0.01
Jun	0.01	0.00	0.00	0.01
Jul	0.01	0.00	0.00	0.01
Aug	0.01	0.00	0.00	0.01
Sep	0.02	0.01	0.00	0.01
Oct	0.02	0.01	0.01	0.01
Nov	0.02	0.01	0.01	0.02
Dec	0.03	0.01	0.01	0.02

For example, this indicates that the computed two-day mean water level for Toledo in January will be within +/- 2 cm of the true mean 48-hour water level approximately two-thirds of the time. To determine the total uncertainty in the average lake level due to deviation of the true instantaneous water levels from the mean at each gauge, the correlation between errors at the different gauge locations used to compute the mean must be considered. The deviation of each water level gauge from the mean of the four gauges was computed. The correlation

coefficients of these deviations were also computed and are given in Table 9-3 below.

Table 9-3: Correlation coefficients of deviations from 4-gauge lake-wide mean water level

Gauge	Toledo	Cleveland	Pt. Stanley	Pt. Colborne
Toledo	1.00	0.54	-0.87	-0.97
Cleveland	0.54	1.00	-0.61	-0.69
Pt. Stanley	-0.87	-0.61	1.00	0.82
Pt. Colborne	-0.97	-0.69	0.82	1.00

The deviations between Toledo and Port Colborne, for example, have a high negative correlation. Therefore, errors at one of these gauges tend to cancel out errors at the other gauge. Similar results are seen for Port Stanley and Toledo, and Port Stanley and Cleveland, albeit to a lesser degree. The opposite case is observed at Port Stanley and Port Colborne, where a positive correlation is seen between deviations at these gauges. The total uncertainty in the 4-gauge average is then found from:

$$s_{48-hr} = \left(\frac{1}{4^2} \cdot \sum_{i=1}^4 s_i + 2 \cdot \frac{1}{4^2} \cdot \sum_{i=1}^3 \sum_{j=2}^4 s_i s_j \cdot r_{i,j} \right)^{1/2} \quad (102)$$

where s_i is the uncertainty taken as the standard deviation of the mean at each gauge i , and $r_{i,j}$ is the correlation coefficient computed between deviations from each gauge pair i and j .

The results are given in Table 9-4 below. As can be seen, when the correlation of the errors between gauges is taken into consideration, the standard error estimate is less than 0.2 cm for all months. Therefore, using either method to determine the uncertainty in the mean of the four-gauge average showed it to be small, indicating that use of the two-day mean water level is acceptable and reduces errors caused by temporal variability to a nearly negligible level. The more conservative standard uncertainty estimate of 0.3 cm, having normal error distribution, was assumed for the remainder of this study.

Table 9-4: Standard error of the two-day lake-wide mean water level.

Month	Standard Error (No Correl., cm)	Standard Error (w/Correl., cm)
Jan	0.6	0.1
Feb	0.4	0.1
Mar	0.7	0.1
Apr	0.5	0.1
May	0.5	0.1
Jun	0.5	0.1
Jul	0.4	0.1
Aug	0.4	0.1
Sep	0.5	0.1
Oct	0.6	0.1
Nov	0.8	0.2
Dec	0.9	0.2

9.4 Spatial Variability

By computing the change in storage of Lake Erie over a month as the change in mean Lake Erie water level from the beginning to the end of the month, it is assumed that the lake is essentially a flat plane, and that the mean water level computed from a network of gauges, in this case Toledo, Cleveland, Port Stanley and Port Colborne, represents the centre of mass of that plane. However, even though the lake is assumed to be a level plane, as stated by Hayford (1922), the lake surface is likely never truly level at any instant in time “except by accident”. Quinn (2009) also questioned the validity of this assumption. The reason is that additional factors affect the water levels of the lakes. Large scale winds, barometric pressure and seiche effects can cause changes in the slope of the water surface as a whole. The physical geography of the lake and local impacts can cause the surface of the lake to vary further from the planar assumption: for example, seiches are known to occur between different areas of the lake (Hunt, 1959); local harbour impacts on water levels result from resonance and reflection of waves off piers and breakwaters; and even significant local runoff, precipitation or evaporation can cause small local variations in the water level of Lake Erie.

The errors in measured Lake Erie water levels caused by winds, barometric pressure, seiche and other local effects can be easily observed. For example, Figure 9-2 below shows a comparison of daily water levels for the months of November and December, 2007, from all four water level gauges used to compute the coordinated lake-wide average water level for Lake Erie. The effects of meteorological influences are clearly seen in the deviations of water levels at individual gauges from the lake-wide mean level. This is especially true at Toledo and Port Colborne. The reason for this is that, being located at the western and eastern ends of the lake, respectively, these two gauges are impacted to a greater degree by storm-surge and large magnitude seiche effects.

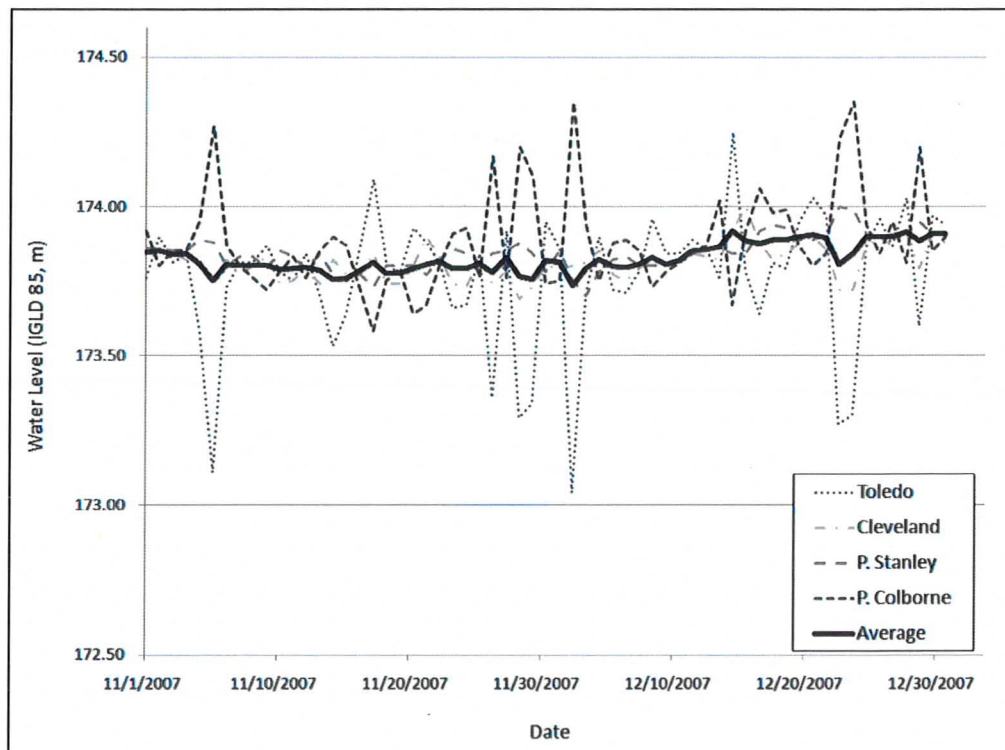


Figure 9-2: Lake Erie daily mean water level comparison

Similar to what was done by Quinn (2009), in order to assess the uncertainty in Lake Erie water levels resulting from spatial variability, the two-day mean water levels computed from each gauge and from various averaged gauge networks, including the average from the coordinated set of four water level gauges, were compared to the two-day mean computed using various Thiessen networks as reported by Quinn and Derecki (1976). In that study,

Thiessen polygons were derived for Lake Erie gauge networks, with the weights adjusted in some cases to account for dominant physical features of the lake. Specifically, it was noted that the Thiessen weight applied to the Toledo gauge was adjusted because, being at the extreme constricted end of the lake, it was deemed not to be a suitable estimate of lake levels other than in the immediate vicinity of the actual gauge, and would bias the mean lake level if given an unadjusted Thiessen weight; furthermore, the Thiessen polygons around Long Point were adjusted to account for the local effect it causes on the surface of the lake. Quinn and Derecki (1976) found that little benefit was gained from using more than a 9-gauge Thiessen weighted network. Furthermore, gauge networks of 10 or more for Lake Erie involved the gauge station located at Barcelona, which has since been discontinued. Therefore, only the 2- through 9-gauge Thiessen networks suggested by the authors were used in this analysis (Table 9-5).

Table 9-5: Lake Erie water level gauge Thiessen weights (Quinn and Derecki, 1976)

Gauge	Thiessen Weight					
	2-gauge	3-gauge	4-gauge	5-gauge	8-gauge	9-gauge
Buffalo	0.184	0.184	0.012	0.012	0.012	0.012
Cleveland	0.816	0.769	0.769	0.399	0.292	0.141
Toledo	--	0.047	0.047	0.047	0.047	0.047
Port Colborne	--	--	0.172	0.172	0.082	0.082
Port Stanley	--	--	--	0.37	0.154	0.147
Erieau	--	--	--	--	0.167	0.167
Erie	--	--	--	--	0.189	0.189
Port Dover	--	--	--	--	0.057	0.057
Marblehead	--	--	--	--	--	0.158

Croley (1987) used a hydrodynamic model to estimate error at each gauge on Lake Erie resulting from long-term wind setup, and found spatial-optimum network gauge weights that minimized the resulting error. These weights were also considered for use in this study, but since the network weights reported for Lake Erie included the gauge at Fairport, OH, which is now believed to be subject to local subsidence (Bruxer and Southam, 2008), the weights suggested could not be used as reported.

Thiessen networks provide a better estimate of the mean Lake Erie water level because they spatially balance the weighting given to individual gauged water levels, which reduces any bias caused by persistent spatial errors. For example, even if all active gauges were used to compute the mean Lake Erie water level using straight averaging, the computed mean would be disproportionately impacted by errors in the western basin, since five gauges are located in relatively close proximity of each other in this area (i.e. Kingsville, Bar Point, Fermi Power Plant, Toledo and Marblehead). Since in a straight average each gauge is given the same weighting, a bias will result, caused by whatever impacts might be affecting this local area. Such errors will be even more prevalent when averaging water levels from a lesser number of gauges.

Two-day mean water levels were computed using each of the Thiessen networks given by Quinn and Derecki (1976). Assuming that these water levels represent the true mean water level of Lake Erie, or at least the best estimate, they were compared to two-day means determined from each gauge individually, and from a number of gauge networks using straight averaging. The two-day mean water levels were computed for the 30-year period from 1980 to 2009, as these data were readily available.

The gauge network used by the Coordinating Committee was computed and denoted as the Coordinated* gauge network in this analysis. The Coordinating Committee uses water levels from the gauge stations at Cleveland (CL), Toledo (TO), Port Stanley (PS) and Port Colborne (PC) when water level data for all four gauges are available; if Toledo or Port Colborne are missing, the average of Cleveland and Port Stanley is used; and if Cleveland or Port Stanley are missing, the average of Toledo and Port Colborne is used. An asterisk was used to indicate that the Coordinated* values computed in this study may differ slightly from the actual Coordinating Committee values due to rounding (simple rounding, i.e. 0.005 was always rounded up to 0.01, was used as opposed to engineering rounding used by the Coordinating Committee), and since only readily available water level data were used (in some cases the Coordinating Committee will obtain additional data directly from the agencies when data are missing, but this was not pursued for this analysis). In addition to the Coordinated* gauge network, the “All Gauges” network was also computed, which was a straight average of water levels reported from all 13 active Lake Erie water level gauge stations.

The mean, standard error, maximum and minimum error estimates determined from the differences between the 9-gauge Thiessen network and the single gauges and straight-averaged networks are shown in Table 9-6. The highest standard errors reported again show that water levels at the eastern (Toledo) and western (Port Colborne) ends of the lake are subject to greater error than water levels in the central basin. The fact that the standard error at Toledo is greater than that at Port Colborne indicates that use of this gauge pair may cause a bias due to disproportionate errors affecting water levels at Toledo. The other gauge pair (Cleveland and Port Stanley) is more balanced, though errors are still somewhat greater at Cleveland. Table 9-6 also shows that the Coordinated* two-day water levels are somewhat less accurate than both the Cleveland-Port Stanley gauge pair, and the average of all thirteen gauges.

Table 9-6: Lake Erie water level differences (9-gauge Thiessen network)

Statistic	Difference (9-gauge Thiessen Network minus Gauge or Gauge Network, cm)								
	CL	TO	PS	PC	CL,TO, PS,PC	CL, PS	TO, PC	Coord*	All Gauges
Mean	0.5	0.9	-0.6	-1.3	-0.3	-0.3	-0.5	-0.3	0.1
SE	2.7	11.8	2.2	8.5	1.2	0.9	2.3	1.2	0.8
Max	19	101	10	35	9	5	16	9	7
Min	-14	-60	-19	-68	-7	-6	-15	-7	-4

The final estimates of uncertainty caused by spatial variability were determined by comparing the 9-gauge Thiessen network averages to the Coordinated* network averages. A simple GIA correction was first applied to the water levels by adjusting water levels at each gauge for the mean annual water level difference between the gauge in question and the Buffalo gauge (it was also noted, however, that the results were nearly identical with or without the correction). Furthermore, since meteorological effects resulting from winds, differences in barometric pressure and seiche vary seasonally, with greater effects from fall through spring, and lesser effects during the summer months, as was shown in Figure 9-2, the results were also divided by the beginning of month that they applied to. That is, it was assumed that days one to 15 of any month applied to the beginning of that month, whereas days 16 to 31 applied to the following month.

A review of the probability distributions of the errors showed them to be bell-shaped and symmetric, but subject to higher kurtosis (peakedness) than a normal distribution. Upon reviewing the histograms and empirical CDFs using “R” (Appendix C), it was determined that the logistic distribution described the data well. The parameters are given in Table 9-7 below. They include a location parameter, which is equal to the mean, and a scale parameter, which describes the spread of the measurements. The logistic distributions were used in the Monte Carlo uncertainty analysis. The variance of the logistic distribution can be determined from:

$$Var = \frac{\pi^2}{3} s_l^2 \quad (103)$$

where s_l is the scale parameter of the logistic distribution. The square root of the variance gives the standard error, or the standard uncertainty estimate, which was used in the FOSM analysis. These results are also provided in Table 9-7.

Table 9-7: Spatial variability errors: logistic distribution parameters and standard error estimates

Month	Logistic Dist. Parameters		SE (cm)
	Location (cm)	Scale (cm)	
Jan	0.0	0.7	1.2
Feb	-0.2	0.6	1.1
Mar	-0.3	0.6	1.1
Apr	-0.5	0.7	1.2
May	-0.4	0.5	1.0
Jun	-0.3	0.4	0.7
Jul	-0.1	0.4	0.7
Aug	0.0	0.3	0.6
Sep	-0.2	0.4	0.7
Oct	-0.1	0.6	1.0
Nov	0.0	0.7	1.4
Dec	0.3	0.9	1.6

The location parameter reflects the mean difference between the 9-gauge Thiessen and the Coordinated* gauge network water levels. This parameter indicates that, depending on the month, on average the lake-wide mean water level may be overestimated ($Location < 0$) or underestimated ($Location > 0$) due to the gauge network currently used. This could be the result of a systematic effect, such as prevailing winds affecting certain gauges more than others. However, since the 9-gauge Thiessen network provides only an additional estimate of the mean Lake Erie level, and not necessarily the true mean water level, it is unclear whether this apparent bias truly exists. The scale parameters and the standard errors computed indicate that the uncertainty caused by spatial variability varies by month, with largest errors occurring from fall to early spring, and the smallest occurring in the summer months.

9.5 *Glacial Isostatic Adjustment (GIA)*

GIA has long been recognized as having an impact on measured water levels and water balance studies in the Great Lakes (Clark and Persoage, 1970). The rate of rebound varies across the region, and causes water levels measured at gauge stations on each of the Great Lakes to appear to be increasing or decreasing with time relative to other gauges on the same lake. However, while the apparent changes in water level due to GIA are an important factor needing consideration in many studies involving Great Lakes water levels, in particular those looking at long term impacts (e.g. IUGLSB, 2009), on a short term basis, the effects of GIA on measured water levels are so small that any errors can safely be assumed negligible. For example, on Lake Erie, GIA generally causes apparent water levels to change by less than 10 cm/century relative to the lake outlet (Bruxer and Southam, 2008). This corresponds to less than 0.1 mm per month. Quinn et al. (1979) also dismissed the effects of GIA on monthly change in storage as negligible.

9.6 *Lake Area*

The change in water level is multiplied by the lake surface area in order to determine the change in volume of Lake Erie each month. The surface area of each Great Lake used in determining the change in storage was first coordinated between Canada and the United States in 1977, and was measured using a

planimeter and a combination of navigation charts and topographic maps, and given to three significant digits (Coordinating Committee, 1977). The total surface area of Lake Erie was reported as 25,700 km². Error in the surface area will cause error in the computed monthly change in storage: if the true surface area is actually larger than the reported value, the computed change in storage will be underestimated; whereas if the true surface area is less than the reported value, the computed change in storage will be overestimated. Though assumed constant, the surface area of the lake varies with water level, complicating the situation.

The accuracy of the surface area estimate is difficult to determine. If the estimated area of 25,700 km² is assumed to be accurate, the resolution error resulting from rounding to three significant digits, which in this case is equivalent to rounding to the nearest 100 km², gives a uniformly distributed uncertainty estimate of +/- 50 km² or 0.2% at a minimum. This was assumed as the minimum uncertainty in the Lake Erie surface area.

Navigation maps are normally drawn at Chart Datum elevation, which for Lake Erie is 173.5 m IGLD 85. This means that the surface area given by the Coordinating Committee (1977) was determined at approximately the Chart Datum elevation, and therefore, when water levels are higher than this elevation, the surface area should be larger than the estimated value, and when water levels are lower than Chart Datum, the surface area should be smaller. Using a geographic information system (ArcGIS) and a digital surface area polygon of Lake Erie obtained from NOAA (http://coastalgeospatial.noaa.gov/data_gis.html), the area of Lake Erie was calculated as approximately 25,695 km², which when rounded to the nearest hundred gives the same estimate of 25,700 km² as determined by the Coordinating Committee (1977). This helps confirm the estimated surface area at Chart Datum elevation. ArcGIS was then used to create buffers of various distances representing uniform increases or decreases in shorefront around the polygon of Lake Erie, and the area of each buffered polygon was computed. From this it was found that for approximately every 1 m of buffer (i.e. shorefront) a 2 km² change in lake area would result. That is:

$$A = 2 \cdot (\Delta Shore) + 25700 \quad (104)$$

where A is the lake area, and $\Delta Shore$ is the increase or decrease (negative) in shorefront over that determined at Chart Datum elevation. It was found that to increase the area of Lake Erie by 1%, for example, the shorefront would have to

change by approximately 130 metres on average. This great an increase in shorefront across the entire lake seems unlikely.

To confirm this, a brief analysis of water levels and near shore slopes was performed. From 1900 to 2008, the mean monthly water level of Lake Erie was determined to be 174.11 m, having a standard deviation of 0.35 m, and minimum and maximum observed values of 173.17 m and 175.04 m, respectively. Near shore bathymetry data for Lake Erie referenced as depths below Chart Datum was reviewed and it was estimated that a near shore slope value of between 0.005 and 0.010 was fairly representative of an average value for the lake below Chart Datum. Assuming the lower value of 0.005, the area at the minimum mean monthly water level of 173.17 m, which is 0.33 m below Chart Datum, would have been approximately 25,568 km², as shown by the following:

$$A = 2 \cdot (\Delta Shore) + 25700 = 2 \cdot \left(\frac{173.17 - 173.5}{0.005} \right) + 25700 = 25568$$

Therefore, at the minimum observed water level the area would only be 132 km² less than the assumed value, or -0.5%.

At the maximum observed water level of 175.04 m, the increase in area given the assumed near shore slope of 0.005 would be approximately 600 km², or 2% greater than the area at Chart Datum. However, this is likely an overestimate, since above Chart Datum elevation, the near shore slope determined from the bathymetry data does not necessarily apply. The slope above Chart Datum is likely to be greater than the slope below, due to steep bluffs, shore protection, and other features of the shoreline that exist around Lake Erie. Therefore, it is unlikely that the rate of change in surface area is as great above Chart Datum as below, although data were not available to confirm this.

Nonetheless, even if the greater uncertainty estimate of 2% is assumed to be the 95% confidence limit, the standard error would be approximately 1%, and the result this error has on the computed change in storage can be shown to be small. The uncertainty in the change in storage can be found from:

$$u(\Delta S)_A = \left(\frac{\partial \Delta S}{\partial A} \right) \cdot u(A) \quad (105)$$

where $u(\Delta S)_A$ is the uncertainty in the change in storage (ΔS) due to error in the area of Lake Erie (A); $\partial S / \partial A$ is the sensitivity coefficient of the change in storage with respect to a change in area; and $u(A)$ is the uncertainty in the area of the lake. The sensitivity coefficient ($\partial S / \partial A$) is simply equal to the change in head (ΔH_t) for month t . The average (absolute) monthly change in head for the 1900 to 2008 period was determined to be approximately 10 cm. The conservative estimate of the standard uncertainty in area of 1% corresponds to approximately 250 km², which when multiplied by the sensitivity coefficient of 10 cm and divided by the approximate number of seconds in a month, gives a standard uncertainty estimate, in discharge units, of less than 10 m³/s. Given that the uncertainty in the area is likely overestimated, it can safely be assumed from this analysis that the uncertainty due to lake surface area can be considered negligible.

9.7 Combined Uncertainty in Change in Storage

The overall combined uncertainty in the change in storage was determined using both the FOSM and Monte Carlo methods. Using the FOSM method and assuming errors in the BOM water levels from the beginning to the end of any given month to be uncorrelated, the uncertainty in the change in storage for month t can be determined from:

$$u(\Delta S)_t = \sqrt{CF^2 \cdot [u^2(BOM_t) + u^2(BOM_{t+1})]} \quad (106)$$

The standard uncertainty in the BOM water level is the result of uncertainty due to gauge accuracy (0.2 cm); rounding to the centimetre (0.3 cm); temporal variability (0.3 cm); and spatial variability (0.6 to 1.6 cm, depending on the month). A summary of the various uncertainty estimates are shown in Table 9-8.

Table 9-8: Summary of standard uncertainty estimates in BOM water levels

Uncertainty Source	Monthly Uncertainty Estimates (cm)											
	Jan	Feb	Mar	Apr	May	Jun	Jul	Aug	Sep	Oct	Nov	Dec
Gauge Accuracy	0.17	0.17	0.17	0.17	0.17	0.17	0.17	0.17	0.17	0.17	0.17	0.17
Rounding Error	0.29	0.29	0.29	0.29	0.29	0.29	0.29	0.29	0.29	0.29	0.29	0.29
Temporal Variability	0.3	0.3	0.3	0.3	0.3	0.3	0.3	0.3	0.3	0.3	0.3	0.3
Spatial Variability	1.2	1.1	1.1	1.2	1.0	0.7	0.7	0.6	0.7	1.0	1.4	1.6

The combined uncertainty in the BOM water levels can be computed from:

$$u(BOM_t) = \sqrt{u^2(h_{gauge}) + u^2(h_{rounding}) + u^2(h_{temporal}) + u^2(h_{spatial})} \quad (107)$$

where h_{gauge} is the uncertainty due to gauge accuracy; $h_{rounding}$ is the uncertainty due to rounding; $h_{temporal}$ is the uncertainty due to temporal variability; and $h_{spatial}$ is the uncertainty due to spatial variability. In addition to the uncertainty estimates provided, the mean systematic error due to spatial variability must also be considered. The mean error can be computed from:

$$\varepsilon(\Delta S)_t = [\varepsilon(BOM)_{t+1} - \varepsilon(BOM)_t] \cdot CF \quad (108)$$

where $\varepsilon(\Delta S)_t$ is the mean error in the change in storage; $\varepsilon(BOM)_t$ is the mean error in the BOM water level of month t , represented by the location parameter determined in Section 9.4; and CF is the monthly conversion factor. The difference $\varepsilon(BOM)_{t+1} - \varepsilon(BOM)_t$ is the error in the change in head ($\varepsilon(\Delta H)_t$). When the change in head is underestimated ($\varepsilon(\Delta H)_t > 0$) for a given month, the change in storage (and subsequently the NBS) will also be underestimated, whereas when the change in head is overestimated ($\varepsilon(\Delta H)_t < 0$) the reverse is true.

The results for both the mean error and standard uncertainty for each month as determined from the FOSM method are shown in Table 9-9. As discussed, the uncertainty in the change in storage is greatest in the fall and winter, and is lowest in the summer months.

Table 9-9: Summary of uncertainty estimates in change in storage

Source	Monthly Error Estimates											
	Jan	Feb	Mar	Apr	May	Jun	Jul	Aug	Sep	Oct	Nov	Dec
$\varepsilon(BOM)_t$ (cm)	0.0	-0.2	-0.3	-0.4	-0.4	-0.3	-0.1	-0.0	-0.2	-0.1	0.0	0.3
$\varepsilon(\Delta S)_t$ (cm)	-0.2	-0.1	-0.1	0.0	0.1	0.2	0.1	-0.2	0.1	0.1	0.3	-0.3
$\varepsilon(\Delta S)_t$ (m ³ /s)	-16	-13	-14	4	9	20	7	-15	11	9	29	-30
$u(BOM)_t$ (cm)	1.3	1.2	1.2	1.3	1.1	0.8	0.8	0.7	0.8	1.1	1.4	1.7
$u(\Delta S)_t$ (cm)	1.7	1.6	1.7	1.7	1.4	1.2	1.1	1.1	1.4	1.8	2.2	2.1
$u(\Delta S)_t$ (m ³ /s)	167	174	166	165	130	117	106	106	137	174	219	203

The uncertainty in the monthly change in storage was also estimated using the Monte Carlo approach. Errors caused by gauge accuracy were randomly sampled from a uniform error distribution having maximum and minimum errors of +/- 0.3 cm; errors caused by rounding water levels to the nearest centimetre were also sampled from a uniform distribution, in this case with maximum and minimum errors of +/- 0.5 cm; errors caused by temporal variability were sampled from a normal distribution having a mean of zero and standard deviation of 0.3 cm; and errors caused by spatial variability were sampled from a logistic distribution having the parameters given in Table 9-7. The randomly sampled errors from each source of uncertainty were summed and added to the computed BOM water level for each month for the period 1900-2008, allowing a random sample of monthly changes in storage for this same period to be computed.

A summary and comparison of the FOSM and Monte Carlo results is given in Table 9-10. The uncertainty in the change in storage was found to be

greatest in the fall through spring months, being almost twice as great as the uncertainty in the summer months. This is the result of greater meteorological effects on water levels in these months, causing greater spatial variability and errors in the mean computed water level. Furthermore, similar to the Niagara River flow analysis (Section 6.7), the change in storage results indicate that the FOSM and Monte Carlo analysis methods produced nearly identical uncertainty estimates. As was the case for the Niagara River flow, the similarity of the FOSM and Monte Carlo analysis results is to be expected, given that the change in storage model is linear (so long as the uncertainty in the area of the lake is assumed constant, which was the case) as well as the fact that the different sources of uncertainty (i.e. gauge accuracy, rounding error, temporal and spatial variability) were combined in a linear fashion. Additional causes of the similarity between methods include the fact that the input probability distributions were found to be symmetric for the most part; the standard error estimates used in the FOSM method were computed from the same distributions as used in the Monte Carlo approach; and the high-dimensionality of the change in storage model, coupled with the similar magnitudes of the model inputs, causes the model output's probability distribution obtained using the Monte Carlo approach to be normally distributed as a result of the central limit theorem.

Table 9-10: FOSM vs. Monte Carlo analysis estimates of change in storage uncertainty

Month	FOSM (m ³ /s)		Monte Carlo (m ³ /s)		Difference (m ³ /s)	
	Mean Error	St. Dev	Mean Error	St. Dev	Mean Error	St. Dev
Jan	-16	167	-16	167	0	0
Feb	-13	174	-13	172	0	2
Mar	-14	166	-13	166	1	0
Apr	4	165	2	164	-1	1
May	9	130	9	130	0	0
Jun	20	117	20	117	0	0
Jul	7	106	7	106	0	0
Aug	-15	106	-14	106	1	0
Sep	11	137	11	137	0	0
Oct	9	174	8	175	-1	-1
Nov	29	219	29	219	0	0
Dec	-30	203	-30	203	0	0

The uncertainty estimates provided account for errors in measurement of change in storage. They do not account for errors resulting from assuming that the entire change in storage is due to increases in the mass volume of water. In reality, some of the measured change in storage results from thermal expansion and contraction of the water body, and this is discussed in the following section.

9.8 Thermal Expansion and Contraction

Water increases or decreases in volume depending on its temperature. When calculating residual NBS, the change in volume (i.e. the change in storage) due to thermal expansion and contraction (thermal volume change) is generally considered negligible and subsequently omitted. For certain time steps, this assumption is acceptable: for example, thermal volume changes over the course of a day are likely too small to be measurable, and the errors due to thermal volume changes over the course of a year likely cancel out as the volume of the lake returns to a similar temperature year after year. However, the effects of thermal volume change over the course of a month could be a significant source of error in monthly NBS calculations. These effects are treated separately from the uncertainty in the computed change in storage described above. The uncertainty in the computed change in storage is a result of errors in measuring the true change in volume of the lake, whereas the uncertainty caused by thermal volume change is not a result of measurement errors, but rather it is a result of the assumption that the entire measured change in volume is related to a true increase or decrease in the mass volume of the lake, when in reality part of that change is the result of thermal changes of the water volume.

Accounting for thermal volume change is difficult due to the limited availability of water temperature data for the Great Lakes. The immense size of the lakes and the fact that water temperature in the Great Lakes varies in three dimensions makes accurate measurement of water temperature impossible. Actual measurements of lake water temperatures are normally made at only a few discrete locations. For example, on Lake Erie, temperature is measured at the Buffalo Water Treatment Plant at a depth of 9.1 metres (30 feet) (see: <http://www.wbuf.noaa.gov/laketemps/lktemp.html>). Buoys are deployed in the Great Lakes to measure water temperature and other meteorological variables at specific locations (<http://www.ndbc.noaa.gov/>). Alternatively, remote sensing provides a means of estimating water surface temperatures across the entire lake.

For example, since 1994 GLERL has produced daily mean surface temperatures for each of the Great Lakes from satellite imagery through the Great Lakes Surface Environmental Analysis (GLSEA), and has made the data available through the internet (<http://coastwatch.glerl.noaa.gov/glsea/doc/>). Water temperature data below the surface is more limited. Vertical water temperature profiles have been collected for Lake Erie, but only periodically. Furthermore, data have been collected more often in the summer months than in winter, and only at discrete points. In more recent years, energy balance models have been developed and applied in the Great Lakes, and these can be used to estimate water temperature profiles and have been shown to give good results (Croley, 1992; Lam and Schertzer, 1987). However, current models developed by EC are not operational in the winter as they do not incorporate ice effects (Ram Yerubandi, EC, personal communication, 20 July, 2010), while GLERL's evaporation model accounts for ice effects and could be configured to produce continuous modelled vertical temperature profiles, but would require significant effort to achieve this (Tim Hunter, GLERL, personal communication, 9 August, 2010). Furthermore, while GLERL models have been calibrated to surface temperature and ice cover, they have not been calibrated to vertical temperature distribution, and in this regard would benefit from greater availability of calibration data (Carlo De Marchi, GLERL, personal communication, 7 July, 2010).

One method to estimate the temperature distribution in a lake that has been proposed by researchers in the past (e.g. Meredith, 1975; Derecki, 1976; Quinn and Guerra, 1986) is to assume one-dimensional variation of temperature with depth, and relate the average surface water temperature of the lake to the one-dimensional vertical temperature profile using a dimensionless profile. The dimensionless profile is obtained by estimating the mean vertical water temperature profile for the lake for each month, and then dividing the mean vertical temperatures at each elevation by the mean surface temperature for that month. The actual measured or estimated mean surface temperature for any given month is then multiplied by the dimensionless profile to give an estimate of the actual vertical temperature profile for the month in question. Such a method was adapted for this study.

Mean surface water temperatures for Lake Erie were obtained from two sources: GLERL's GLSEA remotely sensed data, and from GLERL's one-dimensional energy balance model. The GLSEA data already described was available from November 1994 to 2009. The GLERL energy balance model is

used to estimate lake evaporation, and has been calibrated against surface water temperature and ice cover data (Croley, 1989; Croley and Assel, 1994). Data were obtained directly from GLERL. Daily modelled results were available for the years 1948 to 2009. Both datasets were used and the results compared. The BOM mean surface temperature was estimated using a 6-day running mean to avoid extreme one-day fluctuations from causing anomalous results. A comparison of 6-day mean and 14-day mean results showed good agreement, and therefore the 6-day mean was used primarily for this study.

Vertical temperature profiles were obtained or derived from a number of sources. Meredith (1975) derived temperature profiles from data collected from a number of studies conducted in the 1960s and 1970s. Derecki (1976) derived mean vertical water temperature profiles for each month from data collected from 1960-1963 and published by the University of Toronto, with profiles for the winter months of January to March estimated since no data were available for these winter months. The exact profile values were not given by Derecki (1976), so BOM temperature profiles for this study were estimated from plotted data. An additional set of vertical water temperature profiles were developed specifically for this research from survey data collected by EC's National Water Research Institute between 1967 and 1982 under the Great Lakes Surveillance Program (see Schertzer et al., 1987; Lam and Schertzer, 1967). Bathythermograph readings were taken during ship cruises that traversed the entire lake (Figure 9-3). Data were collected for the months of April through December only. The EC data were grouped by the approximate BOM that they were collected using the 15th day of each month to divide the samples. For example, all temperature readings on or between April 16th and May 15th would be considered May BOM and grouped together. The temperature data for each BOM were plotted against depth and a representative temperature profile was fit to the data by eye (results are shown in Appendix D). A comparison of the three sets of vertical temperature profiles showed them to be in fairly good agreement, especially in the non-winter months (Appendix E).

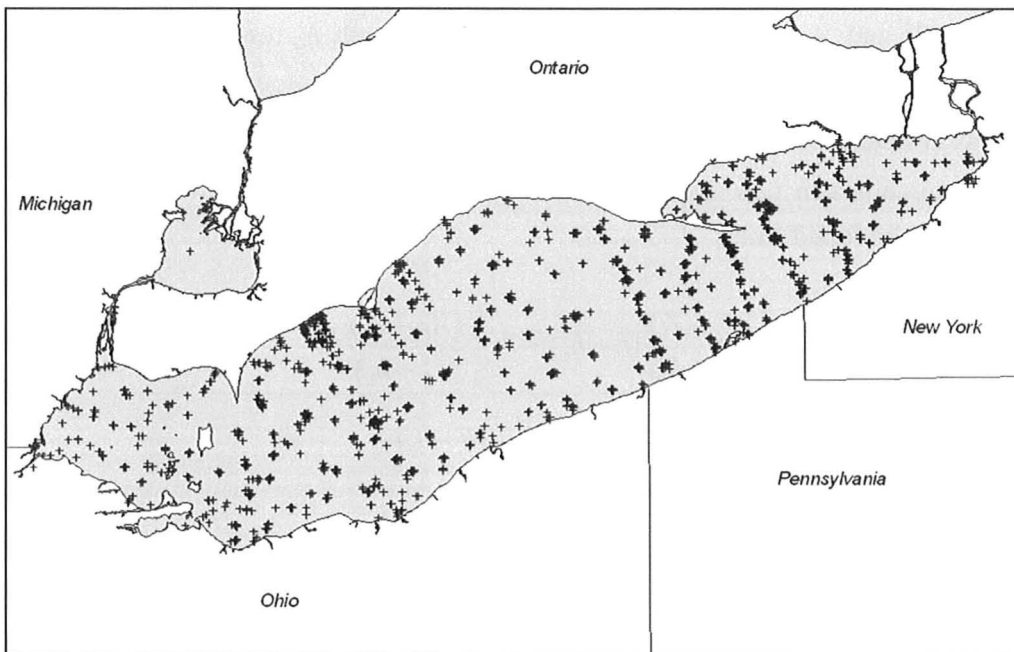


Figure 9-3: EC bathythermograph survey locations (1967-1982)

Lastly, hypsometry data in the form of planar surface areas versus elevations for Lake Erie were obtained from both Meredith (1975) and from data provided by EC, and it was found that the two datasets agreed fairly well. Furthermore, small differences in volume tend to cancel out in this analysis since thermal volume changes are determined by taking the difference in volume from the beginning of one month to the next.

The volume of Lake Erie at the beginning of each month is computed by assuming temperature (T) and area (A) vary linearly with depth, and then relating these to depth as follows:

$$T_h = \frac{(T_2 - T_1)}{(h_2 - h_1)}(h - h_1) + T_2 \quad (109)$$

$$A_h = \frac{(A_2 - A_1)}{(h_2 - h_1)}(h - h_1) + A_2 \quad (110)$$

where T_h and A_h are the temperature and area at depth h , respectively; T_1 and T_2 are the lake temperatures at depths h_1 and h_2 , respectively; A_1 and A_2 are the lake areas at depths h_1 and h_2 , respectively. The mean temperature (\bar{T}) of a volume of water between two depths, h_1 and h_2 , each having known temperature and area, can be found from:

$$\bar{T} = \frac{\int_{h_1}^{h_2} TA \cdot dh}{\int_{h_1}^{h_2} A \cdot dh} = \frac{\int_{h_1}^{h_2} \left[\frac{(T_2 - T_1)}{(h_2 - h_1)}(h - h_1) + T_2 \right] \left[\frac{(A_2 - A_1)}{(h_2 - h_1)}(h - h_1) + A_2 \right] \cdot dh}{\int_{h_1}^{h_2} \left[\frac{(A_2 - A_1)}{(h_2 - h_1)}(h - h_1) + A_2 \right] \cdot dh} \quad (111)$$

Performing the above integration and simplifying gives:

$$\bar{T} = \frac{2A_1T_1 + A_1T_2 + A_2T_1 + 2A_2T_2}{3(A_2 + A_1)} \quad (112)$$

The equation for thermal expansion of water used by Meredith (1975), as reported by Hodgman (1958), is:

$$V_T = V_0(1 - 6.427 \times 10^{-5}T + 8.5053 \times 10^{-6}T^2 - 6.79 \times 10^{-8}T^3) \quad (113)$$

where V_0 is the volume of water at zero degrees Celsius ($^{\circ}\text{C}$); T is the temperature of water in $^{\circ}\text{C}$; and V_T is the volume of water at temperature T . This equation was used to calculate the volume of water at the beginning of each month in each depth layer, with $T = \bar{T}$. The volumes of all layers were then summed, and the difference in total volume from the beginning to the end of each month was taken as the error in the change in storage resulting from thermal expansion and contraction for that month. That is:

$$\Delta S_{m,t} = V_{T,t+1} - V_{T,t} \quad (114)$$

where $\Delta S_{m,t}$ is the change in storage due to thermal expansion and contraction for month t ; $V_{T,t}$ is volume at temperature T for month t ; $V_{T,t+1}$ is volume at temperature T for month $t+1$.

There are obviously limitations with using the method outlined. The assumption of one-dimensional variation of temperature prohibits the accurate determination of the true mean water temperature of the lake, since water temperature varies in three dimensions. Furthermore, in Lake Erie, there are three distinct basins (the western end of the lake forms a small, shallow basin; the central basin is larger and deeper than the western end; the eastern basin is between the other two in area, but is also the deepest), and it has been observed that these behave differently in terms of warming and cooling of the water column (Schertzer et al., 1987). The assumption that the mean temperature at depths below the surface varies with the surface water temperature presents another limitation. The correlation between surface temperatures and temperatures below the surface decreases with depth: however, Derecki (1976) concluded that the “employment of surface temperature differences for the temperature profile estimates in Lake Erie appears to be reasonable”, noting that since the percentage of the lake volume decreases with depth, variations in total heat content at lower depths are relatively small, and therefore relatively less important in terms of volume change for the entire lake. One further limitation of the method is the lack of data for the winter months of December through March. The BOM temperature profiles developed for these months are questionable, and furthermore, in some cold months the water surface temperature may be zero or close to it, which will make the water column temperature zero when multiplied by the surface temperature, which may be unrealistic. However, according to documents referenced in Schertzer et al. (1987), winter temperatures are fairly isothermal, with relatively less variation with depth and from month to month. Therefore, thermal changes, and subsequently errors in the change in storage computations, are more significant in the other months.

The results of this analysis are provided in the tables that follow. The mean thermal volume changes computed for both the GLSEA and GLERL surface temperatures are shown in Table 9-11 and Table 9-12, respectively, with each of the three temperature profiles listed as well as the average of the three. The three profiles give similar results, with the exception of October, which showed a much smaller error using the EC profiles than when using those from Meredith (1975) or Derecki (1976). This is caused by a combination of the considerably different temperature profile developed for November from the EC data than the other datasets, as well as the large thermal effects observed during this month. The other profiles that differed substantially were those developed for

Table 9-11: Mean thermal volume change for each vertical temperature profile using GLSEA surface temperature data.

Month	Mean Volume Change per Month (m ³ /s)			Average
	Meredith (1975)	Derecki (1976)	EC	
Jan	6	6	--	6
Feb	3	1	--	2
Mar	-6	-6	--	-6
Apr	1	2	-6	-1
May	56	92	74	74
Jun	163	190	193	182
Jul	181	133	144	153
Aug	17	13	12	14
Sep	-160	-108	-132	-133
Oct	-153	-191	-79	-141
Nov	-77	-87	--	-82
Dec	-33	-47	--	-40

Table 9-12: Mean thermal volume change for each vertical temperature profile using GLERL modelled surface temperature data

Month	Mean Volume Change per Month (m ³ /s)			Average
	Meredith (1975)	Derecki (1976)	EC	
Jan	12	12	--	12
Feb	1	1	--	1
Mar	-6	-7	--	-7
Apr	-6	-5	-11	-7
May	52	89	70	70
Jun	164	191	195	183
Jul	192	144	154	163
Aug	51	48	46	48
Sep	-143	-80	-110	-111
Oct	-157	-198	-47	-134
Nov	-130	-149	--	-140
Dec	-29	-45	--	-37

the winter months of December through April, but the average results from these were relatively similar due to the small thermal effects these months experience. Overall, for both surface temperature datasets, the mean results agreed fairly well for each of the three different profiles used.

Furthermore, a comparison of the average errors from the two surface temperature datasets shows them to be in good agreement (Table 9-13), with the exceptions of August and November, whose values were greater (in absolute terms) in the GLERL modelled data (48 and -140 m³/s, respectively) than in the GLSEA data (14 and -82 m³/s, respectively). The reason for this is unclear, but it may reflect an issue with the modelled temperature data for one of these months, differences in the temperature profiles, or some other unknown factor. A comparison of the average results from this study to the results of Meredith (1975) and Quinn and Guerra (1986), both of which used a different surface temperature dataset and period of record, is also given in Table 9-13. The results differ to a certain degree, but are of the same order of magnitude, and for the most part of the same sign (positive or negative) except for some months that showed only small mean thermal volume changes.

Table 9-13: Comparison of mean thermal volume change results

Month	Mean Volume Change per Month (m ³ /s)			
	Avg. from Current Study		Meredith (1975)	Quinn and Guerra (1986)
	GLSEA	GLERL Modelled		
Jan	6	12	11	17
Feb	2	1	2	-1
Mar	-6	-7	-10	-15
Apr	-1	-7	-3	4
May	74	70	32	92
Jun	182	183	101	131
Jul	153	163	107	73
Aug	14	48	18	-18
Sep	-133	-111	-92	-105
Oct	-141	-134	-91	-73
Nov	-82	-140	-72	-93
Dec	-40	-37	-6	-15

The standard deviation of the thermal expansion and contraction effects is not a good descriptor of the spread of the observed data, due to the large skewness observed for some months. Also, given the limitations of this analysis, as outlined above, the results are highly uncertain and it was deemed that the data should not be used for the uncertainty analysis directly. Instead, histograms for each month were reviewed and approximate distributions were fit to the data using some judgement.

The GLSEA and GLERL modelled data were combined for the concurrent period of November 1994 to 2009 only. The earlier GLERL data (i.e. 1948 to October 1994) were omitted in order to ensure that the two temperature datasets were given equal weight. Also, the monthly means for the 1994-2009 period did not differ significantly from the full period of record, and given the general assumptions and limitations of this analysis it is unlikely that inclusion of the full period of record would improve the results in any truly meaningful way.

Histograms were plotted for each month using the 1994-2009 combined dataset. Triangular PDFs were fit to the data for all months using the minimum and maximum thermal volume changes determined from the dataset, and assuming the mode was equal to the median of the data; the exception was January, in which a uniform distribution was used as it was found that this fit the data somewhat better. Triangular distributions are useful when one knows or can approximate what the lower and upper limits of a dataset are, as well as the mode. Uniform distributions are useful when one only knows the upper and lower limits, but has no knowledge of the distribution of the values between these limits. Some judgement was also used when fitting the distributions: first, what appeared to be outliers in April, May and December were omitted; second, the maximum value of the September probability distribution was increased from $2 \text{ m}^3/\text{s}$ to $78 \text{ m}^3/\text{s}$ (arbitrarily chosen as one-quarter of the difference between the October and August maximums), since there was a large discrepancy between the maximum in the combined 1994-2009 dataset ($-2 \text{ m}^3/\text{s}$) and the maximum in the full GLERL dataset ($137 \text{ m}^3/\text{s}$), and since the value of $-2 \text{ m}^3/\text{s}$ did not seem to be consistent with the maximum from October through December, which were all positive values. Specifically, it seems unreasonable that thermal expansion would never occur in September given that it was found to occur in the earlier GLERL data and in August through December. The parameters of the distributions for each month used in the uncertainty analysis are given Table 9-15 below, and the histograms and fitted distributions can be seen in Appendix F.

The standard uncertainty estimates were also computed for each distribution for use in the FOSM analysis. The equations given in Table 9-14 (ISO, 2005) were used to compute the mean and variance of the uniform distribution used in January, and the triangular distributions for all other months. The standard uncertainty estimate is the square root of the variance. The results are provided in Table 9-15. Note that the sum of both the modes and the mean errors for each month are close to zero (2 m³/s and -13.7 m³/s, respectively). On an annual basis, it would be expected that the net effect of thermal volume change would be approximately zero; otherwise the lake would be gradually increasing or decreasing in temperature over time. While this may be true to a small degree, the differences in this case are likely a result of the limitations of the analysis itself, and the assumptions made regarding the probability distributions in order to best represent the uncertainty in thermal volume changes on a monthly basis.

Table 9-14: Uniform and triangular distribution mean and variance equations

Distribution	Mean	Variance
Uniform	$\frac{a+b}{2}$	$\frac{(b-a)^2}{12}$
Triangular	$\frac{a+b+c}{3}$	$\frac{a^2 + b^2 + c^2 - ab - ac - bc}{18}$
<i>a = minimum; b = maximum; c = mode</i>		

Table 9-15: Thermal volume change uncertainty PDFs and parameters (m³/s)

Month	Distribution	Min	Mode	Max	Mean Error	Standard Error
Jan	Uniform	-4	--	23	9.5	7.8
Feb	Triangular	-11	0	17	2.0	5.8
Mar	Triangular	-23	-8	11	-6.7	7.0
Apr	Triangular	-23	-1	40	5.3	13.1
May	Triangular	8	68	180	85.3	35.6
Jun	Triangular	44	203	312	186.3	55.0
Jul	Triangular	33	147	277	152.3	49.8
Aug	Triangular	-133	22	148	12.3	57.5
Sep	Triangular	-262	-108	78	-97.3	69.5
Oct	Triangular	-340	-152	55	-145.7	80.7
Nov	Triangular	-368	-128	21	-158.3	80.1
Dec	Triangular	-140	-41	5	-58.7	30.2

9.9 Alternative Change in Storage Estimation Methods

The results of the spatial variability analysis indicated that including the Toledo and Port Colborne gauge stations in the computation of average Lake Erie water level actually increases the error in the computed change in storage as a result of the greater errors that affect these gauges in particular. The Toledo gauge is especially poor. The results also indicate that in order to reduce errors in the change in storage computation it may be better to estimate the lake-wide mean using only Cleveland and Port Stanley, or another combination of gauges in the central basin, as opposed to the four-gauge average. Alternatively, one of the various Thiessen networks suggested by Quinn and Derecki (1976) may be more appropriate. Regardless, the choice of network would require further analysis to determine what network to use in order to minimize errors, and how to adjust the network for periods of missing data, both historically and into the future.

Alternative methods could be used to estimate the mean water level of Lake Erie, including the use of Thiessen or some other weighting scheme, as described above. Another alternative would be the use of an interpolation method such as linear interpolation, for example, or a more advanced method such as kriging. These methods should reduce the uncertainty resulting from using a straight average of only four gauges, though by how much is unclear. To use such a method, however, an analysis should be completed to determine the best weighting or interpolation scheme to use, and also how best to adjust the method during periods when data at a gauge or gauges might be unavailable. Another alternative would be to model the water surface elevation using a hydrodynamic model of the lake and incorporate wind stress and other meteorological factors.

Furthermore, since the error due to temporal variability was found to be small due to averaging, it is possible that a longer averaging period could be used to determine the mean BOM water levels, and this could help reduce the error due to spatial variability. While not investigated as part of this research, another alternative that may reduce temporal and spatial errors would be to integrate the change in storage over the course of a month using a smaller time step, as opposed to taking the beginning minus the end of month water levels as the change in storage. By doing this, short-term errors caused by meteorological impacts affecting BOM water levels might be reduced.

Thermal expansion and contraction should be incorporated into NBS estimates when appropriate. Thermal volume change corrections should be subtracted from the residual NBS when comparing them to component NBS, but should be added to the component NBS if using these to model historic water levels using a routing model. Unfortunately our ability to do this is limited by a lack of data. The dimensionless temperature profile method outlined above is useful for estimating the magnitude of errors, but is likely limited in its ability to model actual thermal volume changes over the course of a month due to the assumptions involved. An alternative method would be to use modelled vertical temperature profiles produced by an energy balance model. This might be especially useful for determining thermal effects in the winter months, where measured vertical temperature profiles are unavailable. It is suggested that this be pursued if accounting for thermal expansion and contraction in the Great Lakes water balance is to be considered further.

10 Sources and Estimates of Uncertainty in Consumptive Use

Consumptive use data are reported to the Great Lakes Commission (GLC) by each of the Great Lakes states and provinces as required by the Great Lakes - St. Lawrence River Basin Water Resources Compact. The GLC is responsible for maintaining and operating the Great Lakes Regional Water Use Database (GLC, 2003b). In this regard, the GLC acts as a data repository for regional water use data, ensuring that data received and transmitted are uniform and consistent across the basin, and providing annual summary reports made available to the public. The regional water use database includes total withdrawals and diversions in addition to consumptive use data.

According to the GLC (2003a), consumptive use is estimated using one of two methods in the Great Lakes basin: the first method involves directly subtracting measured return flow and conveyance losses from overall withdrawals; the second method, which is more predominant in the Great Lakes basin, involves multiplying total withdrawals by a generally agreed-upon coefficient for consumptive use, expressed as a percentage. The coefficients are developed and applied by the different jurisdictions, and differ across the basin. There is very little documentation or knowledge of where the coefficients originate from, and consumptive use data are often described as an “estimate of an estimate”, since the original withdrawal data, along with the coefficients, are both estimated (GLC, 2003a). The reliability of facility-reported withdrawal data is also questioned, and therefore, the uncertainty in consumptive use data is large. In fact, the consumptive use estimates were considered so unreliable by the USGS, that they have omitted consumptive use information from their 5-year water use reports for the United States (Becky Pearson, GLC, personal communication, 16 August, 2010).

According to the GLC Regional Water Use Database annual reports (http://www.glc.org/wateruse/database/downloads_new.html), which are summarized in Table 10-1, when converted to metric discharge units the total withdrawal of water from the Lake Erie basin (which includes Great Lakes surface water (GLSW), other surface water (OSW) and groundwater (GW)) has been approximately 2200 to 3100 m³/s from 1998 to 2006. Of this total withdrawal, approximately 14 to 26 m³/s, or about 1%, was considered

consumptive use (CU). Given the uncertainty in these estimates, for the overall uncertainty analysis the error distribution for Lake Erie consumptive use was assumed uniform, ranging from a low value of $10 \text{ m}^3/\text{s}$ to a high value of $30 \text{ m}^3/\text{s}$. Applying equation (88) for the variance of a uniform distribution, the standard uncertainty was computed as $(30 - 10) / \sqrt{12} = 6 \text{ m}^3/\text{s}$.

Table 10-1: Lake Erie total withdrawals, diversions and consumptive use estimates

Year	Total Withdrawals (m^3/s)				Diversions (m^3/s)		CU (m^3/s)
	GLSW	OSW	GW	Total	Intrabasin	Interbasin	
1998	3076	21	16	3113	248	0	26
1999	2433	21	16	2470	186	0	26
2000	2210	21	17	2248	224	0	23
2001	2094	50	17	2161	224	0	23
2002	2363	49	17	2429	224	0	22
2003	2166	49	17	2231	255	0	22
2004	2477	56	16	2549	255	0	21
2005	2496	64	17	2577	255	0	22
2006	2454	60	18	2533	255	0	14

As Neff and Nicholas (2005) have pointed out, in order to determine how consumptive use estimates should be applied to the NBS computations, the location that the consumptive use is withdrawn from must be determined, since this determines whether it has been accounted for in the component or residual NBS computations. For instance, if water is removed directly from a Great Lake and consumed, the quantity of water should be added to the residual NBS, but not to the component NBS, because the residual method does not account for the consumptive use in the change in storage computations, but the component method has already accounted for the consumed water in the measured runoff and precipitation. On the other hand, if water is removed from a lakes' drainage basin as opposed to the lake itself, this volume of water may need to be added to both residual and component NBS estimates, depending on where the water is removed from.

Given that most of the total withdrawals ($> 97\%$) as reported by the GLC are indicated as being from the lakes themselves (i.e. Great Lakes Surfacewater (GLSW)), and the fact that by far the largest consumptive use categories are

public water supply and industrial uses (~60% of total consumptive use), both of which likely originate primarily in the large population centres located along the shores of Lake Erie (e.g. Buffalo, Cleveland, Toledo) as opposed to upstream, it seems likely that most of the total consumptive use in the Lake Erie basin comes directly from the lake itself. As such, it was assumed that the total consumptive use value estimated above should be added to the residual NBS when comparing to the component NBS estimate.

Despite predictions to the contrary, consumptive use estimates have decreased with time. For example, the total consumptive use for the entire Great Lakes basin was estimated by the IJC to be approximately $140 \text{ m}^3/\text{s}$ in 1975, and it was predicted that this value would increase to 227 to $337 \text{ m}^3/\text{s}$ by the year 2000 (IGLDCUSB, 1981); however, the GLC (2004) estimated total consumptive use in the Great Lakes to be only $85 \text{ m}^3/\text{s}$ in 2000, a decrease of nearly 40% from the 1975 consumptive use estimate, and far from even the lowest predicted values in 2000. Again, these estimates are subject to a large amount of uncertainty, so definitive statements as to the causes of these differences may be inappropriate.

11 Overall Uncertainty in Residual NBS

11.1 Hydrologic Data

The hydrologic data used in this study to determine the overall uncertainty in residual NBS, including monthly estimates of inflows, outflows, change in storage and the NBS itself, were obtained from the USACE Detroit District office. Data were available for the period of 1900 to 2008. For the FOSM analysis, the monthly hydrologic data obtained were averaged by month. The mean monthly hydrologic data are provided in Table 11-1, and the mean monthly residual NBS are plotted in Figure 11-1. For the Monte Carlo analysis, the monthly data were used directly, with subsets of stochastic estimates of each input sampled for each month from the probability distributions derived in this study.

Table 11-1: Lake Erie monthly mean residual NBS and input estimates (1900-2008)

Month	Mean Flow (m ³ /s)					
	$O_{N@Bif}$	D_{NYSBC}	O_{WC}	I_{Det}	ΔS	NBS_E
Jan	5540	10	140	4790	-80	820
Feb	5430	10	140	4650	170	1090
Mar	5590	10	150	5060	1330	2010
Apr	5850	10	160	5340	1260	1930
May	6110	30	160	5480	540	1340
Jun	6110	30	160	5540	160	900
Jul	6020	30	160	5590	-400	190
Aug	5910	30	160	5580	-750	-260
Sep	5790	30	160	5540	-910	-500
Oct	5690	30	160	5510	-910	-570
Nov	5690	30	160	5470	-460	-80
Dec	5700	10	150	5330	80	610
Annual	5788	22	155	5327	1	620

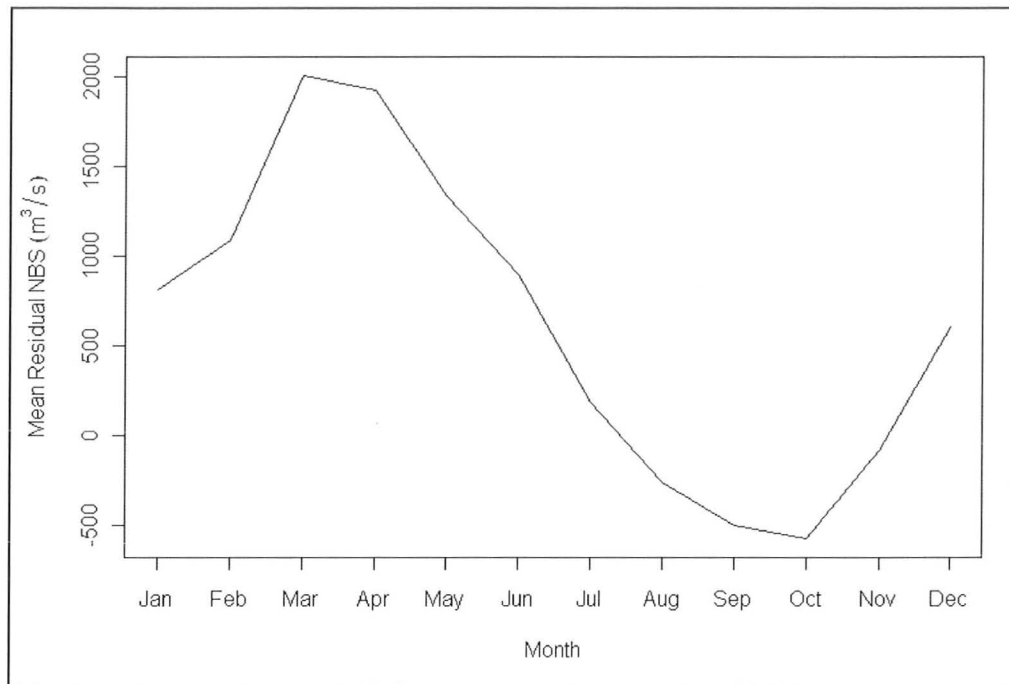


Figure 11-1: Lake Erie monthly mean residual NBS (1900-2008)

It should be noted that the uncertainty estimates in this research were determined from the most recent methods and models used to determine residual NBS for Lake Erie. Models and methods have evolved over time, and it seems likely that through scientific and technological advances, improvements in measurement methods, and even increased care and scrutiny of the data due to heightened awareness of their importance, in at least some cases uncertainty in the most recent data would be less than in the historic data. As such, the uncertainty estimates derived in this study may not apply directly to any data other than the most recently computed values. Nonetheless, the entire period of record (1900 to 2008) was used to provide a longer time series of computed values. A shorter period was also analyzed, running from 1962 to 2008. This represents the period for which discrete Niagara River data are available. It also corresponds to a more stable regime in the Detroit River, since no dredging for navigation purposes has taken place since 1962, and the NYSBC and Welland Canal diversions during this period are also more consistent with current values. In any case, as will be shown, the results from both periods were found to be similar. The mean flow estimates for this period are shown in Table 11-2.

Table 11-2: Lake Erie monthly mean residual NBS and input estimates (1962-2008)

Month	Mean Flow (m ³ /s)					
	$O_{N@Buf}$	D_{NYSBC}	O_{WC}	I_{Det}	ΔS	NBS_E
Jan	5890	0	200	5140	-50	900
Feb	5840	0	200	5170	490	1360
Mar	6040	0	210	5480	1280	2050
Apr	6260	10	240	5530	930	1900
May	6440	30	240	5620	320	1390
Jun	6360	30	240	5680	130	1050
Jul	6270	30	240	5730	-460	320
Aug	6160	30	240	5730	-720	-50
Sep	6030	30	240	5710	-900	-340
Oct	5950	30	230	5680	-980	-470
Nov	5930	20	230	5650	-280	230
Dec	6010	0	220	5550	340	1030
Annual Avg.	6100	18	228	5558	5	777

11.2 Combined Residual NBS Uncertainty: FOSM Method

The FOSM method was applied to the mean monthly discharge estimates. Since the sensitivity coefficients for each input are equal to one, the uncertainty in any month can be determined from:

$$u(NBS_E) = \sqrt{u^2(O_{N@BUF}) + u^2(O_{WC}) + u^2(I_{Det}) + u^2(\Delta S) + u^2(C_E)} \quad (115)$$

The combined uncertainty in the Niagara River flow at Buffalo ($O_{N@Buf}$) was estimated for the 1962-2008 period in Section 6.7 (see Table 6-9). Since flow data for each of the individual Niagara River flow inputs were not available prior to 1962, the relative uncertainty for this period computed for each month as shown in Table 6-9 was used to compute the uncertainty in the $O_{N@Buf}$ for the full period of record (1900-2008). The standard uncertainty in the Welland Canal flow (O_{WC}) was found to be 4% in Section 7.6, and the standard uncertainty in the Detroit River flow (I_{Det}) was found to be 4.3% in Section 8.5. The uncertainty in

the change in storage (ΔS) was computed using the FOSM method in Section 9.7. The uncertainty resulting from thermal volume changes (ΔS_{Th}) was discussed in Section 9.8. Finally, the error caused by considering the consumptive use (C_E) as negligible was determined in Section 10 to be a mean of 20 m³/s, having limits of +/- 10 m³/s, with standard error computed as approximately 6 m³/s.

A summary of the standard uncertainty estimates for 1900-2008 for each input is provided in Table 11-3. This table can also be used to compare the magnitude of the different sources of uncertainty. For example, the largest source of uncertainty can be seen to be the Detroit River inflow, but the outflow and change in storage are of a similar magnitude. This is an interesting result, since the uncertainty in the change in storage is often assumed to be less than the uncertainty in the inflow and outflow terms (e.g. Neff and Nicholas, 2005). The additional uncertainty caused by the change in storage due to thermal expansion and contraction is also seen to be significant.

The combined uncertainty estimates in Lake Erie residual NBS as computed using the FOSM method are provided in Table 11-4. The absolute uncertainty estimates vary by month, but only to a small degree. The relative uncertainty estimates show much more variability by month as a result of the variability in the magnitude of the mean monthly NBS estimates. In three months (July, August and November), the combined standard uncertainty estimate was in excess of the mean computed NBS (i.e. uncertainty was greater than 100%). The highest uncertainty estimates in an absolute sense were November for both periods of record. November was also the highest in a relative sense for the 1900-2008 period, with August being the highest in a relative sense for the 1962-2008 period. Note that these are only relative to the mean NBS for each month. The uncertainty for any individual month will be higher or less than the estimates given depending on the magnitude of the different inputs and the computed NBS.

Table 11-3: Standard uncertainty estimates for Lake Erie residual NBS inputs (1900-2008)

Month	$O_{N@Buf}$			O_{WC}			I_{Det}			ΔS			ΔS_{Th}			C_E		
	\bar{Q} (m ³ /s)	u (%)	u (m ³ /s)	\bar{Q} (m ³ /s)	u (%)	u (m ³ /s)	\bar{Q} (m ³ /s)	u (%)	u (m ³ /s)	\bar{Q} (m ³ /s)	u (%)	u (m ³ /s)	\bar{Q} (m ³ /s)	u (%)	u (m ³ /s)	\bar{Q} (m ³ /s)	u (%)	u (m ³ /s)
Jan	5540	1.86	103	140	4.0	6	4790	4.3	206	-80	209	167	9.5	82	7.8	20	30	6
Feb	5430	1.88	102	140	4.0	6	4650	4.3	200	170	103	174	2.0	290	5.8	20	30	6
Mar	5590	1.88	105	150	4.0	6	5060	4.3	218	1330	12	166	-6.7	104	7.0	20	30	6
Apr	5850	1.92	112	160	4.0	6	5340	4.3	230	1260	13	165	5.3	247	13.1	20	30	6
May	6110	1.86	114	160	4.0	6	5480	4.3	236	540	24	130	85.3	42	35.6	20	30	6
Jun	6110	1.85	113	160	4.0	6	5540	4.3	238	160	73	117	186.3	30	55.0	20	30	6
Jul	6020	1.83	110	160	4.0	6	5590	4.3	240	-400	26	106	152.3	33	49.8	20	30	6
Aug	5910	1.84	109	160	4.0	6	5580	4.3	240	-750	14	106	12.3	467	57.5	20	30	6
Sep	5790	1.87	108	160	4.0	6	5540	4.3	238	-910	15	137	-97.3	71	69.5	20	30	6
Oct	5690	1.87	106	160	4.0	6	5510	4.3	237	-910	19	174	-145.7	55	80.7	20	30	6
Nov	5690	1.81	103	160	4.0	6	5470	4.3	235	-460	48	219	-158.3	51	80.1	20	30	6
Dec	5700	1.86	106	150	4.0	6	5330	4.3	229	80	254	203	-58.7	51	30.2	20	30	6

Table 11-4: Combined uncertainty in Lake Erie residual NBS using FOSM method

Month	1900-2008			1962-2008		
	\overline{NBS}_E (m ³ /s)	u (m ³ /s)	u (%)	\overline{NBS}_E (m ³ /s)	u (m ³ /s)	u (%)
Jan	820	285	35	900	298	33
Feb	1090	284	26	1360	303	22
Mar	2010	293	15	2050	310	15
Apr	1930	305	16	1900	314	17
May	1340	294	22	1390	302	22
Jun	900	294	33	1050	300	29
Jul	190	289	152	320	296	93
Aug	-260	290	111	-50	297	594
Sep	-500	304	61	-340	311	92
Oct	-570	323	57	-470	330	70
Nov	-80	347	434	230	354	154
Dec	610	326	53	1030	334	32
Annual Avg.	620	303	49	777	312	40

The mean error in the residual NBS caused by systematic errors was also computed. Systematic errors were found in the local runoff estimate to the upper Niagara River (Section 6.5) and in the change in storage (Section 9.7); systematic errors also result from assuming thermal volume change and consumptive use as negligible. The mean error in the computed NBS resulting from each of these sources can be found from:

$$\varepsilon(NBS_E) = \varepsilon(\Delta S_{Th}) - \varepsilon(C_E) - \varepsilon(\Delta S) - \varepsilon(R_N) \quad (116)$$

where $\varepsilon(NBS_E)$ is the systematic error in the computed NBS for Lake Erie; $\varepsilon(\Delta S_{Th})$ is the systematic error caused by unaccounted for thermal volume changes; $\varepsilon(C_E)$ is the systematic error cause by not accounting for consumptive use; $\varepsilon(\Delta S)$ is the systematic errors found in the change in storage; and $\varepsilon(R_N)$ is the systematic error in the local runoff to the upper Niagara River,.

The mean error results are given in Table 11-5. It can be seen that not accounting for changes in storage due to thermal expansion and contraction is the primary source of systematic error in NBS: other sources of systematic error provide relatively little additional error. A consequence of this is that even if the apparent bias observed in the change in storage is not real, as discussed in Section 9.4, it has little effect on the mean error in NBS. There may in fact be additional sources of systematic error that have not been accounted for in this research. As one example, runoff from the Lake Erie drainage basin that flows directly into the Detroit River may be measured as part of the Detroit River inflow computed using the stage-fall-discharge equations. This small amount would be accounted for in both the residual and component NBS for Lake Erie. While this example and other similar systematic errors might be quite small, they should be considered in comparisons of residual and component NBS estimates.

Table 11-5: Mean systematic error in Lake Erie residual NBS

Month	Mean Error (m ³ /s)				
	$\varepsilon(\Delta S_{Th})$	$\varepsilon(C_E)$	$\varepsilon(\Delta S)$	$\varepsilon(R_N)$	$\varepsilon(NBS_E)$
Jan	10	20	-16	-19	25
Feb	2	20	-13	-28	23
Mar	-7	20	-14	-13	-1
Apr	5	20	4	9	-26
May	85	20	9	8	48
Jun	186	20	20	3	143
Jul	152	20	7	3	122
Aug	12	20	-15	-2	8
Sep	-97	20	11	-6	-122
Oct	-146	20	9	-5	-169
Nov	-158	20	29	-14	-193
Dec	-59	20	-30	-29	-20
Annual Avg.	-1	20	0	-8	-13

11.3 Combined Residual NBS Uncertainty: Monte Carlo Method

Given that the probability distributions of the error sources were known or estimated, an estimate of the combined uncertainty in the overall NBS was also possible using a Monte Carlo approach. The “R” statistical software was used to randomly sample from the probability distributions of each of the input parameters. The distributions and parameters used are summarized in Table 11-6. For the Niagara River, somewhat different methods were used depending on the year. For the period 1962-2008, the Monte Carlo analysis results computed in Section 6.7 using the individual subcomponent flow uncertainty estimates (i.e. the summation equation) were used directly. For the period 1900-1961, subcomponent data could not be obtained, and only the total Niagara River flow at Buffalo is available. Since the Monte Carlo analysis results from the 1962-2008 period for the total Niagara River flow at Buffalo were found to be normally distributed and vary little from month to month, the Niagara River flow at Buffalo was represented by a normal distribution for the period 1900-1961 as well, with a mean equal to the computed monthly Niagara River flow at Buffalo and standard deviation equal to the average of the monthly standard deviations computed from the 1962-2008 analysis in Section 6.7. For the change in storage, the results previously presented in Section 9.7 for the 1900-2008 period were used.

A summary of the mean monthly results from the Monte Carlo analysis are shown in Table 11-7 for the 1900-2008 period, and Table 11-8 for the 1962-2008 period. The standard error results for both periods are quite similar in absolute terms; the standard errors in relative terms are somewhat different due to the difference in the mean NBS computed for each period. Furthermore, similar to the FOSM method results, there is little monthly variation in the absolute uncertainty estimates, whereas in relative terms the uncertainty varies due to differences in magnitude of the mean monthly NBS values. The differences between the average deterministic and average Monte Carlo results as captured by the mean error columns indicate the bias that results from systematic effects as noted in the previous section.

Table 11-6: Distributions and parameters used in residual NBS Monte Carlo analysis

Input	Month	Distrib.	Par. 1	Value	Par. 2	Value	Par.3	Value
$O_{N@Buf}$	Jan	Normal	Mean	monthly estimates	SD	1.9%	N/A	N/A
	Feb					1.9%	N/A	N/A
	Mar					1.9%	N/A	N/A
	Apr					1.9%	N/A	N/A
	May					1.9%	N/A	N/A
	Jun					1.9%	N/A	N/A
	Jul					1.8%	N/A	N/A
	Aug					1.8%	N/A	N/A
	Sep					1.9%	N/A	N/A
	Oct					1.9%	N/A	N/A
	Nov					1.8%	N/A	N/A
	Dec					1.9%	N/A	N/A
O_{WC}	All	Normal	Mean	monthly estimates	SD	4.0%	N/A	N/A
I_{Det}	All	Normal	Mean	monthly estimates	SD	4.3%	N/A	N/A
ΔS	(See discussion and results presented in Section 9.7)							
ΔS_{Th}	Jan	Uniform	Min	-4 m ³ /s	Max	23 m ³ /s	N/A	N/A
	Feb	Triangular	Min	-11 m ³ /s	Max	17 m ³ /s	Mode	0 m ³ /s
	Mar	Triangular	Min	-23 m ³ /s	Max	11 m ³ /s	Mode	-8 m ³ /s
	Apr	Triangular	Min	-23 m ³ /s	Max	40 m ³ /s	Mode	-1 m ³ /s
	May	Triangular	Min	8 m ³ /s	Max	180 m ³ /s	Mode	68 m ³ /s
	Jun	Triangular	Min	44 m ³ /s	Max	312 m ³ /s	Mode	203 m ³ /s
	Jul	Triangular	Min	33 m ³ /s	Max	277 m ³ /s	Mode	147 m ³ /s
	Aug	Triangular	Min	-133 m ³ /s	Max	148 m ³ /s	Mode	22 m ³ /s
	Sep	Triangular	Min	-262 m ³ /s	Max	78 m ³ /s	Mode	-108 m ³ /s
	Oct	Triangular	Min	-340 m ³ /s	Max	55 m ³ /s	Mode	-152 m ³ /s
	Nov	Triangular	Min	-368 m ³ /s	Max	21 m ³ /s	Mode	-128 m ³ /s
	Dec	Triangular	Min	-140 m ³ /s	Max	5 m ³ /s	Mode	-41 m ³ /s
C_E	All	Uniform	Min	10 m ³ /s	Max	30 m ³ /s	N/A	N/A

Table 11-7: Residual NBS mean Monte Carlo analysis results (1900-2008)

Month	Mean Deterministic (m ³ /s)	Mean Monte Carlo (m ³ /s)	Difference (Mean Error) (m ³ /s)	Mean Standard Error (m ³ /s)	Mean Standard Error (% of NBS)
Jan	819	793	26	286	36
Feb	1092	1068	24	285	27
Mar	2011	2010	1	295	15
Apr	1928	1954	-26	305	16
May	1341	1290	51	295	23
Jun	898	750	148	294	39
Jul	193	68	125	290	427
Aug	-257	-266	9	290	109
Sep	-500	-381	-119	303	80
Oct	-571	-406	-165	325	80
Nov	-84	106	-190	347	328
Dec	610	628	-18	327	52

Table 11-8: Residual NBS mean Monte Carlo analysis results (1962-2008)

Month	Mean Deterministic (m ³ /s)	Mean Monte Carlo (m ³ /s)	Difference (Mean Error) (m ³ /s)	Mean Standard Error (m ³ /s)	Mean Standard Error (% of NBS)
Jan	903	878	24	299	34
Feb	1356	1336	21	303	23
Mar	2054	2053	0	311	15
Apr	1901	1926	-25	314	16
May	1390	1343	47	302	22
Jun	1045	901	144	300	33
Jul	316	194	122	296	153
Aug	-51	-57	6	297	523
Sep	-340	-217	-124	311	143
Oct	-469	-300	-169	332	111
Nov	229	424	-195	354	84
Dec	1027	1046	-19	335	32

By applying the Monte Carlo method to each month individually, additional information on the maximum and minimum uncertainty for each month can be obtained. Table 11-9 shows the maximum and minimum uncertainty for each month for the 1962-2008 period, as well as the standard deviation of the

monthly uncertainty estimates. It can be seen that uncertainty estimates ranged from about 240 m³/s to 390 m³/s, with standard deviations of around 20 m³/s for each month, which is not very significant. However, because the magnitude of the NBS estimates themselves varies significantly, and since the NBS can often be close to zero for any month, the variation in relative terms is quite significant, with the uncertainty in NBS often dwarfing the actual estimate itself.

Table 11-9: Monthly range and SD of 1962-2008 residual NBS Monte Carlo analysis results

Month	Monthly Uncertainty Estimates (m ³ /s)		
	Maximum	Minimum	Standard Deviation
Jan	349	255	23
Feb	349	240	22
Mar	351	269	22
Apr	352	267	22
May	347	256	22
Jun	342	248	23
Jul	337	251	22
Aug	337	252	21
Sep	354	265	21
Oct	381	298	19
Nov	390	310	19
Dec	375	288	20
Overall	390	240	--

The Monte Carlo results for 2008 were plotted (Appendix G) and found to be normally distributed. Some of the error distributions used for the model inputs were not normally distributed, specifically the change in storage due to spatial variability, the change in storage due to thermal expansion and contraction, and the consumptive use distributions. However, by combining the results from a large number of inputs, each of which was described as a statistically independent random variable, and none of which were significantly larger in magnitude than the others, the combined uncertainty estimate in the residual NBS approaches the normal distribution as a result of the central limit theorem.

11.4 Comparison of FOSM and Monte Carlo Analysis Results

A comparison of the standard uncertainty estimates for the two methods is shown in Table 11-10. As can be seen, the results of both methods are nearly identical. As discussed in Section 6.7 and 9.7, the FOSM and Monte Carlo analysis methods provide identical results when the model being investigated is linear. Referring to equation (19) in Section 3.3.6, the residual NBS model is a simple summation of a number of inputs, and is a linear model when the area of Lake Erie is considered constant (as it was in this study) or nearly linear if the area is allowed to vary. Therefore, one can expect the results of the FOSM and Monte Carlo methods to be nearly identical, so long as care is taken to ensure the uncertainty estimates in each of the inputs are computed in comparable fashion for both methods.

Table 11-10: Mean FOSM and Monte Carlo analysis results for residual NBS

Month	Standard Uncertainty (m^3/s)					
	1900-2008			1962-2008		
	FOSM	MC	DIFF	FOSM	MC	DIFF
Jan	285	286	-1	298	299	-1
Feb	284	285	-1	303	303	0
Mar	293	295	-1	310	311	-1
Apr	305	305	0	314	314	-1
May	294	295	0	302	302	0
Jun	294	294	0	300	300	1
Jul	289	290	-1	296	296	0
Aug	290	290	0	297	297	0
Sep	304	303	0	311	311	0
Oct	323	325	-2	330	332	-2
Nov	347	347	-1	354	354	0
Dec	326	327	-1	334	335	0

A comparison of the mean errors is shown in Table 11-11. The results are again quite similar, with differences of less than an absolute value of $5 \text{ m}^3/\text{s}$. These small differences may be the result of rounding or resolution errors, but regardless, the estimates are in close agreement. Again, the mean error in both

cases is dominated by the errors caused by ignoring change in storage due to thermal expansion and contraction.

Table 11-11: Mean systematic error in monthly residual NBS

Month	Mean Error (m ³ /s)		
	FOSM	MC	DIFF.
Jan	25	26	-1
Feb	23	24	-1
Mar	-1	1	-2
Apr	-26	-26	0
May	48	51	-3
Jun	143	148	-5
Jul	122	125	-3
Aug	8	9	-1
Sep	-122	-119	-3
Oct	-169	-165	-4
Nov	-193	-190	-3
Dec	-20	-18	-2
Annual Avg.	-13	-11	-2

In terms of application of the two methods, in practice the FOSM method was found to be much simpler to apply; however, so long as the distributions of the model inputs are known, it was found to be possible and also relatively simple to perform a Monte Carlo analysis given the simplicity of the NBS model, as well as the computing power and statistical software packages now readily available. While the FOSM method is the simpler of the two methods to apply, it may not provide accurate uncertainty estimates if the model is highly non-linear or if the probability distributions of the input values are highly asymmetric; however, as discussed, this was not an issue in the analysis of residual NBS for Lake Erie. Overall, use of the Monte Carlo approach to determine uncertainty in residual NBS is likely unnecessary, given that the results from the FOSM and Monte Carlo methods were nearly identical. The Monte Carlo analysis approach is beneficial in that it provides the full probability distribution of the model output; however, this analysis showed that the overall combined uncertainty in NBS was normally

distributed, a result of the high-dimensionality of the model and the fact that none of the statistically independent random input variables dominated in terms of magnitude, which allows the central limit theorem to apply. Therefore, given similar conditions it might safely be assumed in future studies that the overall uncertainty in the residual NBS is normally distributed, even if only the FOSM method is applied and only the mean and standard deviation of the model output are obtained, thus making application of the Monte Carlo method unnecessary. That said, in order to ensure the FOSM results are accurate, care must be taken to properly describe the standard uncertainty estimates in each of the different inputs.

11.5 Sensitivity Analysis

A sensitivity analysis was performed on the uncertainty analysis results to determine how changes in the uncertainty estimates in each of the various inputs affect the overall combined uncertainty in the Lake Erie residual NBS. Given that the results of the FOSM and Monte Carlo methods were so similar, the sensitivity analysis was performed using only the FOSM method. One of the benefits of the FOSM method is that it makes performing a sensitivity analysis a simple task. This method requires much fewer calculations in comparison to the Monte Carlo method, which requires thousands of simulations in order to properly define the probability distribution of the model output.

A number of scenarios were investigated in this sensitivity analysis. These included:

- (a) reducing the uncertainty in the Detroit River flows to 2.5%;
- (b) reducing the uncertainty in the Detroit River flows to zero;
- (c) reducing the uncertainty in both the inflows and outflows to zero;
- (d) reducing the uncertainty in the change in storage to zero;
- (e) reducing the uncertainty in all sources to zero other than the uncertainty due to thermal expansion and contraction and consumptive use.

These scenarios were chosen specifically to cover a number of realistic possibilities. For example, the uncertainty estimate for the Detroit River flow was difficult to determine, and was somewhat subjective. Other researchers (e.g. Neff and Nicholas, 2005) have suggested the standard uncertainty to be 2.5% (or 5% at

the 95% confidence level), therefore scenario (a) was employed to test the effects of this assumption. With the recent installation of a horizontal ADCP on the Detroit River, it is hoped that the uncertainty in the Detroit River flow will be reduced. Whether this will reduce uncertainty and by how much is unclear, but scenario (b), which reduces the uncertainty in the Detroit River flows to zero, was chosen in order to observe the results of this highly unlikely, best case scenario. Similarly, scenario (c) assumes that all of the inflows and outflows are known without error – again, an extremely unlikely scenario. Since it seems possible that uncertainty in the change in storage may be the easiest source of uncertainty in NBS to reduce, scenario (d) assumes that the uncertainty in the change in storage is zero. Lastly, scenario (e) assumes that each of the inputs currently used to estimate NBS (i.e. inflows, outflows and change in storage) are known without error, and therefore, this scenario provides an estimate of the uncertainty that results from those inputs currently considered negligible, i.e. thermal expansion and contraction and consumptive use. These scenarios were compared to the base case. Only the 1962 to 2008 dataset was used in this analysis.

The sensitivity analysis results (in m^3/s) are given in Table 11-12, and the relative uncertainty results (as a percentage of the mean Lake Erie NBS for each month) are given in Table 11-13. The results generally show that reductions in the estimated uncertainties of each input variable reduce the uncertainty in the computed NBS; however, the uncertainty in both absolute and relative terms remains significant, despite often large changes in the input uncertainty estimates. For example, scenario (a) shows that even if the uncertainty determined for the Detroit River flow in this research is overestimated, the uncertainty in NBS is still large, and not reduced substantially from the base case. Furthermore, even if the Detroit River flow was known without error, scenario (b) indicates that the uncertainty in NBS would still be significant, remaining greater than 100% for both August and November. This remains the case for scenario (c), where even when the uncertainty in the inflows and outflows is reduced to zero, the combined NBS uncertainty was found to be greater than 100% for August and November, indicating the significance of the uncertainty in the change in storage and other inputs. Scenario (d) shows that even if the uncertainty in the change in storage, which may be one of the easiest sources of uncertainty to reduce, is reduced to zero, the uncertainty in NBS would still be quite large. In fact, this scenario showed the smallest decline in NBS uncertainty over the base case. Finally, scenario (e) shows that even if inflows, outflows and change in storage are known without error, the uncertainty in NBS that results from those inputs currently

considered negligible is still large, lending further evidence that these sources should be taken into consideration in residual NBS estimates.

Table 11-12: Residual NBS sensitivity analysis results

Scenario	NBS Uncertainty (m ³ /s)											
	Jan	Feb	Mar	Apr	May	Jun	Jul	Aug	Sep	Oct	Nov	Dec
Base Case	298	303	310	314	302	300	296	297	311	330	354	334
(a)	238	244	244	247	229	225	218	219	239	263	293	272
(b)	200	206	201	205	181	175	164	166	191	222	257	234
(c)	167	175	166	166	135	129	117	121	154	192	233	206
(d)	247	248	262	267	272	277	277	278	279	280	278	265
(e)	10	8	9	14	36	55	50	58	70	81	80	31

Table 11-13: Residual NBS sensitivity analysis results (relative uncertainty)

Scenario	NBS Uncertainty (%)											
	Jan	Feb	Mar	Apr	May	Jun	Jul	Aug	Sep	Oct	Nov	Dec
Base Case	33	22	15	17	22	29	93	594	92	70	154	32
(a)	26	18	12	13	16	21	68	438	70	56	127	26
(b)	22	15	10	11	13	17	51	332	56	47	112	23
(c)	19	13	8	9	10	12	37	241	45	41	101	20
(d)	27	18	13	14	20	26	86	555	82	60	121	26
(e)	1	1	0	1	3	5	16	115	21	17	35	3

Overall, these results show how difficult it is to reduce uncertainty in residual NBS. For the most part, this is the result of the large magnitude of the uncertainty estimates for each input relative to the magnitude of the NBS itself. These results also show that uncertainty in residual NBS arises from a number of sources, and in order to reduce overall uncertainty in the NBS, uncertainty must be reduced in each of the different inputs. Focusing attention on only some of the inputs and not others will not reduce the overall combined uncertainty significantly. Therefore, efforts should be made to improve the measurement of all inputs if NBS estimates using the residual method are to be improved.

11.6 Comparison to Previous Estimates of NBS Uncertainty

11.6.1 Neff and Nicholas (2005)

Neff and Nicholas (2005) provided estimates of uncertainty in the Great Lakes water balance for the purpose of illustrating how well the hydrology of the Great Lakes-St. Lawrence River system is understood. This analysis included estimates of uncertainty in both the residual and component method NBS computations for each lake; however, the authors noted that the uncertainty estimates provided were based primarily on best professional judgment since published uncertainty calculations associated with most of the flows and levels of the Great Lakes were unavailable. Confidence levels were not given for the uncertainty estimates, but rather a range of what were believed to be reasonable monthly estimates of uncertainty were provided.

11.6.2 De Marchi et al. (2009)

De Marchi et al. (2009) completed an assessment of uncertainty in NBS computed using GLERL's component method. GLERL generates runoff by extrapolating flows from gauged basins to the ungauged portion of gauged basins and ungauged basins using area ratios. Uncertainty in GLERL's runoff estimate was determined using a combination of assumed uncertainty estimates for runoff from gauged basins, with uncertainty in ungauged basins determined using a leave-one-out Monte Carlo analysis. GLERL estimates direct precipitation to the lakes by applying Thiessen polygon weights to measured precipitation at gauges located in or near each lake, the vast majority of which are located on land. Uncertainty in precipitation was estimated by comparing GLERL's precipitation estimates to precipitation estimates from more advanced models which incorporate short-term forecast and radar data. Evaporation is estimated by GLERL using a one-dimensional energy balance model calibrated to surface temperature and ice coverage. The uncertainty in evaporation was not computed directly, but rather the estimates provided by Neff and Nicholas (2005) based on best professional judgement of the authors were used. More recent evaporation estimates from the eddy-covariance system recently installed on Lake Superior and Lake Huron have been compared to GLERL's modeled estimates and have been used to compute uncertainty in evaporation estimates, but these results have

not been published to date (Carlo De Marchi, GLERL, written communication, 10 October, 2010)

11.6.3 NBS Uncertainty Results Comparison

The uncertainty estimates given by Neff and Nicholas (2005) for each of the three major input variables (inflow, outflow and change in storage) were compared to the estimates determined in this study. Neff and Nicholas (2005) gave uncertainty estimates as lower and upper limits (denoted by the authors as “*Low*” and “*High*”, respectively) as opposed to specific confidence intervals. The standard error and 95% confidence intervals from the current study were used in the comparison, and therefore the uncertainty estimates provided by Neff and Nicholas (2005) are not necessarily equivalent to those from the current research. Nonetheless, the comparison allows for differences in magnitude between the two studies to be assessed.

Furthermore, while Neff and Nicholas (2005) noted the existence of seasonal differences in the uncertainty of each of the different inputs, monthly estimates of uncertainty were not given, and instead any seasonal variation in the uncertainty for each input was presumably captured within the overall low and high relative uncertainty estimates provided. As a result, the average results presented by Neff and Nicholas (2005) were compared to the range of monthly estimates of uncertainty presented in this research. Recalling that the Lake Erie outflow consists of both the Niagara River and Welland Canal flows, combining the results from this research the total Lake Erie outflow was found to have a standard error of about 1.8 to 1.9%, depending on the month. Also, for the change in storage, a relative uncertainty estimate with respect to the mean annual change in storage is inappropriate since the water level of Lake Erie is subject to seasonal cycles (rising and then falling over the course of each year), and therefore the average annual change in storage is close to zero. As a result, Neff and Nicholas (2005) did not provide an average change in storage estimate, nor did they estimate uncertainty in the change in storage in relative terms (i.e. as a percent). On the other hand, computing the average change in storage and relative uncertainty on a monthly basis as performed in this research is acceptable, and therefore the range of monthly mean estimates was used in the comparison that follows. Lastly, the uncertainty estimates for the change in storage determined by Neff and Nicholas (2005) include the effects of thermal expansion

and contraction. In the current study, the uncertainty in the measured change in storage was determined separately from the uncertainty that results from thermal expansion and contraction, so both of these sources of uncertainty are noted in the comparison that follows.

Table 11-14 shows the comparison of the input uncertainty estimates. The uncertainty estimates in the inflow and outflow from the current study are somewhat less than those provided by Neff and Nicholas (2005). The high uncertainty estimate of 15% provided by Neff and Nicholas (2005) for the Detroit River inflow was chosen by the authors considering the large uncertainty in ice-affected flows. On a short term basis the uncertainty in the inflows may approach or even exceed this value when ice is affecting flow; however, as discussed in Section 8.4, ice jams are not a significant issue in the Detroit River, and on a monthly basis other ice effects are unlikely to increase the overall uncertainty in the Detroit River flow substantially. Of more significance are uncertainty caused by channel changes, which are difficult to identify and were not assessed directly in either study. The uncertainty in the Lake Erie outflow was estimated at the 95% confidence level in this study to be less than even the low uncertainty estimate given by Neff and Nicholas (2005). This appears to be primarily the result of two issues: first, Neff and Nicholas (2005) overestimate the magnitude of the Niagara River flow at the MOM pool, which was believed by the authors to be the largest component of the Niagara River flow at Buffalo and was estimated to be approximately 60% of the total, when in fact it is the second largest component (behind the combined Niagara hydropower flows) and is closer to 30 to 40% of the total Niagara River flow at Buffalo; and second, the fact that Neff and Nicholas (2005) account for uncertainty resulting from ice and weeds, neither of which is believed to be a significant issue at the MOM pool, as discussed in Section 6.2.

Also of note in the comparison is the significant difference in the estimated change in storage uncertainty. In contrast to the inflow and outflow uncertainty estimates, the uncertainty in the change in storage was found to be greater in magnitude in the current study than in Neff and Nicholas (2005). The estimates provided by Neff and Nicholas (2005) considered primarily the accuracy of the water level gauge measurements themselves and the effects of thermal expansion and contraction. The current study found that in addition to the water level gauge measurements themselves, temporal variability and spatial

Table 11-14: Comparison of residual NBS input uncertainty estimates

Input	Neff and Nicholas (2005)					Current Study				
	Average Magnitude (m ³ /s)	Uncertainty Estimate (% or mm)		Uncertainty Estimate (m ³ /s)		Mean Monthly Magnitude (m ³ /s)	Uncertainty Estimate (% or mm)		Uncertainty Estimate (m ³ /s)	
		Low	High	Low	High		Standard Error	95% Conf. Level	Standard Error	95% Conf. Level
Inflow	5330	5%	15%	267	800	4650 to 5590	4.3%	8.6%	200 to 240	400 to 480
Outflow	5840	4%	10%	234	584	5570 to 6270	1.8 to 1.9%	3.6 to 3.8%	102 to 114	204 to 228
ΔS	N/A	3 mm	12 mm	30	119	-910 to 1330	11 to 22 mm	22 to 44 mm	106 to 219	212 to 438
ΔS_{Th}^*						-158.3 to 186.3**	0.5 to 8.4 mm	1 to 16.8 mm	6 to 81	12 to 162

* The ΔS_{Th} is included in the overall change in storage uncertainty estimate provided by Neff and Nicholas (2005)

** Since ΔS_{Th} is not currently accounted for in the residual NBS, the estimated mean monthly magnitude of this input becomes an additional source of error

variability of water levels contributed greatly to the uncertainty in the change in storage. The result is that the uncertainty in the measured change in storage alone as estimated in this study is greater than the combined uncertainty resulting from measurement errors and thermal volume change as estimated by Neff and Nicholas (2005).

Table 11-15 provides a comparison of the overall relative uncertainty estimates provided by Neff and Nicholas (2005), De Marchi et al. (2010), and those determined in this study. Again, Neff and Nicholas (2005) provided low and high estimates of uncertainty in both the residual and component NBS. De Marchi et al. (2009) provided 95% confidence levels for the GLERL component NBS estimates. The difference between the lower and upper limits is a result of a bias noted between the deterministic and stochastic results of that study. The estimates provided for this study are the annual average relative standard uncertainty and the 95% confidence level. While these estimates are not directly comparable, they again provide an idea of the relative magnitude of the uncertainty estimates from each study for comparison purposes.

The residual NBS results are of a similar magnitude, with the estimates from this study being only slightly greater in relative terms, at least on average. However, as noted in previous sections, the relative uncertainty varies significantly by month, such that in some cases the overall uncertainty in NBS could be much higher or lower than the average estimates given. The monthly variation is due to the magnitude of the input uncertainties relative to the monthly NBS. Monthly variation was not noted specifically in the Neff and Nicholas (2005) study, but it is expected that a similar effect would be observed. A comparison of the residual NBS uncertainty estimates and the estimates provided for the GLERL component NBS shows the residual uncertainty to be generally higher than the component uncertainty estimates. Neff and Nicholas (2005) noted that this was a result of the magnitudes of the different inputs and their associated uncertainties relative to the computed residual NBS. It was also noted in that study that uncertainty in residual NBS is relatively greater on the lower lakes (Erie and Ontario) than the upper lakes (Superior and Michigan-Huron) since inflows and outflows are greater moving downstream, and that the reverse is true for the component NBS. In terms of monthly variation, De Marchi et al. (2009) state that seasonal effects are observed, in particular in the runoff component, where relative uncertainty in summer flows (when measured flows are quite low) is greater than spring flows (when snowmelt is more uniform across the basin),

but the overall uncertainty estimates in NBS were only provided on an annual basis. A monthly comparison of the residual NBS estimates provided in this study and monthly estimates of uncertainty in the component NBS would be interesting. Also of note is that the component NBS uncertainty estimate provided by De Marchi et al (2009) is greater than that provided by Neff and Nicholas (2005), and that De Marchi et al. (2009) did not consider the uncertainty that results from assuming direct groundwater flow to be negligible. This assumption itself will increase the overall uncertainty, and causes a systematic error in any comparisons with residual NBS estimates.

Table 11-15: Comparison of overall uncertainty estimates in NBS

NBS Estimate	Source	Uncertainty Estimate			
		Estimate	Value	Estimate	Value
Residual	Neff and Nicholas (2005)	Low	36%	High	101%
Residual	Current Study	SE	48%	Upper/Lower 95% CL	96%
GLERL Component	Neff and Nicholas (2005)	Low	14%	High	41%
GLERL Component	De Marchi et al. (2010)	Lower 95% CL	-52%	Upper 95% CL	60%

11.7 Summary of Overall NBS Uncertainty

The overall uncertainty estimates determined in this study indicate that the uncertainty in residual NBS estimates can be great, in some months being greater than the actual NBS estimate itself on average. It should also be noted that the uncertainty estimates provided are the mean monthly results. The actual uncertainty in any given month could be much larger or smaller, depending on the magnitude of the input variables and the conditions at the time of measurement.

The uncertainty estimates also assume relatively stable conditions. Any deviations from the current conditions will cause increases in the uncertainty estimates provided. As an example, during periods when gauged measurements of connecting channel flow data are not collected, discharge models cannot be validated, the result being that the actual discharge could be subject to unknown

errors (such as changes to the channel geometry resulting from erosion, for example) and subsequently greater uncertainty than what might be suggested by the data reviewed in this study. As another example, for periods when Lake Erie water level data are unavailable at a certain gauge or combination of gauges, the uncertainty in the mean Lake Erie water level may be greater than suggested in this study. This is particularly true if one of the Port Stanley or Cleveland gauges were missing, since errors in water levels measured at Port Colborne and Toledo were shown to be larger and would cause the lake-wide average water level to be subject to greater uncertainty.

Overall, the uncertainty estimates provided give a good indication of the major sources of error in residual NBS. They also suggest methods of reducing uncertainty in residual NBS, which would require reducing uncertainty in each of the individual model inputs.

12 Conclusions and Recommendations

12.1 Conclusions

This research involves a complete uncertainty analysis of Lake Erie residual NBS. The analysis involves estimating the uncertainty in each of the different inputs used to compute the NBS from available data and information, including the inflow, outflow and change in storage, as well as the uncertainty in those inputs often omitted from the NBS computations, including the change in storage due to thermal expansion and contraction, and consumptive use. This was done through both analysis of available data and through more general means. The uncertainty estimates for each of the different inputs were then combined to estimate the uncertainty in the residual NBS using both the FOSM and Monte Carlo methods.

The results of the two uncertainty analysis methods were found to be nearly identical when applied to the residual Lake Erie NBS. This is to be expected given the linearity of the model. As expected, the inputs that contributed the most uncertainty in the residual NBS for Lake Erie were the inflows and outflows; however, the uncertainty in the change in storage was found to be of a similar magnitude, and much more significant than previous research suggests. Another notable source of uncertainty is the change in storage due to thermal expansion and contraction, an input normally omitted from residual NBS computations.

Estimating the uncertainty in each of the NBS model inputs was found to be the most difficult and time consuming component of this study, and also the component prone to the most subjectivity. Uncertainty in the inflows and outflows in particular was found to be difficult to estimate given the many sources of error and the difficulty in determining whether errors were correlated or not. However, sensitivity analysis can be used to test the effect of different inflow and outflow uncertainty estimates, allowing for a more robust and convincing uncertainty estimate.

Determining the combined uncertainty estimate for the overall NBS proved to be a simpler task than determining the uncertainty in each of the various

inputs, the result of the mathematical simplicity and linearity of the NBS model. As expected, the FOSM method proved simpler to apply than the Monte Carlo method, due to the greater computational resources required when performing the latter. However, the Monte Carlo method was manageable, due to the simplicity of the model and currently available computer software. Since it is able to provide the full probability distribution of the model results, the Monte Carlo method may be the preferred approach when this is desired. That said, the combination of the high dimensionality of the model, and the fact that none of the statistically independent random variables used as model inputs dominated the uncertainty in the model output, caused the overall NBS uncertainty results to be normally distributed due to the central limit theorem. This suggests that, given similar conditions, the overall uncertainty in the residual NBS can be assumed normally distributed, even if only the FOSM method is applied. The FOSM method also makes it easier to perform a sensitivity analysis on the results, making it possible to quickly and easily determine the effects on the overall NBS uncertainty of each individual input uncertainty estimate. This can be useful in determining how improvements in measurement of the different inputs will improve the accuracy of the NBS estimate, or how error in defining the input uncertainties themselves affects the final result.

12.2 Recommendations

An uncertainty analysis on the residual NBS for each of the remaining Great Lakes should be performed using the FOSM approach and the methods of estimating uncertainty in the various inputs outlined in this study. The FOSM method is simple to apply and makes performing a sensitivity analysis on the combined uncertainty results relatively straightforward. The FOSM results are also nearly identical to those obtained using the Monte Carlo method, and since these results were found to be normally distributed, use of the more difficult to apply Monte Carlo method is unnecessary. This research also suggests that the smallest sources of uncertainty can be omitted from the NBS analysis, possibly making application to the other Great Lakes less cumbersome.

Comparisons of residual and component NBS estimates should be performed with consideration given to both the uncertainty analysis results from this study and estimates of uncertainty in the component NBS. The two different methods, component and residual, provide two separate estimates of the same

quantity, that being the true NBS for a given lake. The two estimates and their associated uncertainty distributions can allow for cross-validation and estimation of the uncertainty in the true NBS. To make this possible, systematic errors caused by assuming certain inputs are negligible (e.g. thermal expansion and contraction, consumptive use and groundwater) or resulting from other factors (e.g. the gauge network used to compute the change in storage) should be identified and accounted for accordingly to ensure that the comparisons of the different NBS estimates themselves are consistent and unbiased. In addition, monthly variation in the uncertainty estimates for the component NBS should be documented.

In order to significantly reduce uncertainty in the residual NBS, uncertainty in each of the different inputs themselves must be reduced. This may be possible given the additional estimates of the model inputs that are becoming available, including the horizontal ADCP recently installed to measure flow in the Detroit River and the new stage-discharge relationship being developed in the upper Niagara River, for example. Such alternative methods of computing the different inputs to the residual NBS model may be found to provide more accurate estimates, but this is not guaranteed; however, these additional estimates will at least allow for comparison and cross-validation with the current estimates, and an estimate of the true value of the input and its associated uncertainty can be better determined by taking into account the multiple estimates and their associated uncertainty distributions. Furthermore, this research has identified a number of improvements in estimating residual NBS inputs that could be made relatively easily to reduce uncertainty. This includes: computing the BOM water levels and change in storage using a more sophisticated averaging scheme such as a Thiessen weighted average or one of a number of available interpolation techniques; accounting for change in storage due to thermal expansion and contraction using the methods outlined in this research, or perhaps by using an improved method of computing this input, such as by using modelled vertical temperature data; and determining local runoff to the upper Niagara River on a monthly basis using measured local tributary flows and area ratios or some other more advanced model. As stated, only by reducing the uncertainty in each of the various inputs will the overall uncertainty in the residual NBS be reduced substantially.

13 References

Ang, A.H-S. and Tang, W.H. 1984. *Probability concepts in engineering planning and decision, Volume II: Decision, Risk, and Reliability*. John Wiley and Sons, New York, USA.

Beck, M.B. 1987. “Water quality modeling: A review of the analysis of uncertainty”. *Water Resources Research*, 23 (8), pp. 1393-1442.

Blasone, R-S., Madsen, H., and Rosbjerg, D. 2007. “Uncertainty assessment of integrated distributed hydrological models using GLUE with Markov chain Monte Carlo sampling”. *Journal of Hydrology*, 353, pp. 18-32.

Bruxer, J. and Southam, C. 2008. “Review of Apparent Vertical Movement Rates in the Great Lakes Region”. Report to the International Upper Great Lakes Study, St. Clair River Task Team, Hydraulic-04. Environment Canada, Burlington, ON.

Carter, R.W and Anderson, I.E. 1963. “Accuracy of current meter measurements.” *Am. Soc. Civil Engineers Proc., Hydraulics Division Journal*, 89 (HY4), pp. 105-115.

Carter, R. W. 1970. “Accuracy of current meter measurements”. *Hydrometry, Proceedings of the Koblenz Symposium*. UNESCO, pp. 86-94.

Clark, R.H. and Persoage, N.P. 1970. “Some implications of crustal movement in engineering planning”. *Canadian Journal of Earth Sciences*, 7 (628), pp. 628-633.

Coleman, H.W. and Steele, W.G. 1995. “Engineering application of experimental uncertainty analysis”. *American Institute of Aeronautics and Astronautics (AIAA) Journal*, 33 (10), pp. 1888-1896.

Coleman, H.W. and Steele, W.G., 1999, *Experimentation and Uncertainty Analysis for Engineers*, 2nd Edition, John Wiley & Sons, Inc., New York, NY.

Cooper, R.A. and Weekes, A.J. 1983. *Data, models, and statistical analysis*. Barnes and Noble Books, Totowa, New Jersey.

[Coordinating Committee] on Great Lakes Basic Hydraulic and Hydrologic Data. 1962. *Niagara River Local Inflows, 1913-1960*.

[Coordinating Committee] on Great Lakes Basic Hydraulic and Hydrologic Data. 1976. *Lake Erie Outflow 1860-1964 with Addendum 1965-1975*.

[Coordinating Committee] on Great Lakes Basic Hydraulic and Hydrologic Data. 1977. *Coordinated Great Lakes Physical Data*.

[Coordinating Committee] on Great Lakes Basic Hydraulic and Hydrologic Data. 1979. *Establishment of International Great Lakes Datum (1955)*, 2nd Ed.

[Coordinating Committee] on Great Lakes Basic Hydraulic and Hydrologic Data. 1982. *Lakes Michigan-Huron Outflows: St. Clair and Detroit Rivers 1900-1978*.

[Coordinating Committee] on Great Lakes Basic Hydraulic and Hydrologic Data. 1985. *Establishment of International Great Lakes Datum (1985)*.

[Coordinating Committee] on Great Lakes Basic Hydraulic and Hydrologic Data. 2001. *Apparent Vertical Movement Over the Great Lakes – Revisited*.

Croley, T.E. 1987. “Wind set-up error in mean lake levels.” *Journal of Hydrology*, 92, pp.223-243

Croley, T. 1989. “Verifiable evaporation modeling on the Laurentian Great Lakes”. *Water Resources Research*, 25 (5), pp. 781-792.

Croley, T.E. II. 1992. “Long-term heat storage in the Great Lakes”. *Water Resources Research*, 28 (1), pp.69-81.

Croley, T.E. II. and Assel, R.A. 1994. “A one-dimensional ice thermodynamics model for the Laurentian Great Lakes”. *Water Resources Research*, 30 (3), pp. 625-639.

- Croley, T.E. II. and Hunter, T.S. 1994. *Great Lakes monthly hydrologic data*. NOAA Technical Report TM-083, Great Lakes Environmental Research Laboratory (GLERL), Ann Arbor, MI.
- DeMarchi, C., Dai, Q., Mello, M.E. and Hunter, T. S. 2009. *Estimate of overlake precipitation and basin runoff uncertainty*. Report to the International Upper Great Lakes Study, Hydroclimate Technical Working Group Tasks 3.1.2 and 3.3.3.
- Derecki, J. A. 1976. "Heat storage and advection in Lake Erie". *Water Resources Research*, 12 (6), pp. 1144-1150.
- Derecki, J.A. and Quinn, F.H. 1986. "Natural regulation of the Great Lakes by ice jams". *Proceedings of the Fourth Workshop on Hydraulics of River Ice*, Ecole Polytechnique de Montreal, June 19-20, 1986
- Dettinger, MD and Wilson, JL. 1981. "First order analysis of uncertainty in numerical models of groundwater flow". *Water Resources Research*, 17 (1), pp. 149-157.
- Dickenson, W.T. 1967. "Accuracy of discharge determinations," Hydrology Papers, No. 20, Dept. of Civil Engineering, Colorado State University.
- Draper, N.R. and Smith, H. 1998. *Applied Regression Analysis*, 3rd Edition. John Wiley and Sons, Inc., New York, NY. 706 pp.
- Duncker, J.J., Over, T.M., and Gonzalez, J.A. 2006. *Computation and error analysis of discharge for the Lake Michigan diversion project in Illinois: 1997-99 water years*. U.S. Geological Survey Scientific Investigations Report 2006-5018.
- Espey, W.H., Schmidt, A.R., and Barkau, R.L. 2001. "Findings of the Fourth Technical Committee for Review of Diversion Flow Measurements and Accounting Procedures," 117 p.; in U.S. Army Corps of Engineers, 1998, *Lake Michigan Diversion Accounting Water Year 1998 Annual Report*.
- Fan, Y. and Fay, D. 2003. *Estimation of Lake Erie Outflows for use in the Lake Ontario – St. Lawrence River Study*. Great Lakes – St. Lawrence Regulation Office, Meteorological Service of Canada, Environment Canada, Cornwall, ON.

Fay, D. and Noorbakhsh, N. 2010. *Revision of Historic Monthly Mean Flow Estimates and Development of Lake-to-Lake Stage-Fall-Discharge Equations for the St. Clair and Detroit Rivers 1987-2009* (draft report). Environment Canada and U.S. Army Corps of Engineers, Burlington, ON, and Detroit, MI. 28 May 2010.

Freeman, G.E., Copeland, R.R., and Cowan, M.A. 1995. “Quantifying stage discharge uncertainty at gaging stations”, *Water Resources Engineering* (Proceedings of the First International Conference, vol 2), ed. By W.H. Espey and P.G. Combs, American Society of Civil Engineers, Water Resources Engineering Division, pp. 1779-1783.

Freeman, G.E., Copeland, R.R., and Cowan, M.A. 1996. “Uncertainty in stage-discharge relationships”, *Stochastic Hydraulics*. '96. (Proceedings 7th IAHR Symposium on Stochastic Hydraulics), International Association for Hydraulic Research, pp. 601-608.

Fuller, K., Shear, H., and Wittig, J. (principal editors). 1995. *The Great Lakes: An Environmental Atlas and Resource Book*, 3rd Edition. Jointly produced by Government of Canada, Toronto, ON, and U.S. Environmental Protection Agency, Great Lakes National Program Office, Chicago, Illinois.

[GLC] Great Lakes Commission. 2003a. *Measuring and Estimating Consumptive Use of the Great Lakes Water*. Report prepared by the Great Lakes Commission for the Great Lakes States and Provinces. Ann Arbor, MI.

[GLC] Great Lakes Commission. 2003b. *Toward a Water Resources Management Decision Support System for the Great Lakes-St. Lawrence River Basin: Status of Data and Information on Water Resources, Water Use, and Related Ecological Impacts*. Report prepared by the Great Lakes Commission for the Great Lakes States and Provinces. Ann Arbor, MI.

[GLC] Great Lakes Commission. 2004. *Annual Report of the Great Lakes Regional Water Use Database Repository Representing 2000 Water Use Data in Gallons*. Report prepared by the Great Lakes Commission for the Great Lakes States and Provinces. Ann Arbor, MI.

González-Castro, J. A. and Ansar, M. 2003. “Applicability of Hydraulic Performance Graphs for flow estimation in open channels”. American Society of Civil Engineers. World Water Congress 2003.

González-Castro, J. A. and Muste, M. 2007. “Framework for estimating uncertainty of ADCP measurements from a moving boat by standardized uncertainty analysis.” *Journal of Hydraulic Engineering*, 133 (12), pp. 1390-1410.

Grannemann, N.G. and Weaver, T.L. 1998. *An annotated bibliography of selected references of the estimated rates of direct ground-water discharge to the Great Lakes*. US Geological Survey Water Resources Investigations Report 98-4039, Lansing, MI. 24 p.

Guo, Y. and Adams, B.J. 1998a. “Hydrologic analysis of urban catchments with event-based probabilistic models: 1. Runoff Volume”. *Water Resources Research*, 34 (12), pp. 3421-3431.

Guo, Y. and Adams, B.J. 1998b. “Hydrologic analysis of urban catchments with event-based probabilistic models: 2. Peak discharge rate”. *Water Resources Research*, 34 (12), pp. 3433-3443.

Haan, C.T. 2002. *Statistical methods in hydrology*, 2nd ed. Iowa State Press, Ames, Iowa. 496 p.

Haefeli, C.J. 1972. *Groundwater Inflow into Lake Ontario from the Canadian Side*. Scientific Series No. 9, Inland Waters Branch, Department of the Environment, Ottawa, Canada. 101 p.

Hayford, J.F. 1922. *Effects of winds and of barometric pressures on the Great Lakes*. Carnegie Institution of Washington. The Rumford Press, Concord.

Herschy, R.W. 1970. “The magnitude of errors at flow measurement stations”, International Symposium on Hydrometry, Koblenz, International Association of Hydrological Sciences, Publication No. 99, pp. 109-131

Herschy, R.W. 1978. *Hydrometry: Principles and Practices*. John Wiley and Sons, New York, NY.

Herschy, R.W. 2009. *Streamflow measurement*, 3rd Edition. Taylor & Francis, NY.

Holtschlag, D.J. and Koschik, J.A. 2002. *A two-dimensional hydrodynamic model of the St. Clair and Detroit Rivers within the Great Lakes Basin*. U.S. Geological Survey Water Resources Investigations Report 01-4236. Lansing, MI.

Hunt, I.A. 1959. *Winds, wind set-ups and seiches on Lake Erie*. U.S. Lake Survey Research Report No. 1-2. Department of the Army, Lake Survey District, Corps of Engineers, Detroit, MI.

Ibbitt, R.P. 1975. "Compression of time series data". *Journal of Hydrology (New Zealand)*, 14 (1), pp. 30-41.

Iman, R.L. and Helton, J.C. 1988. "Investigation of uncertainty and sensitivity analysis techniques for computer models". *Risk Analysis*, 8 (1), pp. 71-90.

[IEC] International Electrotechnical Commission. 1982. *International code for the field acceptance tests of hydraulic turbines*, 2nd Edition. IEC Standard. Bureau Central de la Commission Electrotechnique Internationale. Geneva, Switzerland.

[IJC] International Joint Commission. 1985. *Great Lakes Diversions and Consumptive Uses*. A Report to the Governments of the United States and Canada under the 1977 Reference. Ottawa, ON, Canada.

[INC] International Niagara Committee. 1990. *On the Trial Installation of an Acoustic Velocity Meter on Tonawanda Creek at North Tonawanda, New York*. Report by the U.S. On-Site Representative to the International Niagara Committee. September, 1990.

[INBC] International Niagara Board of Control. 2009. *Revised Ashland Avenue Gauge Stage-Discharge Relationship for the Maid-of-the-Mist Pool Outflow*.

[INWC] International Niagara Working Committee. 1985. *Report on Diversions of Water from the Niagara River into the New York State Barge Canal*.

[ISO] International Organization for Standardization. 1979. *Liquid flow measurement in open channels – velocity-area methods*. International Standard ISO 748: 1979(E).

[ISO] International Organization for Standardization. 1995. *Guide to the Expression of Uncertainty in Measurement*. 1st Edition. ISO/IEC Guide 98:1995. Geneva, Switzerland.

[ISO] International Organization for Standardization. 1997. *Assessment of uncertainty in calibration and use of flow measurement devices – Part 1: Linear calibration relationships*, 1st Edition. Technical Report ISO/TR 7066-1: 1997(E).

[ISO] International Organization for Standardization. 2005. *Measurement of fluid flow – procedures for the evaluation of uncertainties*, 2nd Edition. International Standard ISO 5168: 2005(E).

[IUGLSB] International Upper Great Lakes Study Board. 2009. *Impacts on Upper Great Lakes Water Levels: St. Clair River*. Final report to the International Joint Commission, International Upper Great Lakes Study.

Khan, M.S., Coulibaly, P. and Dibike, Y. 2006. “Uncertainty analysis of statistical downscaling methods”. *Journal of Hydrology*. 319. pp. 357-382.

Kim, D. and Yu, K. 2010. “Uncertainty estimation of the ADCP velocity measurements from the moving vessel method, (I) Development of Framework”. *KSCE Journal of Civil Engineering*, 14 (5), pp. 797-801.

Lam, D.C.L. and Schertzer, W.M. 1987. “Lake Erie Thermocline Model Results: Comparison with 1967-1982 Data and Relation to Anoxic Occurrences”. *Journal of Great Lakes Research*, 13 (4), pp. 757-769.

Lee, D.H. 1992. *Computation of Net Basin Supplies: A comparison of two methods*. Final Report Subtask 19.1.2(a) to the International Joint Commission Levels Reference Study. Great Lakes Environmental Research Laboratory, Ann Arbor, MI. 18 p.

Libicki, C. and Bedford, K.W. 1990. “Sudden, extreme Lake Erie storm surges and the interaction of wind stress, resonance, and geometry”. *Journal of Great Lakes Research*, 16 (3), pp 380-395.

Lipscomb, S.W. 1995. *Quality Assurance Plan for Discharge Measurements Using Broadband Acoustic Doppler Current Profilers*. USGS Open-File Report 95-701.

Meredith, D.M. 1975. “Temperature effects on Great Lakes water balance studies”. *Water Resources Bulletin (American Water Resources Association)*, 11 (1), pp.60-68.

Mishra, S. 2009. “Uncertainty and sensitivity analysis techniques for hydrologic modeling”. *Journal of Hydroinformatics*. 11 (3-4), pp. 282-296.

Morlock, S.E. 1996. *Evaluation of Acoustic Doppler Current Profiler Measurements of River Discharge*. USGS Water-Resources Investigations Report 95-4218.

Muste, M., Yu, K., Gonzalez-Castro, J.A., Ansar, M., and Startzman, R. 2004a. “Methodology for estimating ADCP measurement uncertainty in open-channel flows”. *Critical Transitions in Water and Environmental Resources Management Proceedings of World Water and Environmental Resources Congress 2004*.

Muste, M., Yu, K. and Spasojevic, M. 2004b. “Practical aspects of ADCP data use for quantification of mean river flow characteristics; Part 1: moving-vessel measurements.” *Flow Measurement and Instrumentation*, 15, pp. 1-16.

Neff, B. P. and Nicholas, J. R. 2005. *Uncertainty in the Great Lakes Water Balance*. U.S. Geological Survey Scientific Investigations Report 2004-5100.

[NOAA] National Oceanic and Atmospheric Administration. 2009. *Collection of 6-Minute Water Level Data to produce Hourly, Daily, Monthly and Annual Averages for the Great Lakes (Draft Report)*. SOP No. 7.3.

[NOAA] National Oceanic and Atmospheric Administration. 2008. *NOAA's Ocean Service Center for Operational Oceanographic Products and Services*

(CO-OPS) Environmental Measurement Systems Sensor Specifications and Measurement Algorithm (Draft Document).

Oberg, K., and Mueller, D.S. 2007. "Validation of Streamflow Measurements Made with Acoustic Doppler Current Profilers." *Journal of Hydraulic Engineering*, 133 (12). pp. 1421-1432.

Olson, R.M. 1966. *Essentials of engineering fluid mechanics*, 2nd Ed. International Textbook Company, Scranton, Pennsylvania

Pelletier, P. M. 1988. "Uncertainties in the single determination of river discharge – a literature review". *Canadian Journal of Civil Engineering*, 15, pp. 834-850.

Pietroniro, A., Fortin, V., Kouwen, N., Neal, C., Turcotte, R., Davison, B., Verseghy, D., Soulis, E.D., Caldwell, R., Evora, N. and Pellerin, P. 2006. "Using the MESH Modelling System for Hydrological Ensemble Forecasting of the Laurentian Great Lakes at the Regional Scale", *Hydrology and Earth System Sciences Discussions*, 3, pp. 2473-2521.

Quinn, F. and Edstrom, J. 2000. "Great Lakes Diversions and Other Removals". *Canadian Water Resources Journal*. 25 (2), pp. 125-151.

Quinn, F. H. 1976. *Lake St. Clair hydrologic transfer factors*. NOAA Technical Memorandum ERL GLERL 10, Great Lakes Environmental Research Laboratory, Ann Arbor, MI, 16 pp.

Quinn, F.H. 1979a. "Relative accuracy of connecting channel discharge data with application to Great Lakes studies". *Journal of Great Lakes Research (International Association of Great Lakes Research)*, 5 (1), pp. 73-77.

Quinn, F.H. 1979b. *Derivation and calibration of stage-fall-discharge equations for the Great Lakes connecting channels*. GLERL Open File Report, Great Lakes Environmental Research Laboratory, Ann Arbor, Michigan.

Quinn, F.H. 1988. "Detroit River flow reversals". *Journal of Great Lakes Research (International Association of Great Lakes Research)*, 14(4), pp. 383-387.

Quinn, F.H. 2009. *Net basin supply comparison analysis*. Report to the International Upper Great Lakes Study.

Quinn, F. H. and Derecki, J. A. 1976. *Lake Erie beginning-of-month water levels and monthly rates of change of storage*. NOAA Technical Report ERL 364-GLERL 9, Great Lakes Environmental Research Laboratory, Ann Arbor, MI.

Quinn, F.H., Derecki, J.A., and Kelley, R.N. 1979. "Great Lakes Beginning-of-Month Water Levels and Monthly Rates of Change of Storage". *Journal of Great Lakes Research*, 5 (1), pp. 11-17.

Quinn, F.H. and Guerra, B. 1986. "Current perspectives on the Lake Erie water balance." *Journal of Great Lakes Research*, 12 (2), pp. 109-116.

Quinn, F.H. and Noorbakhsh, N. 2001. *Niagara River rating equation for the post-1973 directive period*. Report to the Coordinating Committee on Great Lakes Basic Hydraulic and Hydrologic Data. Great Lakes Environmental Research Laboratory, NOAA, Ann Arbor, Michigan, and U.S. Army Corps of Engineers, Detroit, Michigan.

Sauer, V.B. and Meyer, R.W. 1992. *Determination of error in individual discharge measurements*. U.S. Geological Survey Open-File Report 92-144. Norcross, Georgia.

Schertzer, W.M., Saylor, J.H., Boyce, F.M., Robertson, D.G. and Rosa, F. 1987. "Seasonal Thermal Cycle of Lake Erie". *Journal of Great Lakes Research*. 13 (4), pp. 468-486.

Schmidt, A. 2002. *Analysis of stage-discharge relations for open-channel flows and their associated uncertainties*. Ph. D. dissertation. Civil and Environmental Engineering, University of Illinois at Urbana-Champaign.

Schmidt, A., Choi, N.J., and Banjavcic, S. 2009. *Review of Discharge Measurements and Rating Equations on the St. Clair and Detroit Rivers since 1962*. Report to the International Upper Great Lakes Study.

Sellinger, C. E. and Quinn, F. H. 2001. *Assessment of impacts of increased weed growth on Detroit River flows*. NOAA Technical Memorandum GLERL-119, Ann Arbor, MI.

Simpson, M.R. 2001. *Discharge measurements using a broad-band Acoustic Doppler Current Profiler*. USGS Open-File Report 01-1. Sacramento, CA.

[SINB] Special International Niagara Board. 1930. *The Preservation of Niagara Falls*. F.A. Acland, Printer to the King's Most Excellent Majesty, Ottawa, Canada.

Spence, C., Blanken, P.D., Hedstrom, N., Mackay, M.D., Hunter, T. 2009. *A Comparison of Modelled and Observed Evaporation from Lake Superior*. Report to the Hydroclimatology Technical Working Group, International Upper Great Lakes Study, International Joint Commission.

Stellato, Joseph R. 1981. *Amount and use of waters diverted from the Niagara River by Barge Canal*. New York State Department of Transportation Report, Albany, NY, September 1981.

Thompson, A., Guo, Y. and Moin, S. 2006. "Uncertainty analysis of a two-dimensional hydrodynamic model." *Journal of Great Lakes Research*, 34, pp. 472-484.

Tsokos, C.P. 1972. *Probability distributions: An Introduction to Probability Theory with Applications*. Wadsworth Publishing Company, Inc. Belmont, CA.

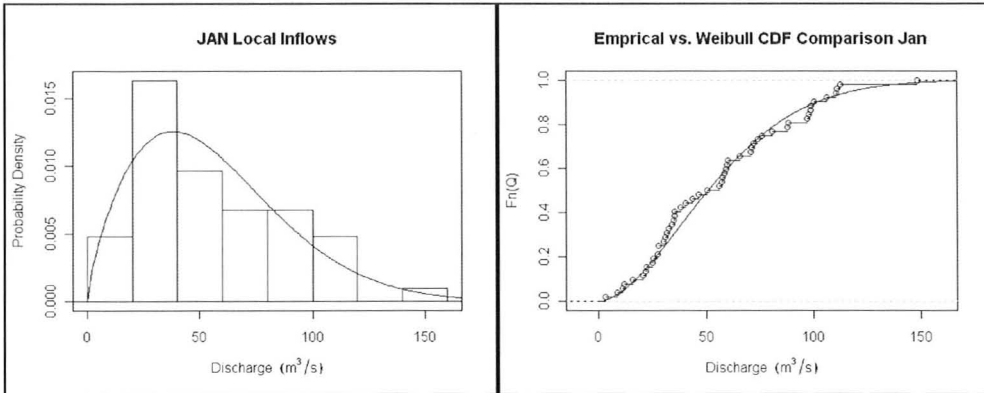
Tung, Y.K., and Yen, B.C. 2005. *Hydrosystems Engineering Uncertainty Analysis*. McGraw-Hill, New York.

Venetis, C. 1970. "A note on the estimation of the parameters in logarithmic stage-discharge relationships with estimates of their error," *Bulletin of the International Association of Scientific Hydrology, International Union of Geodesy and Geophysics*, XV (2), pp. 105-111.

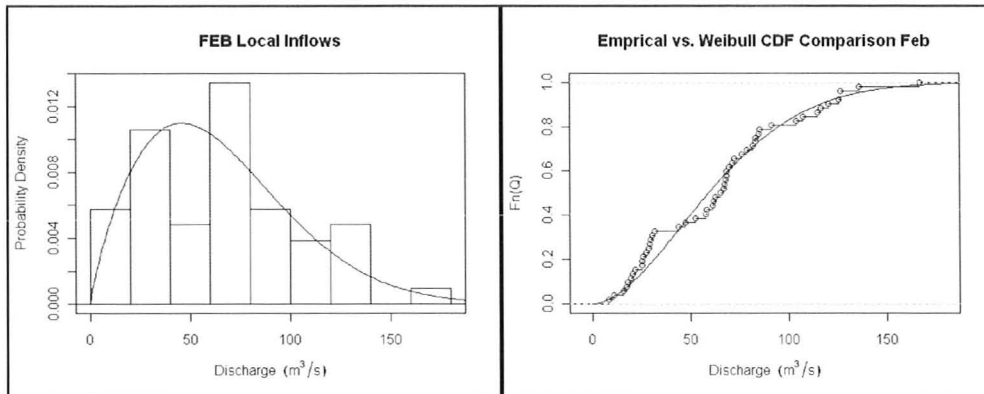
Yen, B.C., Cheng, S.T., and Melching, C.S. 1986. "First-Order Reliability Analysis," in: *Stochastic and Risk Analysis in Hydraulic Engineering*. Edited by B.C. Yen, Water Resources Publications, Littleton, CO, pp. 1-36.

**Appendix A: Comparison of Upper Niagara River Local
Runoff to fitted probability distributions**

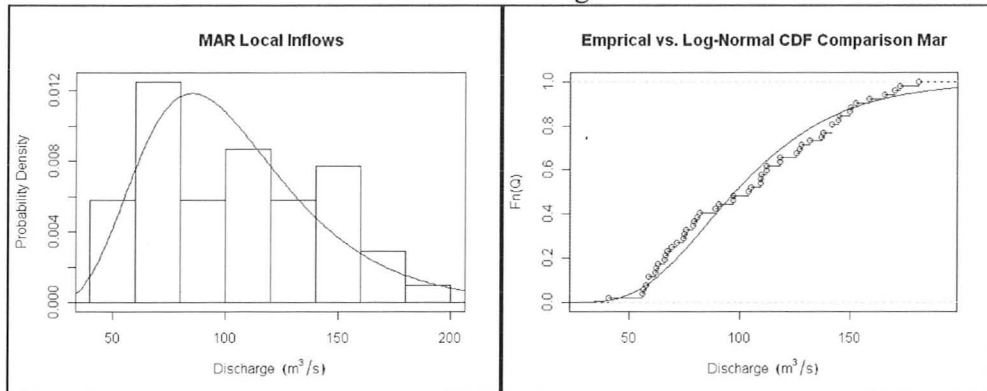
Month: January
Distribution: Weibull
Parameter 1: Shape = 1.73
Parameter 2: Scale = 62.77



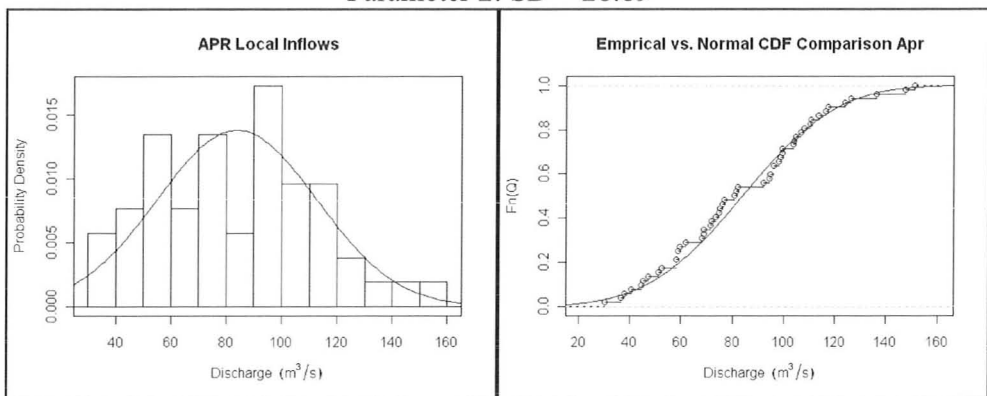
Month: February
Distribution: Weibull
Parameter 1: Shape = 1.78
Parameter 2: Scale = 72.80



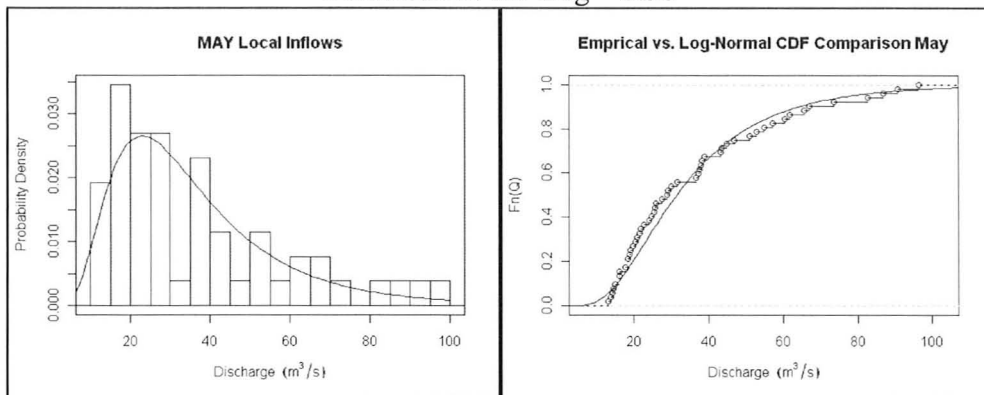
Month: March
 Distribution: Log-normal
 Parameter 1: Mean-Log = 4.58
 Parameter 2: SD-Log = 0.37



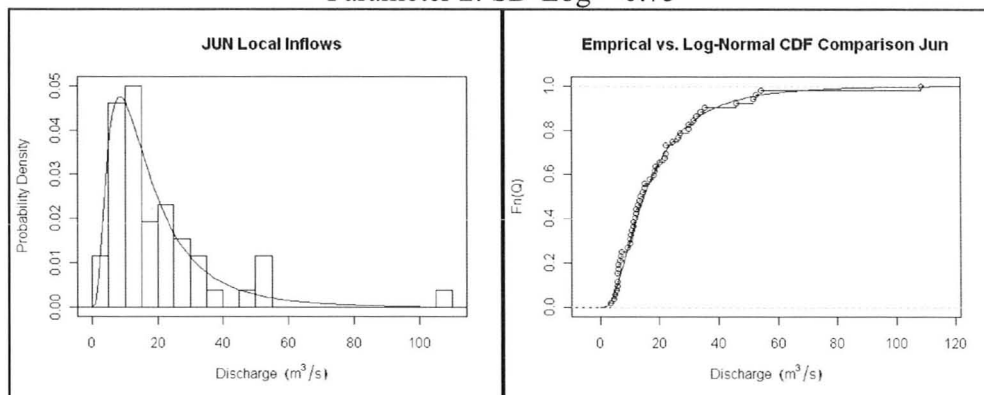
Month: April
 Distribution: Normal
 Parameter 1: Mean = 83.81
 Parameter 2: SD = 28.89



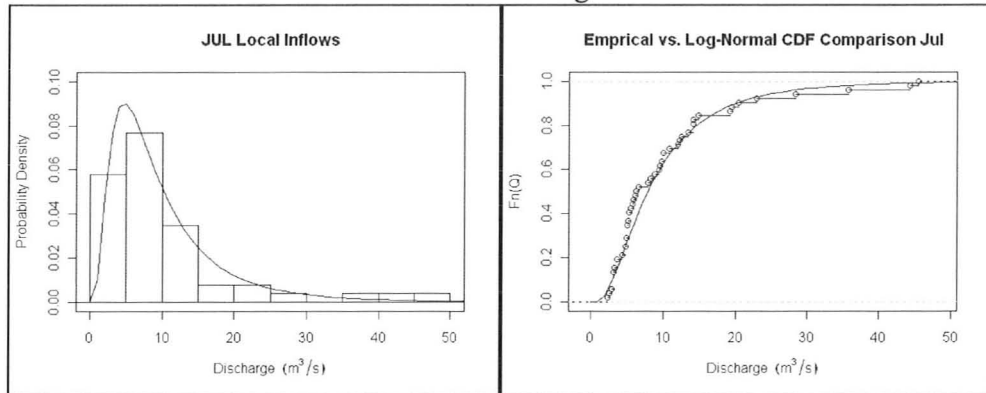
Month: May
 Distribution: Log-normal
 Parameter 1: Mean-Log = 3.45
 Parameter 2: SD-Log = 0.56



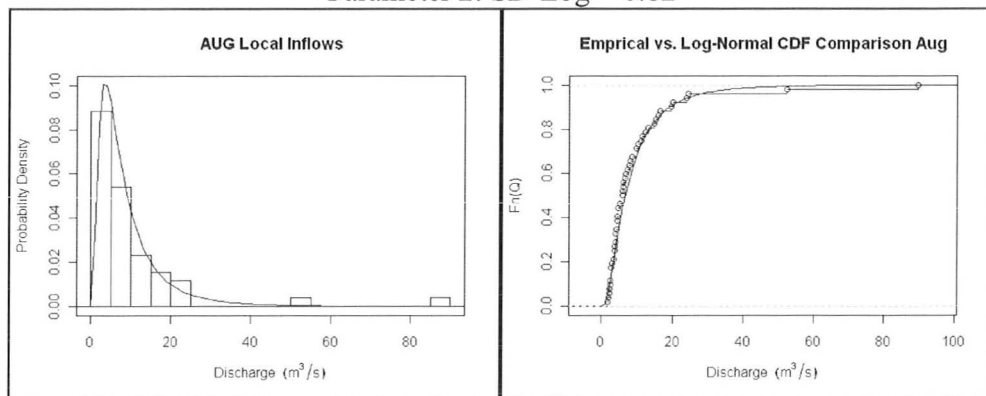
Month: June
 Distribution: Log-normal
 Parameter 1: Mean-Log = 2.70
 Parameter 2: SD-Log = 0.75



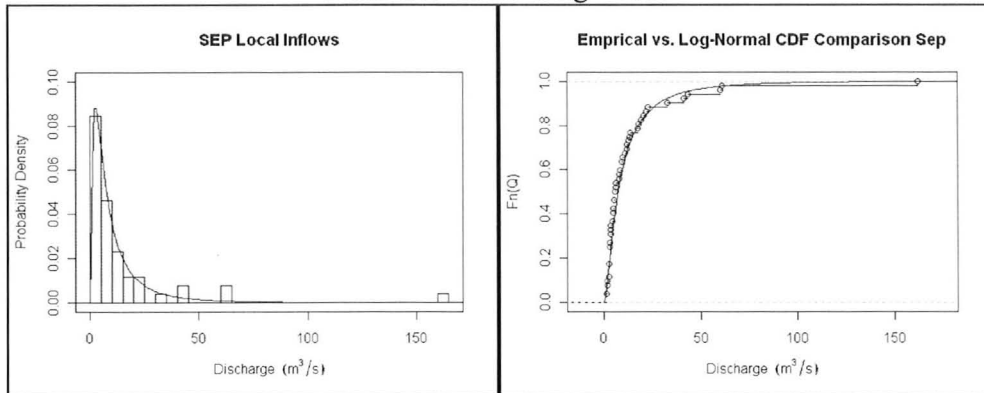
Month: July
 Distribution: Log-normal
 Parameter 1: Mean-Log = 2.06
 Parameter 2: SD-Log = 0.73



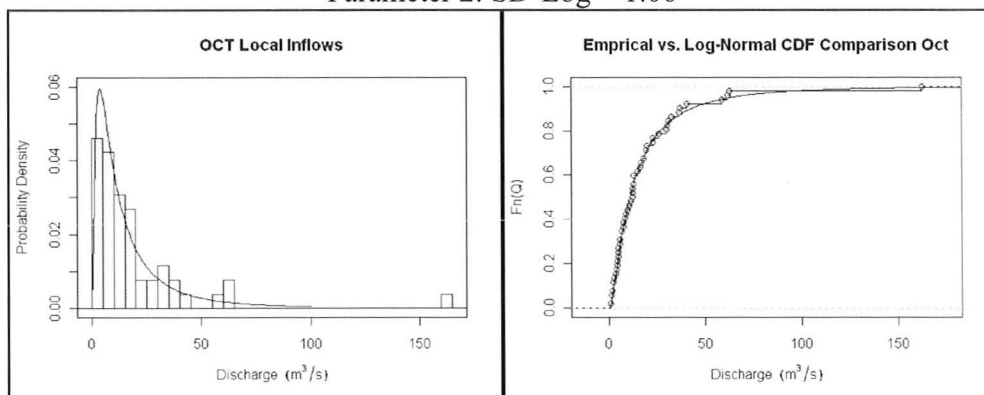
Month: August
 Distribution: Log-normal
 Parameter 1: Mean-Log = 1.90
 Parameter 2: SD-Log = 0.82



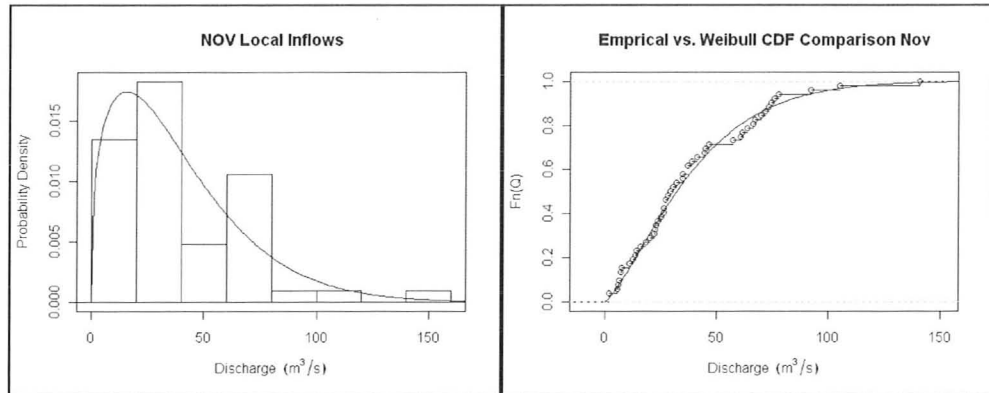
Month: September
 Distribution: Log-normal
 Parameter 1: Mean-Log = 2.00
 Parameter 2: SD-Log = 1.05



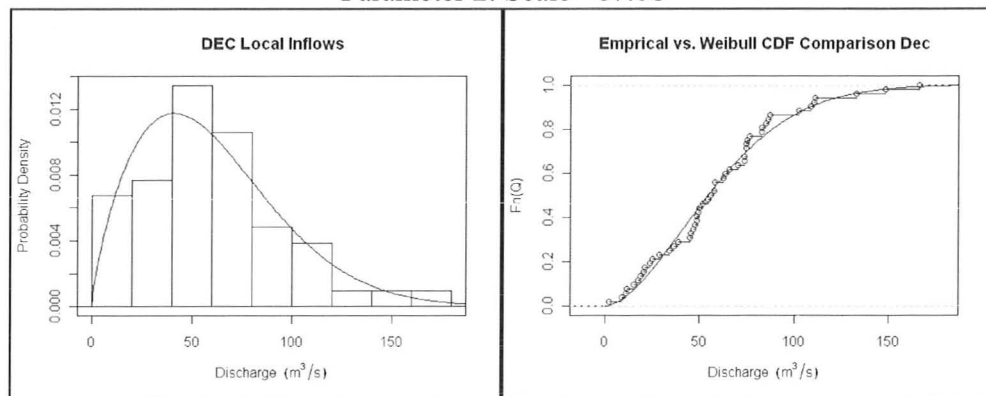
Month: October
 Distribution: Log-normal
 Parameter 1: Mean-Log = 2.40
 Parameter 2: SD-Log = 1.06



Month: November
 Distribution: Weibull
 Parameter 1: Shape =1.35
 Parameter 2: Scale =42.16

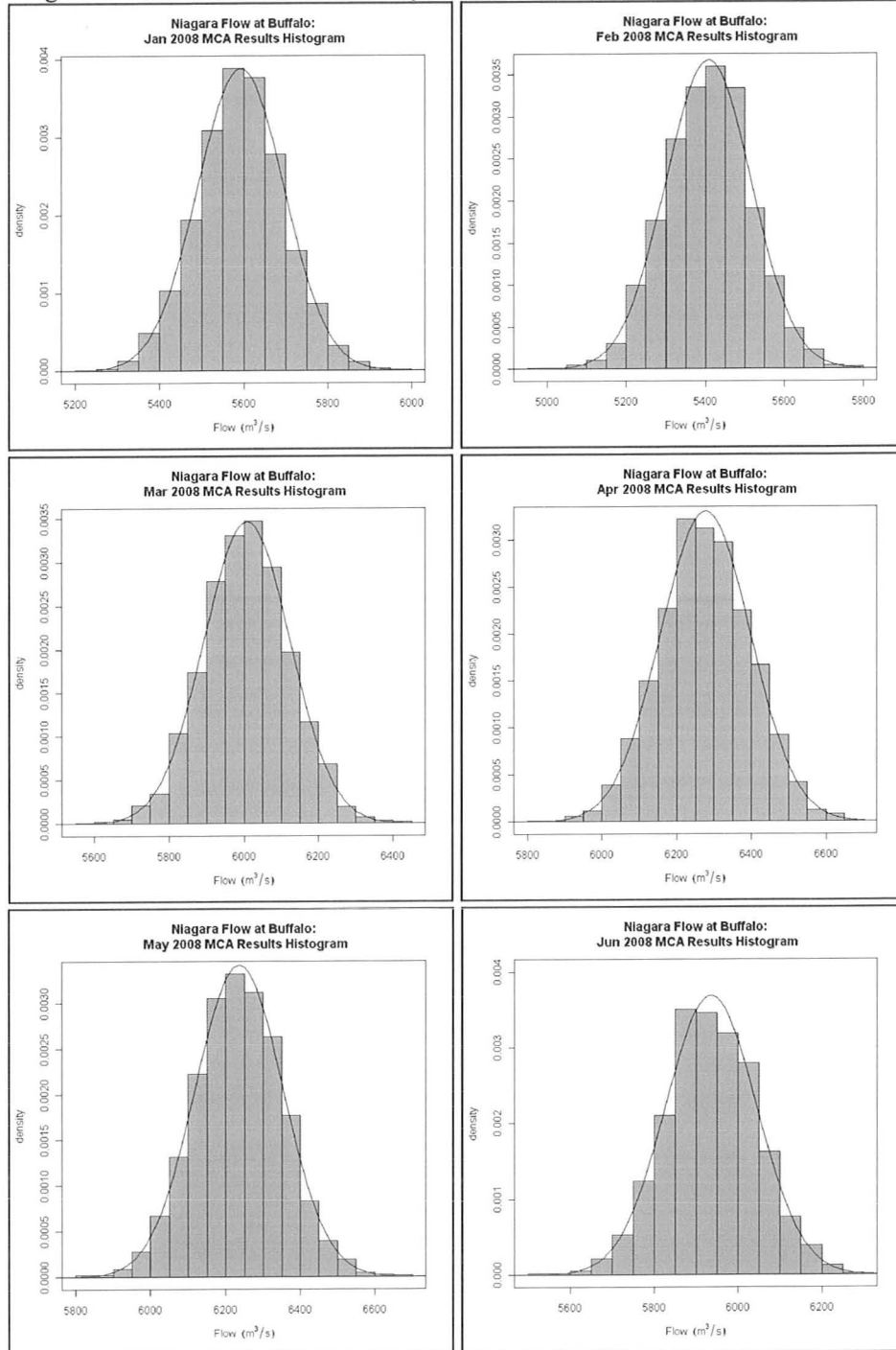


Month: December
 Distribution: Weibull
 Parameter 1: Shape =1.73
 Parameter 2: Scale =67.08

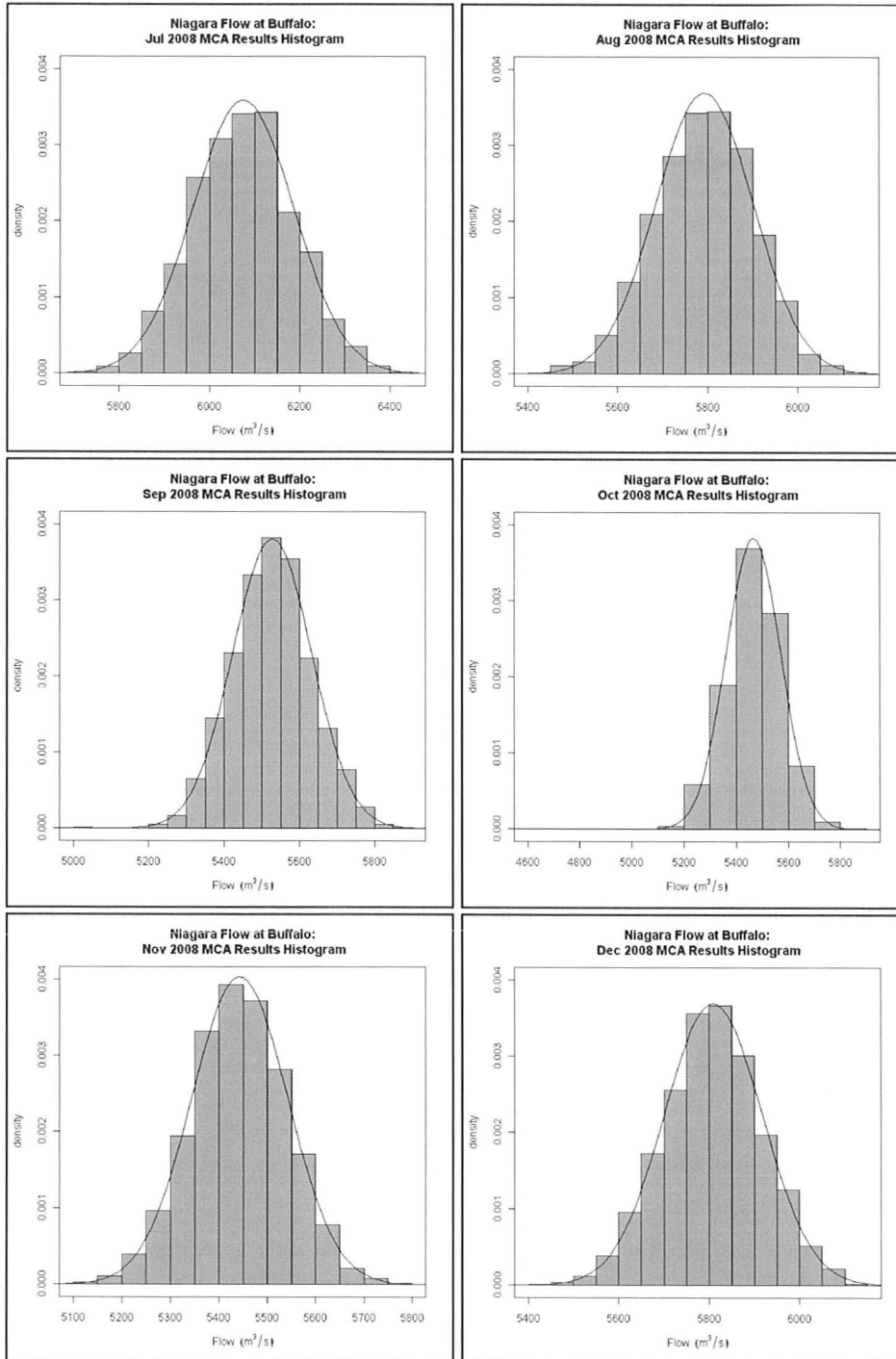


Appendix B: Niagara River flow at Buffalo 2008 Monte Carlo analysis results histograms

Niagara River flow Monte Carlo analysis results histograms vs. fitted normal PDFs

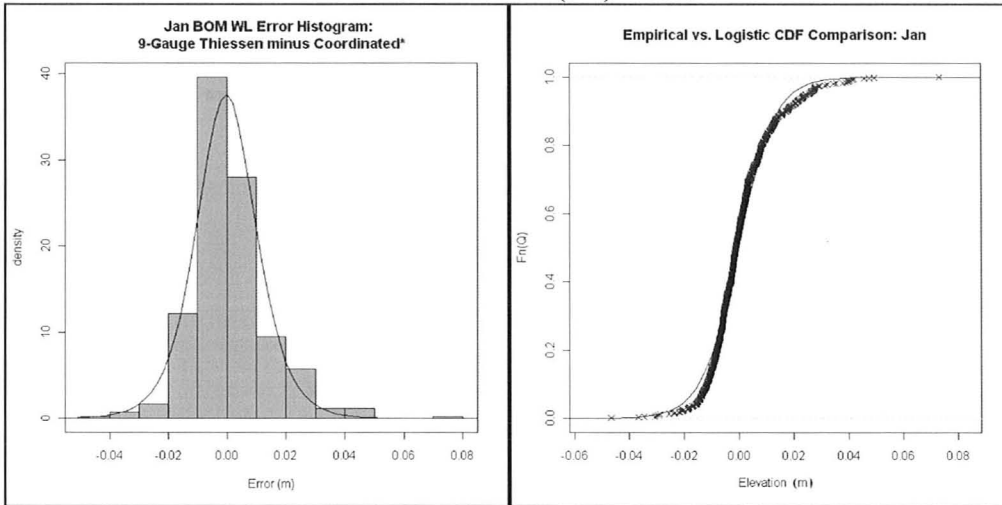


Niagara River flow Monte Carlo analysis results histograms vs. fitted normal PDFs

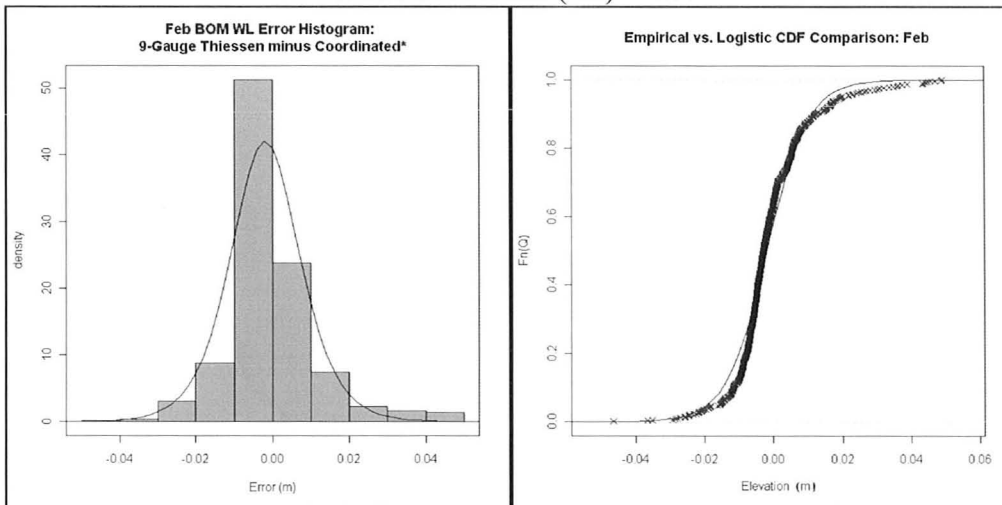


**Appendix C: Spatial variability in mean Lake Erie
water level error comparison to fitted
probability distributions**

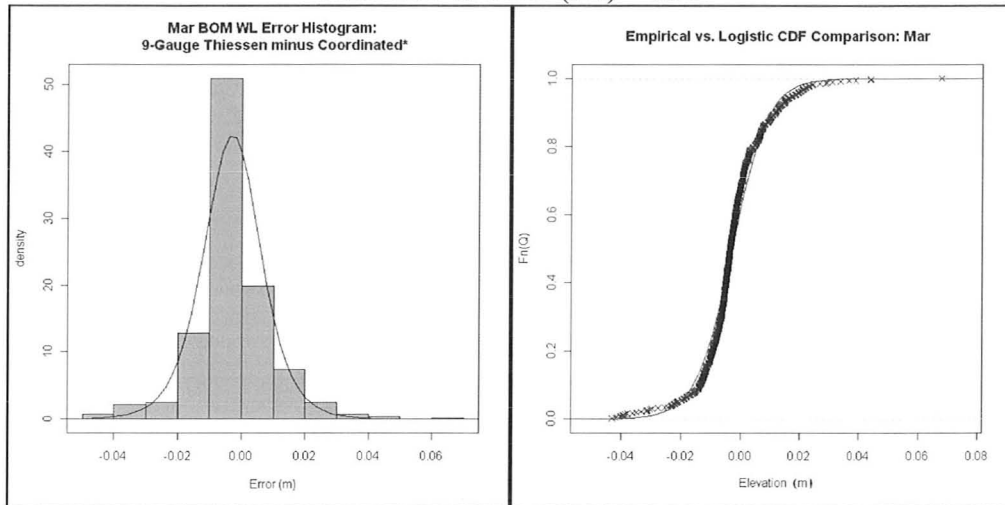
Month: January
 Distribution: Logistic
 Parameter 1: Location (cm) = -0.02
 Parameter 2: Scale (cm) = 0.67



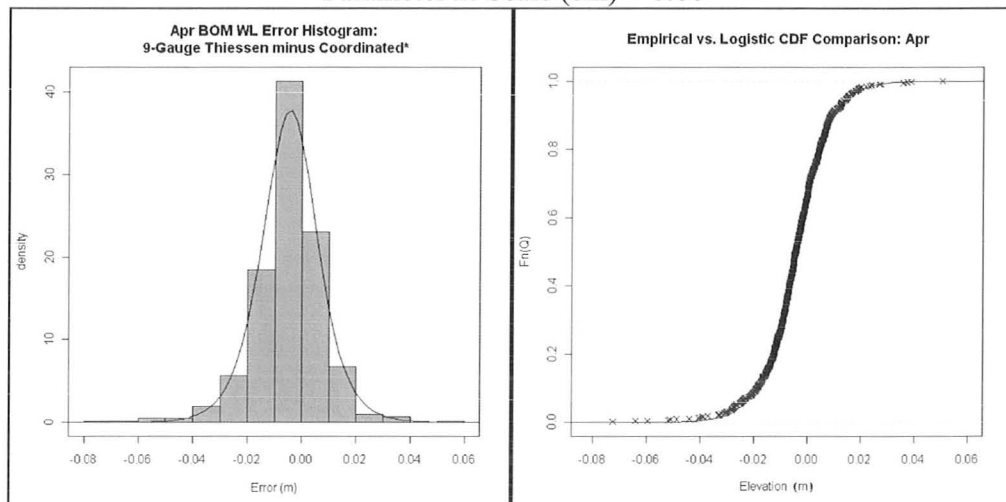
Month: February
 Distribution: Logistic
 Parameter 1: Location (cm) = -0.19
 Parameter 2: Scale (cm) = 0.59



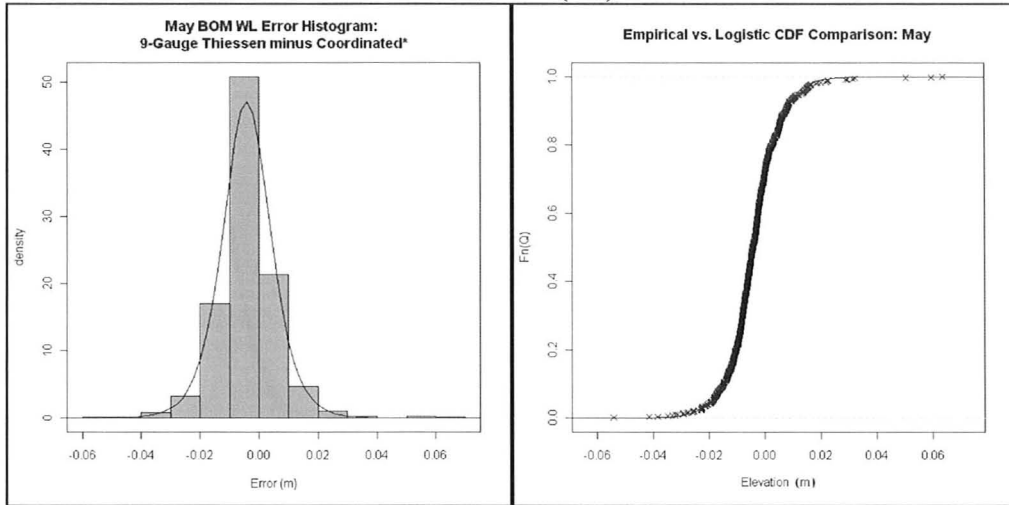
Month: March
 Distribution: Logistic
 Parameter 1: Location (cm) = -0.31
 Parameter 2: Scale (cm) = 0.59



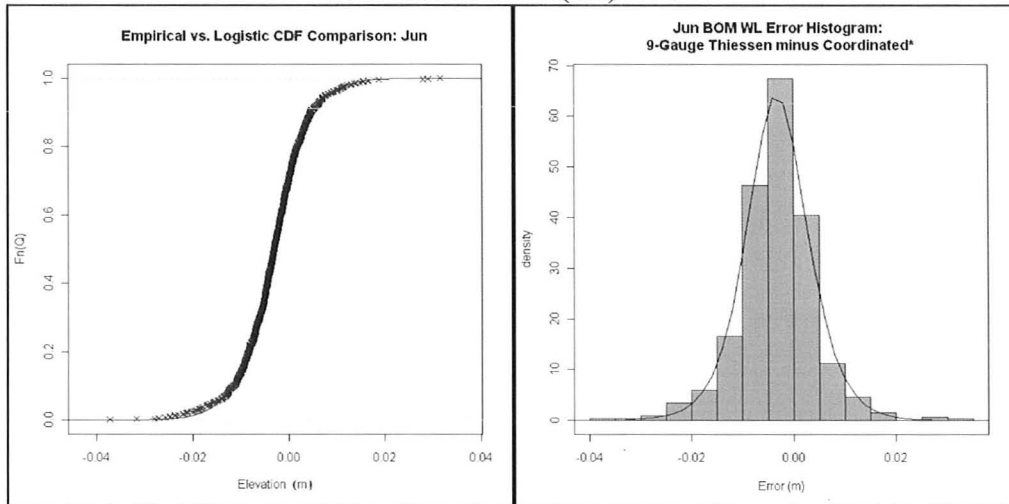
Month: April
 Distribution: Logistic
 Parameter 1: Location (cm) = -0.45
 Parameter 2: Scale (cm) = 0.66



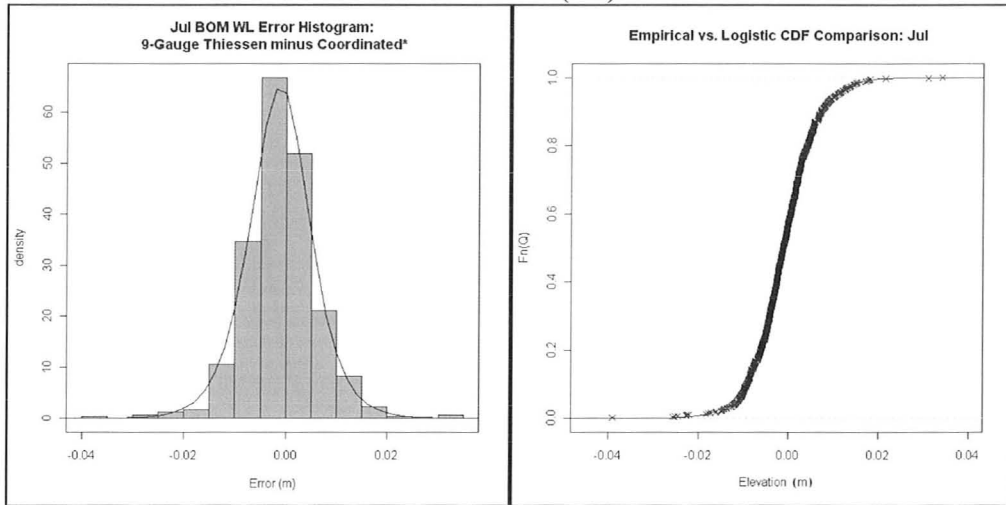
Month: May
 Distribution: Logistic
 Parameter 1: Location (cm) = -0.42
 Parameter 2: Scale (cm) = 0.53



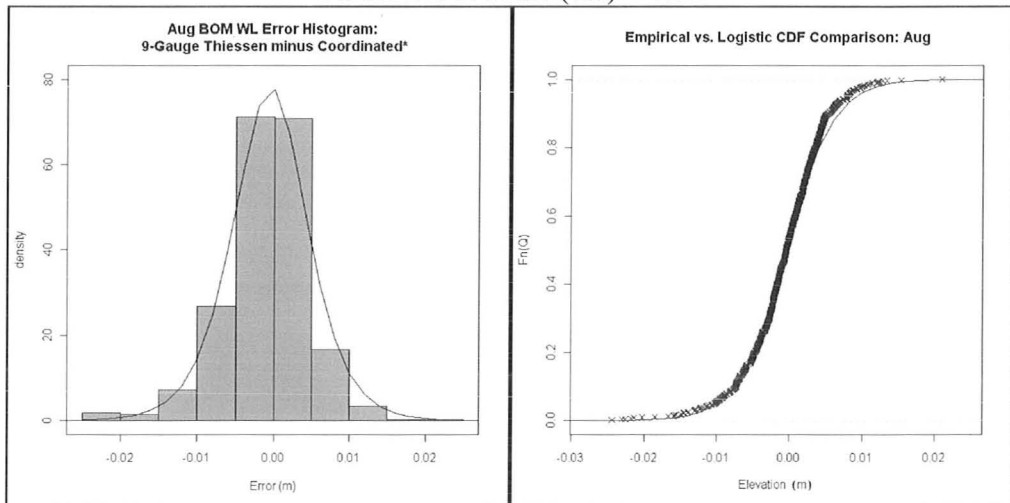
Month: June
 Distribution: Logistic
 Parameter 1: Location (cm) = -0.32
 Parameter 2: Scale (cm) = 0.39



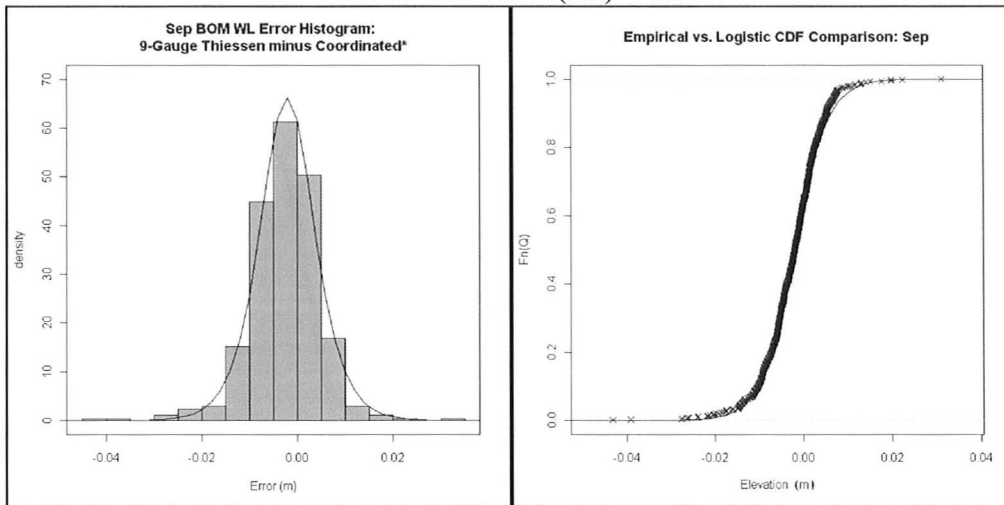
Month: July
 Distribution: Logistic
 Parameter 1: Location (cm) = -0.12
 Parameter 2: Scale (cm) = 0.38



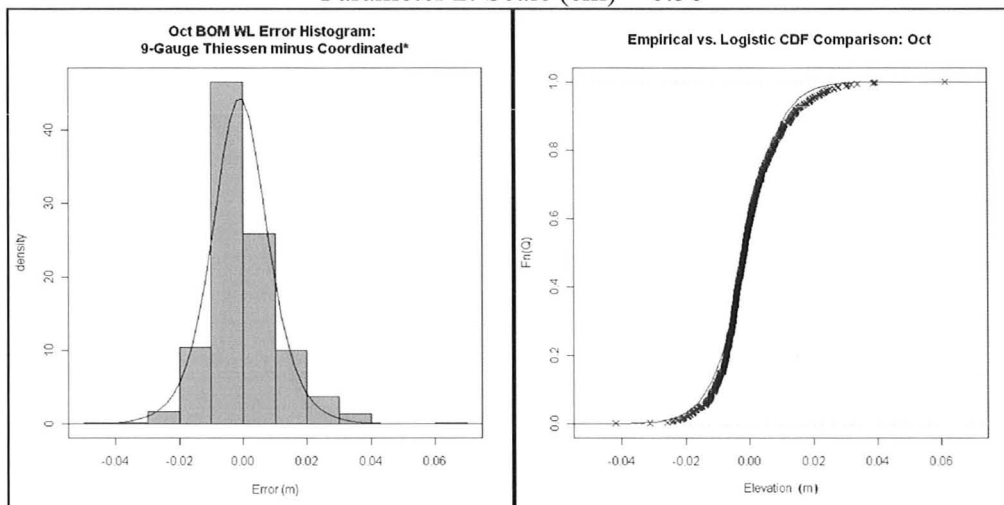
Month: August
 Distribution: Logistic
 Parameter 1: Location (cm) = -0.05
 Parameter 2: Scale (cm) = 0.32



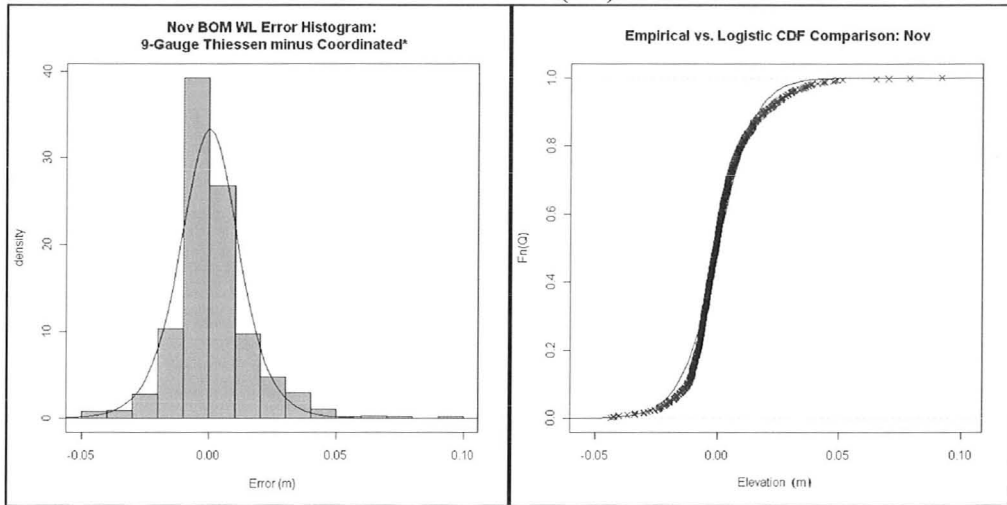
Month: September
 Distribution: Logistic
 Parameter 1: Location (cm) = -0.20
 Parameter 2: Scale (cm) = 0.38



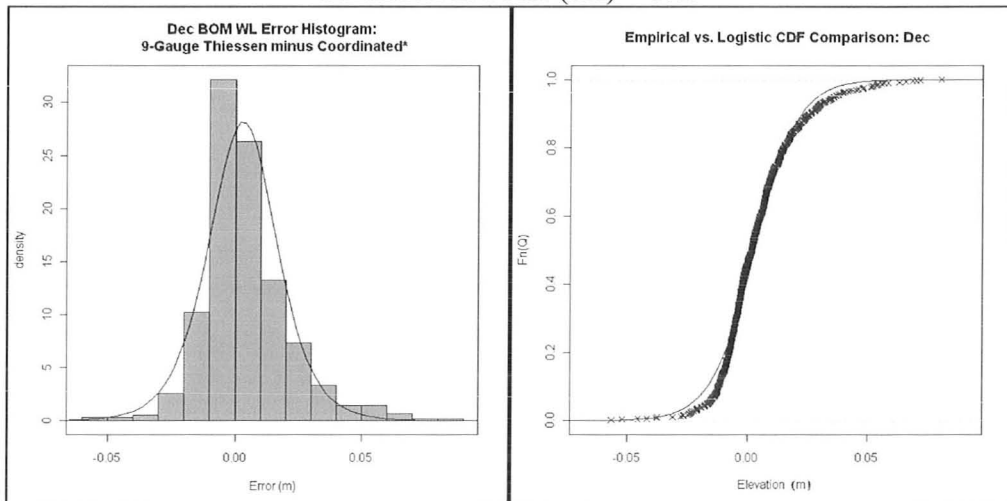
Month: October
 Distribution: Logistic
 Parameter 1: Location (cm) = -0.09
 Parameter 2: Scale (cm) = 0.56



Month: November
 Distribution: Logistic
 Parameter 1: Location (cm) = 0.00
 Parameter 2: Scale (cm) = 0.75



Month: December
 Distribution: Logistic
 Parameter 1: Location (cm) = 0.29
 Parameter 2: Scale (cm) = 0.89



**Appendix D: Environment Canada 1967-1982
bathythermograph survey vertical
temperature data for Lake Erie and fitted
temperature profiles**

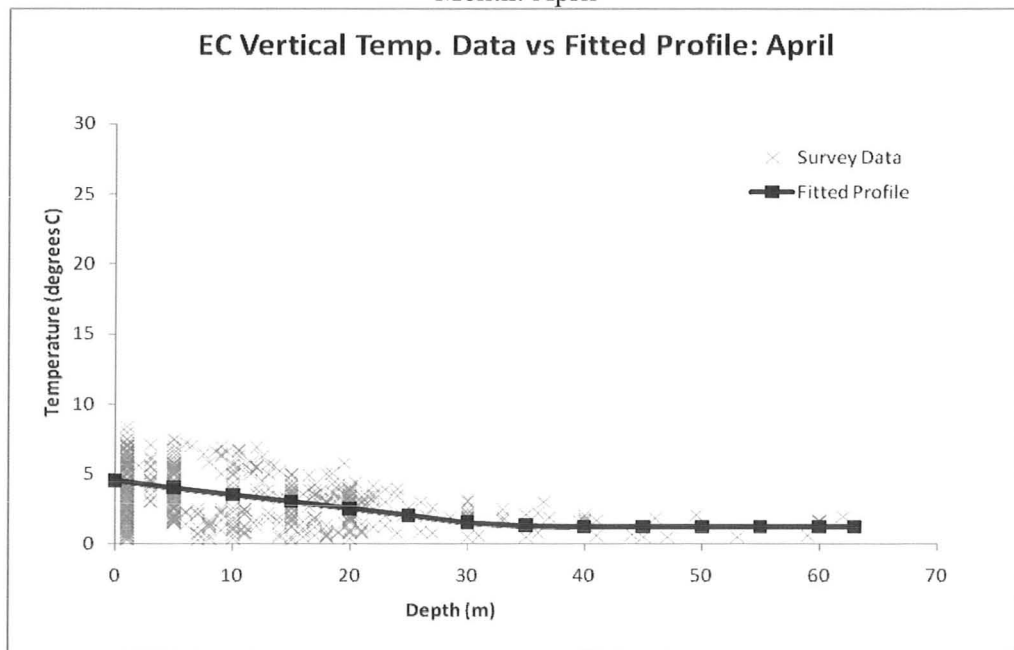
Table D-1: Fitted monthly vertical temperatures as estimated from Environment Canada NWRI data collected between 1967 and 1982.

Month	Fitted Temperature (°C) at Depth (m)													
	0 m	5 m	10 m	15 m	20 m	25 m	30 m	35 m	40 m	45 m	50 m	55 m	60 m	63 m
JAN	--	--	--	--	--	--	--	--	--	--	--	--	--	--
FEB	--	--	--	--	--	--	--	--	--	--	--	--	--	--
MAR	--	--	--	--	--	--	--	--	--	--	--	--	--	--
APR	4.5	4	3.5	3	2.5	2	1.5	1.3	1.2	1.2	1.2	1.2	1.2	1.2
MAY	8	6.5	5	4	3.5	3	2.8	2.7	2.6	2.5	2.4	2.4	2.4	2.4
JUN	14	12.5	10	8	6.5	5.5	5	4.5	4.5	4.5	4.4	4.3	4.3	4.3
JUL	18	17.5	15.5	12	9	6.5	5.5	5	4.5	4.5	4.5	4.5	4.4	4.4
AUG	22	22	21	16	10	7	5.5	5	4.5	4.5	4.4	4.4	4.4	4.4
SEP	21.5	21.5	21	19.5	13.5	8	6	5.5	5.2	5	4.6	4.5	4.5	4.5
OCT	18	18	18	17.5	15	12	7.5	6	5.5	5	5	5	5	5
NOV	9	9.5	11	12	12.5	12.5	12	11	10	9	8.5	8	8	8
DEC	6.5	7	8	9	9.5	10	10	10	10	10	10	10	10	10

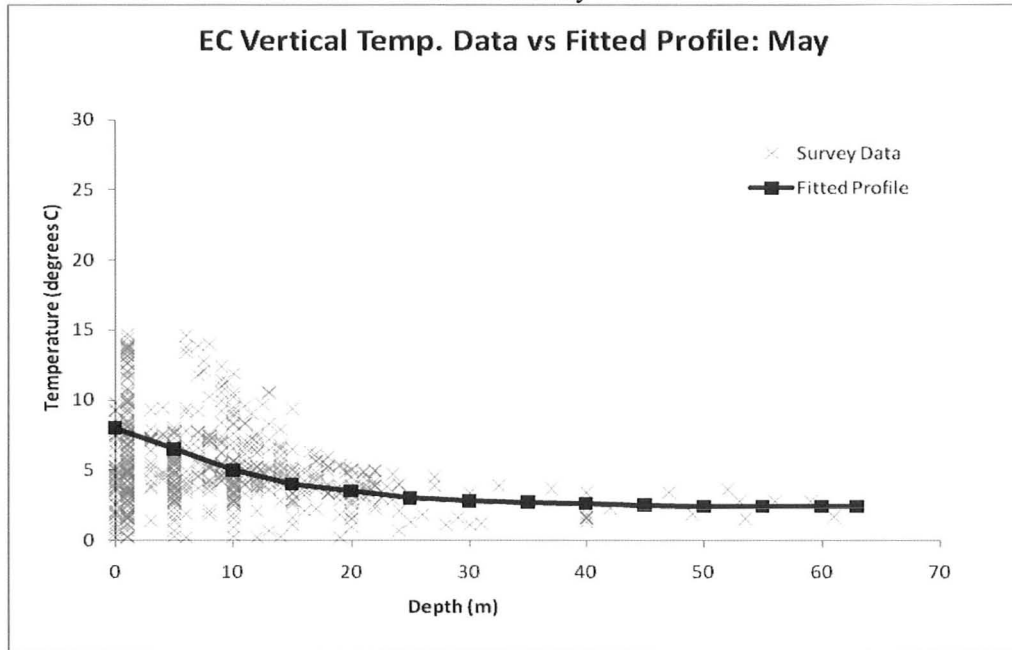
*Data not collected for months of January through March

Plotted Survey Data vs. Fitted Profiles

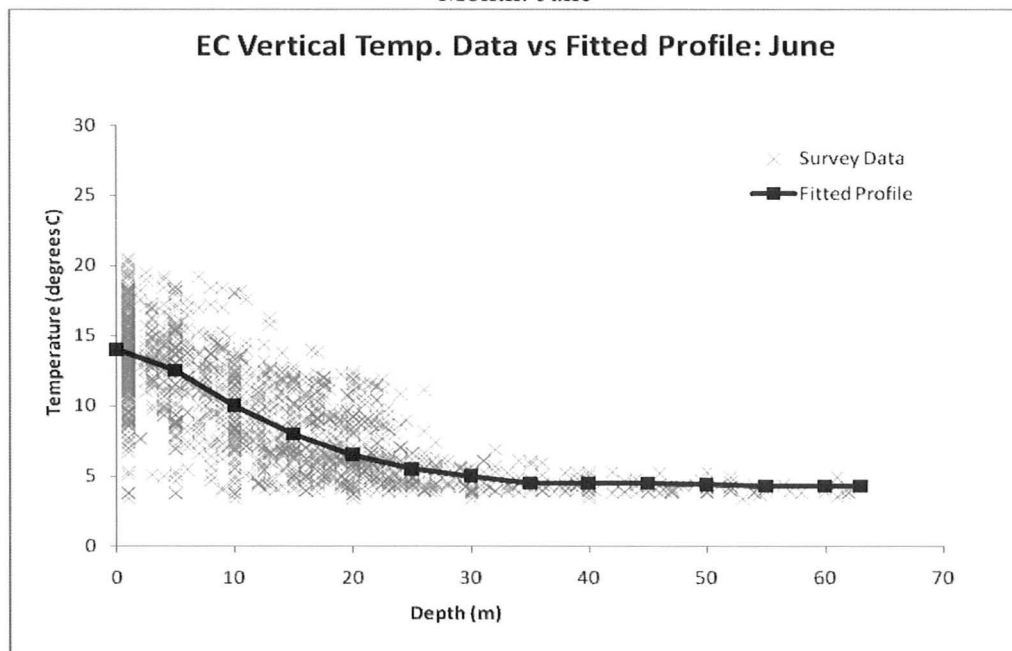
Month: April



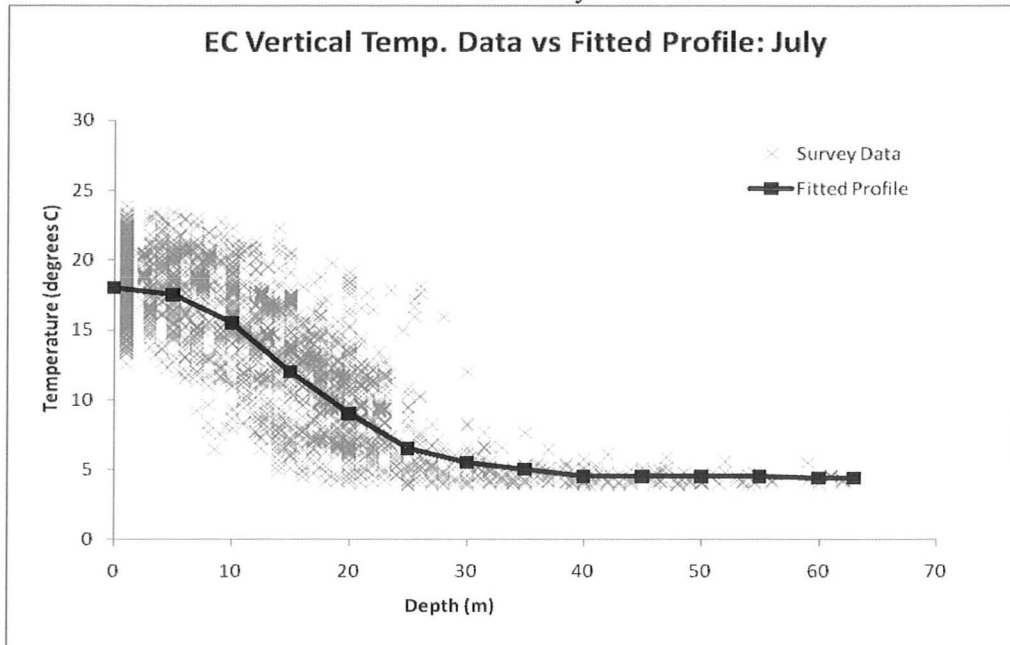
Month: May



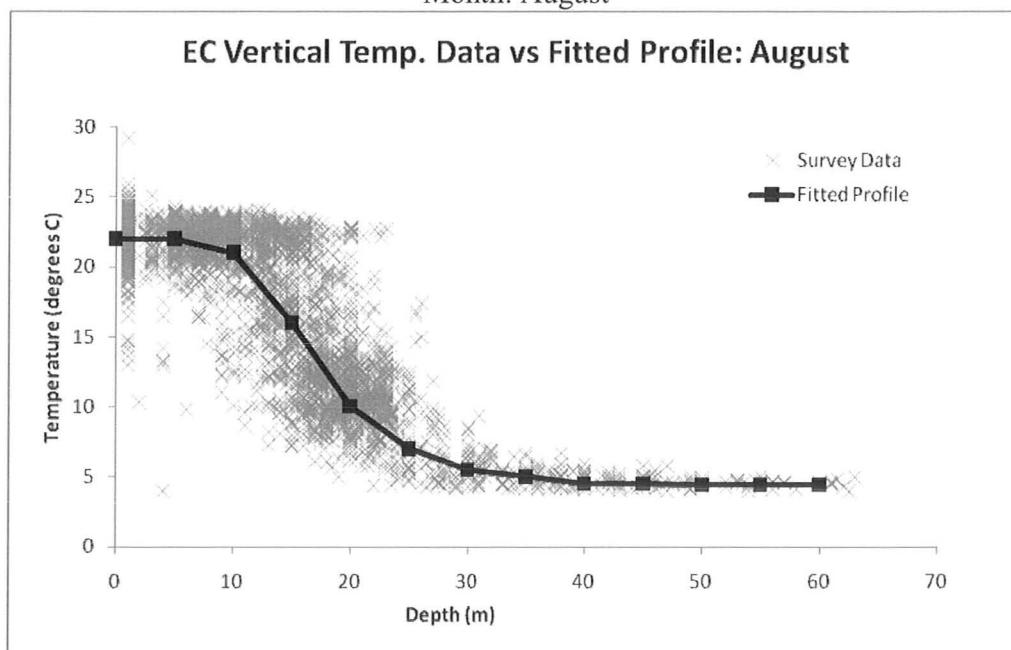
Month: June



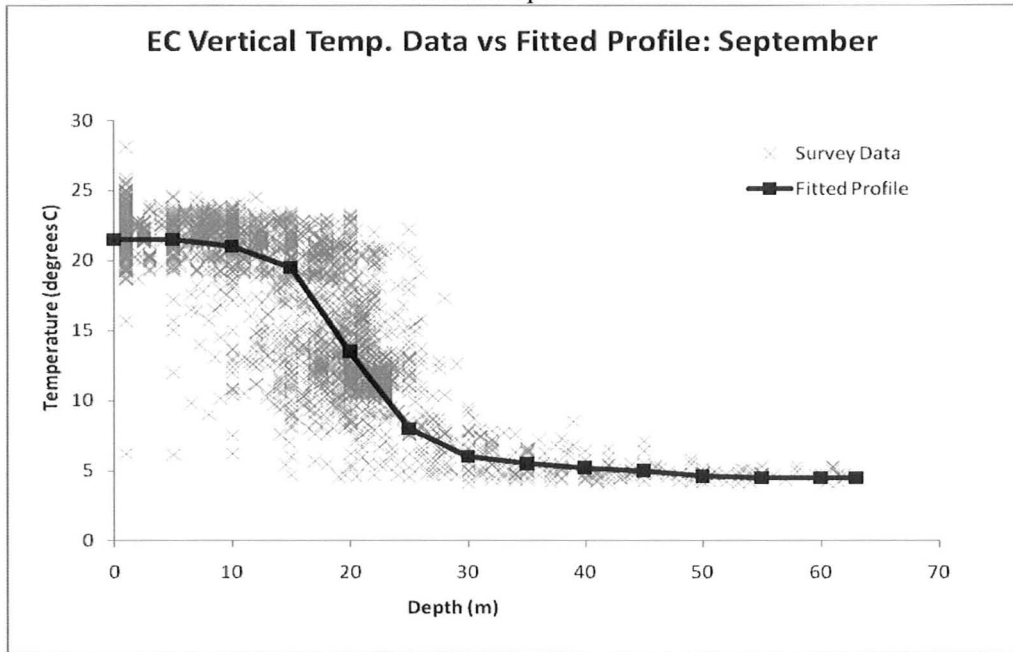
Month: July



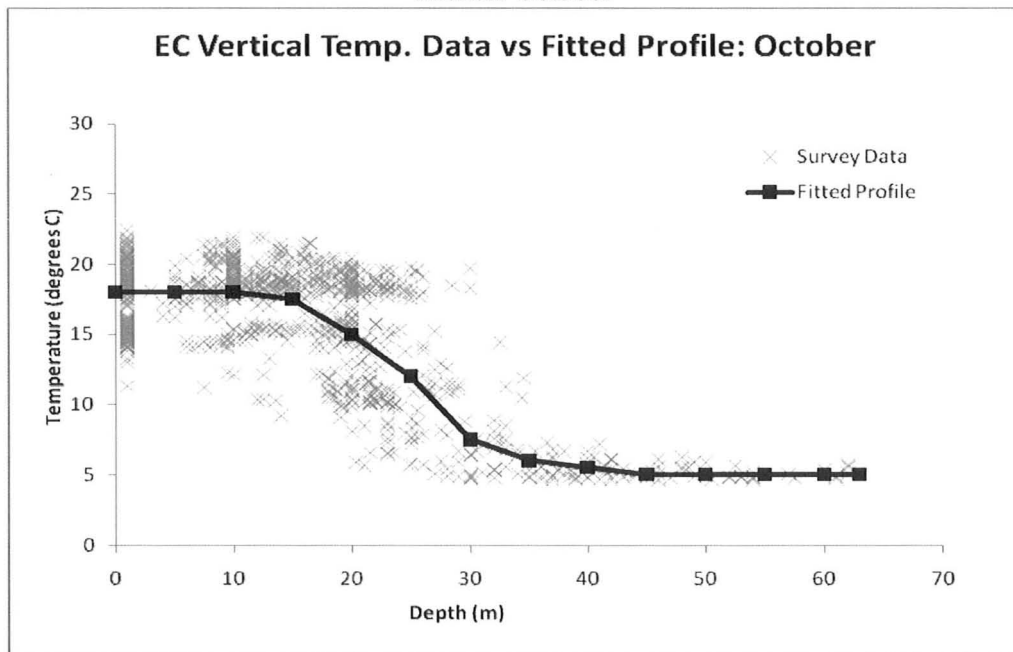
Month: August



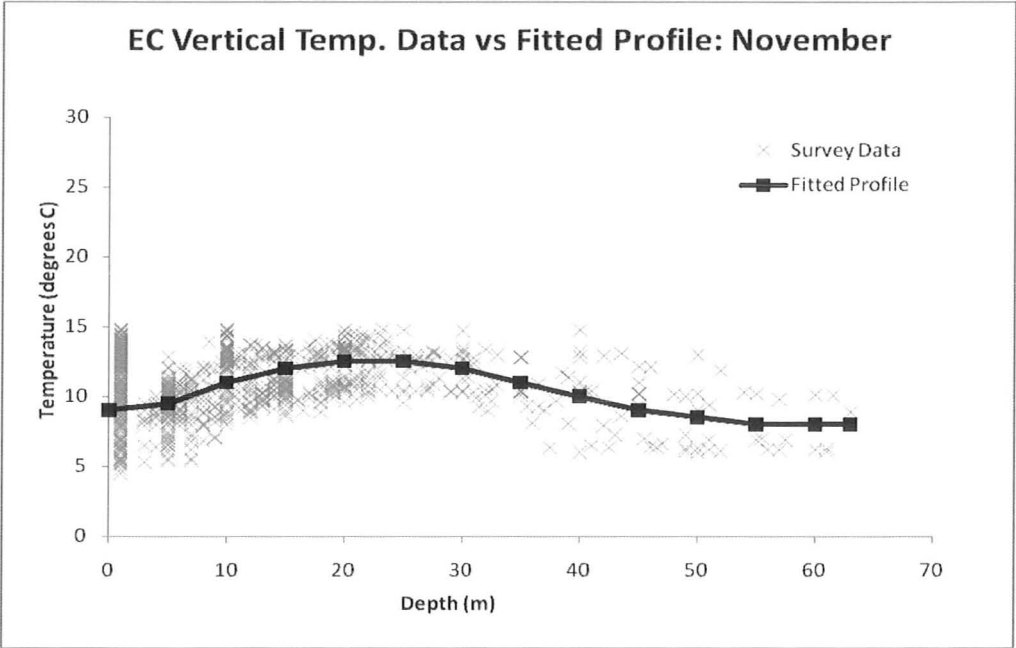
Month: September



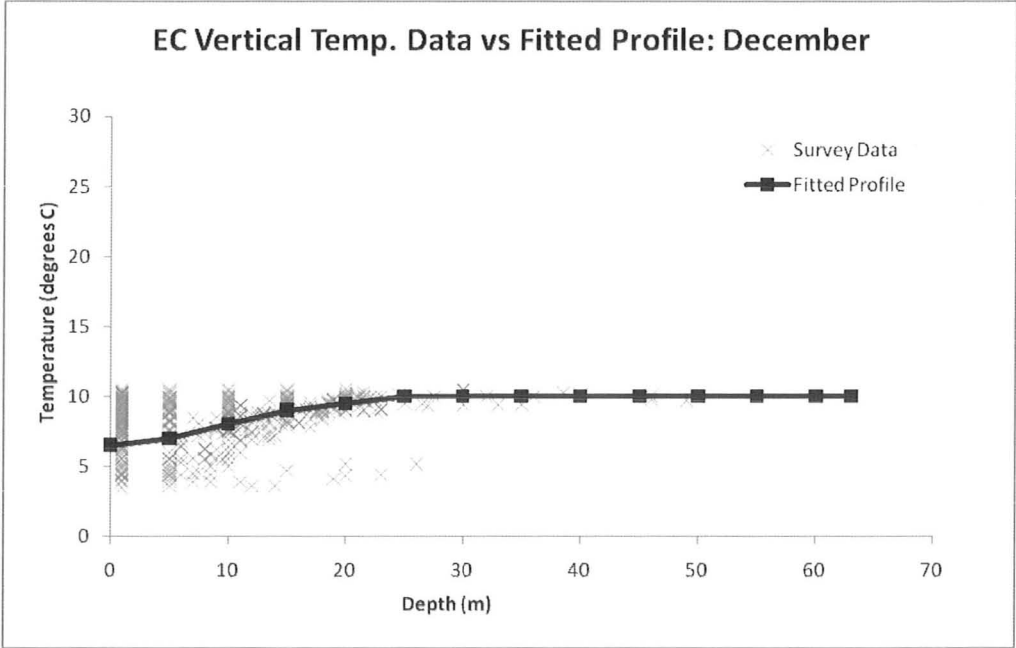
Month: October



Month: November

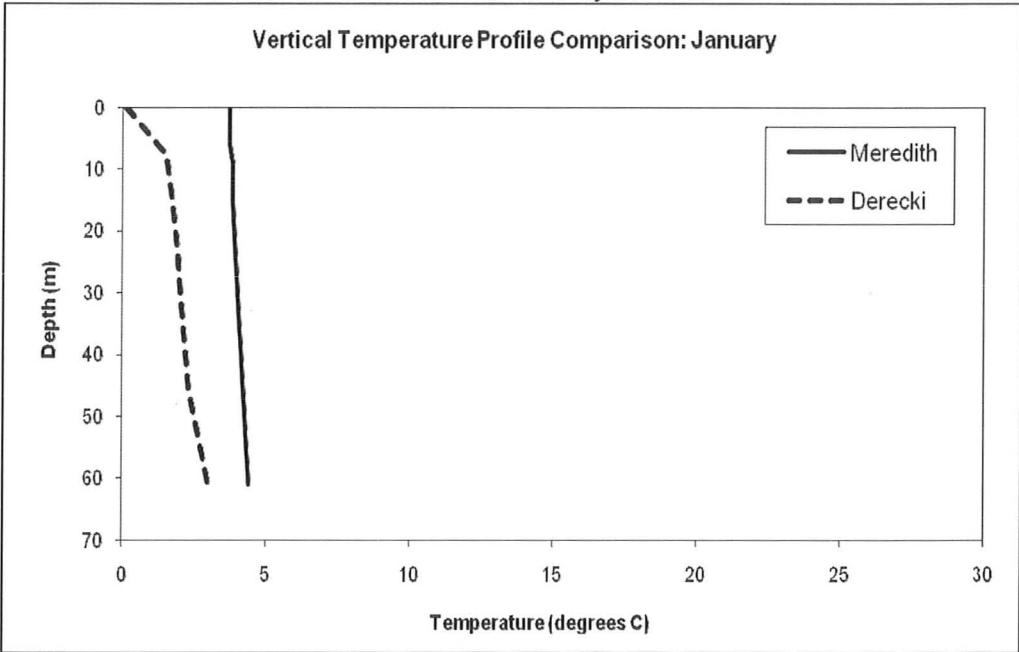


Month: December

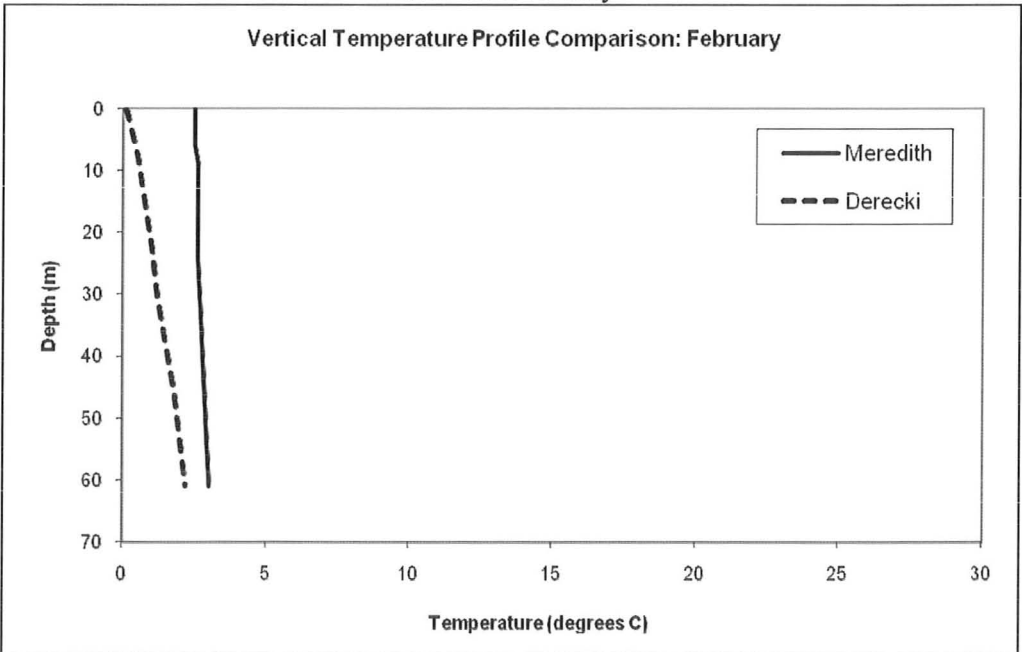


**Appendix E: Lake Erie beginning-of-month fitted vertical
temperature profile comparisons**

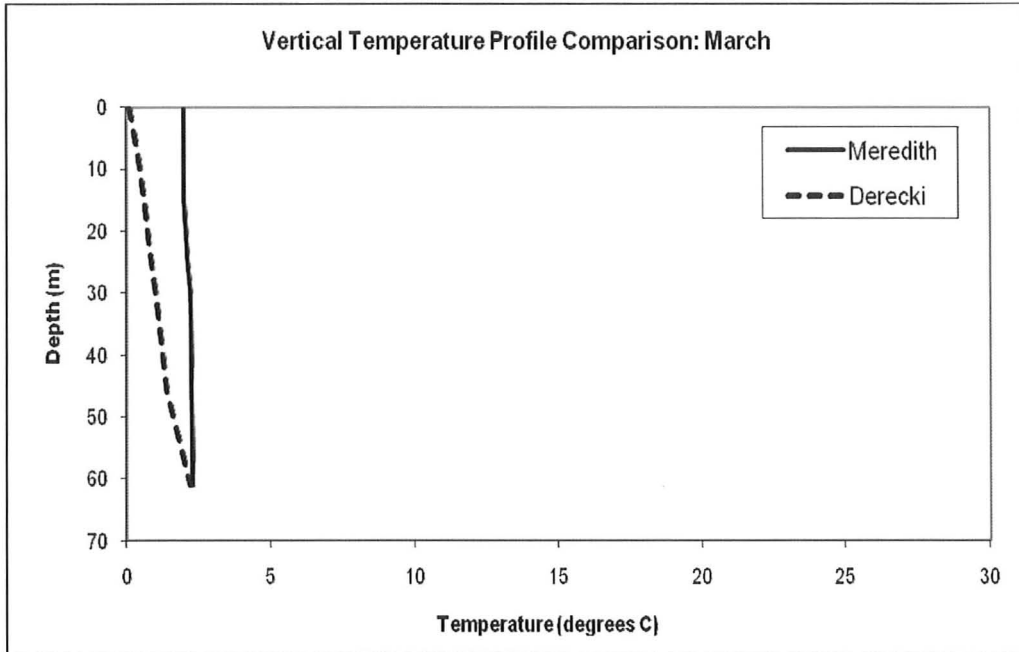
Month: January



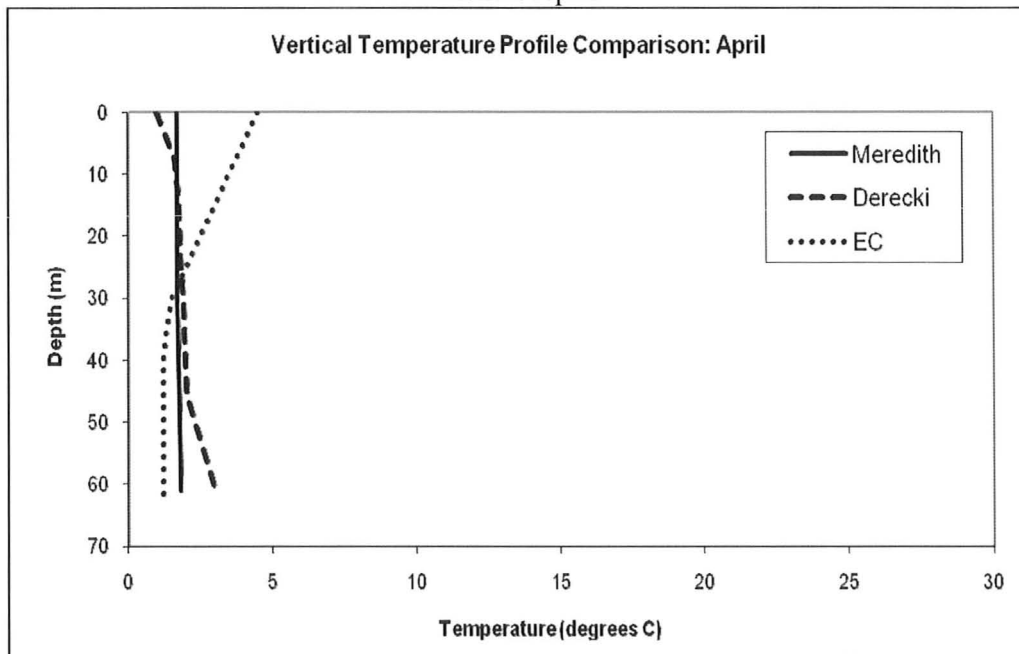
Month: February



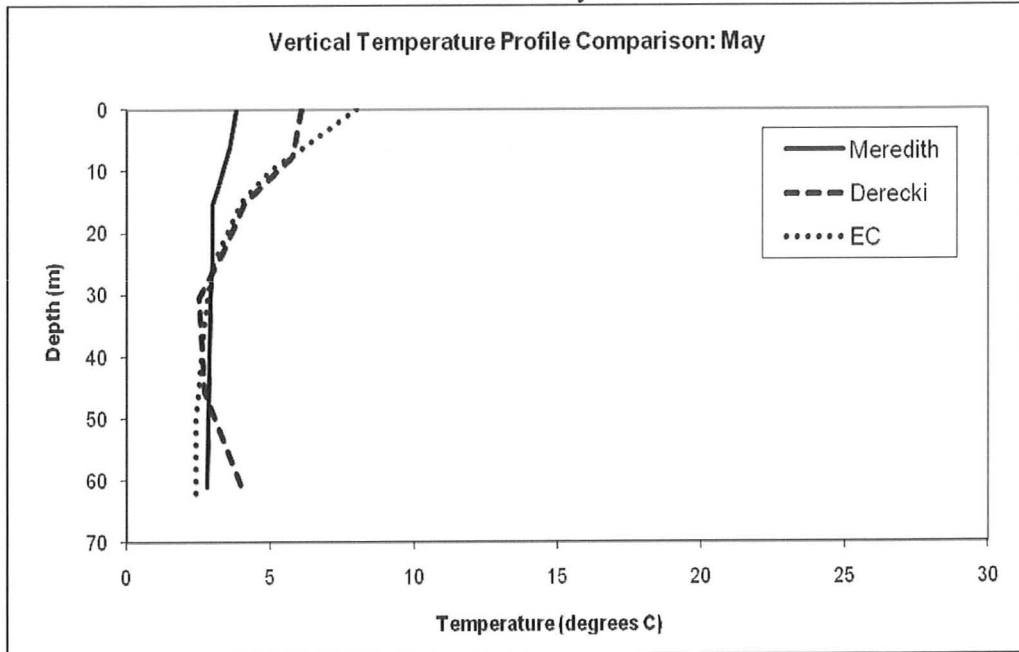
Month: March



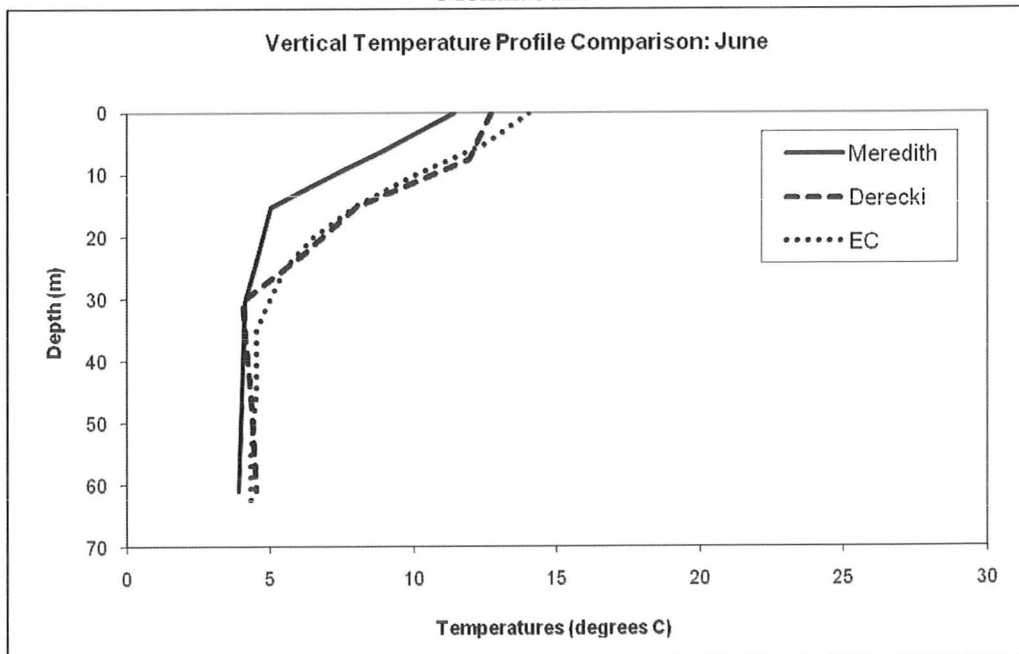
Month: April



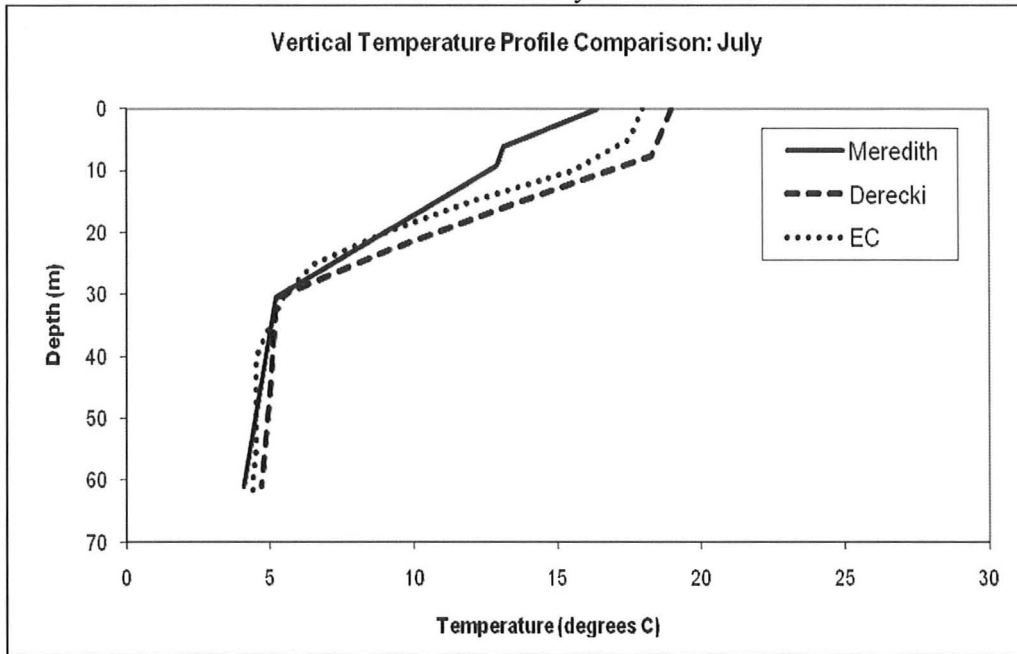
Month: May



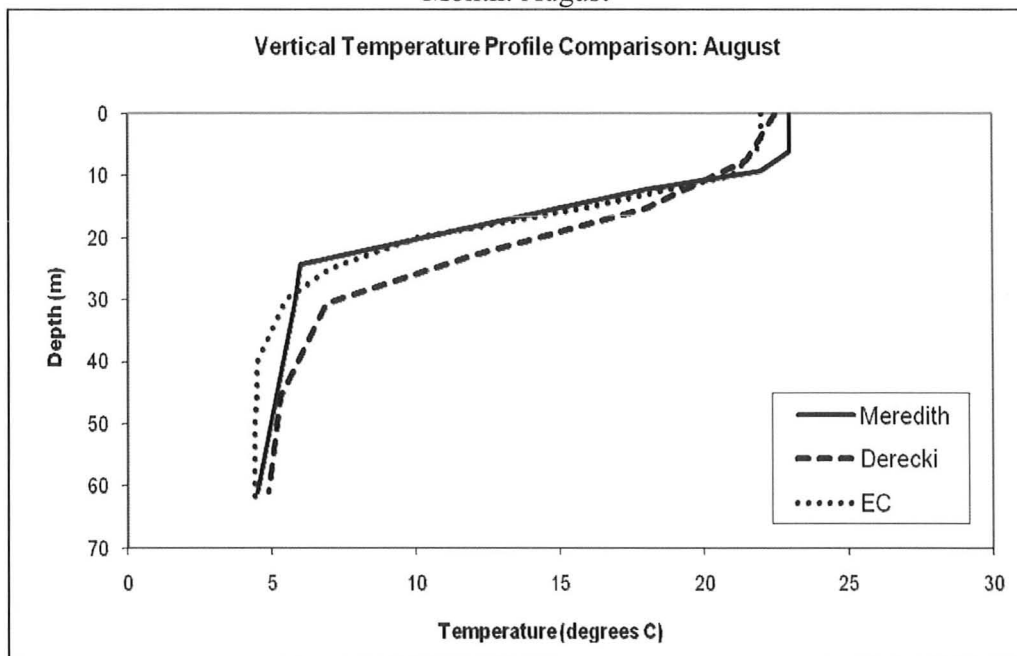
Month: June



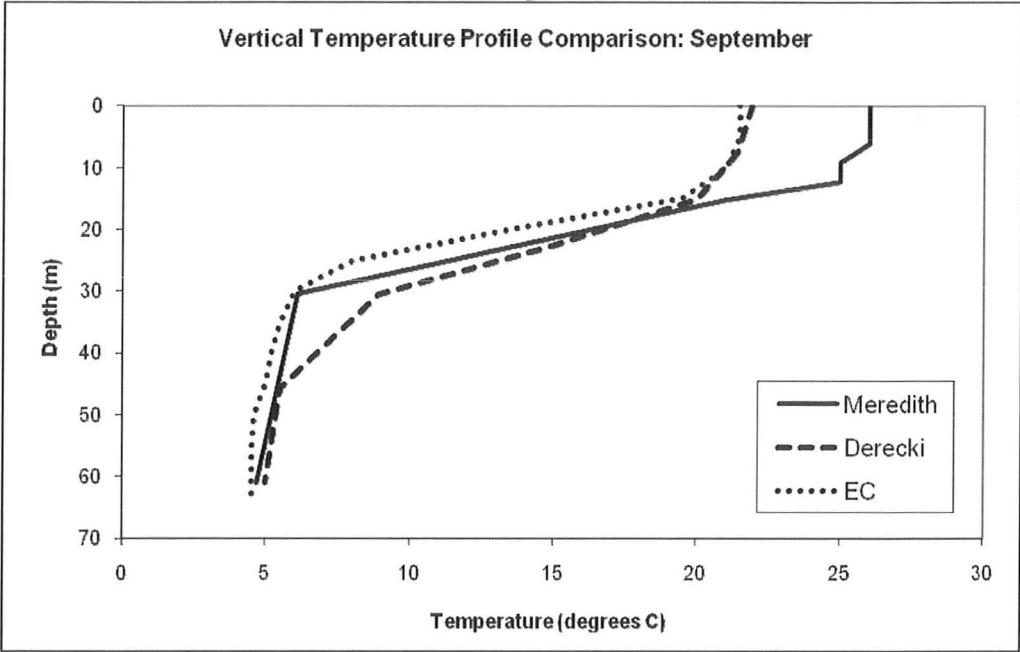
Month: July



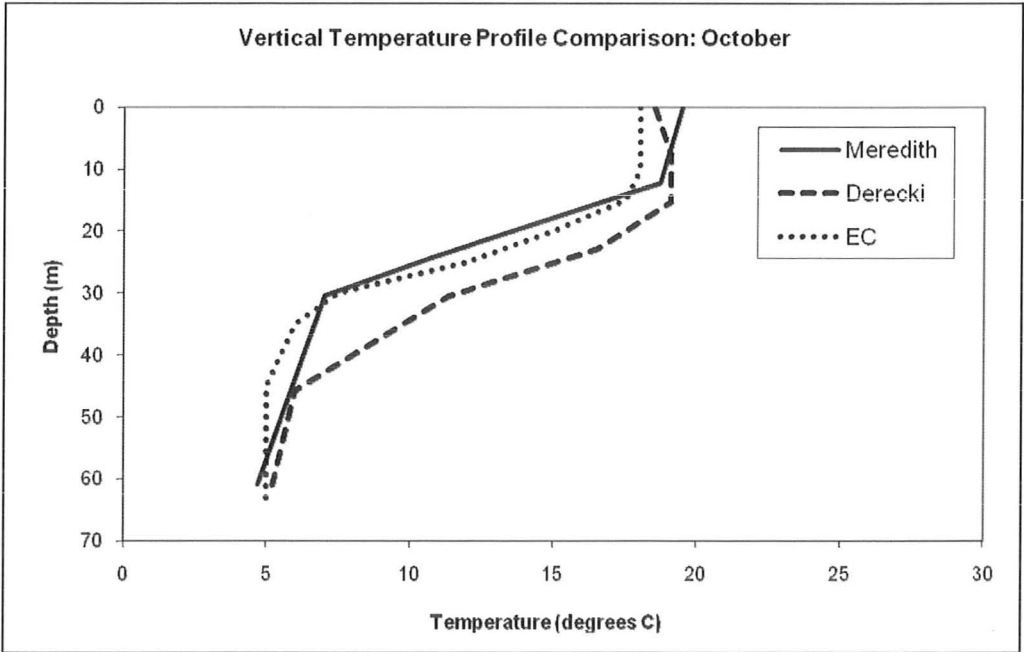
Month: August



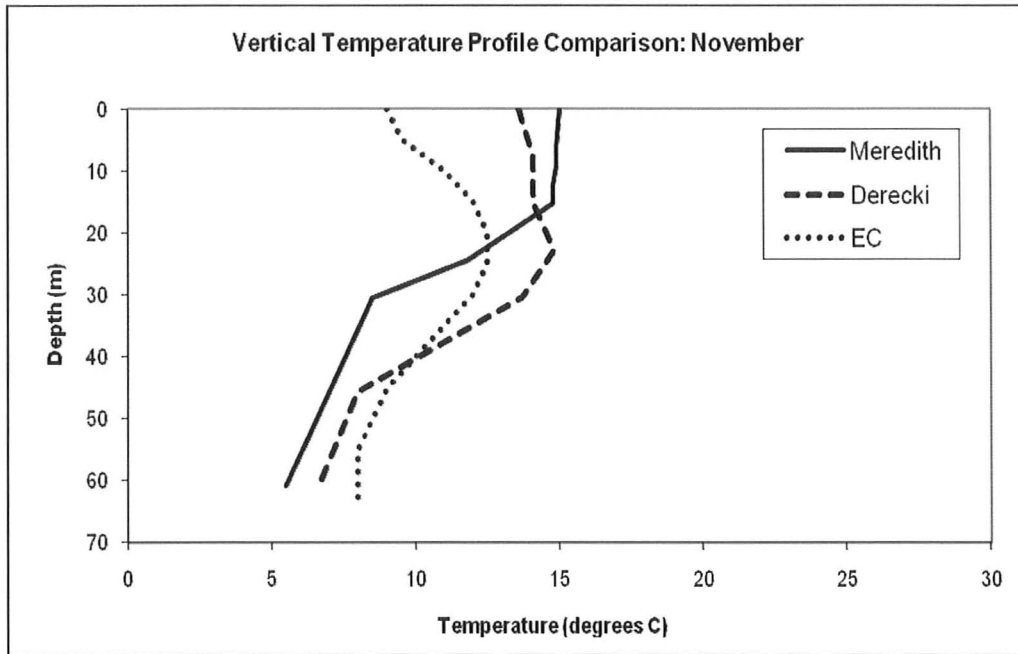
Month: September



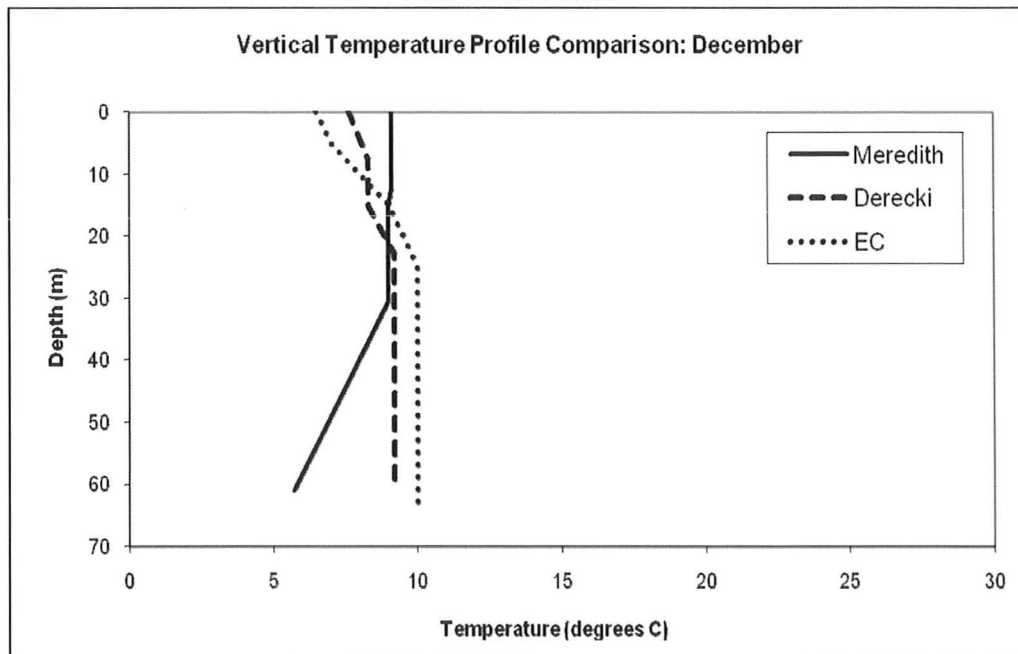
Month: October



Month: November

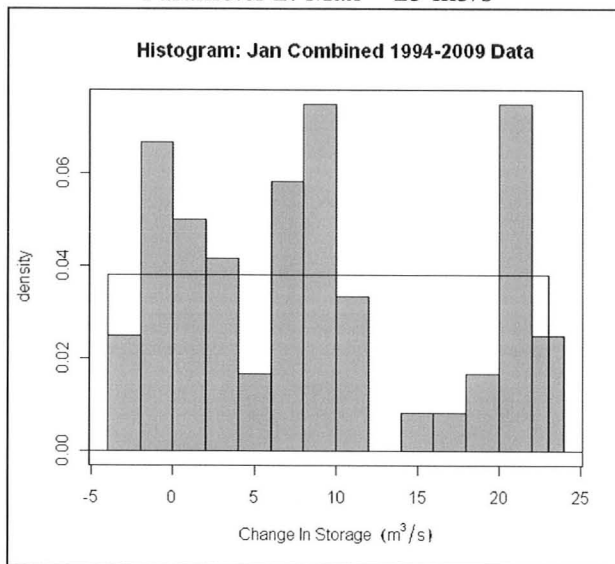


Month: December

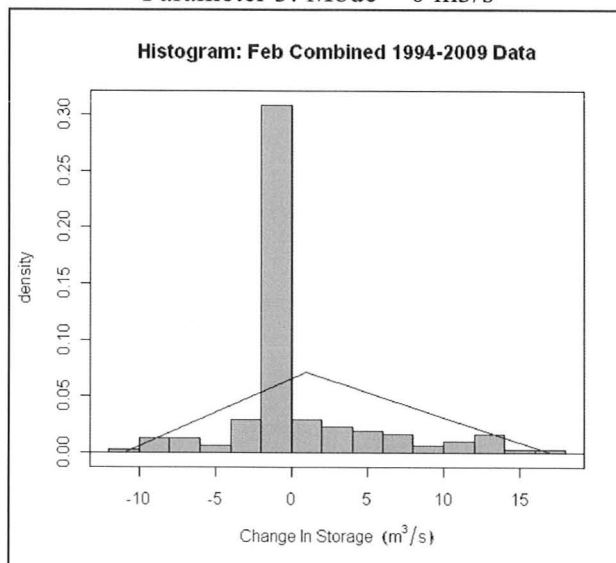


**Appendix F: Thermal expansion and contraction results
comparison to fitted probability
distributions**

Month: January
 Distribution: Uniform
 Parameter 1: Min = -4 m³/s
 Parameter 2: Max = 23 m³/s



Month: February
 Distribution: Triangular
 Parameter 1: Min = -11 m³/s
 Parameter 2: Max = 17 m³/s
 Parameter 3: Mode = 0 m³/s



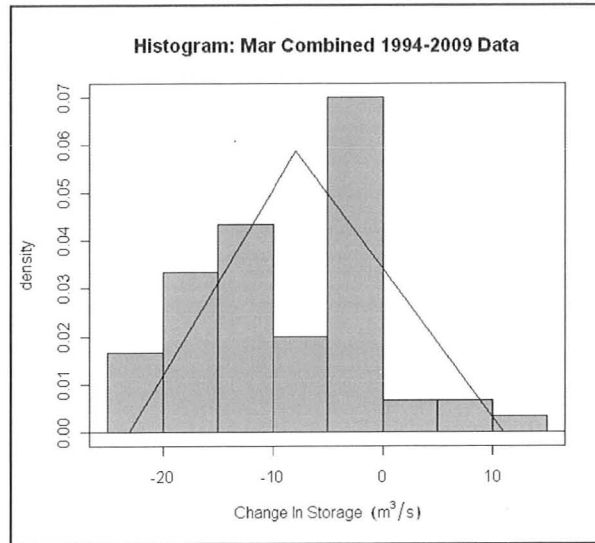
Month: March

Distribution: Triangular

Parameter 1: Min = -23 m³/s

Parameter 2: Max = 11 m³/s

Parameter 3: Mode = -8 m³/s



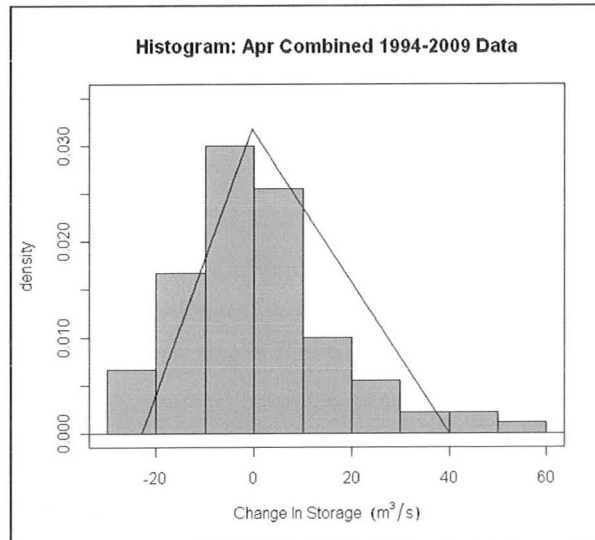
Month: April

Distribution: Triangular

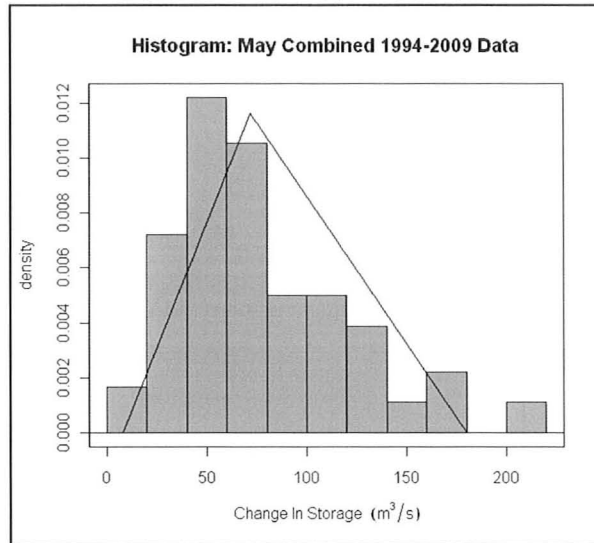
Parameter 1: Min = -23 m³/s

Parameter 2: Max = -1 m³/s

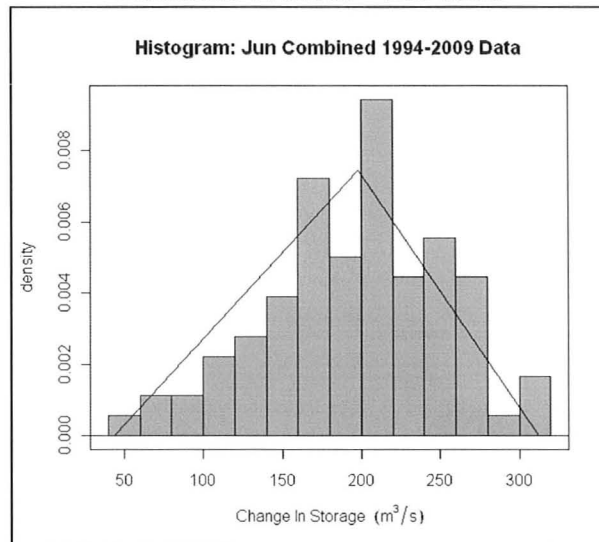
Parameter 3: Mode = 40 m³/s



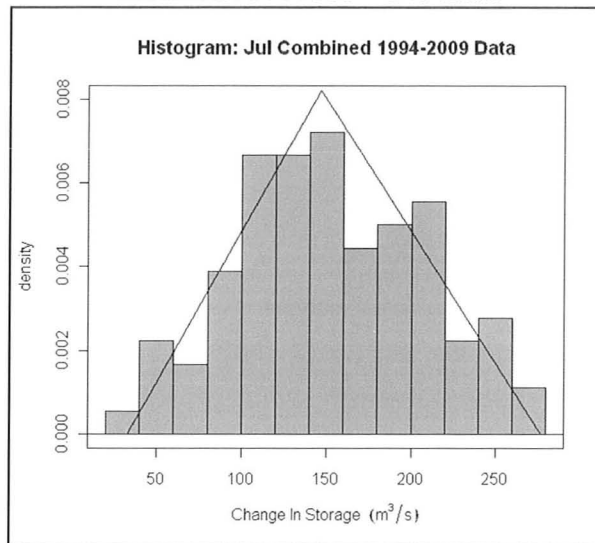
Month: May
 Distribution: Triangular
 Parameter 1: Min = 8 m³/s
 Parameter 2: Max = 180 m³/s
 Parameter 3: Mode = 68 m³/s



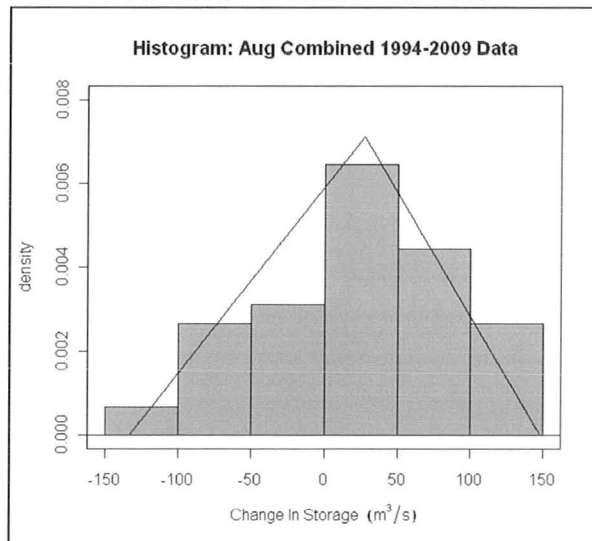
Month: June
 Distribution: Triangular
 Parameter 1: Min = 44 m³/s
 Parameter 2: Max = 312 m³/s
 Parameter 3: Mode = 203 m³/s



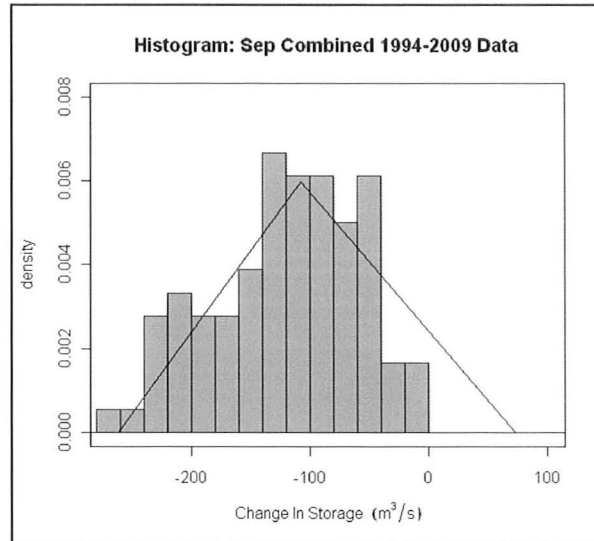
Month: July
 Distribution: Triangular
 Parameter 1: Min = 33 m³/s
 Parameter 2: Max = 277 m³/s
 Parameter 3: Mode = 147 m³/s



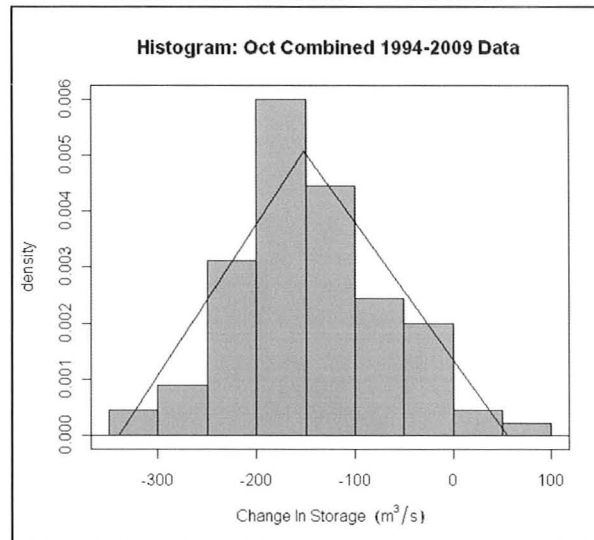
Month: August
 Distribution: Triangular
 Parameter 1: Min = -133 m³/s
 Parameter 2: Max = 148 m³/s
 Parameter 3: Mode = 22 m³/s



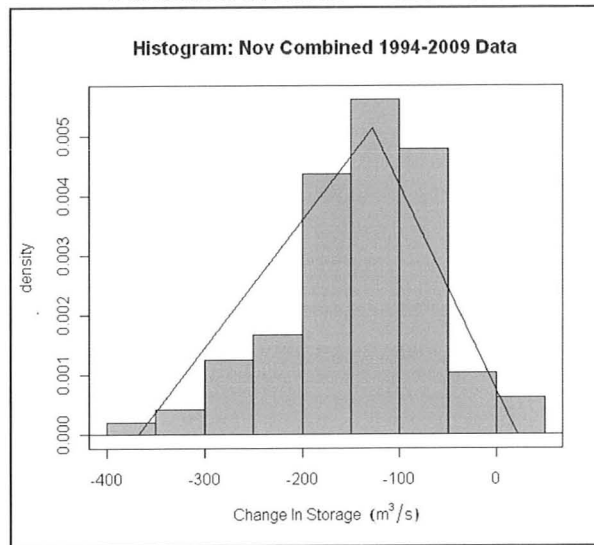
Month: September
 Distribution: Triangular
 Parameter 1: Min = -262 m³/s
 Parameter 2: Max = 78 m³/s
 Parameter 3: Mode = -108 m³/s



Month: October
 Distribution: Triangular
 Parameter 1: Min = -340 m³/s
 Parameter 2: Max = 55 m³/s
 Parameter 3: Mode = -152 m³/s



Month: November
 Distribution: Triangular
 Parameter 1: Min = -368 m³/s
 Parameter 2: Max = 21 m³/s
 Parameter 3: Mode = -128 m³/s



Month: December
 Distribution: Triangular
 Parameter 1: Min = -140 m³/s
 Parameter 2: Max = 5 m³/s
 Parameter 3: Mode = -41 m³/s

